

Sheffield Hallam University

The rheological and honing characteristics of polyborosiloxane/grit mixtures.

DAVIES, Peter John

Available from the Sheffield Hallam University Research Archive (SHURA) at:

<http://shura.shu.ac.uk/3165/>

A Sheffield Hallam University thesis

This thesis is protected by copyright which belongs to the author.

The content must not be changed in any way or sold commercially in any format or medium without the formal permission of the author.

When referring to this work, full bibliographic details including the author, title, awarding institution and date of the thesis must be given.

Please visit <http://shura.shu.ac.uk/3165/> and <http://shura.shu.ac.uk/information.html> for further details about copyright and re-use permissions.



VOL.1

Sheffield Hallam University

REFERENCE ONLY

ProQuest Number: 10694418

All rights reserved

INFORMATION TO ALL USERS

The quality of this reproduction is dependent upon the quality of the copy submitted.

In the unlikely event that the author did not send a complete manuscript and there are missing pages, these will be noted. Also, if material had to be removed, a note will indicate the deletion.



ProQuest 10694418

Published by ProQuest LLC (2017). Copyright of the Dissertation is held by the Author.

All rights reserved.

This work is protected against unauthorized copying under Title 17, United States Code
Microform Edition © ProQuest LLC.

ProQuest LLC.
789 East Eisenhower Parkway
P.O. Box 1346
Ann Arbor, MI 48106 – 1346

**THE RHEOLOGICAL AND HONING CHARACTERISTICS OF
POLYBOROSILOXANE/GRIT MIXTURES**

by

**Peter John Davies BSc.(Hons)
Metallurgy and Microstructural Engineering**

**A THESIS SUBMITTED IN PARTIAL FULFILMENT OF THE
REQUIREMENTS OF SHEFFIELD HALLAM UNIVERSITY FOR
THE DEGREE OF DOCTOR OF PHILOSOPHY**

SEPTEMBER 1993

Collaborating Establishment:

**Extrude Hone Limited
6 Centurion Court
Brick Close
Kiln Farm
Milton Keynes.**

PREFACE

The work reported in this thesis was carried out at Sheffield Hallam University between October 1990 and September 1993.

The candidate has not during the above period of registration for the degree of PhD been registered for any other university degree.

The results presented here are, as far as can be certain, original except where reference has been made to previous work.

Courses were attended at Sheffield Hallam University in the following subjects:

Computer studies, Polymer processing, and Machining.

ACKNOWLEDGEMENTS

I wish to express my thanks to Extrude Hone Limited for supplying materials, machine time, and for their financial support over the three years of research. I would also like to thank the Director of the School of Engineering at Sheffield Hallam University for providing both technical and financial support. In addition thanks must also be expressed to the Science and Engineering Research Council for their financial support.

All the technicians at both Sheffield Hallam University and Extrude Hone Limited are acknowledged for their constant assistance throughout the duration of the work.

The relationship with a supervisor is an important factor that should not be underestimated, therefore sincere gratitude is expressed to Dr. A. J. Fletcher for his constant help, time, and not forgetting his many thought provoking comments.

To my parents a simple thank you for your constant support, encouragement, belief, and wisdom. I would like to thank Susan for allowing me the indulgence of time and for her constant patience. Finally I would like to thank Vikki and the remaining members of my family for being there when needed.

THE RHEOLOGICAL AND HONING CHARACTERISTICS OF POLYBOROSILOXANE/GRIT MIXTURES

P. J. DAVIES

SYNOPSIS

Abrasive Flow Machining, (AFM), is a non-traditional machining process that is achieved by extruding polyborosiloxane, (a viscoelastic polymer), containing abrasive grit additions, across surfaces, edges, and through component cavities. The AFM process is a complex one and its machining mechanism is still only partially understood since previous research into the process has mainly been limited to qualitative study. The present work undertook to investigate the relationship between the rheological characteristics of polyborosiloxane/grit mixtures and the associated machining parameters. A significant increase in the quantitative data available with respect to both the rheological and machining characteristics of these mixtures has been provided as a consequence of the investigations.

Experiments were conducted using low viscosity, (LV), medium viscosity, (MV), and high viscosity, (HV), polyborosiloxane base media, in conjunction with silicon carbide abrasive grit of 60 and 100 Mesh size; the ratios of grit to base polymer utilised in the experiments were 0, 1, and 2. The test pieces used in the experimental work were mild steel dies having a diameter of 15mm and a length of 15mm, and the equipment used to conduct the experiments was an Extrude Hone mark 7A machine.

The investigations conducted have revealed that for all polymer/grit mixtures an increase in the number of extrusion cycles results in an increase in the stock removed, an improvement in the surface roughness, and an increase in the temperature of the mixture. Furthermore as the usage of the medium increases the grit particle wear increases so that there is a corresponding decrease in the machining parameters.

For all mixtures there appears to be no correlation between the viscosities of the base media types and the machining parameters. However, a relationship is demonstrated between the machining parameters and variations in the viscosities of the grit/polymer mixtures based on a specific polymer base. The factors that appear to influence this relationship are the grit to polymer ratio, the grit size, and the temperature. The most important of these parameters are suggested to be the grit to polymer ratio and temperature since these variables appear to affect the viscosity behaviour and the associated machining parameters.

In addition the investigations showed that the viscosities and associated rheological dependent parameters correspond to the qualitative viscosity nomenclature given to the different media types by the manufacturer. A shear history effect is also exhibited in each of the polymer types.

CONTENTS

		Page Number
1.0	INTRODUCTION	9
2.0	MACHINING	11
2.1	Mechanics of Machining	12
2.2	Other Factors that Influence Machining	17
2.3	Abrasive Machining Processes	20
2.4	Non-Traditional Machining Processes	22
2.5	Surface Integrity	23
3.0	RHEOLOGY	26
3.1	The Fundamentals of Polymer Rheology	26
3.1.1	Types of Fluid	28
3.1.1.1	Time-independent Fluids	28
3.1.1.2	Time-dependent Fluids	30
3.1.1.3	Viscoelastic Fluids	31
3.1.2	Tensile Flow	32
3.1.3	Normal Stresses	34
3.1.4	Viscosity Dependent Parameters	35
3.2	Measurement of Flow Properties	38
3.2.1	Rotational Viscometers	39
3.2.1.1	Coaxial (Concentric-Cylinder) Viscometer	39
3.2.1.2	Cone and Plate Viscometer	40
3.2.2	Capillary (Extrusion) Viscometers	40
3.2.2.1	Corrections Applicable to Capillary Viscometers	42

4.0	ABRASIVES	45
4.1	Assessment of Abrasive Particles	45
4.1.1	Particle Size	45
4.1.2	Particle Shape	46
4.2	Abrasive Wear	47
5.0	ABRASIVE FLOW MACHINING	48
5.1	Fundamental Constituents of the AFM System	50
5.2	The AFM Procedure	53
5.3	Surface Integrity Related to the AFM Process	54
5.4	Review of Previous Research Related to the AFM Process	55
5.4.1	Research Related to the Machining Aspects of the AFM Process	55
5.4.2	Research Related to the Rheological Aspects of the AFM Process	59
6.0	EXPERIMENTAL	61
6.1	Preliminary Work	61
6.1.1	The Effect of Medium Reuse on the Stock Removal and Surface Roughness	62
6.1.2	Abrasive Particle Assessment	63
6.2	Principal Work	65
6.2.1	Materials	65
6.2.2	Investigation of Process Parameters and Machining Characteristics	66
6.2.2.1	Stock Removal	66
6.2.2.2	Surface Integrity	67
6.2.2.3	Pressure and Temperature	68

6.2.3	Machining Procedure	69
6.2.3.1	Machining Equipment	69
6.2.3.2	Machining Procedure	70
6.2.4	Data Assessment	72
6.2.4.1	Pressure Data Assessment	72
6.2.4.2	Calculation of the Volume of Medium Extruded	73
6.2.4.3	Determination of Rheological Parameters	73
6.2.5	Processing Parameter Variations and their Effect on the Measurements Made	75
6.2.5.1	Machining Parameter Variations	75
6.2.5.2	Rheological Parameter Variations and Assumptions	77
7.0	RESULTS	82
7.1	Preliminary Work	83
7.1.1	AFM Surface Features	83
7.1.1.1	Castle Nut Component	83
7.1.1.2	Bearing Component	84
7.1.2	Medium Reuse	84
7.1.3	Abrasive Grit Wear	86
7.2	Principal Work	87
7.2.1	Die Diameter Change	87
7.2.2	Die Mass Change	90
7.2.3	Surface Integrity	91
7.2.3.1	Surface Roughness Improvement	91
7.2.3.2	Surface Photomicroscopy	94
7.2.4	Processing Time	95

7.2.5	Pressure Drop Measurements	97
7.2.5.1	The Effect of the Number of Extrusion Cycles Performed on the Pressure Drop Across the Die	98
7.2.5.2	Average Pressure Drops	104
7.2.6	Determination of the Apparent Viscosities	106
7.2.7	Temperature Measurements	110
7.2.8	Shear History	115
8.0	DISCUSSION	117
8.1	Errors Associated with the Measured and Calculated Parameters	118
8.1.1	The Method of Calculation of the Viscosities	119
8.1.1.1	Comparison of the Calculated Viscosities to Published Values	120
8.1.2	The Effect of Surface Friction on the Pressure Drop	121
8.1.3	Errors Associated with the Normal Pressure Measurements	122
8.2	The Effect of the Number of Extrusion Cycles on the Machining Parameters	124
8.3	Entrapped Air Contained within the Polyborosiloxane/Grit Mixtures	127
8.4	The Shear History Effect	128
8.4.1	Factors Governing Viscoelastic Effects	129
8.4.2	Frozen-in-Orientation	130
8.4.3	The Explanation for the Occurrence of the Shear History Effect in the Present Work	131
8.5	The Rheological Parameters	133
8.5.1	The Temperature and Pressure Variables	133
8.5.1.1	The Effect of Temperature on the Viscosity	133
8.5.1.2	The Effect of Average Pressure Drop on the Viscosity	134

8.6	The Relationship Between the Rheological Behaviour and the Machining Characteristics	135
8.6.1	The Effect of Temperature on the Rheology and the Machining Performance	135
8.6.2	The Overall Effect of Rheology on Machining	137
8.6.2.1	The Effect of Shear Stress on the Machining Performance	139
8.7	The Effect of Alterations in the Base Viscosity, Grit Size, and Grit to Polymer Ratio on the Rheological and Machining Parameters	140
8.7.1	Viscosity of the Base Polymer	141
8.7.2	Grit to Polymer Ratio	145
8.7.3	Grit Size	148
8.7.4	The Combination of the Effects of Base Viscosity, Grit Size, and Grit to Polymer Ratio on the Machining Performance	149
8.8	The Proposed Machining Mechanism	152
8.8.1	The Polyborosiloxane/Grit Mixtures	152
8.8.2	The Machining Mechanism	154
8.8.3	Slip-Stick	157
9.0	CONCLUSIONS	159
10.0	FURTHER WORK	165
11.0	REFERENCES	
	Tables 1 - 58	
	Figures 1 - 135	
	Appendix 1	

1.0 INTRODUCTION

Abrasive Flow Machining is a non-traditional machining process that has been in use since the mid-1960's. It essentially involves metal removal by abrasion that is achieved by a mixture of polyborosiloxane and abrasive grit which is forced through orifices in a variety of metal components, such as dies.

The process is a complex one and the machining mechanism remains only partially understood. It is obvious that the machining mechanism will be dependent on both the polymer rheology and the machining conditions employed. Therefore the intention of the present work is to examine and quantify:

- 1) the behaviour of the various polymer mixtures utilised in the Abrasive Flow Machining process, and
- 2) the machining action at the die wall.

This allows the development of a correlation between the rheological characteristics of the mixture and the machining mechanisms occurring in the Abrasive Flow Machining process.

The programme of work involved the examination of the effect of medium viscosity and grit to polymer ratios on the polymer rheology and the correlation of these effects with changes in the machined component, (which has included surface integrity, stock removal, and component profile).

The literature review has aimed to unite the relevant subjects that pertain to the Abrasive Flow Machining process, viz:

- i) Section 2.0 Machining,
- ii) Section 3.0 Rheology of Polymers,
- iii) Section 4.0 Abrasives,
- iv) Section 5.0 Abrasive Flow Machining.

2.0 MACHINING

A workpiece which has undergone a primary process such as hot rolling, forging, or casting, will require a secondary process to produce high dimensional tolerance, good surface finish and if required complex geometry. This secondary process is termed machining and encompasses turning, boring, drilling, and forming, as well as shaping and planing. Machining involves the removal of selected areas of a workpiece, by the use of a tool, and is accomplished by straining a local region of the workpiece to fracture by the relative motion of the tool to the workpiece. This is usually achieved by mechanical energy; however, developments in the machining process have resulted in the use of electrical, chemical, and thermal energy.

The main motion in the machining process is termed the primary motion. This is provided by the tool and causes relative motion between itself and the workpiece in such a way that the face of the tool approaches the workpiece. A further motion, termed the feed motion, is applied to either the tool or workpiece; which when added to the primary motion results in the development of a cutting zone. In this zone the tool compresses the workpiece, which eventually shears by the action of the advancing tool, resulting in the formation and removal of a chip; thus the desired surface finish is obtained. The majority of the power required to perform machining is usually absorbed by the primary motion.

Machine tools can be either those which generate surfaces of rotation or those which generate flat or formed surfaces by linear movement.

2.1 Mechanics of Machining

Several reviews (1,2,3) stipulate that there is no universal theory of the basic mechanics of the machining process because of the complex phenomena and the interdependence of the parameters that control the process, e.g tool forces, tool/chip contact length, and tool temperature.

However, the machining process is dependent upon the applied forces occurring in the cutting zone. Therefore the cutting zone is an important area that is comprised of one type of machining action and chip formation respectively. The different types of machining action and chip formation (4,5), as shown in figures 1 and 2, consist of:

a) Machining Action

- i) Orthogonal - a two dimensional cutting action where the tool cutting edge is perpendicular to the direction of movement.
- ii) Oblique - a three dimensional cutting action along more than one edge of the cutting tool.

b) Chip Formation

- i) Discontinuous (Type I) - chips break away in segments. Characteristic of brittle materials, as well as ductile materials machined at very low speeds and high feeds.
- ii) Continuous (Type II) - Chips breakaway like 'ribbons'. Characteristic of ductile materials under steady-state conditions.

- iii) Builtup edge (Type III) - chips with continuous form and a high affinity for the tool face material, forming a highly compressed layer at the tool/chip interface. Predominates with high feeds and low rake angle.

"The continuous chip has been extensively studied because it frequently occurs in practice" (6). Furthermore, since orthogonal machining is two dimensional rather than three dimensional, it has been widely used in theoretical and experimental work because several dependent variables are eliminated by the reduction in the number of dimensions.

The present work will consider a simple model of orthogonal machining (7,8) since the Abrasive Flow Machining process employed is considered to be orthogonal, i.e the abrasive grit (the cutting tool) produces a plane surface parallel to the original plane surface and the cutting edge is perpendicular to the flow direction.

Figure 3 represents the simple orthogonal model utilising a single-point tool with a rake angle α , a clearance angle θ , and a wedge angle ω ; ($\alpha + \theta + \omega = 90^\circ$). The rake face of the tool is the surface over which the chip flows, and the surface of the tool clearing the machined surface is termed the flank. Intense shearing action on the metal ahead of the tool is created by the imposed forces in a zone termed the primary deformation zone. This shear produces a chip. A secondary deformation zone exists between the chip and tool interface where the forces are sufficient to deform the lower layers of the chip as it slides along the tool face. The metal in the chip is deformed from an original thickness, h , to a deformed thickness, h_c , leading to a chip thickness ratio C_h ($= h/h_c$). A localised region of

intense shear in the vicinity of OA will exist together with severe frictional work along OB (9). The localised region of shear is usually represented by a well-defined shear plane OA occurring at a shear angle ϕ . A general model (10) applicable to commercial cutting conditions discusses the existence of three zones within the tool/chip contact length:

Zone 1 - a transient sliding zone adjacent to the cutting edge.

Zone 2 - a sticking zone close to the cutting edge.

Zone 3 - a second sliding zone at the back of the contact area.

As machining continues the transient sliding zone is absorbed by the sticking zone and eventually under steady-state conditions only two zones are observed, i.e. sticking and sliding.

For chips without curl there are three velocities to consider, viz:

- 1) The cutting speed v ; this is the velocity of the tool relative to the workpiece.
- 2) The chip velocity v_c ; this is the velocity of the chip relative to the tool face.
- 3) The shear velocity v_s ; this is the velocity of the chip relative to the workpiece.

The force system associated with orthogonal machining requires the chip to be held in equilibrium by the action of two equal and opposite forces, R and R' . R' is the force which the tool exerts on the back surface of the chip whilst R is the force which the workpiece exerts on the base of the chip (shear plane); see figure 4. The force R' is resolved into a component F , the frictional force experienced by

the chip sliding over the tool face, and a component N , the normal force perpendicular to F . The force R is resolved into a component F_s , the shearing force required to shear the metal, and a component F_n , the compressive stress on the shear plane which is perpendicular to F_s . The force R can also be resolved into a component F_v , the cutting force acting on the rake face of the tool which is perpendicular to the cutting edge, and a component F_p , the thrust force acting on the tool parallel to the direction of feed.

The shear stress is the main parameter affecting the energy requirement in the machining process. It has been stated (7) and demonstrated elsewhere (11), that for simple orthogonal machining the force F_s acting on the shear plane is:

$$F_s = F_v \cos\phi - F_p \sin\phi \quad (1)$$

providing shearing occurs on plane OA and there is continuous chip formation.

The shear stress, which is derived from the shear force, F_s , and the shear plane area, A_s , is;

$$\tau = \frac{F_s}{A_s} = \frac{F_s \sin\phi}{bt} \quad (2)$$

where,

$$A_s = \frac{bt}{\sin\phi} \quad (3)$$

and b = width of the chip

The rate of energy consumption during machining, P_m , is the product of the cutting speed, v , and the cutting force F_v :

$$P_m = F_v V \quad (4)$$

The cutting speed is proportional to both the rate of energy consumption and the metal removal rate, Z_w . Therefore an indication of the process efficiency, independent of the cutting speed, is provided by the energy consumed per unit volume of metal removed, i.e. the specific cutting energy U :

$$U = \frac{P_m}{Z_w} = \frac{F_v V}{btv} = \frac{F_v}{bt} \quad (5)$$

The specific cutting energy depends on the type of material being machined as well as the cutting speed, feed, and rake angle.

Since no cutting tool is completely sharp other forces in the machining process are present to produce chip formation, and it has been reported (12) that "the tool edge 'ploughs' its way through the work material" to produce the sheared chip. For a large depth of cut the ploughing force acting on the tool cutting edge is a small percentage of the total force. However, the ploughing force becomes a large percentage of the total force if the depth of cut is small. This phenomena results in the "size effect" which stipulates that the specific cutting energy required for processes which remove very thin chips, e.g. grinding, is higher than for processes that produce thicker chips.

One of the most important parameters in the machining model is the rake angle because upon it are dependent the cutting force and the strength of the tool edge. An increase in the rake angle, i.e making it more positive, lowers the cutting force and feed force, simultaneously, thus reducing the strength of the tool edge with consequent higher wear rates and shorter tool life. On the other hand negative rake angles increase the strength of the tool edge but result in metal removal by the action of "ploughing" of the workpiece rather than chip formation.

2.2 Other Factors that Influence Machining

Cutting tools are affected by the forces, pressures, stresses, and temperatures present in the machining process. Therefore the type of material used in the cutting tool is critical to the application under consideration. The most common types of tool material are:

- 1) High speed tool steels (0.7-1.5%C with additions of Cr, V, W, Co)
Limited to low cutting speeds due to the rapid decrease in hardness above 150°C.
- 2) Cast nonferrous tools (40%Co-35%Cr-20%W)
Retain hardness up to 815°C but since they are brittle, these tools must be used in situations with mild vibrations and impact.
- 3) Cemented carbides (WC)
Retain hardness up to 1095°C and speeds of upto five times that of high speed tools can be used. However, they are extremely brittle and should be used without vibrations or impact.
- 4) Ceramic or oxide tools of sintered Al_2O_3
These are more brittle than WC but speeds of upto two times that of WC can be employed.
- 5) Diamond
Possesses the highest hot hardness.

Although most machining operations are performed at ambient temperatures, the nature of the machining process itself, and the large shearing energy required to produce chips, cause conversion of considerable amounts of mechanical energy into heat (13,14,15). There will therefore be significant temperature increases which will be dependent upon the cutting velocity employed and consequently the

heat transfer within the workpiece. The cutting fluid therefore plays a critical role in the machining operation, since it dissipates the heat generated, reduces the friction and wear, removes the chips from the cutting zone, and protects the newly machined surface. It has been found (16,17) that the cutting fluid penetrates along the chip/tool interface to form compounds that reduce the chip/tool metal-to-metal contact area resulting in reduced adhesion and friction forces.

The most important operating variable in the machining process is the cutting speed, which influences the tool temperature and hence tool precision and life. Taylor (18) established a completely empirical relationship between the cutting speed, v , and the tool life, t :

$$vt^n = C \quad (6)$$

where, n = material constant particular to the tool material.

C = material constant related to both tool and workpiece.

However the International Standard (19) for tool testing has proposed that this equation should be:

$$vt^{-\frac{1}{K}} = C \quad (7)$$

where, K = tool material constant

There is virtually no difference between the Taylor and British Standard equations except for the exponent employed and the more accurate calculation of the tool material constant in the British Standard case.

The Taylor equation was further developed to encompass depth of cut, d , and feed, f (7). Thus:

$$vt^n d^x f^y = constant \quad (8)$$

Tool life has an important effect on the economics of metal cutting and is affected by tool wear and failure. The life of a tool can be terminated by either progressive wear of the cutting edge, or by premature failure of the artifact, viz:

a) Progressive Wear

Progressive wear may be classified by:

1) Adhesion wear

Adhesion wear occurs during machining when bonds are formed between the chip and tool as part of the friction process. When these bonds fracture small fragments of the tool material are torn out and carried away by either the chip or the machined surface.

2) Abrasion wear

This type of wear is produced by the mechanical action of hard particles on the underside of the chip which pass over the tool face. These hard particles may be unstable fragments of a built-up edge, fragments produced by adhesion wear, or hard elements in the work material.

3) Diffusion wear

At elevated temperatures and extremely close contact between the tool and workpiece diffusion of the atoms from tool to the workpiece may occur. This process takes place in a very narrow reaction zone at the tool/chip interface.

b) Premature Wear

Premature failure occurs because many tool materials are very brittle, and failure may be caused by mishandling, or by thermal stresses arising from intermittent machining or localised cooling from the cutting fluid. The latter may be sufficiently large enough to cause fracture of the tool.

2.3 Abrasive Machining Processes

Abrasives may be regarded as microminiature cutting tools used for surface finishing processes. Materials cut by abrasives tend to be confined to those that are so hard that other tools do not affect them. The chips thus produced generally require magnification to be seen clearly. In addition abrasives provide better finishes and closer tolerances than the more conventional machining operations such as turning, drilling, etc. They may be used in three principal ways:

- a) cemented together onto wheels
- b) cemented onto backing cloth/paper
- c) used loose, without being held together in any way. (20)

Grinding is the principal abrasive machining process, which utilises abrasive grit particles bonded to a wheel. The grinding action of the abrasive results in the removal of short chips, and eventually through continual use the abrasive grit particles will suffer attritious wear. The major difference between grinding and other metal-removing processes is that grinding employs large negative rake angles due to the shape of the abrasive grit particles. Therefore there is a tendency for the abrasive grit particles to slide over the workpiece rather than cut, resulting in a small depth of cut. The properties of the grinding wheel depend upon the type of abrasive grit employed (21); the most widely used being aluminium

oxide, Al_2O_3 , or silicon carbide, SiC.

The major application of grinding is as a finishing operation since it produces highly finished surfaces. Rubenstein (22) concluded that this metal removal process could be simulated by a turning operation using a single abrasive grain with the grinding action distributed over many cutting points. The depth of cut was very small, and the cutting point had a relatively large negative rake angle compared with tools used in other metal removal processes.

Work conducted into the abrasive wear of metals utilising abrasive papers (23) developed a general relationship applicable to a large range of metals, polymers, and abrasive papers. The wear per unit distance, W , was calculated thus:

$$W = K \mu_p \frac{L}{p} \quad (9)$$

where, K = numerical constant determined by the specimen's material properties.

μ_p = ploughing contribution to friction; dependent upon the shape of the abrasive particle.

L = normal load.

p = dynamic hardness of the metal.

It was further concluded that ahead of the abrasive grit particle a prow formed. The material from the prow flowed around the abrasive particle and formed a built-up edge on either side of the groove, which eventually fractured to produce wear debris.

It has been reported by Misra and Finnie (24) that with particles below approximately $100\mu\text{m}$ the efficiency of the machining process decreases dramatically. The physical basis of this "size effect" remains obscure.

Further processes which use abrasives include honing and lapping. These processes are principally employed to attain smooth surfaces with minimal stock removal, in essence the converse to grinding.

2.4 Non-Traditional Machining Processes

The term non-traditional machining describes either emerging processes or processes that are not used extensively in industry. The development of such processes arose from the need to machine complex shapes in ceramics, superalloys, fibre-reinforced composites, and plastics. None of these materials can easily be machined by traditional machining processes without excessive tool wear and high cost (25,26,27,28). In addition to machining high strength, high temperature materials many non-traditional processes permit the attainment of better surface finishes as an inherent characteristic of the process (29). Non-traditional processes can be classified into two groups, those in which there is non-traditional contact between the tool and workpiece, and those in which non-traditional media are employed to transfer the energy from the tool to the workpiece. A selection of such processes are:

1) Electro Chemical Machining (ECM)

ECM can be considered to be the opposite process to electroplating, i.e. stock removal is achieved by anodic dissolution in an electrolytic cell where the workpiece is the anode and the tool is the cathode.

2) Electro Discharge Machining (EDM)

EDM requires an electrically conductive material since stock removal is achieved by the melting or vaporization of the material by a high frequency spark discharge whilst both the tool and workpiece are submerged in a dielectric fluid.

3) Abrasive Waterjet Machining (AWJ)

AWJ is achieved by impacting the workpiece surface with a high velocity jet of water laden with abrasive grit.

4) Abrasive Flow Machining (AFM)

Stock removal in AFM is achieved by flowing an abrasive-laden medium over/through the workpiece surfaces which require machining. This, as the process under consideration in the present work, is discussed in detail in section 5.0.

5) Thermal Energy Machining (TEM)

TEM achieves stock removal by intense heat. The workpiece is placed in a pressure chamber with a combustible gas and oxygen. The chamber is then pressurized and the gases ignited.

2.5 Surface Integrity

The surface integrity of a machined component is the inherent or enhanced condition of a surface produced in machining or other surface generating processes. It is directly related to the amount of force used to remove material from a component and the time taken to complete the operation (30). Surface integrity is an important factor because the nature of a component's surface

determines how effectively the component performs during its operation. This property involves both surface topography and surface metallurgy (31). The relevant parameters encompass surface finish, chemical change, thermal damage, and residual stresses, the most important factor of which is the surface finish (32).

Surface finish is affected by (i) the microstructure of the component material, (ii) the action and instability of the machining action, and (iii) deformations due to stress patterns in the component.

There are five surface finish characteristics (33) see figure 5, viz:

- 1) Profile - the contour of any section through a surface.
- 2) Roughness - finely spaced surface irregularities produced, for example, by a cutting tool during a machining process.
- 3) Waviness - surface irregularities of greater spacing than roughness; which may be caused by vibrations, warping, etc.
- 4) Flaws - surface irregularities or imperfections occurring at irregular and random intervals; these are usually visual defects, e.g. holes, scratches, and cracks.
- 5) Lay - the direction of the predominant surface pattern.

The standard notation of surface finish is surface roughness, R_a , and is a quantitative assessment of the vertical and horizontal elements of a machined surface. The magnitude of this parameter is attained from the mean deviation of the peaks from the centreline of a corresponding surface profile, thus:

$$R_a = \left(\frac{1}{L} \right) \int_{x=0}^{x=L} (Y) \delta x \quad (10)$$

where, Y = ordinate of the surface profile trace

L = assessment length

The centreline bisects the profile in such a way that the area enclosed above and below the line are equal. Since surface finish is dependent upon several different factors, that can give highly irregular and spurious fluctuations, two filters are available to eliminate unwanted readings on the profiles, viz:

- 1) A roughness filter may be selected to analyse the component performance, e.g. wear characteristics, friction; or
- 2) A waviness filter may be selected to analyse the machine tool performance, e.g. noise or vibration.

Each manufacturing process produces surface finishes in a certain range, some of which may overlap although each possesses a unique surface pattern; for example turning and shaping leave parallel lines, grinding produces directional lines varying in length, and honing produces multidirectional or crisscross lines.

3.0 RHEOLOGY

Rheology is the science of the deformation and flow of matter in response to mechanical forces (34). There are two general categories of deformation which are based upon the fundamental laws of rheology:

- 1) Reversible spontaneous deformation on the removal of an applied stress, termed Hookean behaviour i.e. elasticity.
- 2) Deformation irreversible on the removal of an applied stress, termed Newtonian behaviour i.e. flow.

The most significant type of deformation in rheology is that of flow. The most important material property connected with this phenomena is considered to be the viscosity, i.e. the material's resistance to flow, as detailed in section 3.1; Table 1 illustrates some material viscosities at room temperature (35).

3.1 The Fundamentals of Polymer Rheology

The fundamental parameters in the study of polymer rheology are shear stress, shear rate, and viscosity. These parameters are defined by Newtonian fluid motion, as illustrated in figure 6, which is exhibited by all gases and simple fluids:

A fluid is confined between two flat parallel plates A and B a distance h apart. Plate B is stationary and plate A is moving. In order to move plate A by a velocity v , a shearing force F must be applied. This shearing force is transmitted to plate B which requires an equal and opposite force in order to remain stationary. The viscous drag of the fluid, i.e. the velocity gradient between the plates, v/h , is the means by which the shearing force is transmitted between the plates. Therefore:

$$F = \eta A \frac{V}{h} \quad (11)$$

where, η = viscosity

$$\Rightarrow \eta = \frac{F}{A \frac{V}{h}} \quad (12)$$

Viscosity is defined as the frictional force exerted on unit area in a region of unit velocity gradient. However, linear velocity gradients are not the norm and a generalised velocity gradient is used, i.e. shear rate $\dot{\gamma}$, i.e. the change in the flow velocity over a measured distance perpendicular to the direction of flow:

$$F = \eta A \dot{\gamma} \quad (13)$$

$$\Rightarrow \frac{F}{A} = \eta \dot{\gamma} \quad (14)$$

A generalised form of F/A is used and is termed the shear stress τ :

$$\tau = \eta \dot{\gamma} \quad (15)$$

i.e. Newton's Law

The Newtonian viscosity η depends only upon temperature and pressure and is independent of shear rate. Therefore η is a single constant which completely characterises the rheology of the fluid.

3.1.1 Types of Fluid

Newton's Law stipulates viscosity to be independent of shear rate and any fluid which exhibits this type of behaviour is termed a Newtonian Fluid. However, the viscosities of many fluids are not independent of shear rate and are termed non-Newtonian. Three categories of non-Newtonian flow behaviour are recognised:

a) Time-independent

These fluids exhibit a range of shear viscosities which are dependent upon the shear stress. Since a range of viscosities may be exhibited the term apparent shear viscosity η_a is employed.

b) Time-dependent

These fluids are more complex than time-independent fluids since their viscosities are dependent upon both the shear rate and the duration of shear. Furthermore, the shear history of the fluid has a significant effect on their behaviour.

c) Elasticoviscous

These fluids have characteristics of both solids and fluids and possess a degree of elasticity after deformation.

3.1.1.1 Time-independent Fluids

There are four types of time-independent fluids, see figure 7:

i) Newtonian

The Newtonian fluid is the simplest form of these fluids as already discussed.

ii) Bingham plastic

The Bingham plastic body behaves like a solid which will not flow unless the applied shear stress is greater than the yield stress, τ_y . At higher shear stresses the fluid behaves like a Newtonian fluid with a viscosity η_p :

$$\tau - \tau_y = \eta_p \dot{\gamma} \quad (16)$$

iii) Pseudoplastic (Shear thinning)

Pseudoplastic fluids do not possess a yield stress. However as the shear rate increases so the apparent viscosity decreases. The apparent viscosity tends to become constant at high shear stresses. The power-law relationship, as proposed by Ostwald (36), is used to describe pseudoplastic behaviour:

$$\tau = k \dot{\gamma}^n \quad (17)$$

where, n = shear thinning index

k = temperature dependent constant

For shear-thinning fluids $n < 1$, whereas for Newtonian fluids $n = 1$ and $k = \eta$:

$$\eta_a = \frac{\tau}{\dot{\gamma}} = \frac{k \dot{\gamma}^n}{\dot{\gamma}} = k \dot{\gamma}^{(n-1)} \quad (18)$$

Shear thinning arises because the long asymmetric molecules, initially entangled and randomly orientated, become less entangled and more aligned as the shear increases. Therefore the molecules

interact less and the fluid tends towards Newtonian behaviour.

iv) Shear thickening

Shear thickening fluids possess the opposite characteristics to pseudoplastic materials, i.e. the apparent viscosity increases as the shear rate increases. In general, this behaviour does not occur in polymer fluids; but the power-law is still valid with $n > 1$.

3.1.1.2 Time-dependent Fluids

These fluids can be categorised into two types:

1) Thixotropic

In this process, as the fluid is sheared from rest the apparent viscosity decreases as the shear rate increases. In addition, when the fluid is permitted to rest for sufficient time after shearing, the viscosity returns to its original value.

2) Anti-thixotropic

This term is employed when the apparent viscosity increases as the shear rate increases, and as in the case of thixotropic fluids the viscosity returns to its initial value after a sufficient rest period.

Investigations into time-dependent behaviour have been few and have had limited success (37,38). Possible explanations for time-dependent behaviour have been proposed in terms of a dynamic equilibrium that exists between two types of rheological structures within which there occur irreversible changes and reversible changes. Structure I was classified as non-Newtonian and structure II as Newtonian. The degree of thixotropy was dependent upon the reaction rates

between these two structures. The forward reaction represented structure degradation and the reverse reaction represented structure recovery.

3.1.1.3 Viscoelastic Fluids

The term viscoelastic means the simultaneous existence of viscous and elastic characteristics. Therefore a viscoelastic fluid is capable of indefinite deformation on the application of a stress, but on the release of the stress the fluid may exhibit some recovery. This behaviour is attributed to the fact that long-chain molecules become orientated on the application of a stress, and on the release of this stress the bonds rotate causing the molecule arrangement to become random. Therefore there is a contraction in one direction and an expansion in the other. There are two idealised models for elasticoviscous fluids, (39,40), which use springs and dashpots to represent Hookean and Newtonian behaviour respectively; viz:

a) The Maxwell model

The Maxwell model consists of a single dashpot and a single spring in series where the total shear rate is equal to the sum of the shear rates of the two elements, i.e.:

$$\dot{\gamma} = \dot{\gamma}_s + \dot{\gamma}_D \quad (19)$$

where, $\dot{\gamma}_s$ = Hookean shear rate

$\dot{\gamma}_D$ = Newtonian shear rate

thus

$$\dot{\gamma} = \frac{\dot{\tau}}{G} + \frac{\tau}{\eta} \quad (20)$$

b) The Kelvin (or Voigt) model

The Kelvin model consists of a single spring and a single dashpot in parallel where the total stress is equal to the sum of the stresses in each element, i.e.:

$$\tau = \tau_D + \tau_s \quad (21)$$

where, τ_D = Newtonian stress

τ_s = Hookean stress

thus

$$\tau = \eta \dot{\gamma} + G \gamma \quad (22)$$

where, G = shear modulus

3.1.2 Tensile Flow

The preceding discussion considered shear flow in polymer fluids, however in many commercial processes the flow behaviour is a combination of both shear and tension. Tensile flow arises from the effect of converging streamlines which are the result of:

- a) a change in shape or size of the chamber through which the fluid moves,
- b) the deformation of a hanging melt under its own weight,
- c) the expansion of a melt,

All these processes produce tensile stress in the direction of the tension.

The tensile or elongational viscosity, $\bar{\eta}$, is the material's resistance to tensile flow.

The relationship between tensile stress, σ , and tensile strain rate, $\dot{\epsilon}$, is similar to that of shear flow (41,42):

$$\sigma = \bar{\eta} \dot{\epsilon} \quad (23)$$

where the tensile strain rate is given by the Hencky strain:

$$\dot{\epsilon} = \frac{\delta \left(\ln \frac{l}{l_0} \right)}{\delta t} \quad (24)$$

where, l = initial length
 l_0 = final length at time t

For Newtonian fluids:

$$\bar{\eta} = 3 \eta \quad (25)$$

For all other fluids the tensile viscosity may be significantly greater than the shear viscosity, so that the former becomes an important factor in flow through chambers of decreasing cross-section.

A further factor in tensile flow is the tensile elasticity. When abrupt changes in the flow path of a fluid occur, minimum energy is maintained by the adjustment of the angle of convergence at the restriction. This produces streamline flow. At this point both shear and tensile stresses occur simultaneously. However, in long dies the tensile stress decays by stress relaxation, whereas in zero length dies the stress is entirely tensile.

From a knowledge of the die entry pressure drop and the rheology under simple shear a method has been proposed for the calculation of the rheological parameters due to tension (43). This method assumes that (i) the flow field at the point of convergence is comprised of both tensile and shear components, and (ii) these components are separate quantities that can be added to calculate the total

interaction. Therefore in terms of pressure drops:

$$P_{Total} = P_{Shear} + P_{Tension} \quad (26)$$

Tensile viscosity is calculated thus:

$$\bar{\eta} = \left(\frac{9}{32}\right) \left[\frac{(n+1)^2}{\eta}\right] \left(\frac{P_o}{\dot{\gamma}}\right)^2 \quad (27)$$

where, P_o = pressure drop through zero length die
 η = shear viscosity
 $\dot{\gamma}$ = shear rate
 n = power law index

and tensile stress thus:

$$\sigma = \left(\frac{3}{8}\right) (n+1) P_o \quad (28)$$

3.1.3 Normal Stresses

Normal stresses are a further rheological phenomena associated with non-Newtonian fluids at points of changes in the flow path, for example changes in cross-section.

The normal stress develops at right angles to the applied force, and consists of two components, see figure 8, viz:

- 1) The first (or primary) normal stress difference, $\sigma_{11}-\sigma_{22}$, which forces the shear plates apart, and
- 2) The second and third normal stresses which create bulges in the polymer at the edges of the plates either parallel or perpendicular to the force.

The definitions and relationships applicable to the normal stresses (41) are:

$$\sigma_{11} + \sigma_{22} + \sigma_{33} = 0 \quad (29)$$

$$\sigma_{11} - \sigma_{22} = \textit{first normal stress difference} \quad (30)$$

$$\sigma_{22} - \sigma_{33} = \textit{second normal stress difference} \quad (31)$$

3.1.4 Viscosity Dependent Parameters

The flow and hence the viscosity of a material is dependent upon the mobility of the molecular chains and the forces or entanglements holding the molecules together. Factors affecting the viscosity are:

i) Temperature

Viscosity is highly susceptible to temperature changes and a relationship for Newtonian fluids is given by the Arrhenius equation:

$$\eta = A e^{-B/T} \quad (32)$$

where, A and B = constants

T = the absolute temperature

This relationship illustrates that as the temperature increases the viscosity decreases.

The external temperature rise does not have to be very significant because the act of shearing itself generates heat, which may be sufficient to cause the molecules to increase significantly in mobility, with a corresponding decrease in viscosity.

ii) Pressure

The volume of a material is dependent upon the applied pressure, and increasing this pressure reduces the volume. This results in a reduction in the free volume and a corresponding reduction in the molecular mobility. Therefore an associated increase in viscosity is observed.

Temperature and pressure can therefore be said to be inter-related since both use the free volume hypothesis to interpret the viscosity behaviour. The pressure influence on viscosity is qualitatively similar to that of temperature but opposite in sign. Therefore, this relationship can be defined as (44):

$$\eta \propto \frac{\Delta P}{\Delta T} \quad (33)$$

iii) Plasticisers and Lubricants

Plasticisers are added to polymers to modify the mechanical behaviour either by improving the processability, or by acting as stabilising agents. Plasticisers should be both compatible and miscible with the polymer to which they are added, since they may be used to modify the rheological behaviour of a polymer by lowering the glass transition temperature, T_g , of the blend, decreasing the density of the entanglements, and acting as a low viscosity diluent.

The simplest and crudest estimate of the blend's viscosity at a temperature well above its glass transition temperature T_g is:

$$\log \eta = \phi_{pp} \log \eta_{pp} + \phi_p \log \eta_p \quad (34)$$

where, η_{pp} and η_p = the respective pure polymer and plasticiser viscosities.

ϕ_{pp} and ϕ_p = the respective pure polymer and plasticiser volume fractions.

More detailed relationships are given elsewhere (41).

iv) Molecular Weight Average (\bar{M}_w)

This is the most influential factor involving the molecular structure that determines the rheological behaviour, see figure 9. Below a critical molecular weight M_c the viscosity is approximately proportional to \bar{M}_w , i.e. :

$$\eta = K_1 \bar{M}_w \quad (35)$$

At low shear rates where \bar{M}_w is above M_c , the viscosity is dependent on \bar{M}_w by a power factor of 3.5:

$$\eta = K_2 \bar{M}_w^{3.5} \quad (36)$$

where, K_1 and K_2 = temperature dependent constants

The existence of M_c is attributed to the length of the molecules, i.e. below M_c the molecules are of insufficient length to cause entanglements, and flow is easier.

v) Chain Branching

Branches can be short or long, randomly spaced, or several branches may originate from the same location. Short branches tend not to affect viscosity whereas long branches have a significant affect.

vi) Chain Rigidity

The covalent bonds in a polymer with a linear chain fix the distance between the atoms. Different orientations can only be achieved by rotation around the bonds. Therefore flexible chains such as silicones have lower viscosities than rigid chains such as C-C.

3.2 Measurement of Flow Properties

Viscometers are instruments used to characterise the behaviour of fluids and as such require careful selection to meet the required specifications of an investigation. Furthermore temperature control is an important factor in viscometry since viscosity is highly dependent upon temperature. Therefore to obtain accurate results from viscometers the temperature must be carefully controlled.

There are many types of viscometer, but the most widely used fall into two categories, rotational or capillary (see figure 10). Rotational viscometers tend to be more versatile than capillary viscometers because in this case fewer difficulties are encountered in the examination of non-Newtonian fluids.

However, since capillary rheometry was the method utilised in the present work a detailed consideration is given here to capillary viscometers.

3.2.1 Rotational Viscometers

Rotational viscometers incorporate two basic components which are separated by the fluid under test. These parts consist of either concentric cylinders or a combination of a low angle cone and a plate; in both cases a shearing action is produced by the rotation of one component against the other. Shear-thinning and time-dependent behaviour can be analysed by rotational viscometers since viscosities over a range of steady shear rates at various time durations can be measured. The viscosity is measured by the torque required to produce a specified angular velocity.

3.2.1.1 Coaxial (concentric-cylinder) Viscometer

This type of instrument is the most common viscometer, and consists of two cylinders, one within the other, with the fluid in between. The relationship between viscosity, angular velocity, and torque for a Newtonian fluid is given by the Margules equation (45):

$$\eta = \left(\frac{M}{\Omega 4 \pi h} \right) \left(\frac{1}{R_i^2} - \frac{1}{R_o^2} \right) = \frac{k M}{\Omega} \quad (37)$$

where,

M	= the torque on the inner cylinder
h	= the length of inner cylinder
Ω	= the cylinder angular velocity in radians per second
R_i	= the inner cylinder wall radius
R_o	= the outer cylinder wall radius
k	= an instrument constant

3.2.1.2 Cone-and-plate Viscometer

This type of viscometer consists of a low angle ($\leq 3^\circ$) cone which rotates against a flat plate with the fluid in between. Usually in rotational viscometry the rate of shear varies with the distance from a wall or the axis of rotation. However, this variation is virtually eliminated in this case since both the linear velocity and the gap between the cone and plate increase with increasing distance from the rotation axis. The viscosity relationship for Newtonian fluids is (45):

$$\eta = \frac{3 \alpha M}{2 R_c^3} \quad (38)$$

where, α = the angle between the cone and plate
M = the torque
 R_c = the cone radius

3.2.2 Capillary (Extrusion) Viscometers

Capillary viscometers utilise a fine bore tube through which the fluid under test is drained or forced. The viscosity is determined from the measured flow, tube dimensions, and the applied pressure. The basic equation used is that due to Hagen-Poiseuille for flow of a fluid in a circular pipe (46):

$$\eta = \frac{\pi r^4 \Delta P}{8 Q L} \quad (39)$$

where, r = capillary radius
 ΔP = pressure drop through the capillary
Q = volumetric flow rate of fluid
L = length of capillary

The Hagen-Poiseuille method of viscosity assessment is only suitable for Newtonian fluids because the identical assumptions are made, i.e there is no-slip at the wall, the fluid is time-independent and incompressible, and steady-state, laminar conditions exist.

The shear stress at the wall for Newtonian fluids is calculated from:

$$\tau = \frac{\Delta P r}{2 L} \quad (40)$$

and applies to all time-dependent and time-independent fluids.

The shear rate at the wall for Newtonian fluids is calculated from:

$$\dot{\gamma} = \frac{4 Q}{\pi r^3} \quad (41)$$

Since non-Newtonian fluids are dependent upon the duration of shear the above expression cannot be used. A correction factor was developed by Rabinowitsch and Mooney (47,48) to enable the true shear rate at the wall, $\dot{\gamma}_{tw}$, for non-Newtonian fluids to be calculated. The applicable correction factor is:

$$\frac{(3n + 1)}{4n} \quad (42)$$

where

$$n = \frac{\delta (\log \tau)}{\delta (\log \dot{\gamma})} \quad (43)$$

thus

$$\dot{\gamma}_{tw} = \frac{(3n + 1) \dot{\gamma}}{4n} \quad (44)$$

Therefore a true viscosity η_t can be calculated:

$$\eta_t = \frac{\tau}{\dot{\gamma}_{tw}} \quad (45)$$

(For a Newtonian fluid $n = 1$.)

3.2.2.1 Corrections Applicable to Capillary Viscometers

Corrections must be made to any data collated by capillary viscometers due to the following energy transfers:

- 1) An effective pressure loss arises if the pressure measurements are taken at the top of the capillary rheometer's reservoir. This occurs because during a test the fluid contained within the reservoir decreases and results in a corresponding decrease in the applied pressure. This pressure loss is best avoided by measuring the pressure just above the entrance to the capillary.
- 2) Kinetic energy losses arising from the discharge of fluid from a capillary into air. If the kinetic energy represents a sizeable portion of the total applied pressure the pressure loss may be corrected by:

$$\Delta P = \Delta P_{obs} - \frac{\rho v^2}{2} \quad (46)$$

where, ΔP_{obs} = observed pressure drop

ρ = density

v = velocity

As can be seen this correction is negligible when v is small.

- 3) The ideal pressure behaviour along a capillary, (see figure 11), is one where the pressure is constant in the reservoir, the pressure drop along the capillary is linear, and the pressure is zero at the capillary exit. However, some studies have shown (39) deviations from the ideal behaviour, see figure 12. These deviations result in energy transfers due to viscous and elastic effects encountered on entry and exit from the capillary. These give rise to end effects; viz:
- a) a substantial pressure drop in the capillary entrance,
 - b) the pressure at exit does not fall to zero, and
 - c) downstream from the entrance there is a degree of non-linearity.

Various methods are available to correct for errors due to end effects:

i) The Couette-Hagenbach method

This method employs two dies of different lengths L_1 and L_2 . At a given shear rate the entrance pressure drop across each die is assumed to be identical. The pressure and length values obtained with the shorter die are subtracted from those related to the longer die and a shear stress calculated using:

$$\tau = \frac{(P_1 - P_2) r}{2 (L_1 - L_2)} \quad (47)$$

ii) The Bagley method

This method employs dies of varying length to diameter ratios, L:D. For a given shear rate the pressure drops attained are plotted against the L:D values and the curve extrapolated back to the Y-axis. The Y-axis intercept, which is non-zero, is assumed to be the pressure drop corresponding to a

capillary of zero length, P_o . The shear stress can then be calculated thus:

$$\tau = \frac{(P - P_o)}{2 \left(\frac{L}{2R} \right)} \quad (48)$$

iii) The Orifice Die

This method is a combination of the Couette-Hagenbach and Bagley methods. Two dies are utilised, one of a large L:D ratio, the other with an identical diameter but with a "zero" die length. The pressure from the "zero" length die is subtracted from the pressure of the long die thereby eliminating the pressure drop to end effects. The shear stress is then calculated using:

$$\tau = \frac{(P - P_o) r}{2 L} \quad (49)$$

4.0 ABRASIVES

There are two abrasive group classifications, viz:

- | | |
|--------------|---|
| 1) Natural | - FeO ₄ , Al ₂ O ₃ , Diamond |
| 2) Synthetic | - SiC, Al ₂ O ₃ , CBN, Diamond |

The important properties of an abrasive particle are:

- i) Hardness - resistance to penetration.
- ii) Toughness - resistance to fracture.
- iii) Friability - ability to fracture into smaller parts under pressure.
- iv) Resistance to Attrition - resistance to deterioration by the loss of fine particles.

4.1 Assessment of Abrasive Particles

The definition of a particle is "a solid material of small size with an immensely high ratio of surface area to volume" (50). The usual assessment of a particle is in terms of its size and shape and surface area.

4.1.1 Particle Size

The simplest assessment method of particle size is by microscopy, but this requires a highly accurate sampling technique. The particle size is always expressed as an average diameter although only spherical particles have a true diameter. The size of irregular particles is dependent upon the method of assessment employed, a fact due to the asymmetry of a particle, for example the orientation of a needle like particle during a sieve analysis could be critical to its retention on a sieve. Therefore the assessment method utilised should be taken

into account when comparing data from one method to another. The alternative assessment methods to microscopic sizing were initially developed for materials in powder form and are:

- a) Sieving
- b) Microscopic sizing
- c) Methods based on Stoke's Law
- d) Coulter-Counter and particle size analysis by light obscuration
- e) Laser light scattering

These methods are described elsewhere in more detail, (51,52,53)

Sieving is the most important assessment method for particles larger than $44\mu\text{m}$ and is the method by which grain sizes are based with respect to abrasive machining. Methods (b) to (e) are more suitable for particles smaller than $44\mu\text{m}$ (i.e. sub-sieve).

4.1.2 Particle Shape

The particle shape is not attainable from the particle size and cannot be accurately described. Particle shape is therefore purely a qualitative assessment. However, the International Standards Organisation have issued a standard number 3252 which gives qualitative descriptions, as shown in figures 13(a) to 13(c), viz:

- | | | | |
|----|-----------|---|-------------------------------------|
| 1) | Acicular | - | needle shaped |
| 2) | Angular | - | sharply edged/roughly polyhedral |
| 3) | Dendritic | - | branched shaped |
| 4) | Fibrous | - | regular/irregular thread appearance |

- 5) Flaky - plate like
- 6) Granular - almost identical dimensions but irregular shapes
- 7) Irregular - no symmetry
- 8) Nodular - rounded irregular shape
- 9) Spheroidal - roughly spherical

4.2 Abrasive Wear

Abrasive wear involves the change in particle shape and dimensions as a result of mechanical work, i.e. the friction and abrasion process. In addition there is also strength wear which occurs by particle attrition produced when the abrasive fatigue strength is exceeded. Both processes occur simultaneously but in general the strength wear prevails.

Work (54) examined the re-use of angular and rounded abrasive particles and suggested that angular abrasive particles should not be re-used since the angularity of the abrasive decreased significantly during use. On the other hand rounded abrasive particles could possibly be re-used.

5.0 ABRASIVE FLOW MACHINING

As outlined in section 2.0 metal surfaces can be refined to any desired smoothness or accuracy by various cutting methods; the greater the degree of refinement the greater the cost.

Abrasive Flow Machining (AFM) is a rapid, controllable non-traditional machining process offering precision, repeatability, and flexibility in conventionally "inaccessible" areas (55). Surface improvement, deburring, edge treatment, and stock removal are accomplished by the AFM process, with several or all of these operations being achieved simultaneously in some circumstances (56). The AFM process is suitable for processing external as well as internal areas.

The initial development of the AFM process in the mid-1960s involved the deburring of inaccessible areas within aerospace parts (57). The current applications of the AFM process include the die, aerospace, automotive, and medical component industries (58) where close dimensional tolerances or microscopic inspection requirements are necessary. Illustrations and details of successful applications of the AFM process are given in (59,60,61,62,63).

Abrasive machining is usually achieved by means of stock removal with abrasive wheels, stones, or belts. However, the AFM process achieves stock removal by the extrusion of polyborosiloxane, containing abrasive grit additions, across the surfaces, edges, and cavities of machined parts. The media consistency is such that uniform extrusion through the part is attained. This is necessary to obtain uniform abrasive action regardless of part geometry (64). Additionally the AFM process permits the simultaneous abrasion of two restrictions in the same flow path providing the cross-sectional areas are identical; otherwise the smaller of the

two restrictions will receive the most abrasion (65).

Polyborosiloxane is an inorganic polymer with important properties of inertness and heat resistance, so that it does not undergo degradation readily. A preparation method of polyborosiloxane by Kasgoz has been published (66) which involves initial condensation polymerisation of silicon tetracetate with boron trialkoxide to produce low molecular weight polyborosiloxane. Further processing involving various stages yields high molecular weight polyborosiloxane.

Polyborosiloxane would appear to be a viscoelastic polymer since it exhibits both flow and elasticity, but unlike most polymers polyborosiloxane illustrates these properties at ambient temperature. This apparent viscoelasticity permits polyborosiloxane to behave as a semi-solid viscous fluid. That is, at restrictions in its flow path the viscosity of the polyborosiloxane increases and the flow becomes more "solid" ; however, once the restriction is passed its viscosity returns to its original value and the flow becomes that of a fluid once again (65). This behavioral characteristic coupled with abrasive grit additions facilitates machining at any restrictions in the flow path. Therefore polyborosiloxane has the exceptional characteristic of enabling selective surface improvement and stock removal of components due to the ability to vary its machinability. This makes polyborosiloxane the ideal polymer for use in the AFM process.

Due to the low stock removal rate the AFM process is unsuitable with respect to mass stock removal; hence it is used as a fine finishing operation to attain uniform stock removal economically. The final finishes attained are dependent upon the original surface finish, permissible stock removal, and the nature of the material; whilst the metal hardness has no significant effect on the AFM process.

There are however limitations to the process, viz:

- i) the amount of stock removed from a component must be strictly controlled if the part dimensions must be kept within specified tolerances.
- ii) the process is unable to remove blind holes or cavities without detrimental effects to the component because the process requires conventional, controlled flow of a medium which is not available in these circumstances (67).
- iii) the process is also incapable of correcting out-of-roundness and taper since material is removed equally from all surfaces.

5.1 Fundamental Constituents of the AFM System

There are three fundamental elements to the AFM system, viz:

- 1) Machine - to accomplish and control media flow (68,69), (see figure 14).

The basic components of all AFM machines are a hydraulic power unit, two vertically opposed chambers that contain the honing medium, hydraulic clamping cylinders, a support and head structure, and a control system. One of the chambers is held stationary in the machine base whilst the other, (in the head structure), moves vertically on guide rails. Each medium chamber contains a hydraulic ram to move the medium from one chamber to the other. The diameter and length of the medium chambers determines the machine's volumetric capacity. Every machine has adjustable controls to permit a wide range of applications in order to meet specific finishing requirements. These adjustable parameters are i) the medium flow

pressure, ii) the medium flow rate, iii) a cycle counter, and iv) an optional medium displacement control.

- 2) Medium - To perform stock removal, surface improvement, and deburring operations (70,71,72).

A honing medium is composed of a mixture of abrasive particles, the base polymer polyborosiloxane, and additives. The abrasive grit is held in the polyborosiloxane matrix such that a uniform dispersion is obtained throughout the medium. Polyborosiloxane conforms exactly to the part geometry insuring 100 percent contact on all surfaces that it flows through or over. Polyborosiloxane also has good cohesion and little tendency to adhesion. Therefore it tends to "fuse" to itself and remains as a coherent entity during machining. The size, type, and percentage of the abrasive grit coupled with the viscosity of the polymer employed determines the amount of surface improvement and stock removal attained. The AFM process utilises an abrasive chosen from silicon carbide, boron carbide, aluminium oxide, and diamond abrasive grits. Silicon carbide is the most widely used abrasive in the AFM process since it lasts longer and is cheaper than the alternatives. Aluminium oxide is also used in a variety of applications, since it performs well, but is used less frequently than silicon carbide on account of cost. Due to the high cost of both diamond and boron carbide they are only used to machine very hard materials such as tungsten carbide. Larger abrasive particle sizes tend to be employed to achieve aggressive stock removal and to attain the required radii on the components, whereas smaller abrasive sizes are used when surface improvements are required. To reduce the friction of the medium as it is extruded lubricants are added

to the base polymer. The type of lubricant used determines the effectiveness and the machining productivity of the medium (73). Furthermore to alter the polyborosiloxane viscosity plasticisers or reducers may be added, the viscosity being determined by the ratio of polymer to diluent. The media also "absorb" the stock removed, but up to ten percent by volume of stock removed is the maximum acceptable limit before the machining efficiency diminishes (74). During machining the abrasive grit wears by attrition or becomes dull. The efficiency of the media is therefore also dependent upon the initial batch quantity, quality, and the aggressiveness of the work performed. It has also been reported (75) that the medium loses part of its effectiveness over time since the added lubricants are consumed during its use. The loss of lubricant affects the medium's consistency and its ability to maintain a uniform dispersion of abrasive grit.

- 3) Tooling - To confine both the component and medium, as well as to direct the medium (76,77), see figure 15.

The tooling plays a critical role since a basic principle of the AFM process is that the greatest abrasion occurs where the medium velocity is high, i.e. at the greatest restriction in the flow path. The tooling fulfils many functions in the AFM process since it not only influences the positions where abrasion occurs but also enables selective abrasion to be achieved, protects critical edges and surfaces, meters medium flow, and assists in loading/unloading. The tooling geometry is dependent upon the component to be machined and its requirements. The majority of toolings are manufactured from steel due to its low cost, but where the quality of the

contact surface must be strictly maintained nylon is employed to avoid damage from the abrasive grit during clamping. Some examples of tooling employed in production are given (78).

5.2 The AFM Procedure (79,80)

The medium is loaded into the lower medium chamber followed by the clamping of the component and tooling in position between the two medium chambers. The media is then forced from one chamber into the other under hydraulic pressure. The medium viscosity temporarily rises during extrusion through any regions of restricted flow, such as burrs or restrictions induced by the tooling, causing the abrasive grit to become held rigidly by the polymer. The medium then acts as a multipoint-cutting tool transmitting the force applied by the machine to the component edges and/or surfaces which results in stock removal and surface improvement. "The amount of force transmitted to the abrasive grit in contact with the component depends upon the medium consistency and the pressure differential from one side of the grit particle to the other" (67). The higher the medium viscosity the greater the percentage of force transferred to the abrasive grit. However, not all the applied pressure is consumed in machining; a fraction of it is expended in internal shearing of the medium as well as in deformation of the medium to the form of the restricted flow path. After passing through the restricted passage the medium viscosity returns to its original value. One extrusion cycle is completed when the medium is extruded from the lower medium chamber to the upper medium chamber and back again. Analogously, the process can be thought of as a flowable file, with capabilities ranging from a light buff to coarse stock removal (81).

Once the component has been machined any medium remaining must be removed. This is achieved by either air or vacuum which removes the vast majority but in the case of very complex components the medium is sacrificed by removal in a solvent wash or bath. The removal of medium need not be immediate since it does not dry-out.

The AFM process parameters are therefore dependent upon:

- a) the medium extrusion pressure.
- b) the abrasive grit type, size, and percentage.
- c) the medium viscosity.
- d) the geometry of the tooling and component.
- e) the number of extrusion cycles.
- f) the component material.

5.3 Surface Integrity Related to the AFM Process

The surface finish due to the use of the AFM process, achieved by the honing action of the abrasive grit on the high spots on the component surface, is parallel to the medium flow (termed uni-directional in the text below), "smear-free", and consists of very fine lines (82,83,84). This type of surface in certain situations is an intrinsic benefit to components such as extrusion dies, since the surface thus produced will produce a low co-efficient of friction and will therefore reduce surface friction.

Surface roughness values after utilising the AFM process have been documented (59,85) and it was found that much finer finishes are obtained with this process than those normally associated with conventional methods. Rhoades states this is

in part due to the cushioning effect of the matrix holding the abrasive in suspension against the component being machined.

The better the starting finish the smaller the abrasive grit size employed since larger abrasive grits abrade at faster rates, while smaller grits provide finer finishes and accessibility to small orifices.

5.4 Review of Previous Research Related to the AFM Process

Although the AFM process has been in use for more than 25 years, the process is a complex one and its machining mechanism still remains unclear. This is in part due to the many interdependent variables and the limited qualitative study which has concentrated on the machining aspect of the process. Furthermore minimal study into the rheology of the process has been performed, and there has been no attempt to correlate the rheological behaviour with the machining characteristics. The only correlation has been in terms which define the different medium in use, i.e. low, medium, and high viscosity or mixtures of these. Furthermore most information available on the AFM process relates mainly to the process description and its applications.

5.4.1 Research Related to the Machining Aspects of the AFM Process

Rhoades (86) performed simple laboratory tests on machined round holes to illustrate the effect of changing some of the AFM process parameters for specific medium formulations. It was concluded that some simple rules could be presented as guidelines, viz:

- 1) increasing the extrusion pressure increases the stock removal per unit time.

- 2) increasing the extrusion pressure increases the media flow rate.
- 3) as the media temperature increases so the flow rate increases.
- 4) increasing the hole length reduces the flow rate.

The extent to which these rules applied was dependent upon the medium used.

Rhoades further concluded that the medium life and therefore stock removal was limited by:

- a) Contamination by machined particles which cause the medium's viscosity to increase due to the additions into the matrix acting as a filler. These machined particles will also reduce the abrasive grit concentration available for machining.
- b) Abrasive grit wear, i.e. grit particle attrition and fracture.

Borchers (87) performed research on cylindrical shaped parts that contained intersecting surfaces. This work assessed the effect of different silicon carbide grits and extrusion pressures on the radius of the component's edges, i.e. the edge radiusing, as well as the effect of tooling design on stock removal. It was found that edge radiusing increased as the extrusion pressure and grit size increased; whereas finer grit produced improved surface finishes with lower R_a values. Poor tooling design resulted in uneven stock removal, out-of-roundness and bell-mouthing at the base of the bore.

Tests conducted by Przyklenk (88) in conjunction with the German Research Community demonstrated:

- 1) An increase in the bore length increased the processing time, and an increase in the extrusion pressure decreased the processing time.
- 2) Stock removal was proportional to the volumetric flow rate and the number of cycles performed.
- 3) The most significant surface improvement was achieved within the first ten cycles, after which there was no significant improvement.
- 4) Edge radiusing decreased if the length and diameter of the die increased, and the bore roundness remained virtually unchanged provided the die was axially mounted.
- 5) The media viscosity was an important variable which was itself dependent upon the percentage of abrasive held in suspension. An increase in the proportion of abrasive increased the medium viscosity, resulting in an increase in processing time. Furthermore as the media viscosity increased the amount of stock removed increased.
- 6) Increasing the abrasive grit size increased the stock removal rate.
- 7) The type of abrasive grit employed was found to affect the stock removal. In order of increasing stock removal rate the effect of the different grits were:

SiC, Al₂O₃, Zircon Corundum, B₄C

In addition an increase in extrusion pressure or the number of cycles performed produced ripples on the component surface. The process variables of greatest significance were percentage of abrasive grit, grit size, and the viscosity of the base medium. The influence of the component material, temperature, and type of abrasive grit were considered to be minimal.

Kohut (89) published results in relation to the effect of medium re-use on stock removal. Both fresh and used medium-viscosity polymer with 70 Mesh grit were employed. It was found that the new medium removed approximately twice the amount of stock as the used medium after identical volume flows had passed through the machine. Also the processing time required for the new medium to process the same size component as the used medium was significantly less in the former case.

The most recent research into the machining aspect of the AFM process, upon which the present work was based, was conducted by Williams, Rajurkar and Rhoades (90,91,92). The parameters investigated were:

- 1) the effect of medium viscosity and extrusion pressure on the stock removal and surface finish.
- 2) the relationship between the flow rate and the stock removal with flow volume held constant.
- 3) the effect of extrusion pressure, medium volume, and the number of extrusion cycles on the rate of stock removal and the quality of surface finish.

All these experiments were conducted using relatively low viscosity media with additions of 66% by mass silicon carbide 70 grit. The samples used were mild steel which contained orifices with a length to diameter ratio of 3.2 and an average initial surface roughness of $2.5\mu\text{m}$. Each sample used was run for ten cycles. The reported results from this study if all other factors remained constant were:

- 1) an increase in the extrusion pressure increased the stock removal and produced smoother surfaces.
- 2) higher viscosity media removed stock uniformly while lower viscosity media caused greater edge radiusing.
- 3) an increase in the media viscosity increased the amount of stock removed and increased the amount of surface improvement.
- 4) changes in the flow rate , with the media flow volume held constant, did not significantly change stock removal.
- 5) scanning electron microscopy indicated that conventional machining marks were removed within a small number of extrusion cycles. The major effects were seen after a few extrusion cycles. Thereafter the flow lines became smoother and were spaced further apart.
- 6) the widely used relationship $R_{\max} = 4R_a$ for turning operations became $R_{\max} = kR_a$, where k was the proportionality constant which varied between 1.4 and 2.2 in the case of the AFM process.

5.4.2 Research Related to the Rheological Aspects of the AFM Process

The earliest reference to the rheology of the AFM process was presented by Perry (93). Four base media of varying viscosities were examined and the temperature of each base was adjusted to 30°C prior to use. It was found that all the bases examined exhibited shear-thinning (pseudoplastic) behaviour. Also it was suggested that high pressures should be avoided because their use led to high heat generation, and since the media are insulators, the heat generated could not be conducted away by conventional methods at a rate sufficiently fast to maintain a constant temperature.

Rhoades has also published rheological findings in association with the National Science Foundation, Washington (94). The objective of this research was to achieve further knowledge of the flow mechanics of polyborosiloxane. The initial investigation of two different polyborosiloxane media reported that under normal operating conditions the existence of stick-slip behaviour was observed which appeared to have a considerable influence on the stock removal.

Research by Trengove (95,96) employing low, medium and high viscosity media at temperatures $\geq 30^{\circ}\text{C}$ and a Davenport capillary rheometer, has suggested that:

- 1) these media exhibit shear-thinning thixotropic behaviour and that the temperature change has a significant effect on this behaviour.
- 2) the viscosity dependence on temperature is significant.
- 3) the low viscosity medium exhibits evidence of stick slip, and that this phenomena is more pronounced at low strain rates than high strain rates where it is almost negligible.

As a consequence of point 2 it is believed that at some values of viscosity the abrasive grit held in the matrix separates under the influence of the gravitational force. This is because the density difference between the base medium and abrasive is insufficient to maintain the buoyancy force required to maintain the abrasive in suspension in the polymer.

6.0 EXPERIMENTAL

To determine the various parameters that affect the AFM process and to permit correlation and comparison of results, the procedures employed were based on work carried out by previous investigations (97).

6.1 Preliminary Work

The preliminary work performed enabled practical experience to be gained in both the machining and measurement methods. The results obtained from the preliminary work are not of sufficient accuracy to be used on a quantitative basis but they do provide background knowledge of the AFM process.

The work undertaken initially consisted of the examination of a variety of test pieces that had undergone the AFM process. These were provided by the collaborating establishment and consisted of a castle nut and bearing components. Each piece was examined using a Phillips 500 Scanning Electron Microscope at various magnifications to provide photomicrographs of surfaces that had been subject to AFM.

Further preliminary work was conducted to determine the effect of abrasive grit wear during the AFM process; this consisted of:

- i) the examination of the effect of the reuse of the same medium on the stock removal and surface roughness.
- ii) the examination of the effect of the machining process on the abrasive grit particles.

The determination of the abrasive grit wear as outlined above involved three experimental procedures. The investigation of medium reuse involved one procedure method and the abrasive grit particles examination involved two individual techniques. The medium used throughout the preliminary work was 935/60, i.e. low-medium viscosity, polyborosiloxane containing 60 Mesh, (406 μ m), Silicon Carbide (SiC) abrasive grit.

6.1.1 The Effect of Medium Reuse on the Stock Removal and Surface Roughness

This method consisted of three experimental sets, each of which used an Extrude Hone Mark 7A machine, with an extrusion pressure of 2210kPa, and individual dies of 15mm diameter and 15mm length. The first and second sets consisted of eleven runs, whilst the third consisted of three; each run was conducted on a fresh die but with the same medium reused. The set of experiments involved the following number of extrusion cycles in ascending sequential order:

Experiment One	1, 2, 3, 5, 10, 15, 20, 25, 40, 50, 70
Experiment Two	1, 2, 3, 5, 10, 15, 20, 25, 40, 50, 70
Experiment Three	5, 10, 20

This resulted in a set of medium samples whose abrasive grit particles had been subject to extrusion cycles of:

Experiment One	1, 3, 6, 11, 21, 36, 56, 81, 121, 171, 241
Experiment Two	242, 244, 247, 252, 262, 277, 297, 322, 362, 412, 482
Experiment Three	487, 497, 517

The stock removal parameters measured were die mass and die diameter change, together with the surface roughness improvement.

6.1.2 Abrasive Particle Assessment

As already stated the determination of the characteristics of abrasive grit particles which had been subject to the AFM process consisted of two techniques, viz:

a) Technique One

This comprised one experiment that utilised an Extrude Hone Vector machine, with an extrusion pressure of 2069kPa, and individual dies of 6mm diameter and 6mm length. The experiment consisted of nine runs involving the following number of extrusion cycles which were performed in ascending sequential order on fresh dies; viz:

1, 2, 4, 6, 8, 10, 15, 20, 25 Extrusion Cycles

This produced a medium whose abrasive grit particles had been subject to:

1, 3, 7, 13, 21, 31, 46, 66, 91 Extrusion Cycles

To determine the resultant abrasive grit wear a sample of the medium was taken before machining commenced, with a similar sample taken after the associated machining had been performed but before the next set of extrusion cycles in the sequential order were performed. The silicon carbide particles were separated from the polyborosiloxane in the medium sample by the addition of trichloroethane to the mixture, which was stirred and left to stand, after which the solution was decanted and further trichloroethane additions made. It should be noted that of the

slurry decanted the vast majority was assumed to be polyborosiloxane. (However, it is inevitable that the slurry would contain fine particles of both abrasive grit and any stock removed.) This process was repeated until the decanted trichloroethane was relatively clear, thereby indicating no more medium remained. The abrasive grit was given a final rinse in trichloroethane and filtered using 52 paper and dried in an oven at 90°C. The abrasive grit particles which remained were examined by scanning electron microscopy. To permit a meaningful SEM examination a representative particle size distribution was desirable; this was achieved by a quartering and coning technique conducted on the filtered sample. The representative sample thus attained was coated with carbon and examined on the Phillips 500 Scanning Electron Microscope.

b) Technique Two

This involved the comparison of both un-processed and exhausted 100 Mesh, (173 μ m), SiC grit, the samples being provided by the collaborating establishment. Since a sieve analysis was performed on the abrasive grit samples and the machining history of the exhausted abrasive grit was not known technique two provided a semi-quantitative determination of the wear rate effect of the abrasive grit. The sieve analysis was conducted with six sieves, the mesh sizes being 125, 106, 75, 63, 53, and 45 μ m assembled from the finest to the coarsest in ascending order. Each sample was placed on the top sieve and mechanically shaken for 30 minutes. The mass of the sample retained on each sieve was recorded and a percentage of the original mass calculated. Furthermore a specimen from each sieve fraction was removed for carbon coating and examination on the Phillips 500 Scanning Electron Microscope. Prior to the study of the exhausted abrasive grit sample the abrasive grit had to be separated; this was achieved by the procedure adopted in Method One.

6.2 Principal Work

Some of the procedures used in the preliminary work were considered in the light of experience gained to be defective. The procedures utilised to determine the rheological and honing characteristics of the medium in the main programme were achieved by either modifications made to the techniques used in the preliminary work, or by the introduction of improved instrumentation.

6.2.1 Materials

Many components machined using the AFM process are manufactured from mild steel. Therefore the specimens used throughout the research programme were individual 15mm diameter x 15mm length mild steel dies, with a length to diameter ratio of 1 and an approximate $12\mu\text{m}$ turned surface finish. Etched on the opposing faces of each die were a unique identification number and locational marks. The locational marks which were etched at 90° intervals around the die's circumference ensured that repeated measurements could be taken at identical locations. An additional locational mark to designate a 0° position was etched; this allowed consistency in the position of the die during re-measurement and permitted correlation of readings taken at identical sites.

Three polymer types were used in the research, low viscosity (LV), medium viscosity (MV), and high viscosity (HV) polyborosiloxane. These are proprietary mixtures of undisclosed composition that contain small quantities of other substances besides polyborosiloxane. The sizes of the abrasive SiC grit were either 60 or 100 Mesh ($406\mu\text{m}$ and $173\mu\text{m}$). The abrasive grit to polymer ratios examined were 0.5, 1 and 2. The above combinations led to a matrix containing 18 parameters, i.e. 18 different polyborosiloxane/grit mixtures were used. 5Kg of fresh, unprocessed polyborosiloxane/grit mixture was used for each experiment. In

addition to this matrix a further three parameters were investigated, i.e. pure LV, MV, and HV polyborosiloxane with no abrasive SiC grit additions.

6.2.2 Investigation of Process Parameters and Machining Characteristics

The measurements taken before and after machining to determine the changes in the die dimensions were stock removal and surface integrity. In addition pressure and temperature measurements were taken during the machining operation.

6.2.2.1 Stock Removal

Stock removal was measured by the changes in die diameter and die mass:

i) Die diameter change

A Ferranti 750M Co-ordinate Measuring Machine was employed to measure the die diameters. This is a computer aided technique incorporating three independent, perpendicular motor driven supports which allow a stylus to locate surface positions to an accuracy of $0.5\mu\text{m}$, see figure 16. Readings were taken at 45° intervals around the bore circumference on five planes along the bore length, the five planes being separated by 2.5mm intervals. This resulted in twenty diameter measurements per die. The die was placed on the workbench in a position such that the identification number was facedown with the 0° location mark towards the operator.

ii) Die mass change

A Stanton Unimatic CL41 mass balance was used to measure the die mass, and permitted readings to an accuracy of 0.0001g.

6.2.2.2 Surface Integrity

A Rank Taylor Hobson Form Talysurf 120L was used to obtain axial micrographs and surface roughness parameters (see figure 17). The Form Talysurf 120L combines a motor driven laser interferometric pick-up with computer software to provide measurements of surface roughness to an accuracy of $0.1\mu\text{m}$.

The die was placed such that the locational marks were facing towards the Form Talysurf stylus. Surface roughness readings were taken clockwise at each 90° locational mark starting at the 0° location site. This permitted four surface roughness readings per die. The readings taken incorporated an ISO-2CR roughness filter of cut-off length 0.8mm over a measurement length of 13.6mm . The bore length over which the resultant surface integrity was measured could therefore be associated with that used in the die diameter measurement.

Qualitative microscopy work was performed in conjunction with the quantitative work. This consisted of optical microscopy of specific machined dies using an Olympus photomicroscope. The machined dies were cut in half after all the quantitative assessments had been completed and subsequent photomicroscopy of the bore cavities at a magnification of $\times 8$ performed. This work permitted a visual inspection of the die surfaces and allowed an examination into the effects of utilising the various medium, with all other parameters held constant, on the condition of the surfaces. In addition the effect of increasing the number of extrusion cycles on the surface finish could be determined.

For all surface integrity and die diameter measurements the samples were cleaned and left in a controlled environment at 20°C for several hours prior to inspection. This allowed thermal stabilisation and prevented errors due to dimensional changes

associated with small changes in temperature.

6.2.2.3 Pressure and Temperature

Pressure and temperature measurements were taken using two Dynisco TPT463E integral pressure-thermocouple transducers coupled with Dynisco μ PR690 microprocessor units. The pressure transducers had a measuring range of 0 - 34,475kPa and an error of $\pm 1\%$ full scale output. The thermocouples were type J (iron/constantan) and were capable of recording temperatures upto a maximum of 400°C. The transducers were also equipped with a calibration function which allowed the μ PR690 microprocessor units to be calibrated to the transducers without the need for a known pressure calibration source.

The integral transducers were mounted in tooling plates used to secure the dies. These were mounted in such a way that the centre of the transducer in each tooling plate was approximately 9mm from the central cavity and 4mm below the die recess. The transducers were recessed from the central cavity to avoid damage to the tips by the abrasive grit content of the media.

Each transducer was coupled with a Dynisco μ PR690 microprocessor unit which provided power to and received signals from the transducers. Each was in turn connected to a computer, see figure 18. The computer stored the pressure transducers' signals by the use of a specific programme written for the research, (which also enabled the corresponding machining times to be recorded). The thermocouples were connected to a Solartron Data Logger which allowed a hard copy of the temperature measurements to be made, see figure 19.

In the case of the LV and MV media, the time intervals between the pressure and temperature measurements were 0.1s and 2.0s respectively. However, since the processing times for the HV medium were significantly longer than those obtained with the other two media, the time intervals between the pressure and temperature measurements for the HV medium were altered to 0.3s and 10s.

Prior to the commencement of this experimental work it was found that the data obtained from the pressure transducer data in its raw state was unsuitable due to electrical noise. Therefore capacitors were used to eliminate the majority of the electrical noise experienced during machining. The resultant data was further modified to a usable format by the elimination of any remaining electrical noise; this was achieved using DADiSP, (Data Analyzing Digital SPreadsheet), software.

6.2.3 Machining Procedure

The machining operation required the use of specialised equipment only available at the collaborating establishment.

6.2.3.1 Machining Equipment

All procedures utilised an Extrude Hone mark 7A machine in conjunction with two mild steel tooling plates, see figure 20. The mark 7A machine has an extrusion pressure range of 690 to 11,032kPa, a clamping pressure range of 690 to 13790kPa, a 15.24cm diameter extrusion chamber, and it comes equipped with a cycle counter.

The extrusion and clamping pressure settings on the mark 7A AFM machine are monitored by dial gauges, where one division on both scales is 138kPa. The pressure settings would therefore be subject to an error of $\pm 138\text{kPa}$.

Both the tooling plates employed throughout all procedures were of a 25.4cm diameter and a 2.2cm thickness. Each contained a 1.5cm central bore and a central 4.5cm diameter recess of 0.75cm depth. This central recess accommodated the die, providing a stable and secure mounting during clamping, and permitted the alignment of each die machined. On the reverse side of the lower tooling plate, a central 15.2cm diameter protrusion, of 0.2cm thickness, was introduced to permit the alignment of the tooling plates, see figure 21(a) and 21(b). As previously stated, the centre of each integral transducer was mounted approximately 0.4cm below the die recess and recessed approximately 0.9cm from the bore cavity to avoid any damage to the transducer tip.

6.2.3.2 Machining Procedure

For each parameter of polymer type, polymer to abrasive grit ratio, and abrasive size within the aforementioned 18 matrix table an experiment was conducted. Each experiment performed contained a set of eight separate runs which involved the following number of extrusion cycles in the following ascending sequential order:

1, 2, 3, 5, 10, 15, 20, 30

In all cases each run was performed on a fresh die.

To determine the pressure drop produced during the use of each of the three pure polymers with no abrasive grit additions a single run of 30 extrusion cycles was also performed.

The clamping and extrusion pressures employed in all cases conducted were 13,790 and 5,516kPa respectively. Furthermore the transducers' recesses were always plugged with the relevant polyborosiloxane/grit mixture employed. This permitted consistency in both the pressure and temperature transmission from the bore cavity through the plug to the transducer tip.

Prior to the commencement of the experiment the volume of medium available was measured. The lower extrusion chamber was then loaded with the appropriate medium, the lower tooling plate placed in position, an un-processed die placed in the die recess, (with the identification number facing the lower tooling plate and the 0° location mark towards the operator), the upper tooling plate placed on the die, and the machine clamped, see figure 22.

Both transducers were placed on the same side of the 7A machine. Ideally, both transducers should have lain in one vertical plane, but the dimensions of the bodies of the transducers outside the tooling plates prevented this. The bodies of the transducers outside the tooling plates were therefore offset in the horizontal plane by approximately 5°. The cycle counter was positioned to the applicable number of extrusion cycles, and with both the data logger and computer activated, machining commenced.

Once machining had been completed the 7A machine was unclamped, the tooling plates and die removed, and the medium extracted from the extrusion chambers. The die was cleaned in solvent and any remaining medium removed in a stream of air. With the aid of a digital thermometer the medium temperature was monitored, and when the temperature of the cooling medium equated with the temperature of the medium prior to machining, the medium was re-loaded into the 7A machine.

The tooling plates and a fresh die were placed in position, the cycle counter positioned to the next number of extrusion cycles in the sequence, and after approximately ten minutes, machining commenced.

6.2.4 Data Assessment

The stock removal, surface integrity and temperature data gathered required no further manipulation to attain the desired parameters. However, since the raw pressure data contained spurious signals the data required further processing.

6.2.4.1 Pressure Data Assessment

The raw pressure data recorded from each transducer during a run produced a "periodic" trace, see figure 23, which in several cases contained electrical noise at various points in the trace. Since the pressure drop through the die would be required to calculate an apparent shear stress, and hence an apparent viscosity. The pressure data would require further modifications to eliminate any electrical noise present. As previously stated DADiSP software was employed which enabled the trace to be modified to eliminate any such electrical noise. This was achieved by setting maximum and minimum limits within the relevant affected cycles, after which the half cycle pressure drop could be determined. From the half cycle pressure drops an average pressure drop for the run was calculated, which was used in the calculation of the various rheological parameters.

The DADiSP software permitted the time taken to perform a half cycle to be recorded simultaneously, which allowed an overall machining time to be calculated.

6.2.4.2 Calculation of the Volume of Medium Extruded

The mixtures of polyborosiloxane and SiC grit were used in quantities of 5kg per run, i.e. half the media chamber capacity of the mark 7A machine. This resulted in mixtures of varying volumes due to the difference in densities between polyborosiloxane and SiC. Due to the mechanics of the mark 7A machine, the variation in the amount of medium available for extrusion was further complicated because on extrusion a certain quantity of medium is retained in both the upper and lower extrusion chambers. Therefore to calculate the volume of medium retained, and hence the actual volume of medium extruded, it was necessary to know the dimensions of both the upper and lower extrusion chambers at the extremity of the forward stroke. At the start of each set of experiments these dimensions were recorded to avoid errors due to possible chamber replacement during the period between each set of experiments.

6.2.4.3 Determination of Rheological Parameters

The basic equations used to calculate viscosities using capillary viscometers are based upon the Hagen-Poiseuille expression as presented in section 3.0, the derivation of which is given elsewhere (45), viz:

$$\eta = \frac{\pi r^4 \Delta P}{8 Q L} \quad (50)$$

where, ΔP = axial pressure drop through capillary

r = capillary radius

Q = volumetric flow rate

L = length of capillary

η = viscosity

Newtonian fluid motion as presented in section 3.0 states:

$$\Rightarrow \eta = \frac{\tau}{\dot{\gamma}} \quad (51)$$

where, τ = shear stress

$\dot{\gamma}$ = shear rate

A force balance based on classical Newtonian fluid flow states the shear stress to be:

$$\tau = \frac{r \Delta P}{2 L} \quad (52)$$

Combining equations 51 and 52

$$\eta = \frac{\Delta P r}{2 L \dot{\gamma}} \quad (53)$$

Combining equations 50 and 53

$$\Rightarrow \dot{\gamma} = \frac{4 Q}{\pi r^3} \quad (54)$$

The present work therefore calculated an apparent viscosity from the pressure drop and the volumetric flow rate measurements. The volumetric flow rates were calculated from the volume of media extruded and the machining times.

The pressure differences calculated are averages based upon each half cycle performed. Therefore any rheological calculations dependent upon the length of capillary are unaffected by the fact that one extrusion cycle is comprised of two passes; one in an upward and one in a downward direction.

6.2.5 Processing Parameter Variations and their Effect on the Measurements Made

Since all measurements are subject to some degree of error precautions were taken to minimise any errors applicable to the experimental data; any limits to which the experimental data are subject have been quoted. However to conduct the present work an established commercial process and its production equipment were utilised. As a consequence, the results thus obtained may sustain further discrepancies due to both processing parameter variations and assumptions made with respect to both the machining and rheological aspects of the process.

6.2.5.1 Machining Parameter Variations

The elements of the machining method and subsequent assessment methods employed which could have caused discrepancies in the accuracy of the measurements made are:

1) The DADiSP software

As explained the DADiSP software was used to obtain the pressure drop measurements. This software enables an entire transducer trace to be imported into the computer programme, which can then be separated into individual half cycles, and a corresponding average half cycle pressure measurement obtained. However, before the half cycle pressures could be attained two further procedures were required, viz:

i) the separation of each half cycle from the complete transducer trace was necessary to enable the calculation of the pressure drop to be made. This required the measurement of the relevant half cycle duration. This evaluation was possible since the change in extrusion direction from one media chamber to the other was indicated by a pronounced change in the

pressure trace, as shown in figure 23. Therefore both the half cycle start and finish times could be evaluated and the cycle duration recorded.

ii) the second evaluation was only necessary if spurious signals were present in the half cycle transducer trace. Spurious signals were accompanied by large deviations in the transducer's trace in the form of significant "spikes", see figure 24. The elimination of these spurious signals required the filtering of the half cycle transducer trace. This was achieved by placing upper and lower pressure limits on the half cycle pressure trace. These limits were made on the basis of the experience gained as the work progressed. The deviations caused by the spurious signals were very significant and lasted for 0.1s for the LV and MV media and 0.3s for the HV media, i.e. the time interval between readings. The consistency of these time intervals enabled the ready identification of the spurious signals to be achieved.

2) Surface improvement measurements

The requested surface roughness finishes of the dies was $12\mu\text{m}$. However, the actual range of surface roughness finishes produced was between $4\mu\text{m}$ and $20\mu\text{m}$. It would have been preferable to keep this parameter a constant through out the present work since initial surface roughness is considered to be a parameter affecting the AFM process. To overcome these variations the surface roughness improvement was expressed as a percentage of the initial surface roughness. This is considered to be a valid surface roughness improvement parameter that is independent of the initial surface roughness.

3) Temperature measurements

When the HV medium with no abrasive grit additions had undergone 30 extrusion cycles and the machine was unclamped, the temperature in the middle of the bulk medium was taken using a handheld digital thermometer whilst the medium was still in-situ. It was found that the temperature of the bulk medium was greater than the temperature of the "plug" recorded by the thermocouple connected to the pressure transducers. The temperature difference was approximately 40°C between the bulk medium temperature and the "plug" temperature. This error could not easily be corrected for from the thermocouple reading since the thermal conditions were transient. Therefore it must be assumed there is an intrinsic error in all the temperature results recorded. However it is further assumed that this discrepancy is identical in magnitude in all cases, and that the results thus obtained may be compared.

4) Media volume

As stated, a consequence of the use of a commercial process was the medium was used in quantities of 5kg. This resulted in media of varying volumes due to both the different densities and compositions of SiC abrasive and polyborosiloxane, see table 2. This variation in volume affected the amount of medium available for extrusion and hence the duration of the machining process.

6.2.5.2 Rheological Parameter Variations and Assumptions

In order to obtain the required rheological parameters, certain assumptions were required due to i) the complex characteristics of the polyborosiloxane/grit mixtures and, ii) the unavailability of a rheological viscometer due to the abrasive grit

additions to the polyborosiloxane. However, it was assumed that the mark 7A AFM machine would simulate an extrusion viscometer and the pressure drops thus obtained could be used to evaluate the viscosities of the media.

These assumptions would of course result in errors in the rheological data. In addition, further variations would be encountered in the rheological data since the rheological parameters would be dependent upon factors associated with the media employed. These assumptions and variations are:

1) As previously stated the transducers were located within the tooling plates and positioned as close as possible to the die "entrance" and "exit". The transducers were also located away from the tooling "entrance" and "exit". Therefore it was assumed that both the "entrance" and "exit" pressure readings were recorded within the laminar flow stream. Furthermore since the actual pressure drop across the die was recorded from the "entrance" and "exit" pressures it was a further assumption that no entrance and exit pressure loss corrections were necessary, and that the flow conditions within the transducers' were independent of the distance along the die axis.

2) All the media exhibited shear thinning time-dependent behaviour, i.e. thixotropic behaviour, where the viscosity is dependent upon both the shear rate and shear stress. However, it has been stated (40) that it is unsatisfactory to characterise time-dependent fluids quantitatively using capillary-tube viscometers due to the dependency of duration of shear, and that rotational instruments, with uniform rates of shear, offer advantages. Nevertheless, it was assumed that since the mark 7A machine was

employed to achieve the machining parameters it could also be used to simulate a capillary rheometer to attain the desired rheological parameters.

3) A further assumption that thixotropy is superficially similar to shear thinning fluids was made on the basis of Wilkinson (40) who states, "At the limiting conditions encountered at start-up and steady-state a thixotropic fluid is not materially different from the simple time-independent fluid". This implied the rheological parameters could be assessed assuming time-independent conditions but the incurred results would contain errors since steady-state would not be achieved.

4) When rheological data was obtained assuming power-law relationships, incorporating the Rabinowitsch and Mooney expression (47,48), the calculated viscosities of the LV and HV media were incompatible with practical experience. Thus the calculated viscosities of the HV medium were less than those of the LV medium. Furthermore, the data thus obtained with respect to the HV medium indicated that the power-law relationship was invalid since evidence of the shear stress being independent of the shear rate was exhibited, see section 8.1.1 for further clarification.

In addition the calculated viscosities of the MV medium appeared to be incompatible with the power-law relationship. In the case of the MV mixture with 60 Mesh grit and a grit to polymer ratio of 2 evidence of the shear stress being independent of the shear rate was also observed, again see section 8.1.1 for further clarification.

However, to enable a comparison of viscosities to be made between all media the rheological calculations were based on Newtonian relationships. The attainment of such apparent viscosities would be subject to error but would permit correlations to be made with other process parameters.

5) The normal pressure was assumed to be measured from the transducers directly due to the measurement of pressure being normal to the direction of flow.

6) Variations in the compositions of the media employed could introduce errors into both the rheological and machining measurements. The stipulated polyborosiloxane media are referred to as pure base medium with abrasive grit additions. In fact the media consist of one base medium with additions in various quantities of other polyborosiloxane compounds, lubricants, and plasticisers and/or reducers, (98). Therefore the properties of the media and subsequent assessments will be dependent upon the quality of mixing and the level of homogeneity obtained.

7) The practical problems of utilising an established commercial process and equipment was a major influence on the quality of the data obtained. To gain access to equipment in continuous use for production, and to ensure maximum usage throughout the duration of access required a certain amount of compromise without endangering the essential requirements of the investigation. In particular, repeat experiments using identical conditions were not made. The overall machining time required to complete two identical trials would have been too great and impractical within the time limits of the project.

8) A fundamental prerequisite of capillary rheometry is the use of a minimum capillary L:D ratio of 16. However, the commercial process could not accommodate this requirement since the extrusion pressure required to use such an L:D ratio would be too large, and the extrusion pressure would need to be altered from medium to medium. The AFM process is also incapable of machining with such L:D ratios with any success and the necessary surface measurements would also be unobtainable. Therefore an L:D ratio of 1 was specified as an initial starting point.

7.0 RESULTS

Section 7.1 details the results obtained from the preliminary experimental work, which was intended to provide qualitative evidence of the AFM process, and section 7.2 reports the results obtained from the principal experimental work, which examined and quantified the behaviour of the various polymer mixtures utilised and the machining action produced by the said mixtures.

To attain the relevant results to permit any correlation to be made in relation to the principal work required the collation of a very large amount of data. The results will be separated into those areas relating to the machining aspect of the process, viz:

- 1) the surface integrity, and
- 2) the stock removal,

and those which have been used to calculate the viscosities, as well as those which had an influence on the machining action, viz:

- 3) the processing time,
- 4) the pressure drops, and
- 5) the temperature.

Furthermore it was evident that there was a shear history effect associated with the usage of certain media. The results indicating such an effect are discussed in section 7.2.8.

7.1 Preliminary Work

The preliminary results as detailed in sections 7.1.1, 7.1.2, and 7.1.3 consist of SEM photomicrographs and graphical representation of (i) the effect of reusing media on the stock removal and surface roughness improvement parameters, and (ii) the effect of repeated medium use on the amount of abrasive grit wear.

7.1.1 AFM Surface Features

SEM photomicrographs were taken of a castle nut, figure 25, and a bearing component, figure 26. The latter was provided in both the unmachined and machined condition which enabled a comparison to be made of the surface topography both before and after AFM processing.

7.1.1.1 Castle Nut Component

The machining objective regarding this component was as an edge deburring operation. This is shown in figure 27(a) and illustrates an inner spur corner that has been deburred by the AFM process. Figure 27(b) depicts a section of the previous figure at a greater magnification and illustrates both the effect the abrasive grit additions have on the surface condition and their direction of flow. Figures 28(a) and 28(b) focus on two of the limitations of the AFM process, i.e. the inability to remove inclusions and voids without significantly affecting the component's dimensions. The selective machining capability of the AFM process is shown in figures 29(a) and 29(b), which illustrate the removal of conventional machining marks on different surface locations of the same spur. The ploughing effect of the grit particles can also be seen in figure 30.

7.1.1.2 Bearing Component

The processing of this component required the use of complex tooling since an apex was required to be machined on the flat areas in between the channels, as illustrated in figures 31(a) and 31(b). Figures 32(a) and 32(b), depict the component surface topography both before and after machining, and illustrate the uni-directional surface pattern generated by the machining process. Figure 33 shows the surfaces on either side of the machined apex and further illustrates the surface pattern generated by the process. The selective machining of one side of the channel wall is shown in figures 34(a) and 34(b) which illustrate the surface characteristics both before and after machining.

7.1.2 Medium Reuse

The parameters used to determine the effect of reusing medium on the machining process were the die diameter change, die mass change and surface roughness improvement. All of these parameters are graphically represented in such a way that the results obtained from the three sets of experiments performed, to determine the parameter under consideration, are presented on a single graph. These three sets of experiments, as detailed in section 6.1.1, were such that experiment one was conducted using fresh medium and experiment two involved the repetition of experiment one reusing the medium, whilst experiment three consisted of limited repetitions reusing the same medium.

Figures 35 and 36 show the effect of increasing the number of extrusion cycles on the amount of stock removed in the former case with respect to the die diameter and in the latter case with respect to the die mass. Similar results relating to both sets of parameters were obtained that indicated as the number of extrusion cycles increased so the amount of stock removed increased. This trend

was observed even when the same medium was reused during a repeat experiment. However, it should be noted that there was a decrease in the amount of stock removed the more the medium was reused. This difference was more pronounced as the cumulative number of extrusion cycles increased, and was most evident after the run that consisted of 20 extrusion cycles. In the cases of experiments one and two the difference between the respective die diameter measurements after 20 extrusion cycles had been conducted, i.e. 56 and 297 cumulative extrusion cycles respectively, was approximately 0.0080mm. However, after 70 extrusion cycles, i.e. 241 and 482 cumulative extrusion cycles, the difference between the respective die diameter measurements had increased to approximately 0.1900mm.

The effect of increasing the number of extrusion cycles on the surface roughness improvement is shown in figure 37. The results in all cases illustrated that the main improvement in surface roughness was achieved within a limited number of extrusion cycles, afterwhich minimal improvement was achieved. The results from the medium used to conduct the first experiment showed an approximate $4.3\mu\text{m}$ improvement in the surface roughness after 15 extrusion cycles, afterwhich there was no significant change in this value. Furthermore the majority of the improvement occurred within the first 5 extrusion cycles. The results of the second experiment showed an identical trend to the first; however the surface roughness improvement achieved was $4\mu\text{m}$, which required 20 extrusion cycles, afterwhich there was minimal improvement. The improvement attained by the third experiment was approximately $3.2\mu\text{m}$ and was achieved after 10 extrusion cycles; thereafter no significant improvement was attained.

7.1.3 Abrasive Grit Wear

These results relate to the two assessment methods as detailed in section 6.1.2,

viz:

1) Method One

The results as presented in figures 38(a) to 38(f) consist of selective photomicrographs of abrasive grit that underwent cumulative extrusion cycles of 0, 1, 7, 21, 46, and 91. These figures show as the cumulative number of extrusion cycles increased gradual deterioration and rounding of the abrasive grit particles was induced.

2) Method Two

Figure 39 illustrates the results obtained from the sieve analysis conducted on both the fresh and exhausted abrasive grit. In the case of the fresh grit there was virtually 100 percent grit retained on the 75 μ m sieve, whereas the exhausted grit required a 53 μ m sieve to achieve approximately 100 percent grit retention. Corresponding photomicrographs of the grit retained on the smaller sieves, i.e. below 75 μ m, are shown in figures 40(a) to 40(d). In the case of the fresh grit there were greater amounts of particles available for examination on the 75 μ m and 63 μ m sieves in comparison to the exhausted grit; whereas the contrary observation was seen in the cases of the material on the 53 μ m and 45 μ m sieves. Furthermore the particle shapes in the case of the fresh grit tended to be irregular on the 75 μ m and 63 μ m sieves and decidedly acicular on the 53 μ m and 45 μ m sieves. However, in contrast the particle shapes of the exhausted grit tended to be irregular whatever the particle size, although there was a minute amount of "spheroidal" particles present on each sieve.

7.2 Principal Work

Unless otherwise stated all the results relating the effect of a specific medium/grit combination on a specific characteristic of the machining process are displayed on one graph, irrespective of the grit to polymer ratio employed. The results thus presented illustrate the effect of increasing the number of extrusion cycles on the:

- a) Die diameter.
- b) Die mass.
- c) Surface integrity.
- d) Processing time.
- e) Average Pressure Drops.
- f) Apparent viscosities.

7.2.1 Die Diameter Change

In all cases of the medium/grit combinations used the die diameter changes produced after 30 extrusion cycles are presented in Table 3.

The effect of increasing the number of extrusion cycles on the die diameter using the LV medium and 60 Mesh grit is illustrated in figure 41. Irrespective of grit to polymer ratios employed the results show that as the number of extrusion cycles increased the die diameter change increased. After 30 cycles the greatest diameter change was produced by the medium with a grit to polymer ratio of 2, this was followed by the medium with a ratio of 0.5, whilst the smallest diameter change was produced by the medium with a ratio of 1. The corresponding results obtained with the LV medium and 100 Mesh grit, figure 42, showed similar results to those of the 60 Mesh grit. The only difference was that there were only very small differences in the results obtained by the mixtures with grit to polymer ratios

of 0.5 and 2.

Figure 43 shows the effect of increasing the number of extrusion cycles on the die diameter change with respect to the MV medium and 60 Mesh grit. After 30 extrusion cycles the greatest change in the die diameter was attained by the mixture with a ratio of 2. The mixture with a grit to polymer ratio of 0.5 produced the next greatest diameter change, whilst that with a ratio of 1 had the least effect on the die diameter. However, at 20 extrusion cycles the mixture with a grit to polymer ratio of 0.5 exhibited a marginal decrease in the die diameter change such that after 30 extrusion cycles the mixtures with ratios of 0.5 and 1 produced virtually identical die diameter changes. The corresponding results relating to the MV medium and 100 Mesh grit, figure 44, showed similar results to those obtained by the 60 Mesh grit. The mixture with a grit to polymer ratio of 0.5 illustrated a similar decrease in the die diameter change as associated with the 60 Mesh grit mixture, the only difference was that in the case of the former mixture this decrease in the diameter change occurred at 15 extrusion cycles. This decrease in diameter change exhibited by the 100 Mesh grit mixture with a grit to polymer ratio of 0.5 was such that after 30 extrusion cycles the diameter change produced was less than that produced by the mixture with a grit to polymer ratio of 1.

The results of the HV medium and 60 Mesh grit with grit to polymer ratios of 1 and 2, (figure 45), show as the number of extrusion cycles increased the die diameter change increased. In the case of the mixture with a ratio of 0.5 errors were encountered that implied the die diameter decreased during the machining operation which would have been an impossible occurrence. It must therefore be concluded that there was in these cases an inaccuracy in the original die diameter

measurements. Therefore only those results that were deemed realistic were plotted. Figure 46 illustrates the corresponding results obtained using the HV medium and 100 Mesh grit. The major difference between the results associated with the 100 Mesh grit mixtures to those of the 60 Mesh grit was that the former mixture with a grit to polymer ratio of 1 produced greater diameter changes than those associated with the same mixture with a grit to polymer ratio of 0.5.

The greatest and least effects on the diameter change after 30 extrusion cycles were produced respectively by the MV medium and 60 Mesh grit with a grit to polymer ratio of 2 and the HV medium and 100 Mesh grit with a ratio of 0.5. However, all the results obtained in relation to the die diameter changes can be summarised with respect to:

- 1) the three grit to polymer ratios employed. The effect of these ratios on the diameter changes in order of ascending magnitude was 1, 0.5 and 2 with the exception of the HV medium and 100 Mesh grit where the order was 0.5, 1 and 2. In all cases the diameter change values of the mixtures with grit to polymer ratios of 2 were much larger than those of the other grit to polymer ratios of 0.5 and 1. In the case of the MV medium with both 60 and 100 Mesh grit in a ratio of 0.5 there was a significant decrease in the stock removed in the latter stages of machining. However, there were no significant distinguishable trends exhibited between the remaining media used, and

- 2) the different grit sizes employed. The results indicate that in the cases of the LV and HV media the stock removal capabilities were improved with the larger grit size, i.e. 60 Mesh; however, in the case of the MV medium the stock removed was independent of the grit size.

7.2.2 Die Mass Change

The change in die mass after 30 extrusion cycles for all mixtures used are given in Table 4. The effect of increasing the number of extrusion cycles on the die mass change in all cases can be seen in figures 47 to 52. Similar analogous trends were observed as in the corresponding figures in section 7.2.1 that related the effect of an increase in the number of extrusion cycles on the die diameter change. Since both the die diameter and mass change are related to the amount of stock removed similarities between these relationships would be expected. However, in some cases there were slight discrepancies between some of the trends, viz:

a) in the case of the MV medium and 60 Mesh grit the die mass change up to 9 extrusion cycles achieved by the mixtures with grit to polymer ratios of 1 and 0.5 were virtually identical, afterwhich this similarity terminated since the die mass change produced by the mixture with a ratio of 0.5 remained approximately constant. This was inconsistent with the results obtained from the die diameter changes where the results from these ratios converged at 30 extrusion cycles, see figures 43 and 49.

b) for the MV medium and 100 Mesh grit the observation of a reversal in stock removal capabilities between the grit to polymer ratios of 0.5 and 1 occurred at 16 extrusion cycles (cf. after 20 cycles in the case of the die diameter change results, see figures 44 and 50.)

c) The stock removal capabilities of the various grit to polymer ratios of the HV medium and 60 Mesh grit altered to 0.5, 1, and 2, (in ascending order), see figures 45 and 51.

The results obtained in relation to the three remaining mixtures after 30 extrusion cycles were similar to those associated with the changes in the die diameter. The results for the LV medium with 60 and 100 Mesh grit are presented in figures 47 and 48, whilst the results for the HV medium and 100 Mesh grit are presented in figure 52.

In the case of die mass change the effect of varying the grit size was the same as for the die diameter change, i.e. the LV and HV media performance increased with an increase in grit size, whereas the MV medium performance was independent of the grit size, and the mixtures with grit to polymer ratios of 2 produced the greatest die mass changes. Furthermore, unlike the die diameter results, after 30 extrusion cycles the greatest die mass change was achieved by the HV medium and 60 Mesh grit with a grit to polymer ratio of 2, and the least die mass change was produced by the HV medium and 100 Mesh grit with a grit to polymer ratio of 0.5.

7.2.3 Surface Integrity

The surface integrity was examined both quantitatively and qualitatively, the former by the determination of the surface roughness improvement and the latter by photography.

7.2.3.1 Surface Roughness Improvement

The effect of increasing the number of extrusion cycles on the percentage surface roughness improvement can be seen in all cases in figures 53 to 58. The characteristic shapes of these graphs illustrated identical behaviours irrespective of the grit to polymer ratio employed, i.e. the main improvement was achieved within a limited number of extrusion cycles, after which minimal improvement was

produced.

The following list presents the percentage surface roughness improvement in terms of (i) the grit to polymer ratios in ascending order of surface roughness improvement, (ii) the number of extrusion cycles required to attain the main improvement, and (iii) the corresponding percentage surface roughness improvement attained at that point, viz:

1) LV medium 60 Mesh grit, (see figure 53)

Grit to polymer ratio in ascending order of surface roughness improvement	-	1, 0.5, 2
Extrusion cycles required to attain the main improvement	-	10, 10, 5
Percentage improvement achieved	-	60, 82, 92

2) LV medium 100 Mesh grit, (see figure 54)

Grit to polymer ratio in ascending order of surface roughness improvement	-	1, 0.5, 2
Extrusion cycles required to attain the main improvement	-	30, 15, 10
Percentage improvement achieved	-	47, 82, 92

3) MV medium 60 Mesh grit, (see figure 55)

Grit to polymer ratio in ascending order of surface roughness improvement	-	1, 0.5, 2
Extrusion cycles required to attain the main improvement	-	5, 10, 5
Percentage improvement achieved	-	61, 84, 94

4) MV medium 100 Mesh grit, (see figure 56)

Grit to polymer ratio in ascending order of surface roughness improvement	-	1, 0.5, 2
Extrusion cycles required to attain the main improvement	-	5, 5, 2
Percentage improvement achieved	-	40, 77, 92

After 15 extrusion cycles in the case of the above mixture the results obtained with the grit to polymer ratio of 0.5 exhibited a deviation from the results as presented above, such that there was a significant decrease in the surface improvement to a value below that obtained with the mixture with a ratio of 1. Therefore after 30 extrusion cycles the percentage surface roughness improvement achieved by the grit to polymer ratios of 0.5 and 1 were 32% and 41% respectively.

5) HV medium 60 Mesh grit, (see figure 57)

Grit to polymer ratio in ascending order of surface roughness improvement	-	1, 0.5, 2
Extrusion cycles required to attain the main improvement	-	5, 15, 10
Percentage improvement achieved	-	40, 71, 94

The results as stated above were only valid when the number of extrusion cycles performed were greater than 5, otherwise the order of grit to polymer ratios was 0.5, 1, 2.

6) HV medium 100 Mesh grit, (see figure 58)

Grit to polymer ratio in ascending order of surface roughness improvement	-	0.5, 1, 2
Extrusion cycles required to attain the main improvement	-	10, 20, 15
Percentage improvement achieved	-	17, 41, 77

In the case of the LV and MV media with grit to polymer ratios of 1 and the HV medium with ratios of 0.5 and 2 an increase in the grit size increased the percentage surface roughness improvement; in all other cases increasing the grit size had minimal effect on the surface roughness improvement. Furthermore an increase in the grit size produced a corresponding decrease in the number of extrusion cycles required to attain the main improvement for the LV and HV media, whereas increasing the grit size in the MV medium produced an increase in the number of extrusion cycles required to attain the main improvement.

7.2.3.2 Surface Photomicroscopy

This work was conducted on dies which had undergone the AFM process using media with a grit to polymer ratio of 1. The photographs presented are of selected die surfaces and are intended to provide a qualitative indication of the effect of increasing the number of extrusion cycles on the condition of the surface. An unprocessed die was used in each case and those presented had undergone either 1, 2, 3, 5, 10, or 30 extrusion cycles as indicated by the figure text.

Figures 59(a) to 59(f) illustrate the effect of increasing the number of extrusion cycles on the associated surface conditions of the die obtained using the LV medium and 100 Mesh grit; whilst figures 60(a) to 60(f) show the effect of using 60 Mesh grit. The surface conditions of the dies after using the MV medium and

100 Mesh grit are presented in figures 61(a) to 61(f); with figures 62(a) to 62(f) illustrating the corresponding effect when using 60 Mesh grit. The effects of the HV medium and 100 Mesh grit on the die surface conditions are presented in figures 63(a) to 63(f), and those of the 60 Mesh grit in figures 64(a) to 64(f).

In all cases as the number of extrusion cycles increased there was a corresponding decrease in the detection of the original turning marks and an increase in the prominence of the uni-directional marks produced by the AFM process. It is also evident that during prolonged treatment any pronounced turning marks are not removed but further exaggerated. For all cases the number of extrusion cycles necessary to achieve a visual improvement in the surface topography are presented in table 5.

7.2.4 Processing Time

Since polyborosiloxane exhibits shear-thinning thixotropic behaviour its rheological characteristics will be dependent upon the processing time required to complete machining. Furthermore a fundamental concept of the AFM process is that the time a component is subject to the abrasive action affects the amount of stock removed. Therefore the processing time data is included since it is considered to be of great significance to the AFM process.

In all cases the effect of an increase in the number of extrusion cycles on the time required to complete each run can be seen in figures 65 to 70. These figures all exhibited similar trends irrespective of the grit to polymer ratio employed, i.e. increasing the number of extrusion cycles increased the total processing time. However, when the number of cycles performed in the experimental sequence was increased, there came a point when the machining time required to complete

the additional extrusion cycles was minimal. This was associated with the changes in the rheological characteristics of the medium. Therefore at this point the difference in the processing times required to complete the specified number of runs was also minimal.

For all medium/grit combinations used the processing times required to complete 30 extrusion cycles are presented in Table 6.

Figure 65 shows that in the case of the LV medium and 60 Mesh grit a grit to polymer ratio of 0.5 required longer processing times than was required with the mixtures with ratios of 1 or 2. The medium with a ratio of 1 required the shortest processing times, and the ratio of 2 required intermediate processing times. The corresponding results obtained from the LV medium and 100 Mesh grit, figure 66, show that the mixture with a grit to polymer ratio of 0.5 again required the longest processing times. However, very similar processing times were required in the case of the mixtures with grit to polymer ratios of 1 and 2.

The results obtained from the MV medium and 60 Mesh grit, figure 67, show that in the case of the mixture with a grit to polymer ratio of 0.5 longer processing times were required than the mixtures with ratios of 1 and 2. The corresponding results obtained from the MV medium and 100 Mesh grit, figure 68, show that the mixtures with grit to polymer ratios of 1 and 0.5 exhibited similar trends until 20 extrusion cycles had elapsed, afterwhich in the case of the mixture with a ratio of 1 the increase in the number of extrusion cycles did not produce a corresponding increase in the required processing time. (This change in the case of the mixture with a grit to polymer ratio of 1 was such that a maximum processing time had been reached). Both the mixtures with ratios of 0.5 and 1 required longer

processing times than the mixture with a ratio of 2.

The results obtained from the HV medium and 60 Mesh grit, figure 69, show the mixture with a grit to polymer ratio of 0.5 required the longest processing times, the mixture with a ratio of 1 intermediate times, and the mixture with a ratio of 2 required the shortest processing times. The corresponding results obtained from the HV medium and 100 Mesh grit, figure 70, are incomplete since only one data point from the 30 extrusion cycle was obtained for the mixture with a grit to polymer ratio of 1. The results acquired from the mixture with a grit to polymer ratio of 0.5 required longer processing times than in the case of a ratio of 2.

When the results obtained from the different media are compared it is seen that the HV medium required significantly longer processing times than both the MV and LV media. Likewise the MV medium required longer processing times than the LV medium. In addition there was a trend in all cases of an increase in processing times as the grit size increased, as well as a general trend of a decrease in the processing time as the grit to polymer ratio increased.

7.2.5 Pressure Drop Measurements

For every run conducted results were obtained which examined the relationship between the number of extrusion cycles and the corresponding pressure drop through the die. From this relationship an average pressure drop was obtained for the run and a corresponding viscosity calculated, thus permitting a correlation to be made between the rheological and machining parameters.

Therefore for every experiment conducted two sets of pressure drop results were obtained, viz:

1) those that illustrated the relationship between the number of extrusion cycles and the corresponding pressure drop through the die, as reported in section 7.2.5.1. This was applicable to every run conducted within an experimental set.

2) those that illustrated the relationship between the number of extrusion cycles performed and the average pressure drops, calculated from the above relationship, and as reported in section 7.2.5.2.

7.2.5.1 The Effect of the Number of Extrusion Cycles Performed on the Pressure Drop across the Die

For the purposes of clarity two sets of results were produced in relation to this section, both of which were relevant to all medium/grit combinations used throughout the principal work, figures 71 to 80. The first set of results, figures 71 to 73, 75 to 76 and 78 to 79, illustrate the relationships between the number of extrusion cycles and the corresponding pressure drops through the dies. (The relevant medium/grit identifications are given by the figure text). These figures were presented in such a way that all the results obtained for each medium/grit combination were all plotted on one graph. Therefore these figures also show the pressure drops from which the corresponding average pressure drop calculations were obtained to enable the correlation between the rheological and machining parameters to be made. Furthermore the first set of results showed evidence of a shear history effect which is discussed in section 7.2.8. The second set of results, figures 74, 77 and 80, extract and present the results obtained from the 30 extrusion cycle run since the trends exhibited in each medium/grit combination were extremely similar, irrespective of the number of extrusion cycles performed, and the 30 extrusion cycle run provided a complete representative set of results. However, if there were any deviations from the reported trend this will be highlighted.

Figures 71(a) to 71(c) show the relationship between the number of extrusion cycles performed and the pressure drop measurements in relation to the LV, MV and HV media with no grit additions. In each case a distinctive trend was exhibited. When the LV medium was employed an increase in the number of extrusion cycles produced an initial increase in the pressure drop from 1700kPa to 2200kPa which then remained virtually constant until 22 cycles had been performed when there was a significant decrease in the pressure drop to a final value of 1300kPa. An increase in the number of extrusion cycles in the case of the MV medium produced a very rapid increase in the pressure drop from 1200kPa to 2750kPa after only 4 cycles, after which there was a smaller increase in the pressure drop to 3250kPa after 10 cycles; this value then remained approximately constant to the end of the experiment. In the case of the HV medium as the number of extrusion cycles increased the pressure drop steadily decreased to the end of the experiment from an initial value of 3350kPa to 2950kPa.

Figures 72(a) to 72(c) show the effect of increasing the number of extrusion cycles on the pressure drop measurements for all runs conducted using LV medium and 60 Mesh grit. The results obtained indicate the existence of three types of pressure drop behaviour which were dependent upon the grit to polymer ratio employed. Furthermore these results show that as the number of extrusion cycles performed in an experimental set were increased from the one cycle run to the 30 cycle run there was a corresponding gradual increase in the overall pressure drops. However, if the material was left to stand without use for a significant period, for example overnight between runs, then the overall pressure drop decreased. This trend was particularly in evidence when grit to polymer ratios of 0.5 and 2 were employed. Figure 74(a) shows the extracted results obtained from the 30 cycle run in relation to all LV medium and 60 Mesh grit mixtures. This

figure indicates the difference between the pressure drop trends was marginal in all cases, and the pressure drops attained by the mixtures which contained grit additions were significantly less than those associated with the pure medium. The results in detail, as shown in figure 74(a), for the LV medium and 60 Mesh grit mixtures were:

- 1) in the case of the mixture with a grit to polymer ratio of 0.5 as the number of extrusion cycles increased the pressure drop remained at a constant value ($\approx 1700\text{kPa}$) until 20 extrusion cycles after which there was a constant decrease in the pressure drop to 1400kPa by the end of the run.
- 2) in the case of the mixture with a grit to polymer ratio of 1 there was a rapid increase in the pressure drop from 1400kPa to 1800kPa by the second extrusion cycle which was followed by a constant decrease to 1200kPa by the end of the run.
- 3) in the case of the mixture with a grit to polymer ratio of 2 the pressure drop decreased from 1900kPa to 1600kPa during the first seven extrusion cycles before remaining almost constant at this value to the end of the run.

The results obtained when the same medium and 100 Mesh grit were used are presented in figures 73(a) to 73(c) and figure 74(b). The major difference between the results obtained using 100 Mesh grit to those associated with the 60 Mesh grit was that in the latter case the pressure drops tended to be greater than those obtained in the former experiments. Figures 73(a) to 73(c) once again illustrated the existence of the same build-up in pressure drop as the experimental runs were incremented up to the 30 extrusion cycle run and the corresponding decrease in pressure drop if the material was left unused for a significant period. Once more this effect was most prevalent in the mixtures with grit to polymer ratios of 0.5

and 2.

Figures 75(a) to 75(c) illustrate the relationships between the pressure drop measurements and the number of extrusion cycles for all cases of MV medium and 60 Mesh grit. The existence of three types of pressure drop were once again exhibited; these were again dependent upon the grit to polymer ratio employed. Also once more an increase in the medium usage produced an increase in the pressure drop unless the material was left overnight when the pressure drop decreased. In addition to this effect which was exhibited in all cases the mixture with a grit to polymer ratio of 0.5 exhibited a further phenomena. Thus as the number of extrusion cycles performed in a run were increased from the one cycle run to the 30 cycle run, there was a corresponding decrease in the rate of pressure drop increase within the first 7 extrusion cycles. The extracted results obtained from the 30 extrusion cycle run in relation to the MV medium and 60 Mesh grit mixtures are shown in figure 77(a). After 4 extrusion cycles the results indicate the pressure drops of the mixtures containing abrasive grit were significantly less than those associated with the pure medium. Furthermore the results show that an increase in the grit to polymer ratio resulted in a decrease in the maximum pressured drop. However, after 19 extrusion cycles there was a convergence of the pressure drops. The mixtures with grit to polymer ratios of 1 and 2 exhibited similar trends, such that an increase in the number of extrusion cycles produced an increase in the pressure drop until the latter stages when the pressure drops tended towards a constant value. The results in detail, as shown in figure 77(a), for the MV medium and 60 Mesh grit mixtures were:

1) in the case of the mixture with a grit to polymer ratio of 0.5 there was a small increase in the pressure drop from 2600kPa to 2800kPa by the ninth extrusion cycle, this was then followed by a decrease in the pressure drop to 2500kPa by the end of the run.

2) in the case of the mixture with a grit to polymer ratio of 1 there was an increase in the pressure drop from 2000kPa to 2600kPa by the twelfth extrusion cycle with this value remaining constant to the end of the run.

3) in the case of the mixture with a grit to polymer ratio of 2 there was a decrease in the pressure drop from 2150kPa to 1800kPa by the third extrusion cycle, after which it increased to 2600kPa by the nineteenth extrusion cycle and was then maintained at this value to the end of the run.

The corresponding results obtained from the same medium and 100 Mesh grit are shown in figures 76(a) to 76(c) and figure 77(b). In all cases the results obtained are similar to those relating to the MV medium and 60 Mesh grit. The major difference between the two sets of results was that the 60 Mesh grit produced greater pressure drops than those associated with the 100 Mesh grit. Figures 76(a) to 76(c) indicate again the effect of an increase in the pressure drop as the medium usage increased unless the material was left overnight. Furthermore the mixture with a grit to polymer ratio of 0.5 exhibited the same decrease in the rate of pressure drop increase as the usage of the medium increased as was the case with the corresponding 60 Mesh grit mixture, (this phenomena was more discernible in the case of the 100 Mesh grit mixture). Figure 77(b) illustrated that the convergence of the pressure drops occurred much later, i.e. the mixtures with grit to polymer ratios of 1 and 2 converged at 24 cycles, and convergence with the mixture with a grit to polymer ratio of 0.5 occurred at 29 cycles.

The relationships between the number of extrusion cycles performed and the pressure drops of all the HV medium and 60 Mesh grit mixtures are presented in figures 78(a) to 78(c). The results obtained showed there were significant differences in the pressure drop values attained in each case even though similar behaviour was exhibited. Furthermore the effect of an increase in the pressure drop as the medium usage increased was once again exhibited but was most significant in the case of the mixture with a grit to polymer ratio of 2. Figure 80(a) presents the extracted results from the 30 extrusion cycle runs in relation to the HV medium and 60 Mesh grit mixture. This figure indicates the pressure drops of the mixtures with grit to polymer ratios of 1 and 2 were less than that associated with the pure medium. However, prior to 15 extrusion cycles the pure medium had greater pressure drop values than the mixture with a grit to polymer ratio of 0.5 but this trend was reversed after 15 extrusion cycles had been performed. The results in detail, as shown in figure 80(a), for the HV medium and 60 Mesh grit mixtures were:

- 1) in the case of the mixture with a grit to polymer ratio of 0.5 a constant pressure drop of 3000kPa was maintained throughout the entire run.
- 2) in the case of the mixture with a grit to polymer ratio of 1 a constant pressure drop of 2800kPa was maintained throughout the entire run.
- 3) in the case of the mixture with a grit to polymer ratio of 2 there was a small variation in the pressure drop from 2100kPa to 2300kPa during the first twenty extrusion cycles, with constant values of this quantity thereafter.

The results corresponding to the same medium with 100 Mesh grit are presented in figures 79(a) to 79(c) and figure 80(b). In all cases the results are similar to those of the 60 Mesh grit. The major difference was that the pressure drop values associated with the 100 Mesh grit were slightly less than those of the 60 Mesh grit. Figures 79(a) to 79(c) showed that the most significant effect of the increase in pressure drop as the medium usage increased was again exhibited by the mixture with a grit to polymer ratio of 2. Figure 80(b) showed the pressure drop trend attained by the pure medium was greater than all other mixtures with grit additions.

7.2.5.2 Average Pressure Drops

The average pressure drop results are of great importance since upon them are dependent the viscosity parameters used to examine the relationships between the rheological and machining characteristics of the media used in the present work.

Figure 81 shows the effect of increasing the number of extrusion cycles on the average pressure drops obtained in relation to all of the LV medium and 60 Mesh grit combinations. The average pressure drops fluctuated in all cases in an irregular manner between the limits of 1250kPa and 1850kPa without any definite trend, except for the possibility of a small reduction towards the end of the runs when the grit to polymer ratios were 1 and 0.5.

Figure 82 shows similar results were obtained when the grit size was decreased to 100 Mesh, although there was a marginal change in the range of the average pressure drop to between 1100kPa to 1750kPa.

The effects of increasing the number of extrusion cycles on the average pressure drops when using the MV medium and 60 Mesh grit combinations are presented in figure 83. The average pressure drops varied between 1650kPa and 2700kPa. In the case of the mixtures with grit to polymer ratios of 0.5 and 1 a steady increase in the average pressure drop was shown as the number of extrusion cycles increased. However, no such increase was produced when the grit to polymer ratio was 2.

Figure 84 shows that the grit to polymer ratio had a significant effect on the average pressure drops obtained with the same medium and 100 Mesh grit. The greatest average pressure drops were associated with the mixture with a grit to polymer ratio of 0.5 and the least were associated with the mixture with a ratio of 2. In all cases there was an increase in the average pressure drops as the number of extrusion cycles performed increased. Furthermore the range in which the results were contained altered significantly to between 1400kPa and 2800kPa, (cf 1650kPa to 2700kPa in figure 83).

Figure 85 showed the effect of increasing the number of extrusion cycles on the average pressure drops for all combinations of the HV medium and 60 Mesh grit. A large range of average pressure drops was evident, (between 1700kPa and 3050kPa). However, the values of this parameter obtained with the mixtures with grit to polymer ratios of 0.5 and 1 were unaffected by the number of extrusion cycles, whilst the mixture with a ratio of 2 experienced significantly smaller average pressure drops which decreased in the initial stages and increased in the latter stages. (This fluctuation was only present in the last-named case.)

The results obtained from the HV medium and 100 Mesh grit, figure 86, showed that the mixtures with grit to polymer ratios of 0.5 and 2 experienced constant average pressure drops of 2450kPa and 1800kPa respectively. The results from the experiment conducted using the grit to polymer ratio of 1 consisted of a single point at 2735kPa since only one set of results was obtainable.

When comparing the data obtained from the LV, MV and HV media it was apparent that the average pressure drops increased as the base medium viscosity increased. The respective ranges in the cases of the LV, MV and HV media were 1250kPa to 1750kPa, 1400kPa to 2800kPa, and 1700kPa to 3050kPa. Furthermore increasing the size of the grit resulted in a shift to the upper boundaries of the relevant average pressure drop range.

The average pressure drop results obtained using the media with no abrasive grit additions were not plotted since they refer only to those values after 30 extrusion cycles had been performed and therefore no trend could be plotted. The average pressure drop results so obtained were:

LV	-	2150kPa
MV	-	3030kPa
HV	-	3075kPa

7.2.6 Determination of the Apparent Viscosities

In the present work the apparent viscosity¹, (termed viscosity in the text below), was that parameter which was calculated from the corresponding average pressure drop measurement obtained during the relevant run. Eight runs were

¹ see section 6.2.5.2

conducted in an experimental set resulting in eight average pressure drop measurements. Therefore in one experimental set eight viscosity calculations were possible. The data thus obtained for all polymer and grit combinations used in the present work are presented in tables 7 to 27. An example of the calculations performed to attain the viscosities in all cases is presented in Appendix 1. (This example applies to the LV medium and 60 Mesh grit with a grit to polymer ratio of 0.5 used during 30 extrusion cycles). Corresponding graphs illustrate the effect of increasing the number of extrusion cycles on the viscosity of all the various mixtures of grit and polymer used.

Figure 87 shows the effect of an increase in the number of extrusion cycles on the medium viscosity for the LV medium and 60 Mesh grit combinations. The results obtained for all the mixtures showed the viscosities were significantly affected by the number of extrusion cycles performed, i.e. there were steady reductions in the viscosities as the number of extrusion cycles increased. The viscosity range within which the mixtures with grit to polymer ratios of 0.5 and 2 were operating was between 800Pa.s and 350Pa.s. The mixture with a grit to polymer ratio of 1 was less viscous than the other two mixtures and operated within a viscosity range of between 400Pa.s and 150Pa.s.

Similar results were obtained for the LV medium and 100 Mesh grit combinations, as shown in figure 88, with the exception that there were marginal differences between the various mixture viscosities after 5 extrusion cycles. The change in grit size also affected the observed viscosity range which now lay between 400Pa.s and 250Pa.s, where the lower values were associated with the highest number of extrusion cycles.

Unusually there was a small increase in viscosity in one mixture as the number of extrusion cycles increased to 5. This was only observed when the grit to polymer ratio was 0.5, (see figures 87 and 88).

Figure 89 shows the results obtained from the MV medium and 60 Mesh grit and indicates that the viscosities of each mixture again generally decreased as the number of extrusion cycles performed increased. In all cases there was virtually no difference between the viscosities after 3 extrusion cycles had been performed, and the viscosity range in evidence was between 3500Pa.s and 2000Pa.s. However, prior to the third extrusion cycle the viscosity of the mixture with a grit to polymer ratio of 2 notably decreased from 6900Pa.s to 3500Pa.s. In the same period the mixtures with ratios of 0.5 and 1 increased in viscosities from 1600Pa.s to 3200Pa.s and from 1150Pa.s to 2100Pa.s respectively.

Where the MV medium and 100 Mesh grit combinations were employed, see figure 90, similar results were obtained as with the 60 Mesh grit mixtures. However the mixture with a grit to polymer ratio of 2 did not experience a significant reduction in viscosity by the third extrusion cycle but underwent an increase in viscosity similar to that observed by the mixtures with grit to polymer ratios of 0.5 and 1. Although these mixtures showed a decrease in their viscosities as the number of extrusion cycles were increased there was a distinct difference in the mean viscosities of each mixture. Thus the mixture with a grit to polymer ratio of 1 was the most viscous while that with a grit to polymer ratio of 2 was the least viscous.

The results obtained from the HV medium and 60 Mesh grit mixtures are presented in figure 91 and indicate that the viscosities in all cases decreased as the number of extrusion cycles increased. The mixture combinations with grit to polymer ratios of 0.5 and 1 had similar viscosities within a range between 25000Pa.s and 10000Pa.s. The mixture with a grit to polymer ratio of 2 had a significantly lower viscosity than those associated with the other two mixtures, the viscosity range in evidence was between 17000Pa.s and 4000Pa.s.

The results obtained from the HV mixtures with 100 Mesh grit are presented in figure 92 and show similar ranges of viscosities to those associated with the 60 Mesh grit. However, the former mixtures with grit to polymer ratios of 0.5 and 2 exhibited similar viscosity trends after 1 extrusion cycle had been performed. The viscosity range for these two mixtures was then between 22000Pa.s and 6000Pa.s. The mixture with a grit to polymer ratio of 2 underwent a major reduction in viscosity between the first and second extrusion cycle (from 62000Pa.s to 22000Pa.s) an effect that was absent in the case of the mixture with a grit to polymer ratio of 0.5.

When comparing the data from the LV, MV and HV media it was evident that there was a viscosity associated with each base media that dominated the various grit to polymer ratios. Thus the viscosity ranges associated with the LV, MV, and HV media were 400Pa.s to 150Pa.s, 3500Pa.s to 500Pa.s, and 25000Pa.s to 4000Pa.s respectively. An increase in the grit size affected the viscosity experienced by the MV medium, whilst the viscosities of both the LV and HV media remained relatively unaffected by the change in grit size.

The viscosity results obtained from the mixtures with no grit additions could not be plotted since these values referred only to 30 extrusion cycles. The viscosity results so obtained were approximately:

LV	-	1050Pa.s
MV	-	1900Pa.s
HV	-	6700Pa.s

7.2.7 Temperature Measurements

The temperature results referred to are those single point measurements taken at the transducers tips. All the results presented consist of the temperature measurements recorded at the end of each extrusion cycle within a run against the corresponding processing time. Furthermore, as was the case with the results of the relationship between the number of extrusion cycles and the pressure drop, the temperature results for each medium/grit combination used are presented in such a way that the results for all the runs conducted within a single experiment are plotted on one graph. In addition both the initial and final temperatures of each run are presented in tables 28 to 34. The trends between temperature and time for each experimental set were similar irrespective of the number of extrusion cycles performed. Therefore since the 30 extrusion cycle run encompassed the entire trend the description will refer to this run only. The overall rates of temperature rise, as referred to in the text below, are presented in Table 35 for all mixtures.

The results showing the effect of the processing time on the temperature of the LV, MV and HV media with no grit additions are presented in figures 93(a) to 93(c). In all cases as the processing time increased there was an increase in the

temperature. In addition as the viscosity of the base polymer increased there was a decrease in the rate of temperature rise. The difference in these values was associated with the significant variations in the processing times of the various media, as presented in section 7.2.4. Furthermore the temperature changes associated with these three media exhibited individual characteristics, viz:

a) in the case of the LV medium there was a constant increase in the temperature until an approximate processing time and temperature of 240s and 26°C had been reached. After this stage had been reached there was a pronounced increase in the rate of temperature rise.

b) in the case of the MV medium there was a constant increase in the temperature until an approximate processing time and temperature of 80s and 25°C had been reached. Thereafter there was a decrease in the rate of temperature rise to a much lower value. However, when the processing time reached approximately 960s there was a further small increase in the rate of temperature rise.

c) in the case of the HV medium there was very little change in the temperature until an approximate processing time of 3400s had been reached, afterwhich there was a significant increase in the rate of temperature rise.

Figures 94(a) to 94(c) illustrate the effect of increasing the processing time on the temperature of the LV medium and 60 Mesh grit combinations. In all cases the temperature increased as the processing time increased. The mixture with a grit to polymer ratio of 1 exhibited the greatest overall rate of temperature rise. With

respect to the mixtures with ratios of 0.5 and 2 there were marginal differences between the rates of temperature rise until the processing time and temperature had reached approximately 240s and 40°C when in the case of the mixture with a grit to polymer ratio of 0.5 the rate increased significantly.

The corresponding results using the LV medium and 100 Mesh grit, figures 95(a) to 95(c), illustrated graphs with characteristic shapes similar to those showing the relationships between temperature and time associated with the 60 Mesh grit mixtures. The increase in the rate of temperature rise as associated with the 60 Mesh grit with a grit to polymer ratio of 0.5 was again exhibited by the corresponding 100 Mesh grit mixture except in the latter case it occurred at approximately the same temperature but at a shorter processing time, i.e. 38°C and 180s.

The effect of the processing time on the temperature of the MV medium and 60 Mesh grit mixtures are shown in figures 96(a) to 96(c). The rate of temperature rise exhibited by the mixture with a grit to polymer ratio of 2 was constant throughout the experiment. However, the temperature changes associated with the mixtures with grit to polymer ratios of 0.5 and 1 were markedly different from that of the mixture with a ratio of 2. The characteristic shape of the graph showing the relationship between temperature and time in relation to the mixture with a grit to polymer ratio of 0.5 was similar to that exhibited by the MV medium with no grit additions. In addition the characteristic shape of the same graph in relation to the mixture with a grit to polymer ratio of 1 exhibited a similar segment to the graph produced by the pure medium. Thus:

a) in the case of the mixture with a grit to polymer ratio of 1 there was a constant increase in the temperature until an approximate processing time and temperature of 360s and 36°C had been reached, after which the rate of temperature rise decreased to such a degree that there was only a small increase in temperature thereafter.

b) in the case of the mixture with a grit to polymer ratio of 0.5 the decrease in the rate of temperature rise occurred at 180s and 17°C, whilst the further increase in the rate of temperature rise occurred when an approximate processing time and temperature of 1120s and 24°C had been reached.

Figures 97(a) to 97(c) show the corresponding results obtained when using the MV medium and 100 Mesh grit mixtures. In all cases the results were similar to those obtained with the 60 Mesh grit. However, the rate of temperature rise of the mixture with a grit to polymer ratio of 2 did not remain constant throughout the experimental run as was the case when 60 Mesh grit was used. Instead the temperature decreased when an approximate processing time and temperature of 300s and 33°C had been reached. In the case of the mixtures with ratios of 1 and 0.5 the initial decrease in the rate of temperature rise occurred when the respective processing times and temperatures were approximately 180s and 27°C, and 120s and 16°C. In the case of the mixture with a grit to polymer ratio of 0.5 the further increase in the rate of temperature rise occurred at approximately 740s and 22°C.

The effect of the processing time on the temperature of the HV medium and 60 Mesh grit mixtures are shown in figures 98(a) to 98(c). In all cases as the processing time increased there was a constant increase in the temperature. However, the mixture with a grit to polymer ratio of 2 underwent the greatest rate of temperature rise. There were very small differences in the rates of temperature rise between the mixtures with grit to polymer ratios of 0.5 and 1. In addition the mixture with a grit to polymer ratio of 0.5 exhibited a small increase in the rate of temperature rise in the latter stages of the run at approximately 5600s.

The corresponding results showing the relationship between the temperature and time of the HV medium and 100 Mesh grit, figures 99(a) to 99(c), exhibited similar characteristic shapes to the graphs associated with the 60 Mesh grit mixtures. The increase in the rate of temperature rise of the 100 Mesh grit mixture with a ratio of 0.5 in the latter stages of the run occurred at 3800s (cf 5600s with the 60 Mesh grit). The major difference between the results obtained by the 100 Mesh grit mixtures and the 60 Mesh grit was that in the former case all the mixtures exhibited similar rates of temperature rise, irrespective of the grit to polymer ratio.

Comparison of the data obtained from the LV, MV and HV media showed that an increase in the grit size had little effect on either the rates of temperature rise or the characteristic shapes of the graphs showing the relationship between temperature and time. In addition as the viscosity of the base medium increased there was a corresponding decrease in the rates of temperature rise. The ranges of these rates of temperature rise in relation to the LV, MV, and HV media were $0.0690^{\circ}\text{Cs}^{-1}$ to $0.1531^{\circ}\text{Cs}^{-1}$, $0.0112^{\circ}\text{Cs}^{-1}$ to $0.0591^{\circ}\text{Cs}^{-1}$, and $0.0012^{\circ}\text{Cs}^{-1}$ to $0.0045^{\circ}\text{Cs}^{-1}$ respectively.

7.2.8 Shear History

Due to the nature of the experimental work and the processing times taken it was frequently not possible to complete a set of experiments on the same day. It became apparent during the course of the work that the overnight pause in machining had a significant effect on the characteristics of the medium. For each medium used a graph illustrating the most prominent occurrence and significance of this effect has been selected, as shown in figures 100 to 102. These figures show the influence of the number of extrusion cycles on the variation in pressure drop across the die when the set of experiments were completed on a single day. In all cases the results presented relate to 60 Mesh grit used with the LV and MV media in a ratio of 0.5 and the HV medium in a ratio of 2.

The results shown in figures 100(a), 101(a) and 102(a) indicate that increasing the number of extrusion cycles performed in an experiment from the one cycle run to the 30 cycle run resulted in an associated increase in the overall pressure drop. In addition to this if there was a significant pause between the runs in the experiment, for example if the medium was left standing overnight, there was a pronounced decrease in the overall pressure drop. Furthermore if the medium was then further used then the overall pressure drop would again increase, as shown in figures 100(b), 101(b) and 102(b). The results further show that the characteristic shapes of the graphs illustrating the relationships between the pressure drops and the number of extrusion cycles were unaffected by this effect which appears to be an inherent characteristic of polyborosiloxane and not of the processing variables.

This shear history effect is of significance because any changes in the relationship between the pressure drop and number of extrusion cycles will affect the average pressure drop calculation, and hence the viscosity measurement would be affected. Therefore Table 36 displays the days on which all of the runs within an experimental set were performed to provide an indication of when the shear history effect could have influenced the results obtained.

As previously stated in section 7.2.5.1 an additional phenomena to the shear history effect was exhibited by the MV medium with 60 and 100 Mesh grit additions with a grit to polymer ratio of 0.5. This was such that as the number of extrusion cycles performed in a run were increased from the one cycle run to the 30 cycle run there was a corresponding decrease in the rate of pressure drop increase. Figures 103(a) and 103(b) illustrates this phenomena in relation to the MV medium with 100 Mesh grit and a grit to polymer ratio of 0.5.

8.0 DISCUSSION

As stated in section 5.4, most research into the AFM process has been limited to qualitative studies which have concentrated on the variables affecting machining. Studies conducted into the rheological behaviour of the polyborosiloxane/grit mixtures have been minimal and principally qualitative. However, some quantitative rheological studies have been performed using the polymer alone. There has been no previous investigation of the quantitative relationships between the rheological behaviour of the polyborosiloxane/grit mixtures and the corresponding machining characteristics of the AFM process. Therefore the results obtained during the present work, as detailed in section 7.0, represent a significant increase in information about these relationships. This data will be analysed and discussed in the following section with the intention of providing increased understanding of the relationships between the rheological characteristics of polyborosiloxane/grit mixtures and the corresponding machining characteristics.

Due to the quantity of results obtained, and their inter-dependence, the discussion section is arranged as follows:

- a) Section 8.1 discusses errors associated with the viscosity, surface friction, and normal pressure parameters.
- b) Section 8.2 analyses the observed machining characteristics.
- c) Sections 8.3 and 8.4 discuss those parameters that influence the rheological behaviour of the polyborosiloxane/grit mixtures.
- d) Section 8.5 analyses the observed rheological characteristics.
- e) Section 8.6 discusses the machining performance in conjunction with the rheological behaviour.

- f) Section 8.7 discusses the effect of alterations in the base viscosity, grit size, and grit to polymer ratios on the rheological and machining behaviour.
- g) Section 8.8 proposes a possible model to interpret the observed AFM operation.

Two points must be made with respect to the data provided. In all figures presented in the discussion section a break in the datapoints plotted indicates an overnight break in the experiments. This was deemed necessary to indicate points where the shear history effect, as detailed in section 7.2.8, may have influenced the results obtained and therefore the analysis of the relationships based upon these results. Also since the trends obtained with respect to the die diameter and die mass changes were very similar, and a complete set of die mass change results were obtained, this latter parameter is used to represent the amount of stock removed.

8.1 Errors Associated with the Measured and Calculated Parameters

As stated in section 6.2.5 the present work utilised an established commercial process. The use of production equipment caused certain difficulties not encountered in a laboratory situation, and so the results obtained may have sustained errors due to both processing parameter variations and the need to make certain assumptions with respect to the type of fluid flow exhibited. These have been detailed previously in sections 6.2.5.1 and 6.2.5.2.

No previous investigations have been conducted into the relationship between the rheological and machining characteristics of the polyborosiloxane/grit mixtures used in the AFM process. However, one of the most important parameters

required to be assessed was the viscosity. This would provide an indication of the flow characteristics of the medium during the AFM process that could then be related to the machining performance. The calculations used to obtain the apparent viscosities, (termed viscosities in the text below), and hence the desired relationship, were performed assuming Newtonian fluid flow and dispensing with surface friction calculations. The reasons for these assumptions are discussed in sections 8.1.1 and 8.1.2. In addition section 8.1.3 explains the absence of Normal force measurements.

8.1.1 The Method of Calculation of the Viscosities

Polyborosiloxane exhibits non-Newtonian behaviour. However, the calculation of viscosities during the present work assumed Newtonian behaviour in order to attain a rheological parameter that could be related to the machining performance. The calculation of viscosities for non-Newtonian fluids should utilise the power-law relationship, as given by equation 17. This relationship requires plots of log shear rate versus log shear stress to enable the shear-thinning index and temperature constant to be attained. However, figures 104 to 109, showing log shear stress against log shear rate for all mixtures used in the present work, indicate deviations from the straight line correlations expected for such plots, revealing that there are other influential factors occurring in the process.

In the case of the MV medium and 60 Mesh grit mixture with a grit to polymer ratio of 2 and all of the mixtures based on the HV medium, figures 106(c), 108, and 109 respectively, it is observed that the shear stress appears to be independent of the shear rate. This flow phenomena is similar to flow exhibited by powders and pastes which is analogous to solid-solid friction (41). Thus "the force required to overcome friction of a solid block pulled across a flat solid surface is

nearly independent of the speed of sliding".

A further analogy of this behaviour may be drawn with flow associated with Bingham plastic fluids immediately after flow occurs since the applied shear stress must be greater than the yield stress for flow to occur after which the fluid behaviour tends towards Newtonian flow where the shear stress is independent of shear rate. Therefore figures 106(c), 108, and 109 would indicate that the flow behaviour of the mixtures illustrated represents characteristics that tend towards solid flow, i.e. the mixtures move as a plug through the die.

8.1.1.1 Comparison of the Calculated Viscosities to Published Values

With respect to polyborosiloxane/grit mixtures no previous viscosity data has been published. Therefore the viscosities calculated in the present work can only be compared to those published values that relate to pure polyborosiloxane. This comparison would enable the assumptions made in the calculation of the viscosities to be verified.

Viscosities obtained using a Power Law relationship in relation to pure LV medium at various shear rates have been published by Trengove (95). The viscosity range of this medium was between 295Pa.s and 57Pa.s with a corresponding range of shear rates between 150s^{-1} and 4500s^{-1} . The viscosity of the pure LV medium obtained from the present work was 223Pa.s at a shear rate of 2300s^{-1} . The difference in these results can be attributed to:

- i) the utilisation of a Power Law relationship in the former and a Newtonian relationship in the latter case.
- ii) the process variables and conditions used during the former and latter work were different.
- iii) the compositions of the media employed may have varied due to the method of medium production, i.e. the constituent elements used and both the quality of mixing and the level of homogeneity obtained.

However, given these possible variations, the comparative similarity of these two sets of results shows the assumptions made in the present work were reasonable.

8.1.2 The Effect of Surface Friction on the Pressure Drop

Some corrections applicable to capillary viscometry work were previously detailed in section 3.2.2.1, viz:

- 1) Reservoir pressure losses.
- 2) Kinetic energy losses.
- 3) Entrance and exit pressure losses.

The first and third of these corrections are recommended to be performed on capillary viscometry data (44). However, with respect to the present work these corrections were assumed to be unnecessary due to the experimental procedure adopted, as discussed in section 6.2.5.2.

A further correction due to surface friction losses between polymer and capillary wall is also applicable to capillary viscometry data, viz:

$$\Delta P_f = 2 \rho f \frac{L}{D} v^2 \quad (55)$$

where, ΔP_f = pressure energy loss due to friction
 f = fanning friction factor

The above correction due to surface friction is considered to be independent of surface roughness when laminar flow conditions prevail. Thus since the present work assumed laminar flow conditions it was deemed unnecessary to perform the correction to assess the effect of surface friction on the pressure drop.

8.1.3 Errors Associated with the Normal Pressure Measurements

The commercial process under investigation utilised abrasive laden polymer. Therefore the pressure transducers used to obtain the pressure drops across the dies were recessed to avoid damage to the transducer tips by abrasive action, as described in section 6.2.2.3. This pressure difference between the two transducers enabled viscosities to be calculated using classical capillary rheometer relationships. Furthermore since the transducers were mounted perpendicularly to the direction of medium flow an average normal pressure could also be obtained.

The mechanics of machining and the nature of the AFM process make the normal stress a parameter of considerable interest. However, the validity of a calculation of the normal stress from the corresponding normal pressure would be uncertain due to errors associated with hole pressure measurements, i.e.:

The first normal stress difference, N_1 , is usually obtained from cone and plate rheometry. However, two examination methods (99) using slit-die rheometers have been considered to enable the first normal stress difference to be obtained,

viz:

- 1) The hole pressure method, (P_H), i.e. the difference between the pressure measured at the bottom of a fluid-filled recessed hole and the pressure measured flush with the die wall.
- 2) The exit pressure method, (P_{ex}), i.e. the extrapolated pressure measurements along the die wall to the die exit.

Controversy exists over the accuracy of these methods but Baird (99) concluded that the first normal stress difference could be obtained from the hole pressure method, whereas the use of the exit pressure method was questionable.

Further studies by Tomita (100) into the use of liquid-filled holes to measure the normal stress difference concluded that most experimental and theoretical studies confirmed the measured normal stress difference to be smaller than the true normal stress difference at the wall.

Since the measurements used to obtain the normal pressures in the present work were a combination of the P_H and P_{ex} methods normal stress calculations could not be carried out. However, as already stated the normal pressure with respect to the AFM process would be of considerable interest since it would be expected to be related to the machining performance. Values of the average normal pressure obtained from the 30 extrusion cycle run for all polymer/grit mixtures used are presented in tables 37 to 39.

These average normal pressure results are relevant to the normal force exerted on the grit particles responsible for machining, as detailed in section 2.1. Therefore if the medium was solid the normal pressure would be expected to be related to the machining performance. However, there was no correlation in evidence between the normal pressure and the associated stock removal. This is shown by tables 40 to 42, which present the corresponding die mass change results obtained from the 30 extrusion cycle run, and show that as the normal pressure decreases there is a corresponding increase in the stock removed. Therefore it is suggested that machining is not solely dependent upon the normal force exerted on the grit particles but must also be dependent upon the rheological behaviour of the medium during the process.

8.2 The Effect of the Number of Extrusion Cycles on the Machining Parameters

The results obtained from the principal work indicated that an increase in the stock removed and a reduction in the surface roughness were achieved as the number of extrusion cycles increased. In all cases the reduction in surface roughness did not increase linearly but tended towards a maximum value which was achieved within a specific number of extrusion cycles, that was specific to each polymer/grit combination: thereafter only minimal improvement was achieved. These results are in accordance with work conducted by Przylenk (88), as detailed in section 5.4.1, who concluded that stock removal was proportional to the number of extrusion cycles and the most significant surface improvement was achieved within the first ten cycles, afterwhich there was no significant improvement. Work conducted by Williams (97) also concluded that "the major improvement in the AFM generated surface occurred just after a few cycles".

Figures 110 to 115 show in all cases the effect of increasing the number of extrusion cycles on (i) the mass change per cycle, (ii) the total mass change, and (iii) the percentage surface roughness improvement. In all cases the total mass change was non-linear with respect to the number of extrusion cycles. This is indicated by the corresponding decrease in the stock removed per cycle as the number of extrusion cycles in a run increased. The results obtained from the percentage surface roughness improvement indicate that the main improvement in surface topography is achieved within a specified number of extrusion cycles and the amount of improvement is dependent upon the viscosity of the base medium, the grit size, and the grit to polymer ratio employed.

At the start of the machining process the die surface consists of relatively large peaks from the turning operation used to produce the specified initial surface roughness. It is suggested that these peaks are gradually abraded by the process until the vast majority of peaks have been honed and it is during this stage that the main improvement in surface roughness is to be expected. In relation to surface roughness improvement the benefits in continuing the AFM process beyond this point are minimal since the machining operation thereafter will only have benefits with respect to stock removal.

The optical photographs of surface topography taken during the present work, as detailed in section 7.2.3.2, indicated that an increase in the number of extrusion cycles led to a decrease in the detection of the original turning marks and an increase in the characteristic uni-directional flow marks of the AFM process. Results by Williams, Rajurkar, and Rhoades (90,91,92,97), as detailed in section 5.4.1, stated that Scanning Electron Microscopy conducted on workpiece surfaces showed that conventional machining marks were removed within a small number

of extrusion cycles. Furthermore the major improvement in surface topography was seen after a few extrusion cycles with the flow lines becoming smoother and spaced further apart.

Therefore the AFM process can be viewed as a two stage processing operation, viz:

- a) Stage One where the improvement in surface roughness is the primary process with an associated stock removal, and
- b) Stage Two where the stock removal is the primary process with minimal improvement in surface roughness.

The optical surface topography photographs taken during the present work also indicated that a prolonged treatment resulted in an undulating surface. Przylenk (88), as reported in section 5.4.1, also detected ripples on the surfaces of components as the number of extrusion cycles increased, and concluded that they were due to a combined effect of an increase in the extrusion pressure and the number of extrusion cycles. However, since the extrusion pressure was kept constant in the present work these undulations are thought to be exaggerations of the original turning marks. It is suggested that as the number of extrusion cycles increased the peaks of the original turning marks were removed, whereas the "troughs", depending upon their severity, were only partially honed. Coupling this effect with the fact that the whole surface in contact with the abrasive media is machined, and not just selective areas, the complete removal of the peaks and the gradual removal of the "troughs" results in a surface which has an undulating appearance. This appearance will therefore be dependent upon the original surface condition.

The results obtained during the preliminary work with respect to the effect of the medium re-use on the stock removed and surface roughness improvement, as detailed in section 7.1.2, indicated that as the usage of the medium increased there was a corresponding decrease in the stock removed as well as a smaller amount of improvement in the surface roughness. This is as expected since the results obtained with respect to the effect of abrasive grit wear on the stock removed, as detailed in section 7.1.3, indicated that an increase in the cumulative number of extrusion cycles resulted in the gradual deterioration and rounding of the abrasive grit particles. This is verified by results obtained by Rhoades (86) who concluded that stock removal was limited by abrasive grit wear.

8.3 Entrapped Air Contained within the Polyborosiloxane/grit Mixtures

Work conducted by Rudin and Leeder (101), consisting of capillary rheometry utilising a commercial polystyrene, concluded that an abrupt increase in the extrusion pressure due to compressibility was associated with a decrease in the free volume and a corresponding increase in the viscosity. The results obtained from the present work, in relation to both the 60 and 100 Mesh grit mixtures of the LV medium with grit to polymer ratios of 0.5 and 1, show that an increase in the pressure drop across the die was associated with a corresponding increase in viscosity, see figures 74, 87, and 88. The same observations were obtained when 60 and 100 Mesh grit was mixed with the MV medium using grit to polymer ratios of 0.5 and 1, see figures 77, 89, and 90. It is tentatively suggested that this phenomena observed in the present work are associated with the expulsion of entrapped air contained within the medium, resulting in a corresponding decrease in the free volume and an associated increase in both the pressure drop and viscosity.

The increase in viscosity associated with the LV medium was exhibited in the first extrusion cycle alone. Thus it is assumed that this was due to entrapped air within the medium which occurred during chamber loading. Furthermore since the viscosity of LV medium was low the entrapped air was expelled easily under the applied extrusion pressure during the first cycle.

The observations of an increase in viscosity experienced by the MV medium in the present work can also be attributed to the removal of entrapped air. This is supported by practical experience that when the medium was left overnight "air bubbles" were seen on the surface of the mixture. Furthermore as the medium usage increased the rate of increase in pressure drop decreased. Thus it is tentatively suggested that the viscosity of the MV medium does not permit expulsion of entrapped air at the same rate as the LV medium but that the increase in viscosity of the base medium results in a greater time required to expel air from the matrix. In addition it is possible that there is an associated effect due to structural changes occurring within the base polymer as a consequence of the shear history effect.

8.4 The Shear History Effect

Polyborosiloxane exhibits shear thinning thixotropic behaviour (95,96) due to its viscoelastic properties resulting from molecular entanglements (102). Work conducted by Benbow (103) on polymethyl siloxanes described the associated viscoelasticity in terms of an entanglement network. The entanglement points of which comprised of either permanent covalent bonds or transient van der Waals interactions, which on the application of a shear stress moved in the direction of flow. Additional applications of larger shear stresses caused further molecular orientation along the direction of flow. It is further documented (39,104) that on

release of the shearing stress the molecules recoil and are pulled back by the covalent bonds/van der Waals forces. These elastic properties coincide with the viscous flow and are manifested by features such as die swell, "melt fracture", "sharkskin, and frozen-in-orientations (39,41). The observation of die swell was observed during the present unclamping procedure, thus providing a visual indication of the presence of viscoelastic effects.

8.4.1 Factors Governing Viscoelastic Effects

The effects of viscoelasticity are influenced by molecular structure, which is itself governed by the molecular weight average, chain branching, and chain rigidity, (as outlined briefly in section 3.1.3). The molecular weight average is the most influential of these three variables.

The polyborosiloxane media utilised in the AFM process consist of one base medium with additions in various quantities of other polyborosiloxane compounds, lubricants, and plasticisers and/or reducers (98). However, the precise compositions of these mixtures are not in the public domain due to the commercially sensitive nature of the information. The only rheological identifications of the base media are qualitative and are based upon the commercial identifications of the base media, i.e. low, medium, and high viscosity. Therefore any effects arising from differences in the molecular weight averages cannot be discussed. This would also have repercussions on any discussion of any effects due to chain branching and rigidity.

8.4.2 Frozen-in-Orientation

The phenomena of frozen-in-orientation is a further consequence of molecular structure and elastic properties.

As a polymer melt flows along a die the molecules tend to align and uncoil. The degree of orientation is dependent upon the molecular structure and process variables. When the polymer melt cools there may be insufficient time for the molecules to regain their original orientations. As a result frozen-in-orientations occur. A measure of the time necessary for the molecules to recoil after deformation is given by the relaxation time (natural time), λ . The derivation of which is obtained from the Maxwell model, as outlined in section 3.1.1.3, viz:

$$\tau = \tau_0 e^{-\left(\frac{t}{\lambda}\right)} \quad (56)$$

where, λ = the relaxation time
t = the processing time

The relaxation times in relation to the Maxwell model for shear and tensile forces are:

a) Shear

$$\lambda = \frac{\eta}{G} \quad (57)$$

where, G = the shear modulus in flow.

b) Tension

$$\lambda = \frac{\bar{\eta}}{E} \quad (58)$$

where, E = Young's modulus

The ratio of the relaxation time to the processing time, t , is known as the Deborah number, N_D . If $N_D < 1$ the fluid behaviour is viscous, whereas if $N_D > 1$ the fluid behaviour is elastic.

8.4.3 The Explanation for the Occurrence of the Shear History Effect in the Present Work

It should be re-emphasised that polyborosiloxane exhibits flow at ambient temperatures similar to that exhibited by polymers at much higher temperatures in their molten state. It is probable that this characteristic of polyborosiloxane in conjunction with frozen-in-orientations and relaxation time effects results in the so called shear history effect.

During the extrusion of the polyborosiloxane medium in the AFM process an increase in the medium temperature occurs with a corresponding decrease in the viscosity, which would be expected to facilitate the alignment of the molecular chains. Once machining is finished the polymer is removed from the extrusion chamber and left to cool in air. It is during this stage that the original molecular orientation is gradually restored. However, the relaxation time required for complete recovery is longer than the time required for the temperature of the medium to fall to such a value that the next run in the experimental sequence could be commenced. This would imply that the Deborah number is less than 1 and the medium behaviour is viscous. Also during this recovery period the cooling

of the medium is associated with an increase in viscosity. Therefore the combination of these two effects results in frozen-in-orientations within the polymer structure. This leads to a degree of molecular alignment which would be expected to facilitate extrusion since greater pressures could be exerted on an aligned structure than on a randomly orientated structure. This effect would account for the observed increase in the overall pressure drop during successive extrusion cycles. Continual extrusion will result in further molecular alignment and corresponding frozen-in-orientations when the medium is left to air cool, resulting in a further increase in the pressure drop across the die. However, there would come a point when all the molecular chains are aligned and there would be no further increase in the pressure drop behaviour; as is shown in figure 100(a). An additional factor in this molecular alignment hypothesis is that as the number of extrusion cycles performed in an experimental run are increased there is an associated increase in the rate of molecular alignment. This would imply that the maximum pressure drop would be attained sooner. All these features are shown in figure 101.

When the polyborosiloxane medium is left to stand overnight a sufficient relaxation time is experienced such that extensive structural recovery is possible. Therefore the Deborah number is greater than 1 and the medium behaviour is elastic. Thus when extrusion is halted for a significant period there is a decrease in the pressure drop associated with the recovery of the molecular structure, as shown in figures 100 and 101.

This hypothesis is applicable to all mixtures of the LV, MV and HV media used in the present work.

8.5 The Rheological Parameters

This section discusses the effect of temperature and pressure on the viscosity of the media used in the AFM process irrespective of the grit to polymer ratio, grit size, and classification of base viscosity.

8.5.1 The Temperature and Pressure Variables

Viscosity is dependent upon both temperature and pressure, and as stated in section 3.1.3 the relationship between pressure and viscosity is qualitatively similar to that of the relationship between viscosity and temperature but opposite in sign (44).

Figures 116 to 121 show in all cases the effect of the change in temperature during a run on both the average pressure drops across the die and the associated viscosity measurements. These figures indicate that an increase in the temperature resulted in a decrease in the viscosity with a corresponding increase in the average pressure drop in all but one case. The exception to this trend was the LV medium with 60 Mesh grit with a grit to polymer ratio of 1 which exhibited a decrease in both the viscosity and average pressure drop as the temperature increased. These results with respect to pressure are not as would be expected and are discussed in section 8.5.1.2.

8.5.1.1 The Effect of Temperature on the Viscosity

It should be expected that as the number of extrusion cycles increases there would be a corresponding increase in the temperature since the act of shearing the medium generates heat. In addition the machining action of the abrasive grit in contact with the die surface would also produce heat. The relationship between viscosity and temperature has been obtained by previous research (95,96), as

detailed in section 5.4.2, which examined the effect of temperature on the viscosity of the pure medium and concluded that the viscosity of the base polymer was significantly affected by temperature. This is confirmed by the present work.

8.5.1.2 The Effect of Average Pressure Drop on Viscosity

As stated above a decrease in viscosity would be expected to be associated with a decrease in pressure. However, in the present work this association was only found with the LV medium and 60 Mesh grit with a grit to polymer ratio of 1. All other mixtures showed an increase in pressure as the viscosity decreased. There are two possible explanations for the occurrence of this increase in pressure, viz:

1) The results used in the presentation of the effect of temperature and pressure on viscosity utilised average pressure drop measurements since from these values the viscosities were calculated. The parameters that should have been used to observe the relationship between the viscosity and pressure was that of the pressure drop across the die. This is illustrated by figure 122 which shows the effect of temperature on the pressure drop across the die for selected mixture combinations and is also illustrated by figures 71(a) and 93(a). All these figures show that when the rate of temperature rise increased significantly there was an associated decrease in the pressure drop across the die corresponding with a decrease in the viscosity of the medium.

2) A further factor which may have accounted for the discrepancy between the viscosity and pressure relationship was that which occurred as a result of the shear history effect as detailed in section 7.2.8. The pressure drop across the die increased as the medium usage increased, therefore the

average pressure drop would have also increased. This would have resulted in an increase in the pressure as the viscosity decreased. The only available means to overcome this effect and to achieve a more representative average pressure drop, would have been to use fresh medium for every run conducted. This would have been unrealistic due to the high cost of the medium. An alternative to this would have been to leave the medium to stand in between each run for a significant period thus permitting "complete" molecular recovery. However, this would have been too time consuming and not feasible given the time constraints.

8.6 The Relationship between the Rheological Behaviour and the Machining Characteristics

The discussion of this relationship involves the examination of two effects, viz:

- 1) the effect of the temperature rise on the viscosity and volumetric flow rate, together with the corresponding die mass change per cycle, and
- 2) the effect of an increase in the number of extrusion cycles on the viscosity and the total die mass change and percentage surface roughness improvement.

Even though the former relationship is a subsidiary of the latter it is discussed first in section 8.6.1 because its explanation simplifies consideration of the data in the latter as discussed in section 8.6.2.

8.6.1 The Effect of Temperature on the Rheology and the Machining Performance

Figures 123 to 128 present the relationships between temperature rise and (i) the viscosity, (ii) the volumetric flow rate, and (iii) the die mass change per cycle.

These figures show for all mixtures, irrespective of grit to polymer ratios, an increase in the number of extrusion cycles produced a corresponding increase in the medium temperature, as detailed in section 8.5.1.1. This temperature rise resulted in an associated decrease in viscosity, which in turn led to a decrease in the overall processing time. Since the volume extruded increased linearly with the number of extrusion cycles and the overall processing time increased non-linearly, an increase in the corresponding volumetric flow rate resulted. The changes in these rheological dependent parameters were associated with a decrease in the amount of stock removed per cycle, as shown by figures 123 to 128. However, although there appears to be a direct relationship between the decrease in viscosity, increase in volumetric flow rate, and decrease in stock removed per cycle within the results obtained from the same medium there is not an overall relationship that can be applied to the results from all the media. There must therefore be an additional influential factor that cannot be isolated in the present work.

The results of previous research as discussed in section 8.5.1 indicated that the base medium viscosity was significantly affected by temperature. As the results obtained from the present work indicate this temperature dependency of the base medium also affects the machining performance of the abrasive containing media.

Figures 123 to 128 would further indicate that the stock removed per cycle was inversely proportional to the volumetric flow rate. This observation would also imply that the total stock removed is dependent upon the volumetric flow rate. However, research by Williams, Rhoades and Rajurkar (90,91,92,97) concluded that changes in the flow rate, with the volume held constant, had no significant effect on the stock removed. This conclusion was based on work where the

volumetric flow rate was controlled by altering the temperature of the medium. Therefore the present work would contradict this conclusion. The reason for this discrepancy is probably that temperature rises have significant effects on the rheological properties of both pure and abrasive-laden polyborosiloxane, which would, as shown by the present work, have significant effects on the volumetric flow rates and the corresponding amount of stock removed.

8.6.2 The Overall Effect of Rheology on Machining

Figures 129 to 134 summarise the relationship between the rheological and the machining characteristics for all mixtures by the examination of the effect of an increase in the number of extrusion cycles on (i) the viscosity, (ii) the total mass change, and (iii) the percentage surface roughness improvement. The corresponding shear stresses are also included in these figures.

All the previous correlations discussed in sections 8.1 to 8.5 indicate that:

- 1) as the number of extrusion cycles increased there was an increase in the total mass change and a corresponding improvement in the surface roughness. The latter parameter achieved a maximum value within a specific number of extrusion cycles after which it did not exhibit significant change. This feature was specific to each medium/grit combination.
- 2) as the number of extrusion cycles in a run increased the viscosity decreased.

For those cases when the medium was left overnight these effects were still observed when machining was recommenced.

There is no single dominating factor governing these effects since all the rheological and machining parameters appear to be inter-dependent. An increase in the number of extrusion cycles results in a decrease in the stock removed per cycle and hence a non-linear increase in the total stock removed. This is probably due to the associated decrease in viscosity and increase in volumetric flow rate associated with the increase in the temperature of the medium. This rise in temperature is due to the combination of the polymer shearing, the machining action of the grit particle, and the friction between the grit/polymer mixture and the die surface. Furthermore as the number of extrusion cycles in an experimental run increase the peaks on the die surface available for honing diminish. This, in conjunction with the decrease in viscosity as the number of extrusion cycles increase, suggests that the greater part of the surface roughness improvement and stock removal is achieved whilst the medium viscosity is relatively high, so that when the viscosity decreases the maximum surface roughness improvement has been achieved with marginal improvement occurring thereafter. However, stock removal will still occur due to the mechanics of the process but at a significantly reduced rate.

An extreme example illustrating the dependence of the machining performance on changes in the medium viscosity is shown by the MV medium with 100 Mesh grit and a grit to polymer ratio of 0.5, figure 132(a). This figure shows that for the 20 and 30 extrusion cycle runs both the total stock removed and the improvement in surface roughness decreased. This reversal in the relationship between the machining parameters and the number of extrusion cycles coincided with changes in the relationship between the number of extrusion cycles and the temperature and pressure profiles, as illustrated by figures 97(a) and 76(a) respectively. Figure 97(a) shows there was a significant increase in the medium temperature during

the latter stages of the 15, 20 and 30 extrusion cycle runs which was associated with a corresponding decrease in the pressure drop, figure 76(a). Therefore an increase in the number of extrusion cycles apparently resulted in a decrease in the viscosity, an associated increase in the volumetric flow rate, and a decrease in the stock removed per cycle. Hence the total amount of stock removed and surface roughness improvement decreased as the viscosity decreased.

8.6.2.1 The Effect of Shear Stress on the Machining Performance

Figures 129 to 134 show the effect of an increase in the number of extrusion cycles on the shear stress together with the machining parameters. These figures show that in all cases the shear stress either increased or remained constant as the number of extrusion cycles increased, and that there were only slight differences between the shear stresses exhibited by the different media. It would be expected that the shear stress would exhibit a correlation with the machining performance. However, this was not the case. This was possibly because the average pressure drop values used to calculate the shear stresses are subject to discrepancies, as discussed in section 8.5.1.2. Therefore these discrepancies and their associated effects would be transferred to the shear stress measurements. An indication of the influence of the shear stress is thought to be possible by the examination of the pressure drop behaviour. This is possible since the calculation of the shear stress is dependent upon both the pressure drop across the die and the die radius. If it is assumed that during a run the die radius remained constant, due to the marginal differences in the amount of stock removed, the shear stress can be related to the trends obtained for the pressure drop across the die, figures 72 to 80. However, when this correlation is examined it is evident that once again the machining performance is not obviously affected by the shear stress alone.

8.7 The Effect of Alterations in the Base Viscosity, Grit Size, and Grit to Polymer Ratio on the Rheological and Machining Parameters

Sections 8.1 to 8.6 discussed the general machining and rheological behaviour exhibited in all cases. However, each of the three variables of base viscosity, grit size, and grit to polymer ratio and their effect on both the machining and rheological parameters will be discussed separately in the following section.

The effect of the viscosity of the base medium and grit to polymer ratio on the aforementioned parameters have been subjected to a semi-quantitative analysis. This involved the averaging of all the relevant results obtained from the 30 extrusion cycle runs applicable to identical medium types and grit to polymer ratios. This would enable an overall assessment to be made in relation to the effect of grit to polymer ratio on the machining and rheological parameters whilst disregarding the effect of the medium viscosity. This method would also enable the effect of the viscosity of the medium to be assessed whilst disregarding the grit to polymer ratio. It must be highlighted that this analysis method ignored any effect due to grit size since it is assumed that any effect manifested would be common to all results. The results thus produced are presented in tables 43 to 50.

A similar analysis was conducted to assess the effect of grit size on the rheological and machining parameters. However, this analysis consisted of averaging the results obtained from the 30 extrusion cycle run in relation to identical base medium and grit size. It must be emphasised that this analysis ignored any effects arising from the different grit to polymer ratios employed since it was again assumed that any discrepancy manifested would be common to all results. The results corresponding to this analysis are presented in tables 51 to 58.

8.7.1 Viscosity of the Base Polymer

The differences in the viscosities of the three media employed in the present work were expected to have a notable effect on the machining performance. This was because an increase in the viscosity of the base medium would be expected to produce an associated increase in the shear stress at the wall. Hence the amount of force transmitted to the grit particles at the wall should have been greater and might be expected to result in a corresponding increase in the amount of machining. However, the actual machining performance realised did not follow this trend but appeared to be independent of the base viscosity, as illustrated by tables 43 to 45. This contradicts the results discussed in sections 8.6.1 and 8.6.2 which suggest that there would appear to be a direct relationship between the variation in the viscosity behaviour during an experimental run, irrespective of the type of medium used, and the associated machining performance. Therefore it is suggested that:

- 1) the type of base medium alone does not affect the machining performance because a clear overall relationship is not exhibited between the viscosity and machining parameters,
- 2) there would appear to be a relationship between the viscosity and machining parameters when the results obtained from a single medium type are considered.

The results in tables 40 to 42 show that the overall effect of the viscosities, irrespective of grit size and grit to polymer ratio, on the stock removal and surface roughness parameters were:

Qualitative Effect of Base
Medium on the Parameter Stated

a) Die diameter change	MV > LV > HV
b) Die mass change	MV > LV >> HV
c) Percentage surface roughness improvement	LV > MV >> HV

These results showed that there was very little difference in the machining performance of the LV and MV media. However, the corresponding machining performance of the HV medium was significantly less than either of the other media.

Research conducted by Przylenk (88) and Rhoades, Williams and Rajurkar (90,91,92) concluded that an increase in the base viscosity resulted in an increase in the stock removed. Therefore there are two sets of opposing data which may once again be accounted for by the differences in the medium compositions employed, i.e. the different constituent elements and the quality of mixing and level of homogeneity obtained. In addition to this the media viscosities examined by Rhoades et al consisted of LV, MV and MHV where it is assumed that the MHV is a composite of the HV and MV media with the principal constituent being the MV medium. Therefore it is not possible to eliminate the possibility that the MHV behaviour is closer to the behaviour exhibited by the MV medium. Hence due to the similar rheological behaviour of these two media and the addition of the higher viscosity material to the MHV medium an increase in the observed machining performance may be exhibited. In contrast in the present work the HV medium exhibited significantly different rheological trends to that of the MV medium. In addition the viscosity results referred to in the present work are quantitative and provide specific values to the media employed. Therefore genuine differences

between the viscosities of the media were attained that could be related with certainty to the corresponding machining data, whereas the previous work used qualitative means of viscosity identification. Therefore even though the differences between the viscosities of the various media used in the previous work appears to be large neither the validity of these viscosities or the relation of such viscosities to the machining performance can be verified due to the qualitative nature of the viscosity identification.

Rhoades et al (90,91,92) also concluded that the higher viscosity media removed stock uniformly whilst the lower viscosity media caused edge radiusing. Evidence obtained from the present work disputes this conclusion, see figure 135. This figure shows the surface edge condition on three separate dies after 30 extrusion cycles using LV, MV and HV media with 100 Mesh grit and a grit to polymer ratio of 1 respectively. The experience gained from the present work would indicate that the machining conditions such as tooling, temperature, and the number of extrusion cycles performed are responsible for both the onset and degree of edge-radiusing sustained. These conditions and their effect on the edge surface conditions are applicable to all media used in the AFM process and are not purely limited to low viscosity media.

Even though there was no correlation between the machining performance and the media viscosities of the three media types used in the present work, the variables affecting the rheological parameters of the media employed showed similar trends to those produced by variations in the viscosities, (tables 43 to 47), i.e.:

The processing times followed the sequence:

HV >> MV >> LV

The temperature rises exhibited were:

LV >> MV >> HV

Since viscosity is inversely proportional to temperature, and volumetric flow rate is inversely proportional to both processing time and viscosity, the expected results for volumetric flow would be:

LV >> MV >> HV

which in fact was the observed order of volumetric flow rates. The results obtained in relation to the pressure drops were:

HV > MV > LV

Since viscosity is proportional to pressure drop it would be expected that the viscosities of the media would also produce the same order, which was the case.

A further observation of the present work was that the energy required to obtain machining using the HV medium was not warranted in terms of its machining performance.

8.7.2 Grit to Polymer Ratio

The average results obtained from the combination of the measurements relating to each of the three grit to polymer ratios with respect to the machining and rheological parameters are presented in tables 43 to 50. The most significant correlation between the machining and rheological parameters was that a grit to polymer ratio of 2 produced the greatest machining action.

Previous work conducted into the effect of grit content (88) concluded that an increase in the grit to polymer ratio resulted in an increase in both the viscosity and the processing time. The present work would concur that the medium viscosity is dependent upon the grit to polymer ratio, although it is suggested that as the grit to polymer ratio increases the viscosity decreases. However, the results obtained from the mixture with a grit to polymer ratio of 1 showed a deviation from this relationship since an increase in the viscosity was exhibited. A further discrepancy between the results of the previous and present work is that in the latter case the processing times decreased as the grit to polymer ratio increased. This latter effect corresponds to the differences between the viscosities, see tables 47 and 50, i.e. the viscosity decreased as the grit to polymer ratio increased hence there was an associated decrease in the processing time.

It is probable that as the grit to polymer ratio is gradually increased the grit/polymer mixture becomes a network of grit containing isolated clusters of polymer. It is suggested that this results in a reduction in the viscous fluid flow characteristics since the mixture now exhibits characteristics more typical of a solid. There is a corresponding decrease in the viscosities and an associated decrease in the processing times.

The average temperature rise, as shown in table 46, decreases as the grit to polymer ratio increases to 1. As stated above there is less polymer present in the matrix as the grit to polymer ratio increases; therefore it is suggested that the heat generated by the shearing action of the polymer diminishes and is not compensated for by the heat generated by the machining action of the grit particles. However, when the grit to polymer ratio is increased from 1 to 2 there is such a large amount of grit present in the matrix that the heat generated by machining results in a substantial increase in the temperature rise.

An increase in the grit to polymer ratio also resulted in a decrease in the pressure drop across the die. However, this effect was not associated with a corresponding change to the stock removal results, except for those mixtures with grit to polymer ratios of 2. In these cases it would appear that the large amount of grit particles contained in these mixtures compensated for the fact that these mixtures were subject to the shortest processing times, the smallest pressure drops, and the smallest viscosities.

Both the die diameter change and the percentage surface roughness improvement results, (tables 43 and 45), show that the effect of the grit to polymer ratios on the machining performance to be:

$$2 > 0.5 > 1$$

Contradictory results were obtained in the case of the die mass change, (table 44), which showed that the effect of the grit to polymer ratio on the machining performance was:

$$2 > 1 > 0.5$$

This is surprising since the results in relation to the die mass change were expected to be similar to those relating to the other machining parameters.

The machining performance of the mixtures with grit to polymer ratios of 0.5 and 1 also produced unexpected results. It is suggested that this was due to associated differences in the rheological characteristics exhibited by these mixtures, irrespective of the type of base medium involved, and their subsequent effect on the machining performance, viz:

The greater machining produced by mixtures with grit to polymer ratios of 0.5 than that obtained from the mixtures with grit to polymer ratios of 1 is possibly associated with the average pressure drop, processing time, and volumetric flow rate results, (tables 47 to 49). The effect of the grit to polymer ratios on these aforementioned variables was:

- a) Pressure drop: $0 > 0.5 > 1 > 2$
- b) Processing Time: $0 > 0.5 > 1 > 2$
- c) Volumetric Flow Rate: $0 > 1 > 2 > 0.5$

It is suggested that the longer processing time and larger average pressure drops associated with the mixtures of grit to polymer ratios of 0.5, in conjunction with the smaller volumetric flow rates, permitted greater machining for longer periods than those of the mixtures with grit to polymer ratios of 1.

It must again be re-emphasised that there appears to be a relationship between the grit to polymer ratio and its associated effect on both the rheological behaviour and the machining performance within the results obtained from the same

medium, but that there is no overall relationship that can be applied to the results from the different types of media used. This is possibly due to the fact that the relationship between the rheological parameters and machining performance is associated with the grit to polymer ratio and not the type of medium employed, i.e. the effect of grit to polymer ratio is not only associated with viscosity, but also some other parameter.

8.7.3 Grit Size

The results in relation to the effect of grit size on the machining and rheological parameters are presented in tables 51 to 58. It would appear that the majority of the variables relating to the rheological parameters, (tables 51 to 55), are independent of grit size. The exception was the pressure drop measurements which showed that an increase in the grit size resulted in an increase in the average pressure drop. The results of increasing the grit size on the machining parameters, (tables 56 to 58), indicate that an increase in grit size produced an improvement in all machining parameters which it is suggested was associated with the increase in the average pressure drops as the grit size increased.

It is also suggested that the rheological parameters in the present work were unaffected by grit size since all the polymer/grit mixtures used contained the same volume of base polymer. This occurred since the mixtures were provided in quantities of 5kg irrespective of grit size; therefore when a grit to polymer ratio was stipulated the quantities of grit and polymer were calculated so as to obtain 5kg of grit/polymer mixture at the specified ratio. Hence the same amount of polymer in the matrix in relation to the grit size should have been present and similar volumes of mixtures should have been provided, as was the case, see table 2.

The present results of the effect of grit size on the machining performance are in accordance with previous work (88), i.e. an increase in the grit size produced an increase in the amount of stock removed.

Work conducted by Borchers (87) concluded that (i) an increase in the grit size resulted in an increase in edge radiusing, and (ii) finer grit produced improved surface roughness. However, the present work refutes the suggestion that edge radiusing was dependent upon grit size alone since as stated in section 8.7.1 edge radiusing is considered to be an effect associated with tooling, medium temperature, and number of extrusion cycles. Therefore the essential conditions must exist in order for edge radiusing to occur and an increase in grit size will only compound this effect. Hence the grit size is not solely responsible for the occurrence of edge radiusing. Furthermore the present work indicates that the greatest improvement in surface roughness was associated with coarse rather than fine grit.

8.7.4 The Combination of the Effects of Base Viscosity, Grit Size, and Grit to Polymer Ratio on the Machining Performance

The combination of the effects of the viscosity, grit size, and grit to polymer ratio indicate that the overall machining performance is affected thus:

Medium type	MV > LV >> HV
Grit to polymer ratio	2 >> 0.5 > 1
Grit size	60 >> 100

Therefore from the above combinations of the present work the best machining action would be expected to be produced by the MV medium with 60 Mesh grit and a grit to polymer ratio of 2. Whilst the least machining action would be

expected to be produced by the HV medium with 100 Mesh grit and a grit to polymer ratio of 1. The former of these predicted results was obtained but the least machining was exhibited by the HV medium with 100 Mesh grit with a grit to polymer ratio of 0.5.

Summarising all the individual results in tables 43 to 58 it can be seen that the best machining actions while utilising the various grit to polymer ratios with respect to the medium type and grit size were:

- i) for a grit to polymer ratio of 0.5 the LV medium and 60 Mesh grit,
- ii) for a grit to polymer ratio of 1 either the LV or MV media with 60 Mesh grit, and
- iii) for a grit to polymer ratio of 2 the results indicate that due to the large grit content there were only marginal differences between the machining actions of all media.

Therefore the variables which have a combined effect on the machining performance are the base medium viscosity, grit size, and grit to polymer ratio. This corresponds to previous work (88) that concluded the variables having the greatest effect on machining were the abrasive grit content, grit size, and base medium viscosity. However, the present work also indicates that the most important variable of these three parameters is the grit to polymer ratio. Increasing this parameter had the most significant consequences on the other variables, (i.e. the temperature, processing time, pressure drop, and viscosity), since the magnitudes of these parameters all decreased. Therefore the combined effect of these changes result in a decrease in the machining performance since as stated previously the viscous fluid flow characteristics of the mixtures are significantly

altered. However, it is not simply the changes in the base viscosity which accounts for the decrease in machining performance since as already stated viscosity does not have any significant effect on the machining behaviour. In addition the changes in machining performance are only highlighted when examined in relation to changing the grit to polymer ratio whilst utilising the same medium. Thus it is tentatively suggested that as the grit to polymer ratio increases changes occur within the matrix which not only affect the viscosity of the base medium, but also have an effect on both the grit distribution within the matrix and the molecular structure which affect the subsequent machining performance. When the machining performance is examined with respect to the different media used there is no relationship between viscosity and machining performance because of the initial differences in the molecular structures of the base media. Furthermore when a grit to polymer ratio of 2 is utilised any detrimental effects associated with the change in fluid flow characteristics is eclipsed by the machining action produced by the large grit content within the matrix.

In addition the present work indicates that the temperature is a variable which affects the machining action. Although it was also concluded in previous work (88) that a minimal effect on the machining action was produced by the temperature. However, since the polyborosiloxane medium is an inorganic polymer with properties of inertness and heat resistance any heat generated during machining would not be dissipated readily and would therefore cause the temperature rise to be further magnified. However, it is suggested that this effect is modified by the addition of grit into the matrix since the grit particles will act as heat conductors. The corresponding data is presented in table 46 and shows that as the grit to polymer ratio increases from 0 to 1 there is a corresponding decrease in the temperature rise. However, the mixtures with grit to polymer

ratios of 2 show an increase in the temperature rise which may be associated with the much larger machining rates produced with these mixtures, as detailed in sections 7.2 and 7.3, and the smaller amount of polymer in the matrix to disperse the heat generated.

The shear history effect of the medium as detailed in section 8.4.4 is an additional factor that influences the machining performance. An increase in the medium usage and hence shear history results in an increase in the pressure drop across the die which will have some beneficial effects with respect to the machining operation.

8.8 The Proposed Machining Mechanism

The results from the complete set of results obtained in the present work show no distinct overall correlation between the rheological parameters and the associated machining performance. Thus there must have been other factors associated with the machining mechanism that were probably occurring on a micro-level, and as such could not be detected during the present work. The next obvious step in attempting to discuss the machining action of the AFM process would be on a micro-scale and in relation to the results obtained from identical medium types.

8.8.1 The Polyborosiloxane/Grit Mixture

In section 8.4 it was stated that polyborosiloxane exhibits viscoelastic properties due to a network of molecular entanglements. It is suggested that the viscoelastic properties of the base polymer used in the AFM process are affected by the following variables:

1) The Grit to Polymer Ratio

The effect of adding grit particles into the base polymer would be to observe a decrease in the viscoelastic behaviour of the base polymer since the amount of polymer present in the matrix decreases. This effect is supported by the results in table 50 that show an increase in the grit to polymer ratio results in a decrease in the averaged viscosities. An inconsistency in the aforementioned relationship was exhibited by the mixture with a grit to polymer ratio of 1, and was such that an increase in the average viscosity was shown. It is suggested that the significant increase in the average viscosity exhibited by the mixture with a grit to polymer ratio of 1 was due to the extremely high value of the viscosity calculated for the HV medium. Therefore even though this increase in viscosity is believed to be representative it must be emphasised that it is thought to be significantly exaggerated and it is suggested that there would be marginal differences in the viscosities of the mixtures with grit to polymer ratios of 0.5 and 1. The effect of the grit additions on the viscoelastic properties of the mixtures with grit to polymer ratios of 0.5 and 1 would appear to be related to the machining performance in relation to the associated pressure drops, processing times, and volumetric flow rates, as discussed in section 8.7.2. However, in the case of the mixtures with grit to polymer ratios of 2 it has been suggested that the quantity of grit particles present in the matrix compensates for the breakdown of the relationship between the viscoelastic properties and the corresponding machining performance.

2) The Shear History Effect

As detailed in section 8.4.4 it was proposed that the shear history effect exhibited by certain media would influence the entanglement network and hence the viscoelastic properties of the medium. Therefore it would be expected that the associated rheological behaviour would affect the machining performance.

3) The Composition of the Base Medium

As already discussed in section 8.4.1 the composition of the base polymer would affect the entanglement network due to the effect of the constituent elements on the molecular structure. However, due to the lack of relevant information in relation to the constituent elements the effect cannot be assessed. It is therefore tentatively suggested that the differences in the constituent elements between the different media may partially account for the lack of correlations between the rheological and machining parameters of the different media used in the present work.

8.8.2 The Machining Mechanism

It is proposed that when the polymer/grit mixture is extruded through the die the grit particles become held "in-situ" in the matrix, and those grit particles in contact with the surface begin to hone. It is a reasonable assumption that the grit particles hone the die surface by the action of a combined shear and normal force that originate from the applied extrusion pressure, (termed the applied force in the text below).

The large negative rake angles associated with machining processes that utilise grit particles result in a machining action that involves ploughing and the formation of a prow ahead of the grit particle, as detailed in sections 2.1 and 2.3. The formation of a prow ahead of the grit particle would be expected to produce a restraining force on it. Hence the restraining force experienced would be expected to continually increase as the prow ahead of the abrasive grit particle increased, thus requiring the applied force to increase in order to maintain the movement of the grit particle and the machining action. However, if the applied force were not to increase then it is a reasonable assumption that the restraining force dominates the force system such that further machining is prevented and the grit particle is forced back into the medium, i.e. the grit particle is "absorbed" by the medium. It is therefore tentatively suggested that when the restraining force is large enough so that either partial or complete "absorption" of the grit particle into the medium occurs, the honing action stops. This would imply that the furrow made by the grit particle decreases as the opposing force increases, evidence of which can be seen in figure 30. Furthermore it is proposed that a single grit particle does not remain in contact with the workpiece surface throughout the honing process but that there is a degree of grit movement and rotation as a result of medium displacement.

As previously stated the applied force is assumed to originate from the applied extrusion pressure that is transmitted to the grit particle via the medium. Therefore it is suggested that the viscoelastic properties of the medium are of significance since this will determine the amount of force that is able to be transmitted to the grit particle. As the number of extrusion cycles increase the medium temperature increases resulting in an increase in the volumetric flow rate and decrease in the medium viscosity. Therefore it is further suggested that as the viscosity decreases

the restraining force becomes larger relative to the applied force, resulting in an increase in the "absorbency" of the medium and a corresponding decrease in the amount of stock removed per cycle, i.e. the medium viscosity would govern the extent to which the grit particle is "absorbed" and thus the amount of machining performed. This would also imply that a decrease in medium viscosity results in a decrease in the duration of contact between the grit particle and the die surface, as well as a corresponding decrease in the length of the abrasive stroke.

It is also suggested that as the grit to polymer ratio increases there is a decrease in the amount of base polymer in the matrix. Hence there will be a corresponding decrease in the "absorbency" of the grit/polymer mixture. This decrease in the absorbency results in a greater machining action since the abrasive particle is more constrained and therefore stays in contact with the workpiece surface for longer periods. This is supported by the results obtained from the mixtures with grit to polymer ratios of 2 since these mixtures exhibited the greatest machining action. In the case of the mixtures with grit to polymer ratios of 0.5 and 1 the machining performance was not as expected; the reasons for which are due to the rheological behaviour of these mixtures as detailed in section 8.7.2. However, the above hypothesis for their machining actions is still applicable.

An additional influencing factor of the machining mechanism observed during the experimental stage of the present work, and confirmed by a previous theory of earlier work (96), was that when significant temperature rises were encountered with corresponding decreases in viscosity the abrasive grit held in the matrix separated under the influence of the gravitational force. This is because the density difference between the base medium and abrasive grit was insufficient to maintain the buoyancy force required to maintain the grit in suspension in the

polymer. Hence further significance is placed on the temperature behaviour of the medium during machining.

8.8.3 Slip-Stick

The observation of slip-stick in previous work (94) was not in evidence during the present investigation. However, since commercial equipment was used without any modifications the procedure may not have been sensitive enough to detect any slip-stick behaviour. If slip-stick were to be observed during the present work it would have been expected to be detected whilst the LV medium was used. This is because of the large temperature rises experienced by this medium which possibly would have caused the medium to experience adhesive behaviour. However, it is suggested that the large volumetric flow rates and grit additions would have disrupted any regions of slip-stick behaviour.

Also any phenomena due to slip-stick would have been expected to be associated with surfaces of low surface roughness values since surfaces with high surface roughness values are honed at a fast rate; therefore if slip-stick was present honing would take longer due to the medium sticking and thus preventing honing of the surface underneath. Additionally the optical photographs shown in figures 59 to 64 illustrate in the majority of cases the presence of uniform surfaces. As stated the observed undulations in the surfaces were due to the exaggeration of the original turning marks by the AFM process. However, if slip-stick had been experienced, areas on the same die surface would have been expected to exhibit large differences in the surface roughness measurements, which was not in evidence.

Furthermore if any degree of stick-slip were to be manifested then it would be suggested that the amount of stock removed per cycle would fluctuate since occasionally there would be no machining action due to a barrier of medium protecting the workpiece surface. However, the present work indicates the decrease in stock removal per cycle coincided with the attainment of the maximum surface roughness before changes in the rheological behaviour of the base polymer had any influential effects on the machining performance, i.e the decrease in viscosity, the corresponding force transmitted to the grit, and the "absorption" of the grit into the polymer.

9.0 CONCLUSIONS

- 9.1 An increase in the number of extrusion cycles results in an increase in the stock removed, an improvement in surface roughness, and an increase in the temperature of the medium.
- 9.2 A maximum improvement in surface roughness is achieved within a specific number of extrusion cycles that is dependent upon the grit to polymer ratio, medium type, and grit size utilised. Any additional machining performed after this point has minimal benefit with respect to the surface roughness improvement. This behaviour is shown to apply to all media types.
- 9.3 The relationship between the number of extrusion cycles and the stock removed is non-linear since the amount of stock removed per cycle decreases as the number of extrusion cycles increases. It is suggested that this is due to a combination of a decrease in the viscosity of the medium in conjunction with the decrease in the surface roughness.
- 9.4 As the medium re-use increases there is a corresponding decrease in both the stock removal and surface roughness improvement capabilities. This is probably due to the increase in grit particle wear as the cumulative number of extrusion cycles increases.
- 9.5 No clear relationship is exhibited between the base media types and the machining performance. However, a relationship is demonstrated between the machining results in relation to a mixture based on a specific medium type and their associated viscosity behaviour.

- 9.6** The greatest viscosities were exhibited by the HV medium, (25000Pa.s to 4000Pa.s), the least by the LV medium, (400Pa.s to 150Pa.s), and intermediate values were exhibited by the MV medium, (3500Pa.s to 500Pa.s).
- 9.7** Progression from the low to high viscosity base medium results in an increase in (i) the pressure drop across the die, (ii) the average pressure drop, and (iii) the processing time. Progression from the low to high viscosity base medium is also associated with a decrease in the rate of temperature rise.
- 9.8** The characteristic profiles illustrating the relationship between the number of extrusion cycles and both the temperature and pressure drop across the die are dependent upon the medium type and the grit to polymer ratio employed.
- 9.9** It is tentatively suggested that entrapped air contained within the matrix can affect the pressure drop across the die and hence the viscosity of the medium. In addition the rate of expulsion of any such entrapped air would be expected to increase as the viscosity of the base medium decreases.
- 9.10** The effect of edge radiusing is suggested to be dependent upon the combination of (i) the tooling design, (ii) the temperature, and (iii) the number of extrusion cycles performed, and not solely upon the viscosity classification of the base medium.

9.11 The results obtained would also imply that the viscoelastic properties of the base medium are affected by (i) the grit to polymer ratio, and (ii) the shear history effect, (see conclusion 9.15). It is also tentatively suggested that the compositions of the base polymer could have affected the viscoelastic properties of the base polymer, but this could not be verified.

9.12 The results in relation to the same medium type indicate that an increase in the grit to polymer ratio leads to a decrease in the processing time. In addition the order of grit to polymer ratios on the improvement in surface roughness, in ascending order, are:

1, 0.5, 2

The greatest stock removal is achieved by the mixtures with a grit to polymer ratio of 2 and the least by those mixtures with grit to polymer ratios of 1. Intermediate values are obtained with the mixtures with grit to polymer ratios of 0.5. The unexpected machining results of the mixtures with grit to polymer ratios of 0.5 and 1 are suggested to occur due to the difference in the parameters of pressure drop, processing time, and volumetric flow rate.

9.13 In relation to individual media types no distinct correlation is exhibited between the grit to polymer ratio and (i) the viscosity of the medium, and (ii) the average pressure drops. However, both the average viscosity and pressure drop results, irrespective of grit size and media type, indicate that an increase in grit to polymer ratio results in a decrease in the aforementioned parameters.

- 9.14** The average results obtained from the 30 extrusion cycle run in relation to identical medium types, grit to polymer ratio, and grit sizes would also indicate that an increase in the grit to polymer ratio up to 1 leads to a decrease in the rate of temperature rise; whereas for grit to polymer ratios greater than 1 the rate of temperature rise increases as the grit to polymer ratio rises. It is suggested that the latter effect is due to the increase in the machining action exhibited by the mixtures.
- 9.15** It has been shown that an increase in grit size from 100 Mesh to 60 Mesh leads to an increase in the machining performance. However, this change in grit size has a minimal effect on the rheological parameters.
- 9.16** An increase in the grit size also leads to an increase in (i) the pressure drop across the die, (ii) the average pressure drop, and (iii) the processing time. In relation to the mixtures with grit to polymer ratios of 0.5 and 2 increasing the grit size produces an improvement in the surface roughness, whereas the corresponding effect produced by mixtures with grit to polymer ratios of 1 are relatively unaffected by an increase in the grit size.
- 9.17** Temperature is an important variable in the AFM process due to its effect on the viscosity and subsequent machining performance. The results in relation to the same medium type show that an increase in temperature appears to result in (i) a decrease in the viscosity of the medium, (ii) an increase in the volumetric flow rate, and (iii) an associated decrease in the stock removal per cycle.

- 9.18** It is shown that there is a shear history effect associated with the amount of medium usage. It has been suggested that the manifestation of the shear history effect is due to a combination of molecular entanglements and frozen-in-orientations.
- 9.19** The shear history effect causes the viscosity and the pressure drop across the die to increase as the usage of the medium increases. It is suggested that the shear history would be of significance on the machining behaviour of a medium where it is manifested.
- 9.20** The results suggest that the machining performance is not solely dependent upon either the shear stress or the normal stress acting at the wall.
- 9.21** The factors that appear to influence the machining performance are the viscosity behaviour of a specific medium type, the grit size, and the grit to polymer ratio. The most influential of these parameters are the grit to polymer ratio and the variation in viscosity of the base medium during an experimental set of runs.
- 9.22** When the viscosity results obtained with a specific base medium are considered it is suggested that the greatest machining action is associated with higher values of this parameter.

9.23 It is suggested that the AFM process is comprised of two stages that are related to the conclusion stated in 9.22, viz:

- 1) Stage One where the improvement in surface roughness is the primary process with an associated stock removal, and
- 2) Stage Two where the stock removal is the primary process with minimal improvement in surface roughness.

9.24 From the results for all the mixture combinations the greatest machining performance is achieved by the MV medium and 60 Mesh grit mixture with a grit to polymer ratio of 2; whilst the least machining performance is achieved by the HV medium and 100 Mesh grit mixture with a grit to polymer ratio of 0.5. The results also indicate that the energy required to obtain machining using the HV medium is not warranted in terms of its performance.

9.25 It is proposed that the undulations observed on the workpiece surfaces are exaggerations of the original turning marks and are produced as a consequence of the AFM machining action.

9.26 The machining model tentatively suggested proposes that the machining action is influenced by the viscosity behaviour of the medium and the corresponding degree of "absorbency" of the grit particles back into the medium.

10.0 FURTHER WORK

- 10.1 Investigate the accuracy of utilising average results in the calculation of viscosities and the subsequent relationship between the rheological and machining parameters. It is proposed that this could be achieved if the relevant data pertaining to the viscosity calculations are made at the end of each extrusion cycle instead of at the end of an experimental run.
- 10.2 Investigate in more detail the effect of the grit to polymer ratio on both the machining and rheological parameters in order to substantiate the trends reported in the present work. It is suggested that this is achieved by the investigation of two further grit to polymer ratios, one of which should be less than 0.5 and the other should be greater than 2.
- 10.3 Investigate in further detail the effect of the grit size on the machining and rheological parameters in order to verify the trends observed in the present work. It is suggested that this is achieved by the investigation of two additional grit sizes, one of which should be between 60 and 100 Mesh, whilst the other should be less than 100 Mesh.
- 10.4 Investigate the possible effect that surface roughness may have on both the machining and rheological parameters in order to clarify the percentage surface roughness results reported in the present work. It is suggested that this is carried out by ensuring all the initial surface roughness values are approximately equal.

- 10.5** Investigate in more detail the effect of both the temperature rise and the rate of temperature rise of the medium with respect to both the machining and rheological parameters. This would enable the verification of the proposal that the machining action is dependent upon the viscosity behaviour of individual medium types. Such an investigation would also permit the effect of the temperature rise on the buoyancy of the grit in the polymer matrix to be examined.
- 10.6** Investigate in more detail the effect of the shear history on the machining and rheological parameters in order to determine whether any relationship exists between the shear history behaviour and the machining performance.
- 10.7** Investigate in further detail the effect of entrapped air on the machining and rheological parameters to corroborate the reported results.
- 10.8** Investigate the proposed machining model. It is suggested that this would require the volume of the AFM media to be kept constant, irrespective of the grit to polymer ratio, since this would permit any effect associated with the amount of polymer in the matrix to be examined by:
- 1) its "absorbency" capability in relation to the amount of grit present.
 - 2) its viscosity behaviour in relation to the machining performance.

- 10.9** Investigate the rheological parameters of the AFM media irrespective of the machining action by the utilisation of a rotational viscometer. If this is not possible due to the detrimental effect of the AFM medium on component surfaces it is suggested that a capillary viscometer is used with a die having a length to diameter ratio of 16.
- 10.10** Investigate any effect on the rheological and machining parameters that may arise as a result of utilising (i) alternative types of abrasive grit, (ii) additional workpiece materials, (iii) varying the extrusion pressure, and (iv) varying the length to diameter ratios of the die.
- 10.11** Investigate the constituent elements of the base media to explain the absence of a correlation between the rheological and machining parameters of the various media types.

11.0 REFERENCES

1. - Schmidt A.O., ASME Publications PED, 1984, Vol. 12, P 69-82.
2. - Komvopoulos K., Erpenbeck S.A., Jrl. of Eng. for Industry, August 1991, Vol. 113, No. 3, P 253-267.
3. - Yellowley I., Int. Jrl. Mach. Tools Manufact., 1987, Vol. 27, No. 3, P 357-365.
4. - Boothroyd G., Fundamentals of Metal Machining and Machine Tools (Book). M^cGraw-Hill 1975.
5. - Merchant M.E., Jrl. of Applied Physics, May 1945, Vol. 16, No. 5, P 207-318.
6. - Strenkowski J.S., Carroll J.T., ASME Conf. 9-14 December 1984. Vol. 12, P 157-166.
7. - Dieter G.E., Mechanical Metallurgy (Book). M^cGraw-Hill 1986.
8. - Juneja B.L., Fundamentals of Metal Cutting and Machine Tools (Book). Wiley and Sons 1987.
9. - Bagchi A., Wright P.K., Proc. of the Royal Soc. of London, 8 January 1987, Vol. 409, No. 1836, P 99-113.
10. - Bagchi A., Mittal R.O., Proc. of Manufact. Int. Conf. 17-20 April 1988. P 157-166.
11. - Trent E.M., Metal Cutting (Book). Butterworths 1978.
12. - Albrecht P., ASME Series B, 1960, Vol. 82, P 348-358.
13. - Rumford Count, Essays Political, Economical and Philosophical (Book). David West (Boston) 1799.
14. - Taylor G.I., Quinney H., Proc. of the Royal Soc., 1934, A143, 307.
15. - Bever M.B. et al, Jrl. of Applied Physics, September 1953, Vol. 24, No. 9, P 1176-1179.
16. - Naerheim Y. et al, Jrl. of Tribology, July 1986, Vol. 108, No. 3, P364-367.
17. - Smith T. et al, Tribology Int., October 1988, Vol. 21, No. 5, P 239-247.
18. - Taylor F.W., Trans. ASME, 1906, Vol. 28, P 31.
19. - International Standard 3685:1977, Tool Life Testing with Single Point Turning Tools.

20. - Zorn F.J., Carbide and Tool Jrl., March/April 1987, Vol. 19, No. 2, P 27-30.
21. - Kaczmarek J., Principles of Machining by Cutting, Abrasion, and Erosion (Book). Peter Peregrinus 1976.
22. - Rubenstein C. et al, Proc. Int. Industrial Diamond Conf., Oxford 1966, P 161-172.
23. - Spurr R.T., Wear, 1981, Vol. 65, P 315-324.
24. - Misra A., Finnie I., Wear, 1981, Vol. 65, P 359-373.
25. - Rajurkar K.P. et al, Proc. Manufact. Int. MI92, 1992, P 23-37.
26. - Missing D.H., South African Machine Tool Review, January 1987, Vol. 20, No. 1, P 27-33.
27. - Hignett J.B., Tooling and Production, November 1984, Vol. 50, No. 8, P 55-57.
28. - Gillespie L.K., Machine and Tool Blue Book, October 1980, Vol. 75, No. 10, P 100-113.
29. - Coleman J.R., Tooling and Production, April 1981, P 80-86.
30. - Anon, American Machinist and Automated Manufact., November 1987, Vol. 131, P 80-83.
31. - Field M., Kahles J.F., Annals of the CIRP, 1972, Vol. 21/2, P 219-236.
32. - Shaw M.C., Metal Cutting Principles (Book). Clarendon Press 1989.
33. - Ault W.N., Proceedings 13th Annual Int. Tech. Conf., p 79.
34. - Van Wazer J.R., Viscosity and Flow Measurement (Book). Interscience Publishers 1963.
35. - Barnes H.A. et al, An Introduction to Rheology (Book). Elsevier 1989.
36. - Hugh W.F., An Introduction to Viscous Flow (Book). Hemisphere 1979.
37. - Mewis, J., Jrl. of Non-Newtonian Fluid Mechanics, 1979, Vol. 6, P 1-20.
38. - Lin O.C.C., Jrl. of Applied Polymer Science, 1975, Vol. 19, P 199-214.
39. - Brydson J.A., Flow Properties of Polymer Melts (Book). George Goodwin 1981.

40. - Wilkinson W.L., Non-Newtonian Fluids (Book). Pergamon Press 1960.
41. - Nielson L.E., Polymer Rheology (Book). Marcel Dekker 1977.
42. - Cogswell F.N., Plastics and Polymers, April 1968, Vol. 36, P 109-111.
43. - Cogswell F.N., Trans. of the Soc. of Rheo., 1972, Vol. 16:3, P 383-403.
44. - Cogswell F.N., Polymer Melt Rheology: A Guide for Industrial Practice (Book). George Goodwin 1981.
45. - Schoff C.K., Encyclopedia of Polymer Science and Eng. (Book). Vol. 14, P 454-541.
46. - M^cCabe W.L., Unit Operations of Chemical Engineering (Book). M^cGraw-Hill 1976.
47. - Bagley E.B., Trans. of thr Soc. of Rheo., 1961, Vol. 5, P 355-368.
48. - Kamal M.R, Nyun H., Polymer Eng. and Science, January 1980, Vol. 20, No. 2, P 109-119.
49. - Edgardo J.G., Steffe J.F., Jrl. of Food Process Eng., 1987, Vol. 9, No. 2, P 93-120.
50. - Beddow K., Testing and Characterisation of Fine Powders (Book). Kings Point 1980.
51. - Lenel F.V., Powder Metallurgy Principles and Applications (Book). Metal Powder Industries Federation 1980.
52. - Fayed M.E., Handbook of Powder Science and Technology (Book). Dupont 1984.
53. - Sands R.L., Powder Metallurgy: Practice and Applications (Book). George Newnes Ltd. 1966.
54. - Swanson P.A., Vetter A.F., ASLE Trans., April 1985, Vol. 28, No. 2, P 225-230.
55. - Rhoades L.J., Non-Traditional Machining Conf., Ohio, USA, 2-3 December 1985, P 111-120.
56. - Hersey A., Tooling and Prod., March 1977, Vol. 42, No. 12, P 70-71.
57. - Rhoades L.J., Pittsburgh High Technology, November/December 1988, p 8-16.
58. - Rhoades L.J., AES 21st Conf., 1983, P 165-173.

59. - Rhoades L.J., SME Technical Paper, 1989, MR89-145.
60. - Perry W.B., AES Magazine, September/October 1982, P 12-15.
61. - Kohut T.A., Aluminium Finishing West, May 1987, P 4.1-4.22.
62. - Perry W.B., Non-Traditional Machining Conf., Ohio, USA, 2-3 December 1985, P 121-127.
63. - Kohut T.A., ET84, Atlanta, USA, 24-26 April 1984, P 193-202.
64. - Rhoades L.J., Winter Annual Meeting ASME, Chicago, 27 November - 2 December 1988, P 149-162.
65. - Rhoades L.J., SME Technical Paper, 1987, MR87-163.
66. - Kasgoz A. et al, Jrl. of Ceramic Soc. of Japan, 1989, Vol. 97, No. 11, P 1432-1434.
67. - Reynolds T.A., Production Eng. (London), June 1978, Vol. 57, No. 6, P 35-38.
68. - Rhoades L.J., SME Technical Paper, 1977, MR77-967.
69. - Rhoades L.J., Siwert D.E., AES Proc. 14th Annual Int. Tech. Conf., 16-18 May 1976.
70. - Hoffman, Tooling and Production, February 1966, P 54-70.
71. - Siwert D.E., SME Technical Paper, 1976, MR76-693.
72. - Spiotta R.H., Machine and Tool Blue Book, February 1976, Vol. 71, No. 2, P 80-87.
73. - Dmitriva T.V. et al, Soviet Jrl. of Friction and Wear, 1987, Vol. 8, No. 4, P 123-127.
74. - Rhoades L.J., Cutting Tool Eng., April 1987, Vol. 39, No. 2, P 53-56.
75. - Rhoades L.J., SME Technical Paper, 1985, MR85-473.
76. - Gillespie L.K., Advances in Deburring (Book). SME 1978. Ch. 15.
77. - Rhoades L.J., Siwert D.E., SME Technical Paper, 1975, MR75-842.
78. - Stackhouse J., SME Technical Paper, 1976, MR76-690.
79. - Rhoades L.J., Modern Machine Shop, December 1982, Vol. 55, No. 7, P 60-71.
80. - Rhoades L.J., AES, May/June 1980, P 5-14.
81. - Stackhouse J., SME Technical Paper, 1975, MR75-484.

82. - Stackhouse J., American Soc. for Abrasive Methods 13th Annual Int. Tech. Conf., 4-6 May 1975.
83. - Weller E.J., Metals Handbook (Book), Vol. 16, P52-61. SME 1984.
84. - Studley N., SME Technical Paper, 1989, FE89-807.
85. - Rhoades L.J., Manufact. Eng., November 1988, Vol. 101, No. 5, P 75-78.
86. - Rhoades L.J., SME Technical Paper, 1977. MR77-366.
87. - Borchers J., SME Technical Paper, 1977, MR77-438.
88. - Przyklenk K., Advances in Surface Treatments Tech. Applications Effects, Paris, 3-4 December 1986, Vol. 5, P 123-138.
89. - Kohut T., 4th Int. Aluminium Extrusion Tech. Seminar, 11-14 April 1988, Vol. 2, P 35-43.
90. - Williams R.E., Rajurkar K.P., ASME Winter Annual Meeting Symposium on Mechanics of Deburring, 1986, P 93-106.
91. - Williams R.E., Rajurkar K.P., SME Technical Paper, 1989, FC89-806.
92. - Williams R.E., Rhoades L.J., Trans. of the ASME, February 1992, Vol. 114, P 74-81.
93. - Perry W.B., SME Technical Paper, 1975, MR75-831.
94. - Rhoades L.J., NSF-SBir Phase I Final Report, August 1985.
95. - Trengove S.A. et al, Proceedings of the 3rd Int. Conf. on Advances in Coating and Surface Engineering for Corrosion and Wear Resistance, Newcastle, May 1992.
96. - Trengove S.A. et al, Proceedings of Int. Conf. on Surface Engineering, Toronto, USA, 1990, P 592-601.
97. - Williams R.E., MSc Thesis, University of Nebraska, August 1989.
98. - Rhoades L.J., Proc. 2nd Int. Aluminium Tech. Seminar, 1977, Vol. 2, P 39-47.
99. - Baird D.G. et al, Polymer Engineering and Science, Mid-February, 1986, Vol. 26, No. 3, P 225-232.
100. - Tomita Y., JSME Int. Jrl., 1987, Vol. 30, No. 270, P 1877-1884.
101. - Rudin A., Leeder D.R., Jrl. of Applied Polymer Science, 1968, Vol. 12, P 2305-2316.
102. - Athey R.D., European Coatings Jrl., 1991, No. 10, P 672-674.

103. - Benbow J.J., Howells E.R., *Polymer*, 1961, Vol. 2, P 429-436.
104. - Fener R.T., *Principles of Polymer Processing* (Book). MacMillan Press 1979.
105. - Bagley E.B. et al, *Jrl. of Polymer Science: Part C*, 1971, No. 35, P 177-188.
106. - Doyle L.E. et al, *Manufacturing Processes and Materials for Engineers* (Book). Pentice-Hall 1985.

Table 1 : Examples of some material viscosities at room temperature.

Liquid	Approximate Viscosity / Pa.s
Glass	10^{40}
Molten Glass (500°C)	10^{12}
Molten Polymers	10^3
Liquid Honey	10^1
Olive Oil	10^{-1}
Bicycle Oil	10^{-2}
Water	10^{-3}
Air	10^{-5}

Table 2 : The volumes of the mixtures used in the present work.

Medium	Grit Size	Grit to Polymer Ratio	Volume / m ³
LV	60	0.5	0.004462
		1	0.003707
		2	0.003416
	100	0.5	0.004602
		1	0.003725
		2	0.003370
MV	60	0.5	0.004509
		1	0.003415
		2	0.003254
	100	0.5	0.004393
		1	0.003451
		2	0.003463
HV	60	0.5	0.004323
		1	0.003612
		2	0.003045
	100	0.5	0.004393
		1	0.003818
		2	0.003114

Table 3 : The die diameter changes produced after 30 extrusion cycles for all mixtures used in the present work.

Medium and Grit Size	Grit to Polymer Ratio	Die Diameter Change / mm
LV60	0.5	0.1516
	1	0.0812
	2	0.1978
LV100	0.5	0.1402
	1	0.0800
	2	0.1382
MV60	0.5	0.0992
	1	0.0954
	2	0.3055
MV100	0.5	0.0367
	1	0.0671
	2	0.2266
HV60	0.5	-
	1	0.0630
	2	0.2250
HV100	0.5	0.0240
	1	0.0639
	2	0.1235

Table 4 : The die mass changes produced after 30 extrusion cycles for all mixtures used in the present work.

Medium and Grit Size	Grit to Polymer Ratio	Die Mass Change / g
LV60	0.5	0.2658
	1	0.1971
	2	0.4787
LV100	0.5	0.3203
	1	0.1848
	2	0.3437
MV60	0.5	0.1372
	1	0.2436
	2	0.6243
MV100	0.5	0.0455
	1	0.1548
	2	0.6417
HV60	0.5	0.0868
	1	0.1515
	2	0.8230
HV100	0.5	0.0349
	1	0.1433
	2	0.3318

Table 5 : The number of extrusion cycles required to achieve a visual improvement in the surface topography for all mixtures used with a grit to polymer ratio of 1.

Medium	Grit Size	Number of Extrusion Cycles to Achieve Visual Improvement
LV	60	10
	100	10
MV	60	2
	100	2
HV	60	5
	100	10

Table 6 : The processing times required to complete 30 extrusion cycles for all mixtures used in the present work.

Medium and Grit Size	Grit to Polymer Ratio	Processing Time / s
LV	0	460
LV60	0.5	383
	1	115
	2	225
LV100	0.5	246
	1	188
	2	171
MV	0	1560
MV60	0.5	1355
	1	820
	2	679
MV100	0.5	991
	1	786
	2	344
HV	0	4563
HV60	0.5	5842
	1	4120
	2	1385
HV100	0.5	4219
	1	5073
	2	2719

Table 7 : The viscosity parameter and associated data for all experimental runs conducted using LV medium and 60 Mesh grit with a grit to polymer ratio of 0.5.

Number of Extrusion Cycles	Processing Time / s	Volume Extruded / $\times 10^{-3} \text{m}^3$	Volumetric Flow Rate / $\times 10^{-4} \text{m}^3 \text{s}^{-1}$	Die Diameter / $\times 10^{-3} \text{m}$	Pressure Drop / kPa	Shear Stress / kPa	Shear Rate / s^{-1}	Viscosity / Pa.s
1	33.2	6.224	1.875	15.0313	1297.80	308.665	562.040	549.187
2	53.5	11.134	2.081	15.0494	1370.42	326.329	621.678	524.917
3	77.1	16.024	2.078	15.0630	1454.70	346.711	619.167	559.964
5	123.3	25.864	2.098	15.0809	1527.75	364.555	622.696	585.445
10	190.9	50.414	2.641	15.0871	1673.47	399.491	782.985	510.215
15	251.5	74.964	2.981	15.0938	1757.36	419.703	882.560	475.552
20	263.8	99.514	3.772	15.1039	1810.99	432.801	1114.724	388.258
30	383.4	148.614	3.876	15.0992	1636.03	390.866	1146.492	340.924

Table 8 : The viscosity parameter and associated data for all experimental runs conducted using LV medium and 60 Mesh grit with a grit to polymer ratio of 1.

Number of Extrusion Cycles	Processing Time / s	Volume Extruded / $\times 10^{-3} \text{m}^3$	Volumetric Flow Rate / $\times 10^{-4} \text{m}^3 \text{s}^{-1}$	Die Diameter / $\times 10^{-3} \text{m}$	Pressure Drop / kPa	Shear Stress / kPa	Shear Rate / s^{-1}	Viscosity / Pa.s
1	15.2	4.165	2.740	15.0130	1461.05	347.069	824.507	420.941
2	23.8	7.271	3.055	15.0192	1611.06	382.860	918.126	417.002
3	32.5	10.377	3.192	15.0234	1681.61	399.740	958.758	416.935
5	46.4	16.589	3.575	15.0320	1732.06	411.968	1071.709	384.402
10	71.4	32.119	4.498	15.0516	1732.42	412.591	1343.201	307.170
15	87.9	47.649	5.420	15.0709	1628.03	388.225	1612.399	240.775
20	91.9	63.179	6.874	15.0760	1567.70	373.967	2042.792	183.066
30	114.8	94.239	8.208	15.0812	1479.15	352.964	2436.724	144.852

Table 9 : The viscosity parameter and associated data for all experimental runs conducted using LV medium and 60 Mesh grit with a grit to polymer ratio of 2.

Number of Extrusion Cycles	Processing Time / s	Volume Extruded /x10 ⁻³ m ³	Volumetric Flow Rate / x10 ⁻⁴ m ³ s ⁻¹	Die Diameter / x10 ⁻³ m	Pressure Drop / kPa	Shear Stress / kPa	Shear Rate / s ⁻¹	Viscosity / Pa.s
1	28.7	4.132	1.440	15.0488	1456.89	346.906	430.128	806.517
2	44.3	6.950	1.569	15.0607	1480.01	352.690	467.596	754.261
3	56.8	9.768	1.720	15.0597	1525.77	363.570	512.665	709.177
5	77.6	15.404	1.985	15.0884	1420.59	339.152	588.393	576.404
10	118.9	29.494	2.481	15.1039	1426.61	340.939	733.010	465.123
15	160.0	43.584	2.724	15.1205	1471.41	352.033	802.295	438.782
20	191.5	57.674	3.012	15.1638	1565.99	375.734	879.453	427.236
30	224.3	85.854	3.828	15.1978	1641.79	394.804	1110.233	355.604

Table 10 : The viscosity parameter and associated data for all experimental runs conducted using LV medium and 100 Mesh grit with a grit to polymer ratio of 0.5.

Number of Extrusion Cycles	Processing Time / s	Volume Extruded / $\times 10^{-3} \text{m}^3$	Volumetric Flow Rate / $\times 10^{-4} \text{m}^3 \text{s}^{-1}$	Die Diameter / $\times 10^{-3} \text{m}$	Pressure Drop / kPa	Shear Stress / kPa	Shear Rate / s^{-1}	Viscosity / Pa.s
1	17.7	6.503	3.674	15.0131	1319.43	313.428	1105.489	283.520
2	37.0	11.693	3.160	15.0276	1431.27	340.325	948.158	358.933
3	54.3	16.883	3.109	15.0352	1444.27	343.590	931.424	368.887
5	89.0	27.263	3.063	15.0524	1467.03	349.405	914.517	382.065
10	154.1	53.213	3.453	15.0861	1534.07	366.189	1024.022	357.599
15	183.6	79.163	4.311	15.1080	1648.79	394.144	1273.074	309.600
20	213.2	105.113	4.930	15.1208	1712.62	409.751	1452.012	282.195
30	246.2	157.013	6.377	15.1402	1593.95	381.846	1871.018	204.085

Table 11 : The viscosity parameter and associated data for all experimental runs conducted using LV medium and 100 Mesh grit with a grit to polymer ratio of 1.

Number of Extrusion Cycles	Processing Time / s	Volume Extruded / $\times 10^{-3} \text{m}^3$	Volumetric Flow Rate / $\times 10^{-4} \text{m}^3 \text{s}^{-1}$	Die Diameter / $\times 10^{-3} \text{m}$	Pressure Drop / kPa	Shear Stress / kPa	Shear Rate / s^{-1}	Viscosity / Pa.s
1	20.6	4.202	2.039	15.0047	1412.45	335.338	614.798	545.445
2	32.1	7.342	2.287	15.0120	1431.85	340.110	688.365	494.083
3	42.7	10.490	2.456	15.0183	1504.97	357.627	738.432	484.306
5	59.6	16.778	2.815	15.0260	1532.98	364.471	844.868	431.934
10	83.1	32.498	3.910	15.0347	1556.65	370.312	1171.646	316.061
15	98.3	48.218	4.905	15.0441	1535.81	365.584	1466.838	249.233
20	136.2	63.938	4.694	15.0540	1523.63	362.923	1401.043	259.038
30	187.7	95.378	5.081	15.0800	1498.91	357.651	1508.708	237.057

Table 12 : The viscosity parameter and associated data for all experimental runs conducted using LV medium and 100 Mesh grit with a grit to polymer ratio of 2.

Number of Extrusion Cycles	Processing Time / s	Volume Extruded / x10 ⁻³ m ³	Volumetric Flow Rate / x10 ⁻⁴ m ³ s ⁻¹	Die Diameter / x10 ⁻³ m	Pressure Drop / kPa	Shear Stress / kPa	Shear Rate / s ⁻¹	Viscosity / Pa.s
1	-	4.040	-	15.0488	-	-	-	-
2	63.0	6.766	1.073	15.0629	1141.24	272.000	319.957	850.116
3	52.7	9.492	1.801	15.0726	1214.97	289.760	535.560	541.041
5	55.0	14.944	2.717	15.0902	1172.12	279.867	805.090	347.622
10	82.3	28.574	3.471	15.1241	1221.51	292.313	1021.851	286.062
15	101.2	42.204	4.170	15.1717	1273.93	305.817	1215.893	251.516
20	130.3	55.834	4.285	15.2091	1383.57	332.958	1240.135	268.485
30	171.0	83.094	4.859	15.2266	1438.84	346.656	1401.490	247.348

Table 13 : The viscosity parameter and associated data for all experimental runs conducted using MV medium and 60 Mesh grit with a grit to polymer ratio of 0.5.

Number of Extrusion Cycles	Processing Time / s	Volume Extruded / $\times 10^{-3} \text{m}^3$	Volumetric Flow Rate / $\times 10^{-4} \text{m}^3 \text{s}^{-1}$	Die Diameter / $\times 10^{-3} \text{m}$	Pressure Drop / kPa	Shear Stress / kPa	Shear Rate / s^{-1}	Viscosity / Pa.s
1	73.7	6.317	0.857	15.0313	1732.05	411.946	256.968	1603.101
2	182.1	11.321	0.622	15.0494	2081.55	495.666	185.713	2668.986
3	284.6	16.325	0.574	15.0630	2265.86	540.042	170.887	3160.227
5	385.9	26.333	0.682	15.0809	2363.96	564.092	202.567	2784.718
10	677.2	51.353	0.758	15.0871	2649.05	632.381	224.831	2812.690
15	685.0	76.373	1.115	15.0938	2426.31	579.466	330.125	1755.290
20	1121.2	101.393	0.904	15.1039	2652.32	633.867	267.229	2372.002
30	1355.2	151.433	1.117	15.0992	2669.23	637.709	330.507	1929.489

Table 14 : The viscosity parameter and associated data for all experimental runs conducted using MV medium and 60 Mesh grit with a grit to polymer ratio of 1.

Number of Extrusion Cycles	Processing Time / s	Volume Extruded / $\times 10^{-3} \text{m}^3$	Volumetric Flow Rate / $\times 10^{-4} \text{m}^3 \text{s}^{-1}$	Die Diameter / $\times 10^{-3} \text{m}$	Pressure Drop / kPa	Shear Stress / kPa	Shear Rate / s^{-1}	Viscosity / Pa.s
1	31.1	3.581	1.151	15.0299	1692.78	402.567	345.304	1165.835
2	74.4	6.103	0.082	15.0347	1961.93	466.724	245.760	1899.103
3	111.4	8.625	0.077	15.0388	2031.37	483.375	231.771	2085.569
5	215.3	13.669	0.063	15.0473	2221.04	528.808	189.733	2787.119
10	379.7	26.279	0.069	15.0526	2302.22	548.330	206.614	2653.891
15	538.5	38.889	0.072	15.0726	2439.49	581.794	214.735	2709.366
20	680.1	51.499	0.076	15.0796	2532.11	604.164	224.844	2687.031
30	819.6	76.719	0.094	15.0954	2523.72	602.794	277.072	2175.589

Table 15 : The viscosity parameter and associated data for all experimental runs conducted using MV medium and 60 Mesh grit with a grit to polymer ratio of 2.

Number of Extrusion Cycles	Processing Time / s	Volume Extruded / $\times 10^{-3} \text{m}^3$	Volumetric Flow Rate / $\times 10^{-4} \text{m}^3 \text{s}^{-1}$	Die Diameter / $\times 10^{-3} \text{m}$	Pressure Drop / kPa	Shear Stress / kPa	Shear Rate / s^{-1}	Viscosity / Pa.s
1	144.7	3.806	0.263	15.0856	2243.89	535.608	78.008	6866.086
2	178.5	6.298	0.353	15.1181	2189.17	523.672	103.968	5036.879
3	180.5	8.790	0.487	15.1257	2111.22	505.280	143.282	3526.479
5	250.6	13.774	0.550	15.1703	2132.80	511.950	160.296	3193.783
10	379.7	26.234	0.691	15.2060	2199.44	529.188	200.080	2644.879
15	483.4	38.694	0.800	15.2593	2042.30	493.102	229.382	2149.704
20	593.3	51.154	0.862	15.2825	2228.73	538.933	245.950	2191.227
30	678.1	76.074	1.122	15.3055	2312.32	559.988	318.585	1757.734

Table 16 : The viscosity parameter and associated data for all experimental runs conducted using MV medium and 100 Mesh grit with a grit to polymer ratio of 0.5.

Number of Extrusion Cycles	Processing Time / s	Volume Extruded /x10 ⁻³ m ³	Volumetric Flow Rate / x10 ⁻⁴ m ³ s ⁻¹	Die Diameter / x10 ⁻³ m	Pressure Drop / kPa	Shear Stress / kPa	Shear Rate / s ⁻¹	Viscosity / Pa.s
1	92.5	6.084	0.657	15.0319	2110.82	502.052	197.166	2546.349
2	182.1	10.854	0.596	15.0430	2229.71	530.720	178.280	2976.894
3	209.4	15.624	0.746	15.0504	2194.35	522.560	222.842	2344.983
5	285.2	25.164	0.882	15.0603	1990.9	474.423	262.999	1803.893
10	487.1	49.014	1.006	15.0903	2253.5	538.070	298.149	1804.699
15	631.8	72.864	1.153	15.0898	2492.5	595.116	341.750	1741.379
20	724.2	96.714	1.335	15.0584	2619.44	624.123	398.217	1567.294
30	990.4	144.414	1.458	15.0367	2609.28	620.806	436.683	1421.639

Table 17 : The viscosity parameter and associated data for all experimental runs conducted using MV medium and 100 Mesh grit with a grit to polymer ratio of 1.

Number of Extrusion Cycles	Processing Time / s	Volume Extruded / $\times 10^{-3} \text{m}^3$	Volumetric Flow Rate / $\times 10^{-4} \text{m}^3 \text{s}^{-1}$	Die Diameter / $\times 10^{-3} \text{m}$	Pressure Drop / kPa	Shear Stress / kPa	Shear Rate / s^{-1}	Viscosity / Pa.s
1	64.9	3.654	0.563	15.0227	1469.37	349.269	169.085	2065.644
2	126.5	6.250	0.494	15.0262	1631.64	387.932	148.275	2616.305
3	172.8	8.846	0.511	15.0366	1685.03	400.903	153.313	2614.926
5	257.9	14.038	0.544	15.0473	1749.71	416.589	162.669	2560.968
10	448.0	27.018	0.603	15.0512	1792.96	426.996	180.089	2371.027
15	587.7	39.998	0.680	15.0616	1992.27	474.791	202.812	2341.037
20	774.8	52.978	0.683	15.0610	2109.85	502.792	203.784	2467.282
30	787.3	78.938	1.002	15.0671	2151.75	512.984	298.457	1718.786

Table 18 : The viscosity parameter and associated data for all experimental runs conducted using MV medium and 100 Mesh grit with a grit to polymer ratio of 2.

Number of Extrusion Cycles	Processing Time / s	Volume Extruded / $\times 10^{-3} \text{m}^3$	Volumetric Flow Rate / $\times 10^{-4} \text{m}^3 \text{s}^{-1}$	Die Diameter / $\times 10^{-3} \text{m}$	Pressure Drop / kPa	Shear Stress / kPa	Shear Rate / s^{-1}	Viscosity / Pa.s
1	40.1	4.225	1.053	15.0488	1236.99	294.545	314.776	935.726
2	76.9	7.137	0.928	15.0629	1341.89	319.821	276.496	1156.694
3	101.3	10.049	0.992	15.0726	1337.20	318.910	294.968	1081.169
5	130.4	15.873	1.217	15.0902	1289.07	307.791	360.680	853.363
10	173.3	30.433	1.756	15.1241	1316.42	315.026	516.848	609.513
15	208.0	44.993	2.163	15.1717	1416.15	339.960	630.673	539.043
20	258.6	59.553	2.302	15.2091	1518.95	365.537	666.484	548.455
30	343.8	88.673	2.579	15.2266	1836.80	442.535	743.879	594.902

Table 19 : The viscosity parameter and associated data for all experimental runs conducted using HV medium and 60 Mesh grit with a grit to polymer ratio of 0.5.

Number of Extrusion Cycles	Processing Time / s	Volume Extruded / x10 ⁻³ m ³	Volumetric Flow Rate / x10 ⁻⁴ m ³ s ⁻¹	Die Diameter / x10 ⁻³ m	Pressure Drop / kPa	Shear Stress / kPa	Shear Rate / s ⁻¹	Viscosity / Pa.s
1	530.1	5.946	0.112	-	2903.30	-	-	-
2	1100.7	10.578	0.096	15.0698	2958.32	705.400	28.592	24671.644
3	1427.4	15.210	0.107	15.1329	2998.75	718.035	31.307	22935.223
5	2069.4	24.474	0.118	-	3023.15	-	-	-
10	3318.0	47.634	0.144	15.1779	2996.98	719.745	41.805	17216.605
15	4833.9	70.794	0.146	15.0973	3011.03	719.279	43.334	16598.583
20	5352.0	93.954	0.176	15.0767	3012.78	718.715	52.156	13780.057
30	5841.9	140.274	0.240	-	3025.21	-	-	-

Table 20 : The viscosity parameter and associated data for all experimental runs conducted using HV medium and 60 Mesh grit with a grit to polymer ratio of 1.

Number of Extrusion Cycles	Processing Time / s	Volume Extruded /x10 ⁻³ m ³	Volumetric Flow Rate / x10 ⁻⁴ m ³ s ⁻¹	Die Diameter / x10 ⁻³ m	Pressure Drop / kPa	Shear Stress / kPa	Shear Rate / s ⁻¹	Viscosity / Pa.s
1	407.4	3.922	0.096	15.0125	2824.45	670.919	28.970	23158.850
2	693.3	6.694	0.096	15.0152	2786.13	661.934	29.040	22793.874
3	919.2	9.466	0.102	15.0252	2774.73	659.666	30.912	21340.438
5	1687.2	15.010	0.088	15.0209	2739.46	651.094	26.727	24360.839
10	2684.4	28.870	0.107	15.0449	2759.75	656.965	32.156	20430.804
15	3002.4	42.730	0.142	15.0469	2792.69	664.895	42.535	15631.646
20	3254.4	56.590	0.173	15.0525	2769.64	659.652	51.912	12707.107
30	4119.9	84.310	0.204	15.0630	2795.48	666.270	60.965	10928.654

Table 2.1 : The viscosity parameter and associated data for all experimental runs conducted using HV medium and 60 Mesh grit with a grit to polymer ratio of 2.

Number of Extrusion Cycles	Processing Time / s	Volume Extruded / $\times 10^{-3} \text{m}^3$	Volumetric Flow Rate / $\times 10^{-4} \text{m}^3 \text{s}^{-1}$	Die Diameter / $\times 10^{-3} \text{m}$	Pressure Drop / kPa	Shear Stress / kPa	Shear Rate / s^{-1}	Viscosity / Pa.s
1	349.8	3.388	0.097	15.0957	2049.11	489.442	28.667	17073.096
2	372.9	5.462	0.146	-	2030.33	-	-	-
3	446.1	7.536	0.169	15.0969	1858.55	443.961	49.989	8881.254
5	522.3	11.684	0.224	15.1832	1709.55	410.703	65.074	6311.333
10	776.4	22.054	0.284	15.1100	1747.63	417.827	83.837	4983.829
15	926.7	32.424	0.350	15.2144	1866.40	449.306	101.155	4441.751
20	997.2	42.794	0.429	15.1691	2065.11	495.662	125.183	3959.492
30	1384.8	63.534	0.459	15.2250	2245.51	540.948	132.365	4086.793

Table 22 : The viscosity parameter and associated data for all experimental runs conducted using HV medium and 100 Mesh grit with a grit to polymer ratio of 0.5.

Number of Extrusion Cycles	Processing Time / s	Volume Extruded / $\times 10^{-3} \text{m}^3$	Volumetric Flow Rate / $\times 10^{-4} \text{m}^3 \text{s}^{-1}$	Die Diameter / $\times 10^{-3} \text{m}$	Pressure Drop / kPa	Shear Stress / kPa	Shear Rate / s^{-1}	Viscosity / Pa.s
1	695.7	5.482	0.079	15.0026	2461.50	584.318	23.760	24592.717
2	1059.9	9.814	0.093	15.0061	2452.65	582.353	27.900	20872.927
3	1322.1	14.146	0.107	15.0082	2485.4	590.213	32.226	18314.701
5	1909.8	22.810	0.119	15.0136	2455.33	583.281	35.934	16231.922
10	3728.7	44.470	0.119	15.0195	2477.90	588.874	35.840	16430.626
15	4325.1	66.130	0.153	15.0158	2497.03	593.274	45.981	12902.481
20	4539.0	87.790	0.193	15.0259	2463.13	585.614	58.048	10088.410
30	4218.0	131.110	0.311	15.0240	2467.26	586.522	93.325	6284.725

Table 23 : The viscosity parameter and associated data for the 30 cycle run using HV medium and 100 Mesh grit with a grit to polymer ratio of 1.

Number of Extrusion Cycles	Processing Time / s	Volume Extruded / x10 ⁻³ m ³	Volumetric Flow Rate / x10 ⁻⁴ m ³ s ⁻¹	Die Diameter / x10 ⁻³ m	Pressure Drop / kPa	Shear Stress / kPa	Shear Rate / s ⁻¹	Viscosity / Pa.s
1	-	3.910	-	15.0066	-	-	-	-
2	-	6.762	-	15.0071	-	-	-	-
3	-	9.614	-	15.0085	-	-	-	-
5	-	17.069	-	15.0175	-	-	-	-
10	-	32.989	-	15.0318	-	-	-	-
15	-	48.909	-	15.0413	-	-	-	-
20	-	64.829	-	15.0523	-	-	-	-
30	5072.7	96.669	0.190	15.0639	2735.47	652.006	56.762	11486.570

Table 24 : The viscosity parameter and associated data for all experimental runs conducted using HV medium and 100 Mesh grit with a grit to polymer ratio of 2.

Number of Extrusion Cycles	Processing Time / s	Volume Extruded / $\times 10^{-3} \text{m}^3$	Volumetric Flow Rate / $\times 10^{-4} \text{m}^3 \text{s}^{-1}$	Die Diameter / $\times 10^{-3} \text{m}$	Pressure Drop / kPa	Shear Stress / kPa	Shear Rate / s^{-1}	Viscosity / Pa.s
1	1281.6	2.926	0.022	15.0236	1764.62	419.478	6.855	61190.533
2	722.4	4.702	0.065	15.0321	1802.84	428.805	19.511	21978.017
3	905.1	6.478	0.071	15.0448	1893.32	450.706	21.400	21061.189
5	1148.0	10.030	0.087	15.0618	1940.17	462.380	26.035	17760.099
10	1724.4	18.910	0.109	15.0669	1930.05	460.124	32.644	14095.095
15	1638.9	27.790	0.169	15.1004	1714.40	409.623	50.141	8169.368
20	1958.1	36.670	0.187	15.0907	1849.10	441.523	55.485	7957.569
30	2718.5	54.430	0.200	15.1235	1973.11	472.157	58.936	8011.405

Table 25 : The viscosity parameter and associated data for the 30 extrusion cycle run conducted using the pure LV medium.

Number of Extrusion Cycles	Processing Time / s	Volume Extruded / x10 ⁻³ m ³	Volumetric Flow Rate / x10 ⁻⁴ m ³ s ⁻¹	Die Diameter / x10 ⁻³ m	Pressure Drop / kPa	Shear Stress / kPa	Shear Rate / s ⁻¹	Viscosity / Pa.s
30	460.0	355.319	7.724	15.0574	2153.45	513.062	2304.681	222.6173

Table 26 : The viscosity parameter and associated data for the 30 extrusion cycle run conducted using the pure MV medium.

Number of Extrusion Cycles	Processing Time / s	Volume Extruded / $\times 10^{-3}\text{m}^3$	Volumetric Flow Rate / $\times 10^{-4}\text{m}^3\text{s}^{-1}$	Die Diameter / $\times 10^{-3}\text{m}$	Pressure Drop / kPa	Shear Stress / kPa	Shear Rate / s^{-1}	Viscosity / Pa.s
30	1560.0	201.899	1.294	15.0574	3028.80	721.612	385.998	1869.470

Table 27 : The viscosity parameter and associated data for the 30 extrusion cycle run conducted with the pure HV medium.

Number of Extrusion Cycles	Processing Time / s	Volume Extruded /x10 ⁻³ m ³	Volumetric Flow Rate / x10 ⁻⁴ m ³ s ⁻¹	Die Diameter / x10 ⁻³ m	Pressure Drop / kPa	Shear Stress / kPa	Shear Rate / s ⁻¹	Viscosity / Pa.s
30	4563.0	168.419	0.3690	15.0574	3076.69	733.021	110.082	6658.872

Table 28 : The initial and final temperatures of the medium for each experimental run conducted using pure LV, MV, and HV medium.

Extrusion Cycle	LV Medium		MV Medium		HV Medium	
	No Grit Additions		No Grit Additions		No Grit Additions	
	Initial Temperature / °C	Final Temperature / °C	Initial Temperature / °C	Final Temperature / °C	Initial Temperature / °C	Final Temperature / °C
30	14.09	45.43	17.62	26.24	18.92	28.70

Table 29 : The initial and final temperatures for each experimental run conducted using LV medium and 60 Mesh grit with grit to polymer ratios of 0.5, 1, and 2.

Extrusion Cycle	LV Medium						60 Mesh Grit					
	Grit to Polymer Ratio of 0.5		Grit to Polymer Ratio of 1		Grit to Polymer Ratio of 2		Grit to Polymer Ratio of 0.5		Grit to Polymer Ratio of 1		Grit to Polymer Ratio of 2	
	Initial Temperature / °C	Final Temperature / °C	Initial Temperature / °C	Final Temperature / °C	Initial Temperature / °C	Final Temperature / °C	Initial Temperature / °C	Final Temperature / °C	Initial Temperature / °C	Final Temperature / °C	Initial Temperature / °C	Final Temperature / °C
1	14.88	17.69	15.93	17.15	14.69	16.64	14.88	17.69	15.93	17.15	14.69	16.64
2	15.20	20.27	16.22	18.70	13.94	16.72	15.20	20.27	16.22	18.70	13.94	16.72
3	15.38	22.25	16.25	18.96	13.31	17.07	15.38	22.25	16.25	18.96	13.31	17.07
5	15.55	24.76	16.38	21.92	13.38	18.60	15.55	24.76	16.38	21.92	13.38	18.60
10	15.89	30.41	17.40	25.58	13.81	22.07	15.89	30.41	17.40	25.58	13.81	22.07
15	16.48	34.55	17.41	29.11	14.21	25.44	16.48	34.55	17.41	29.11	14.21	25.44
20	17.12	38.46	19.73	34.10	15.00	27.38	17.12	38.46	19.73	34.10	15.00	27.38
30	14.31	43.53	20.25	37.83	14.24	31.02	14.31	43.53	20.25	37.83	14.24	31.02

Table 30 : The initial and final temperatures for each experimental run conducted using LV medium and 100 Mesh grit with grit to polymer ratios of 0.5, 1, and 2.

Extrusion Cycle	LV Medium						100 Mesh Grit					
	Grit to Polymer Ratio of 0.5		Grit to Polymer Ratio of 1		Grit to Polymer Ratio of 2		Grit to Polymer Ratio of 0.5		Grit to Polymer Ratio of 1		Grit to Polymer Ratio of 2	
	Initial Temperature / °C	Final Temperature / °C	Initial Temperature / °C	Final Temperature / °C	Initial Temperature / °C	Final Temperature / °C	Initial Temperature / °C	Final Temperature / °C	Initial Temperature / °C	Final Temperature / °C	Initial Temperature / °C	Final Temperature / °C
1	16.17	18.06	16.01	17.66	-	-	16.17	18.06	16.01	17.66	-	-
2	16.16	20.68	16.29	19.25	13.78	16.81	16.16	20.68	16.29	19.25	13.78	16.81
3	16.28	22.60	16.74	20.80	14.14	16.52	16.28	22.60	16.74	20.80	14.14	16.52
5	16.00	25.74	17.26	24.00	15.05	19.98	16.00	25.74	17.26	24.00	15.05	19.98
10	16.40	30.14	18.25	26.28	15.62	24.10	16.40	30.14	18.25	26.28	15.62	24.10
15	17.96	36.10	20.25	30.39	15.75	27.76	17.96	36.10	20.25	30.39	15.75	27.76
20	18.93	43.89	21.07	32.47	16.52	29.48	18.93	43.89	21.07	32.47	16.52	29.48
30	19.00	49.18	21.15	34.11	16.33	33.97	19.00	49.18	21.15	34.11	16.33	33.97

Table 31 : The initial and final temperatures for each experimental run conducted using MV medium and 60 Mesh grit with grit to polymer ratios of 0.5, 1, and 2.

Extrusion Cycle	MV Medium						60 Mesh Grit			
	Grit to Polymer Ratio of 0.5		Grit to Polymer Ratio of 1		Grit to Polymer Ratio of 2		Grit to Polymer Ratio of 1		Grit to Polymer Ratio of 2	
	Initial Temperature / °C	Final Temperature / °C	Initial Temperature / °C	Final Temperature / °C	Initial Temperature / °C	Final Temperature / °C	Initial Temperature / °C	Final Temperature / °C	Initial Temperature / °C	Final Temperature / °C
1	15.05	18.30	19.87	20.72	14.87	16.48	14.87	16.48	14.87	16.48
2	14.52	19.32	20.30	24.03	14.40	16.70	14.40	16.70	14.40	16.70
3	14.69	20.73	21.37	26.05	14.53	17.34	14.53	17.34	14.53	17.34
5	14.67	23.69	22.06	28.17	14.48	18.84	14.48	18.84	14.48	18.84
10	16.16	25.26	22.93	30.61	14.53	21.46	14.53	21.46	14.53	21.46
15	13.32	25.06	23.72	33.03	13.22	21.66	13.22	21.66	13.22	21.66
20	12.78	25.18	25.60	34.56	13.16	23.47	13.16	23.47	13.16	23.47
30	13.78	28.96	25.47	37.77	12.77	26.31	12.77	26.31	12.77	26.31

Table 32 : The initial and final temperatures for each experimental run conducted using MV medium and 100 Mesh grit with grit to polymer ratios of 0.5, 1, and 2.

Extrusion Cycle	MV Medium						100 Mesh Grit			
	Grit to Polymer Ratio of 0.5		Grit to Polymer Ratio of 1		Grit to Polymer Ratio of 2		Grit to Polymer Ratio of 1		Grit to Polymer Ratio of 2	
	Initial Temperature / °C	Final Temperature / °C	Initial Temperature / °C	Final Temperature / °C	Initial Temperature / °C	Final Temperature / °C	Initial Temperature / °C	Final Temperature / °C	Initial Temperature / °C	Final Temperature / °C
1	15.91	19.72	14.62	16.93	12.54	14.34	14.62	16.93	12.54	14.34
2	15.82	20.58	14.81	18.68	12.71	15.58	14.81	18.68	12.71	15.58
3	15.58	21.00	15.13	19.08	12.62	16.17	15.13	19.08	12.62	16.17
5	12.91	20.15	16.05	21.53	13.14	18.27	16.05	21.53	13.14	18.27
10	12.43	22.02	16.89	23.23	13.81	22.31	16.89	23.23	13.81	22.31
15	13.51	24.21	17.92	25.97	14.65	26.49	17.92	25.97	14.65	26.49
20	14.68	29.23	19.59	28.80	14.84	28.60	19.59	28.80	14.84	28.60
30	15.12	32.43	21.10	34.32	15.06	35.38	21.10	34.32	15.06	35.38

Table 33 : The initial and final temperatures for each experimental run conducted using HV medium and 60 Mesh grit with grit to polymer ratios of 0.5, 1, and 2.

Extrusion Cycle	HV Medium						60 Mesh Grit					
	Grit to Polymer Ratio of 0.5		Grit to Polymer Ratio of 1		Grit to Polymer Ratio of 2		Grit to Polymer Ratio of 0.5		Grit to Polymer Ratio of 1		Grit to Polymer Ratio of 2	
	Initial Temperature / °C	Final Temperature / °C	Initial Temperature / °C	Final Temperature / °C	Initial Temperature / °C	Final Temperature / °C	Initial Temperature / °C	Final Temperature / °C	Initial Temperature / °C	Final Temperature / °C	Initial Temperature / °C	Final Temperature / °C
1	13.80	15.02	26.70	27.29	17.26	17.77	13.80	15.02	26.70	27.29	17.26	17.77
2	14.12	15.22	27.13	27.92	17.57	18.65	14.12	15.22	27.13	27.92	17.57	18.65
3	14.63	15.89	27.18	28.43	14.41	15.42	14.63	15.89	27.18	28.43	14.41	15.42
5	14.88	17.19	22.16	23.10	14.22	16.35	14.88	17.19	22.16	23.10	14.22	16.35
10	15.69	19.62	22.92	25.64	14.58	17.86	15.69	19.62	22.92	25.64	14.58	17.86
15	13.92	17.32	23.70	27.35	15.08	18.80	13.92	17.32	23.70	27.35	15.08	18.80
20	14.52	19.48	24.70	28.23	17.15	22.41	14.52	19.48	24.70	28.23	17.15	22.41
30	15.38	22.71	25.31	30.32	18.09	24.38	15.38	22.71	25.31	30.32	18.09	24.38

Table 34 : The initial and final temperatures for each experimental run conducted using HV medium and 100 Mesh grit with grit to polymer ratios of 0.5, 1, and 2.

Extrusion Cycle	HV Medium						100 Mesh Grit	
	Grit to Polymer Ratio of 0.5		Grit to Polymer Ratio of 1		Grit to Polymer Ratio of 2		Initial Temperature / °C	Final Temperature / °C
	Initial Temperature / °C	Final Temperature / °C	Initial Temperature / °C	Final Temperature / °C	Initial Temperature / °C	Final Temperature / °C		
1	22.50	23.19	-	-	22.59	23.15	-	-
2	22.11	23.94	-	-	23.54	24.65	-	-
3	22.72	24.66	-	-	23.87	25.30	-	-
5	22.79	25.21	-	-	24.24	26.30	-	-
10	20.40	-	-	-	24.90	27.26	-	-
15	20.18	24.50	-	-	20.20	23.06	-	-
20	20.46	26.20	-	-	21.09	24.14	-	-
30	22.81	29.92	22.03	28.47	21.22	25.34	-	-

Table 35 : The rate of temperature rise recorded after 30 extrusion cycles for all mixtures used in the present work.

Medium and Grit Size	Grit to Polymer Ratio	Rate of Temperature Rise / °Cs ⁻¹
LV	0	0.0681
LV60	0.5	0.0762
	1	0.1531
	2	0.0748
LV100	0.5	0.1226
	1	0.0690
	2	0.1032
MV	0	0.0119
MV60	0.5	0.0112
	1	0.0150
	2	0.0200
MV100	0.5	0.0175
	1	0.0168
	2	0.0591
HV	0	0.0021
HV60	0.5	0.0013
	1	0.0012
	2	0.0045
HV100	0.5	0.0017
	1	0.0013
	2	0.0015

Table 36 : The days on which the runs within an experimental set were performed for all mixtures used in the present work.

Medium and Grit Size	Grit to Polymer Ratio	Number of Extrusion Cycles Performed	Date Performed
LV60	0.5	1, 2, 3, 5, 10, 15, 20	23/11/92
		30	24/11/92
	1	1, 2, 3, 5, 10, 15, 20, 30	13/03/92
	2	1, 2, 3, 5, 10, 15, 20, 30	24/11/92
MV60	0.5	1, 2, 3, 5, 10	24/11/92
		15, 20, 30	25/11/92
	1	1, 2, 3, 5, 10, 15, 20, 30	13/03/92
	2	1, 2, 3, 5, 10	25/11/92
		15, 20, 30	26/11/92
HV60	0.5	1, 2, 3, 5, 10	14/12/92
		15, 20, 30	15/12/92
	1	1, 2, 3	14/07/92
		5, 10, 15, 20, 30	15/07/92
	2	1, 2	15/12/92
		3, 5, 10, 15, 20, 30	16/12/92
LV100	0.5	1, 2, 3, 5, 10, 15, 20, 30	02/11/92
	1	1, 2, 3, 5, 10, 15, 20, 30	10/03/92
	2	2, 3, 5, 10, 15, 20, 30	02/11/92
MV100	0.5	1, 2, 3	03/11/92
		5, 10, 15, 20, 30	04/11/92
	1	1, 2, 3, 5, 10, 15, 20, 30	11/03/92
	2	1, 2, 3, 5, 10, 15, 20, 30	03/11/92
HV100	0.5	1, 2, 3, 5	11/08/92
		10, 15, 20, 30	12/08/92
	1	1, 2, 3	12/03/92
		5	13/07/92
		30	14/07/92
	2	1, 2, 3, 5, 10	10/08/92
		15, 20, 30	11/08/92

Table 37 : The average normal pressure in relation to the 30 extrusion cycle run conducted using LV medium and either 60 or 100 Mesh grit with grit to polymer ratios of 0, 0.5, 1, and 2.

LV Medium		
Grit Size	100 Mesh	60 Mesh
Grit to Polymer Ratio	Normal Pressure / kPa	Normal Pressure / kPa
0.5	1919.37	2034.5
1	1924.11	1726.6
2	1821.14	1835.5

	Normal Pressure / kPa
Pure LV Medium	2198.91

Table 38 : The average normal pressure in relation to the 30 extrusion cycle run conducted using MV medium and either 60 or 100 Mesh grit with grit to polymer ratios of 0, 0.5, 1, and 2.

MV Medium		
Grit Size	100 Mesh	60 Mesh
Grit to Polymer Ratio	Normal Pressure / kPa	Normal Pressure / kPa
0.5	2458.11	2499.20
1	2355.62	2446.07
2	1996.94	2101.84

	Normal Pressure / kPa
Pure MV Medium	2309.52

Table 39 : The average normal pressure in relation to the 30 extrusion cycle run conducted using HV medium and either 60 or 100 Mesh grit with grit to polymer ratios of 0, 0.5, 1, and 2.

		HV Medium	
Grit Size		100 Mesh	60 Mesh
Grit to Polymer Ratio		Normal Pressure / kPa	Normal Pressure / kPa
0.5		2429.45	2552.06
1		2423.06	2558.37
2		1815.70	1740.86

	Normal Pressure / kPa
Pure HV Medium	2655.35

Table 40 : The changes in die mass produced after 30 extrusion cycles using LV medium and either 60 or 100 Mesh grit with grit to polymer ratios of 0.5, 1, and 2.

		LV Medium	
Grit Size		100 Mesh	60 Mesh
Grit to Polymer Ratio		Die Mass Change / g	Die Mass Change / g
0.5		0.3203	0.2658
1		0.1848	0.1971
2		0.3437	0.4787

Table 41 : The changes in die mass produced after 30 extrusion cycles using MV medium and either 60 or 100 Mesh grit with grit to polymer ratios of 0.5, 1, and 2.

MV Medium		
Grit Size	100 Mesh	60 Mesh
Grit to Polymer Ratio	Die Mass Change / g	Die Mass Change / g
0.5	0.0455	0.1372
1	0.1548	0.2436
2	0.6417	0.6243

Table 42 : The changes in die mass produced after 30 extrusion cycles using HV medium and either 60 or 100 Mesh grit with grit to polymer ratios of 0.5, 1, and 2.

	HV Medium	
Grit Size	100 Mesh	60 Mesh
Grit to Polymer Ratio	Die Mass Change / g	Die Mass Change / g
0.5	0.0349	0.0868
1	0.1433	0.1515
2	0.3318	0.8230

Table 43 : The average die diameter change, ($\times 10^{-3}m$), in relation to identical medium and grit to polymer ratios, irrespective of grit size, after 30 extrusion cycles.

Grit to Polymer Ratio	Medium			Combined averages
	LV	MV	HV	
0.5	0.1459	0.0680	0.0240	0.0793
1	0.0806	0.0813	0.0635	0.0751
2	0.1680	0.2661	0.1743	0.2028
Combined averages	0.1315	0.1385	0.0873	

Table 44 : The average die mass change, (g), in relation to identical medium and grit to polymer ratios, irrespective of grit size, after 30 extrusion cycles.

Grit to Polymer Ratio	Medium			Combined averages
	LV	MV	HV	
0.5	0.2931	0.0914	0.0609	0.1485
1	0.1910	0.1992	0.1474	0.1792
2	0.4112	0.6330	0.5774	0.5405
Combined averages	0.2984	0.3079	0.2619	

Table 45 : The average percentage surface roughness improvement in relation to identical medium and grit to polymer ratios, irrespective of grit size, after 30 extrusion cycles.

Grit to Polymer Ratio	Medium			Combined averages
	LV	MV	HV	
0.5	87.50	58.97	36.01	60.83
1	56.53	57.96	49.42	54.64
2	94.90	95.80	76.18	88.96
Combined averages	79.64	70.91	53.87	

Table 46 : The average temperature rise, ($^{\circ}\text{C}$), in relation to identical medium and grit to polymer ratios, irrespective of grit size, after 30 extrusion cycles.

Grit to Polymer Ratio	Medium			Combined averages
	LV	MV	HV	
0	31.3	18.6	9.8	19.9
0.5	29.7	16.2	7.2	17.7
1	15.3	12.8	5.7	11.3
2	17.2	16.9	5.2	13.1
Combined averages	23.4	16.1	7.0	

Table 47 : The average processing time, (s), in relation to identical medium and grit to polymer ratios, irrespective of grit size, after 30 extrusion cycles.

Grit to Polymer Ratio	Medium			Combined averages
	LV	MV	HV	
0	460	1560	4563	2194
0.5	315	1173	5031	2173
1	152	803	4597	1851
2	198	512	2052	921
Combined averages	281	1012	4061	

Table 48 : The average volumetric flow rate, (m^3s^{-1}), in relation to identical medium and grit to polymer ratios, irrespective of grit size, after 30 extrusion cycles.

Grit to Polymer Ratio	Medium			Combined averages
	LV	MV	HV	
0	7.724	1.294	0.369	3.129
0.5	3.189	1.288	0.276	1.584
1	6.645	0.548	0.197	2.463
2	4.344	1.851	0.330	2.175
Combined averages	5.476	1.245	0.293	

Table 49 : The average pressure drop. (kPa), in relation to identical medium and grit to polymer ratios, irrespective of grit size, after 30 extrusion cycles.

Grit to Polymer Ratio	Medium			Combined averages
	LV	MV	HV	
0	2154	3028	3077	2753
0.5	1615	2639	2746	2333
1	1489	2337	2765	2197
2	1540	2074	2109	1908
Combined averages	1700	2520	2674	

Table 50 : The average viscosity, (Pa.s), in relation to identical medium and grit to polymer ratios, irrespective of grit size, after 30 extrusion cycles.

Grit to Polymer Ratio	Medium			Combined averages
	LV	MV	HV	
0	223	1869	6659	2917
0.5	272	1675	6284	2744
1	191	1946	11207	4448
2	301	1175	6049	2508
Combined averages	247	1666	7550	

Table 51 : The average temperature rise, (°C), in relation to identical medium and grit size, irrespective of grit to polymer ratios after 30 extrusion cycles.

Medium	Grit Size	
	60 Mesh	100 Mesh
LV	21.2	20.3
MV	13.7	17.0
HV	8.9	5.9
Combined averages	14.6	14.4

Table 52 : The average processing time, (s), in relation to identical medium and grit size, irrespective of grit to polymer ratios after 30 extrusion cycles.

Medium	Grit Size	
	60 Mesh	100 Mesh
LV	240	201
MV	947	707
HV	3781	4003
Combined averages	1656	1637

Table 53 : The average volumetric flow rate, (m^3s^{-1}), in relation to identical medium and grit size, irrespective of grit to polymer ratios after 30 extrusion cycles.

Medium	Grit Size	
	60 Mesh	100 Mesh
LV	5.304	5.439
MV	0.778	1.680
HV	0.301	0.234
Combined averages	2.128	2.451

Table 54 : The average pressure drop, (kPa), in relation to identical medium and grit size, irrespective of grit to polymer ratios after 30 extrusion cycles.

Medium	Grit Size	
	60 Mesh	100 Mesh
LV	1585	1510
MV	2501	2199
HV	2688	2392
Combined averages	2258	2034

Table 55 : The average viscosity, (Pa.s), in relation to identical medium and grit size, irrespective of grit to polymer ratios after 30 extrusion cycles.

Medium	Grit Size	
	60 Mesh	100 Mesh
LV	280	229
MV	1954	1244
HV	7507	8594
Combined averages	3247	3356

Table 56 : The average die diameter change, ($\times 10^{-3}\text{m}$), in relation to identical medium and grit size, irrespective of grit to polymer ratios after 30 extrusion cycles.

Medium	Grit Size	
	60 Mesh	100 Mesh
LV	0.1435	0.1195
MV	0.1667	0.1101
HV	0.1440	0.0705
Combined averages	0.1514	0.1000

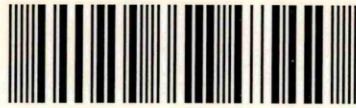
Table 57 : The average die mass change, (g), in relation to identical medium and grit size, irrespective of grit to polymer ratios after 30 extrusion cycles.

Medium	Grit Size	
	60 Mesh	100 Mesh
LV	0.3139	0.2829
MV	0.3350	0.2807
HV	0.3538	0.1700
Combined averages	0.3342	0.2445

Table 58 : The average percentage surface roughness improvement in relation to identical medium and grit size, irrespective of grit to polymer ratios after 30 extrusion cycles.

Medium	Grit Size	
	60 Mesh	100 Mesh
LV	83.90	75.39
MV	86.74	55.09
HV	67.28	40.47
Combined averages	79.31	56.98

101 392 377 4



VOL. 2

Sheffield Hallam University

REFERENCE ONLY

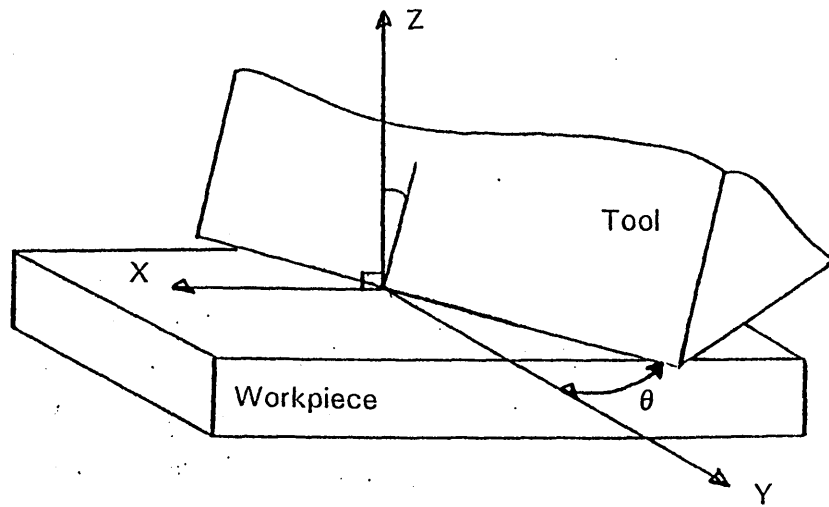
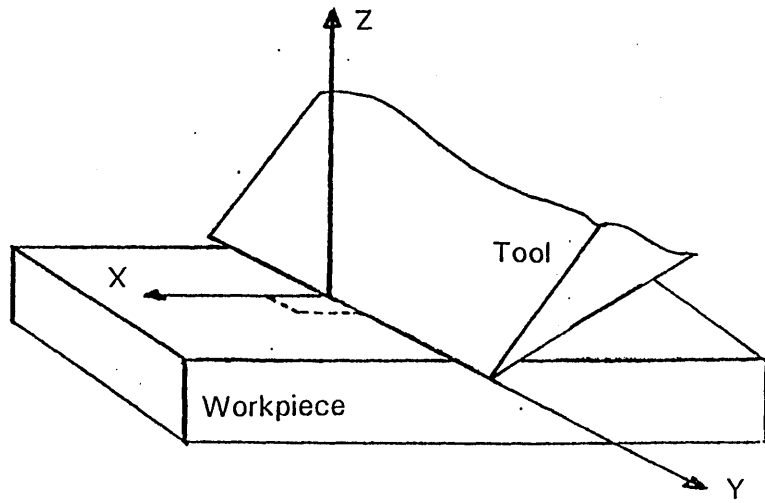
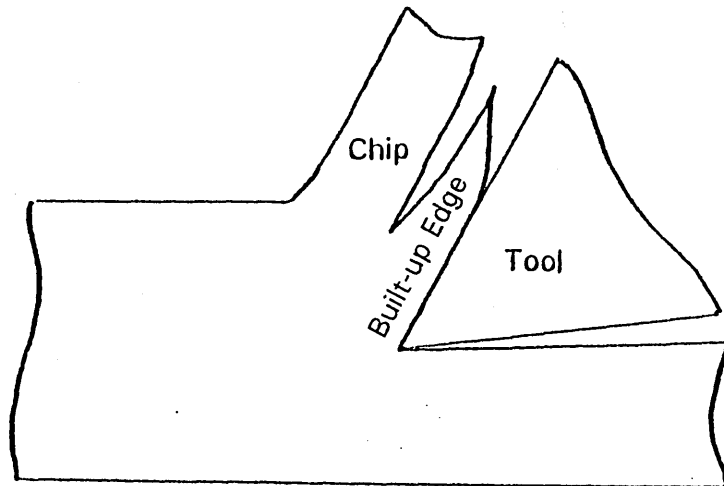
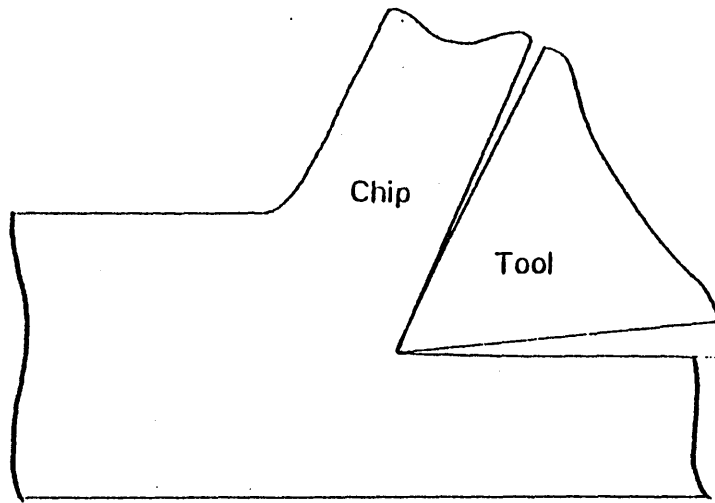
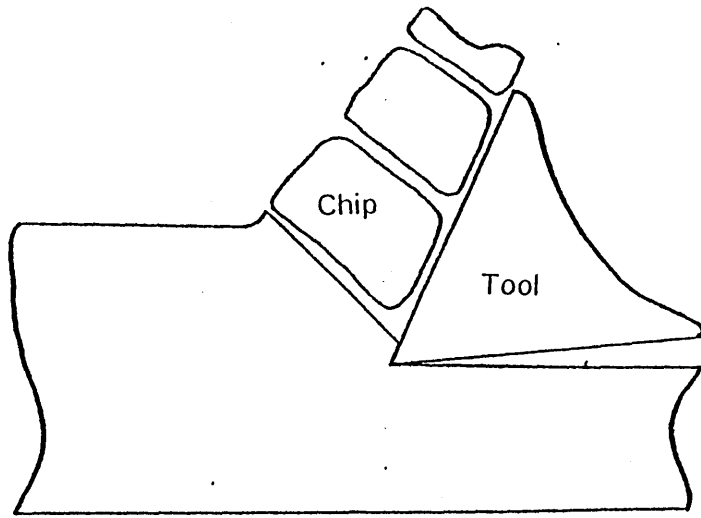
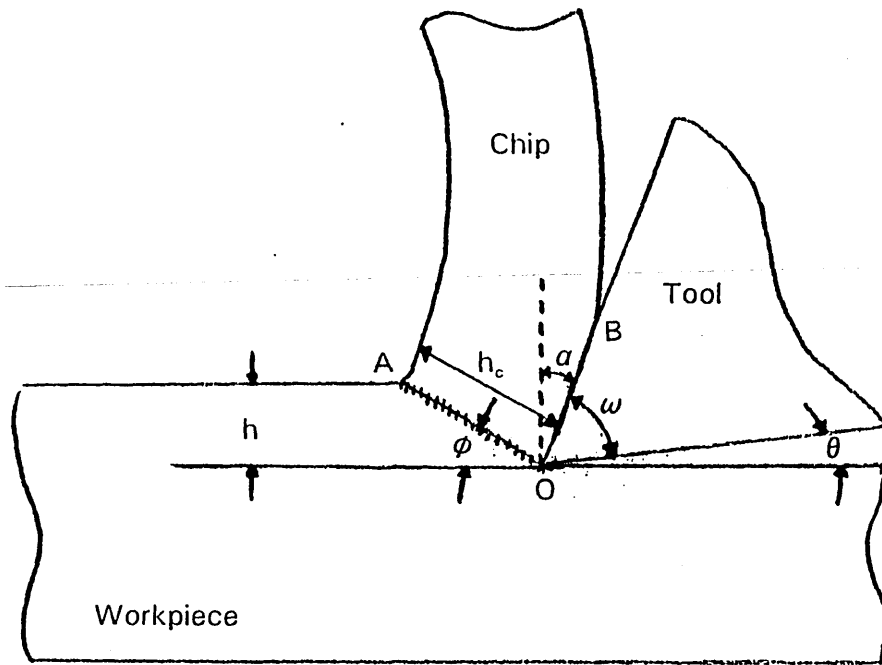


Figure 2(a) : Discontinuous chip (7).

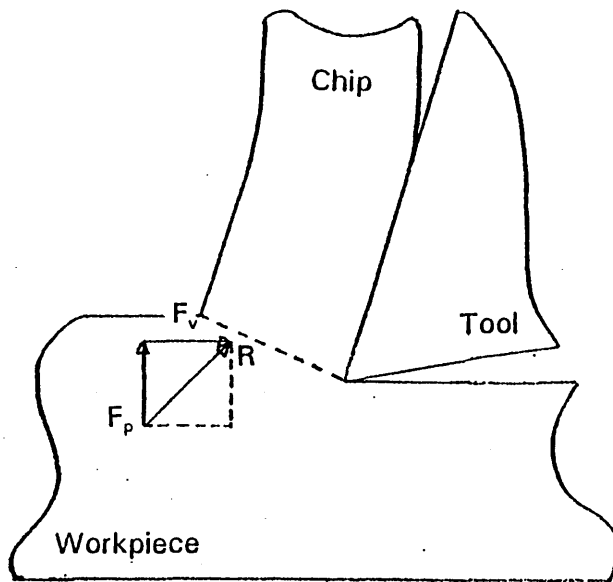
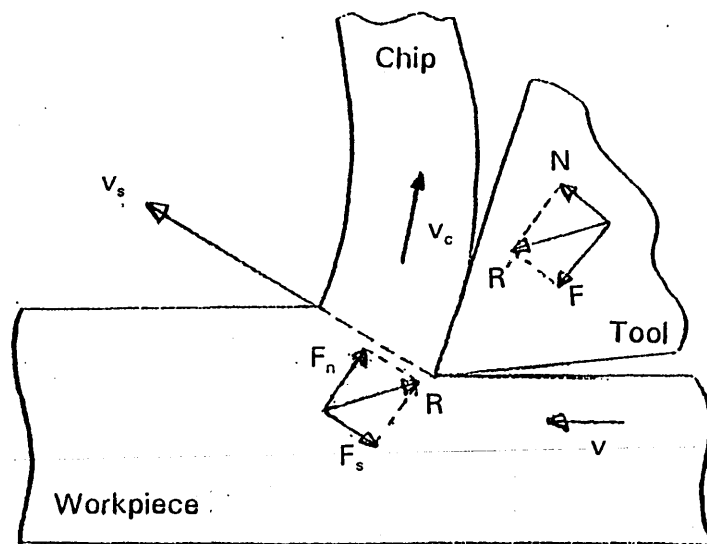
Figure 2(b) : Continuous chip (7).

Figure 2(c) : Built-up edge chip (7).





←
Direction of Movement



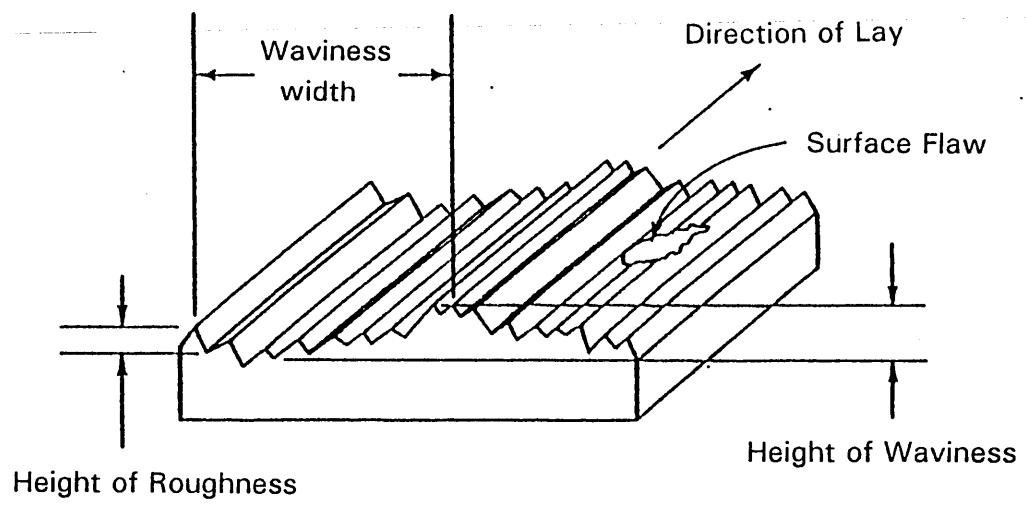


Figure 6 : Diagram to show the parameters used to calculate Newtonian fluid motion (35).

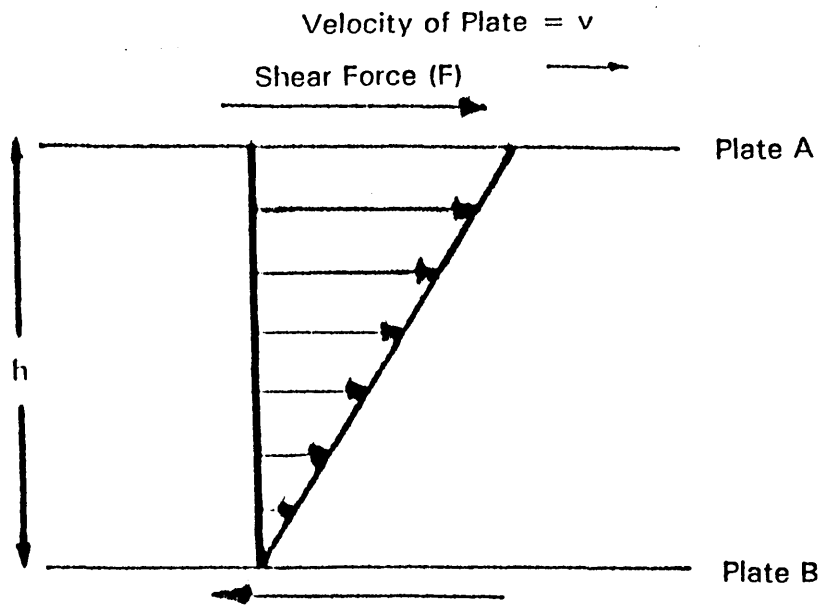


Figure 7 : Graph illustrating the behaviour of the four types of time-independent fluid (39).

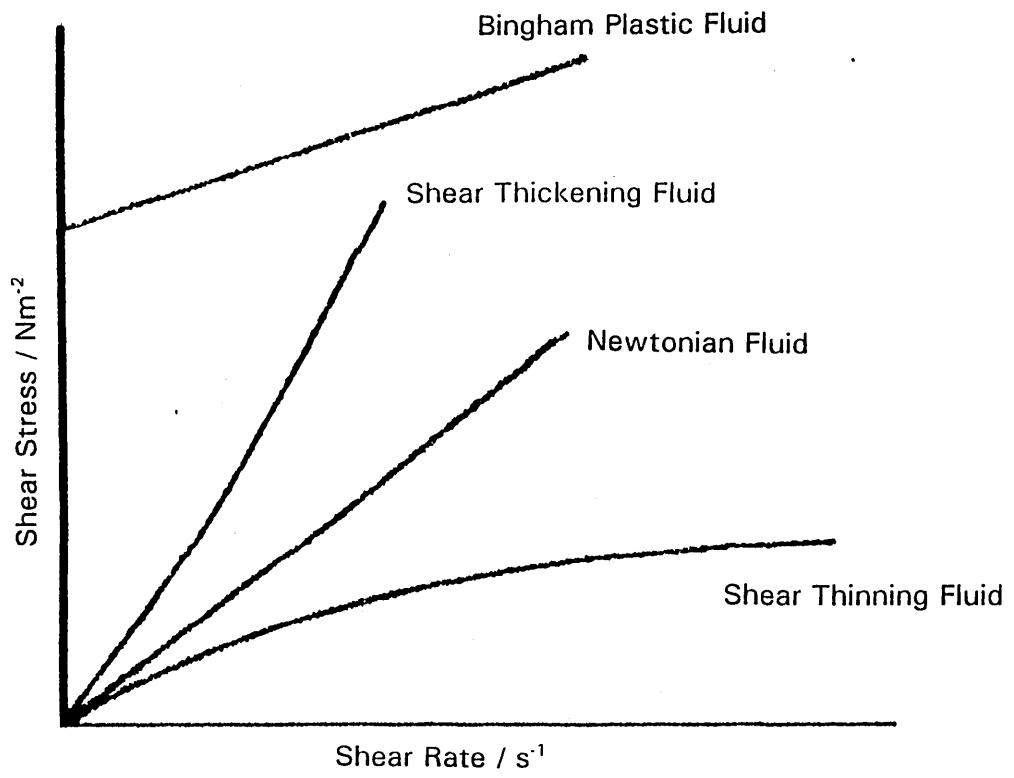


Figure 8 : Diagram showing the Normal stress components in a shear system (41).

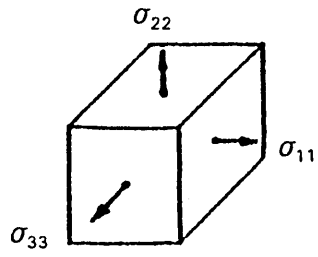


Figure 9 : Graph illustrating the relationship between the viscosity and the molecular weight average (41).

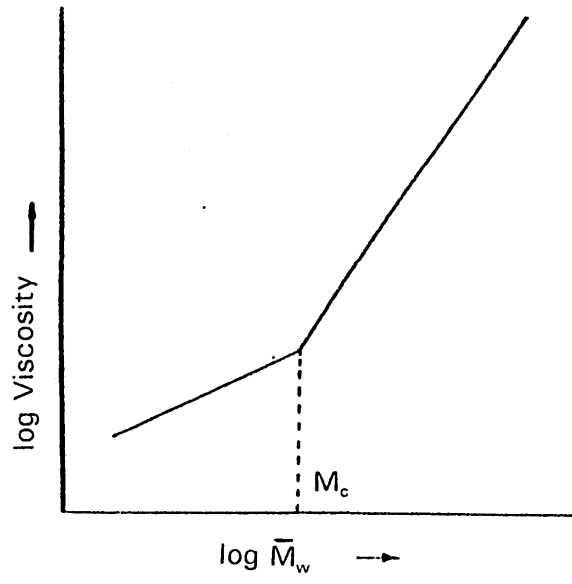


Figure 10(a) : Schematic diagram of a coaxial (concentric-cylinder) rotational viscometer (41).

Figure 10(b) : Schematic diagram of a rotational viscometer (41).

Figure 10(c) : Schematic diagram of a capillary viscometer (41).

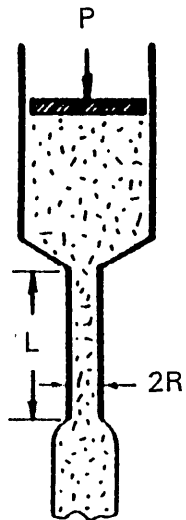
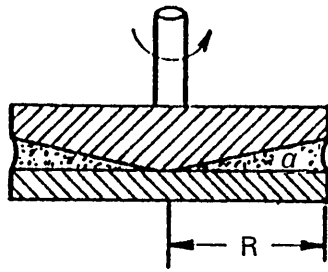
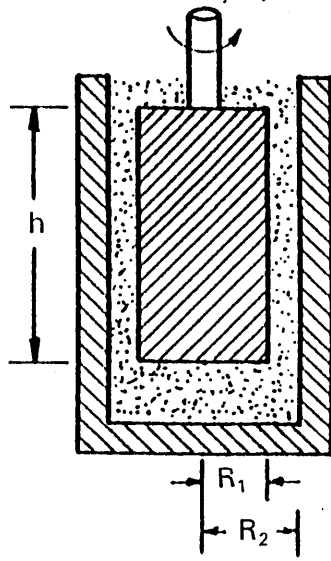


Figure 11 : The ideal pressure behaviour associated with capillary viscometers (39).

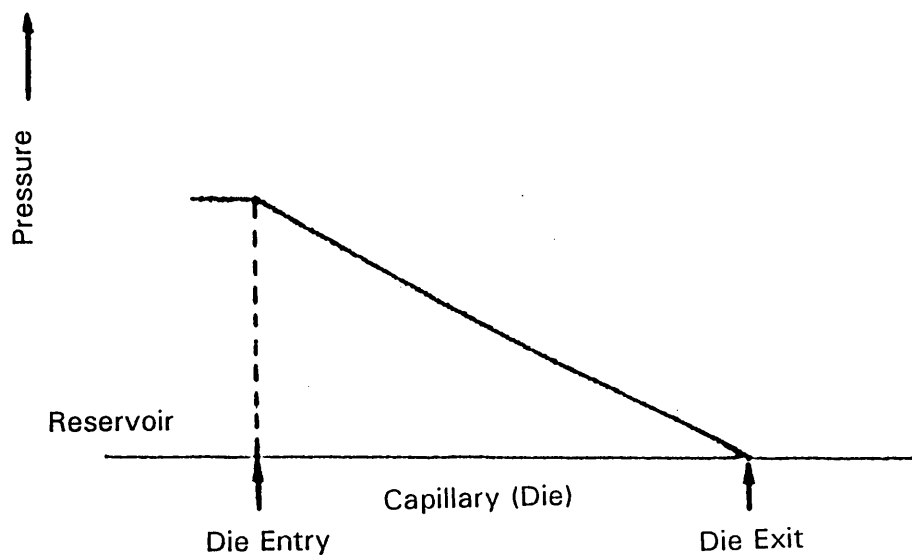
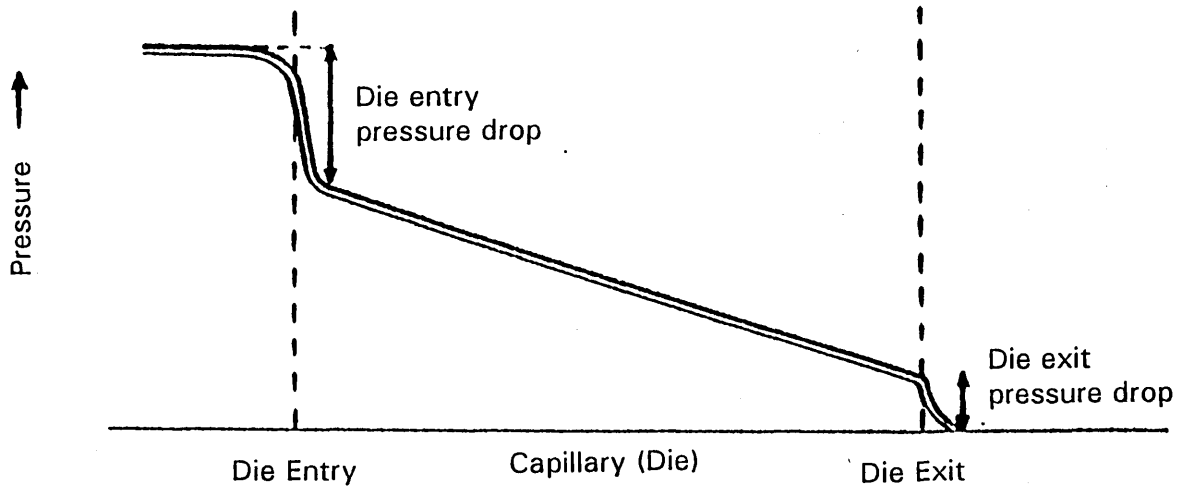
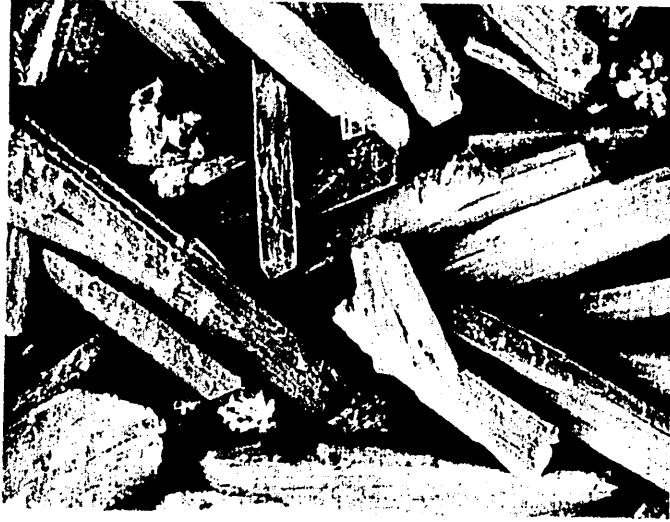
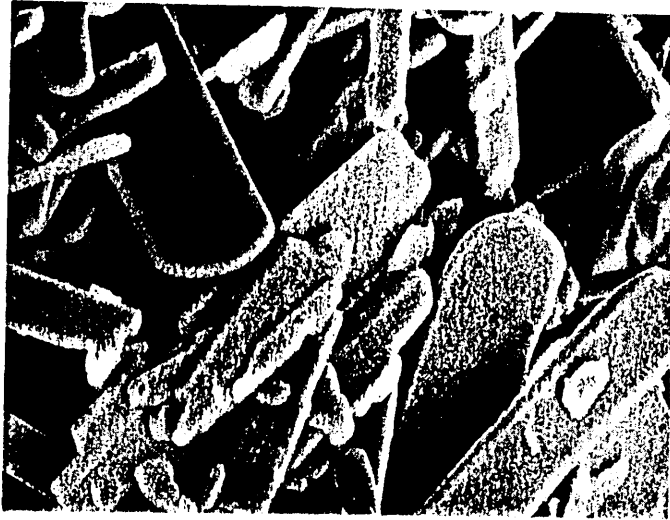


Figure 12 : The deviations from the ideal pressure behaviour in capillary viscometers due to end effects (44).





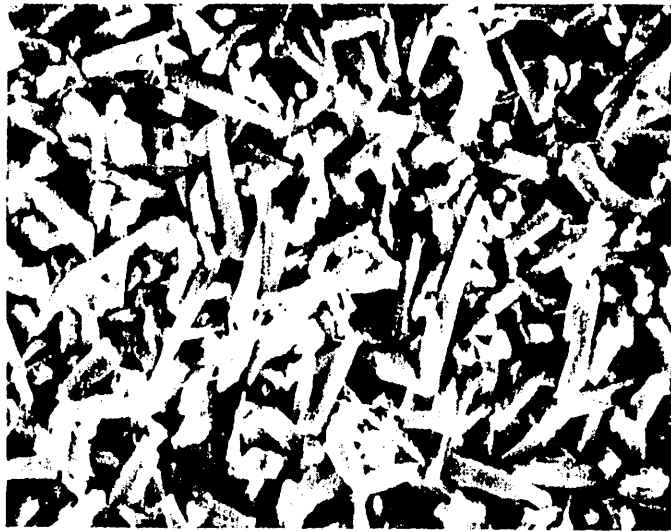
Fibrous



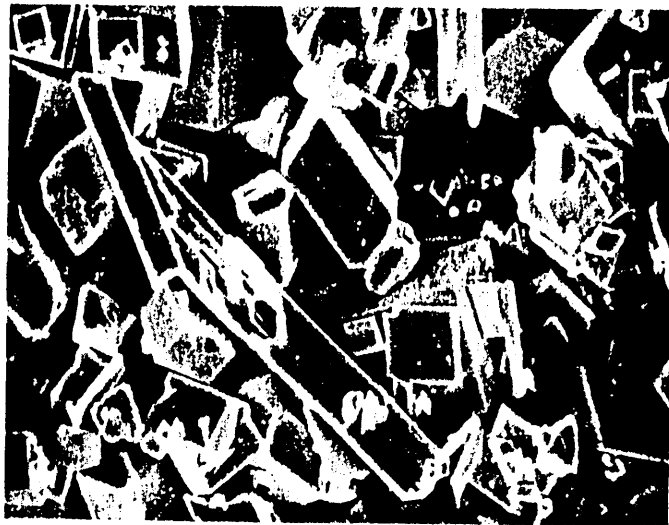
Flaky



Granular



Acicular



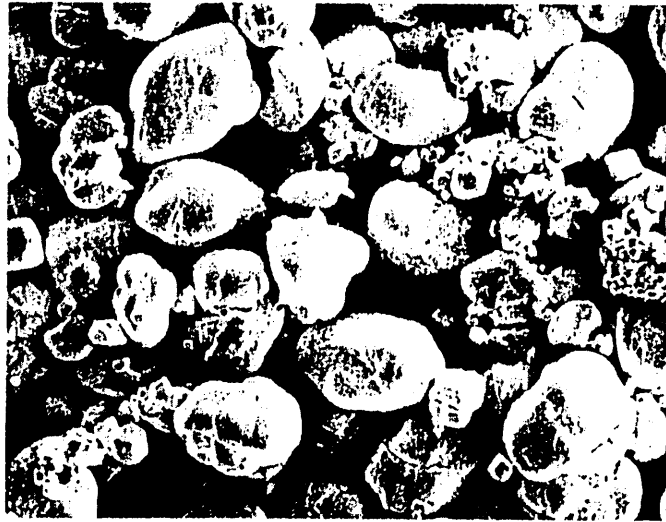
Angular



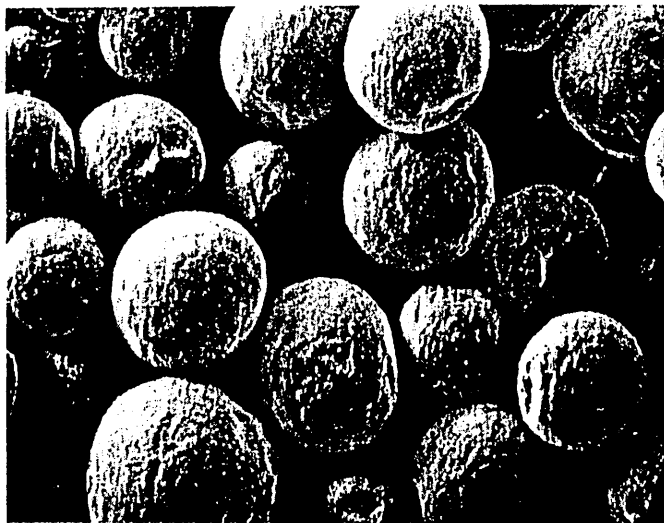
Dendritic



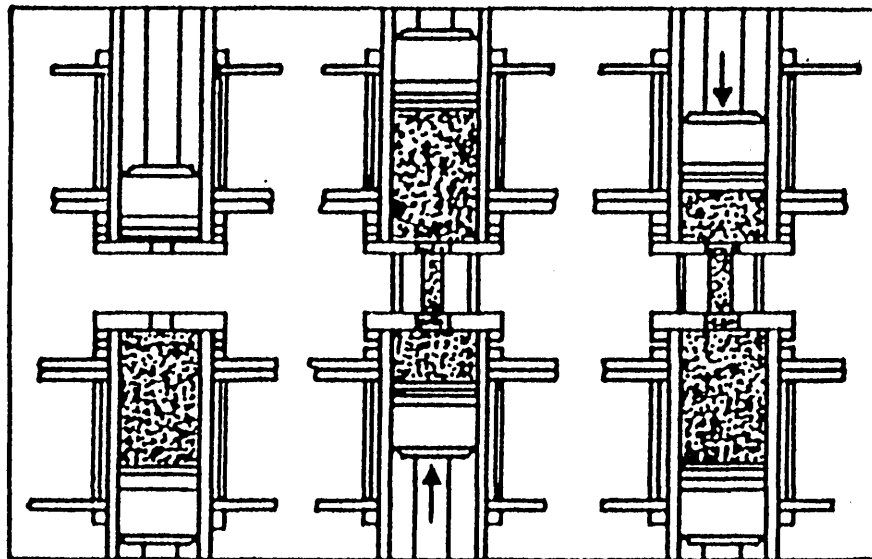
Irregular



Nodular



Spheroidal



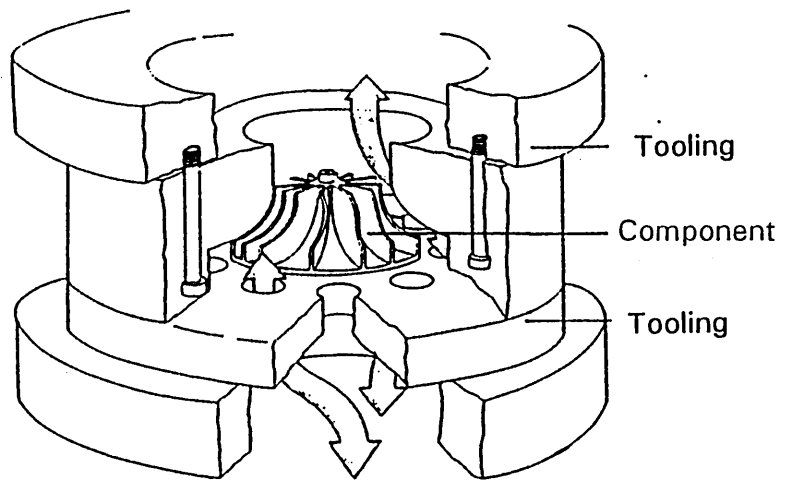






Figure 18 : The Dynisco μ PR690 microprocessor units connection to the computer.

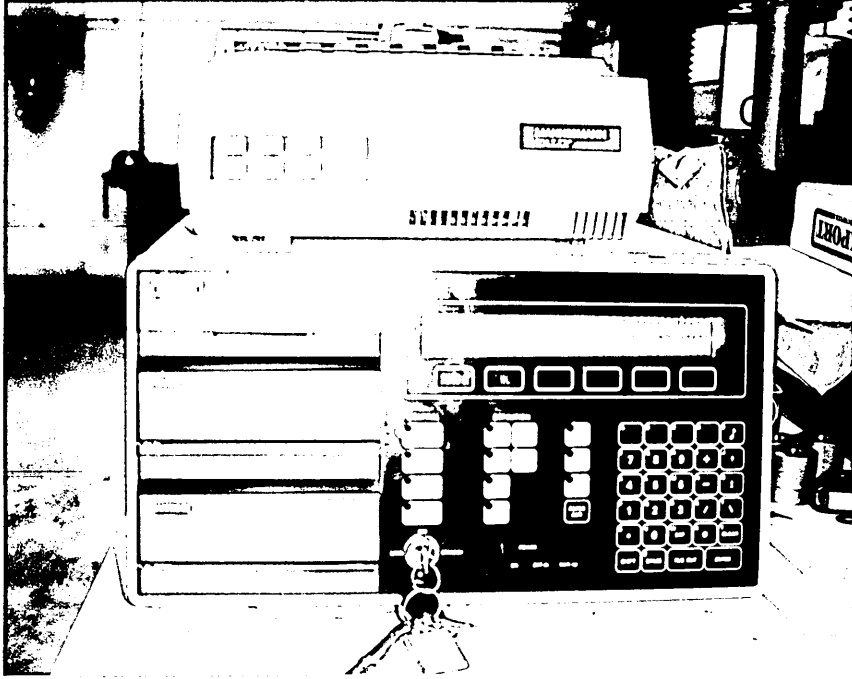


Figure 21(a) : Upper surface of tooling plate illustrating die location cavity.

Figure 21(b) : Transducer locations and protrusion on lower surface permitting alignment of tooling plates.

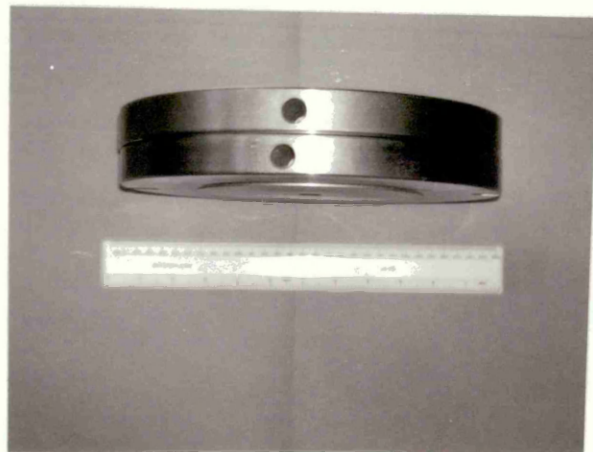
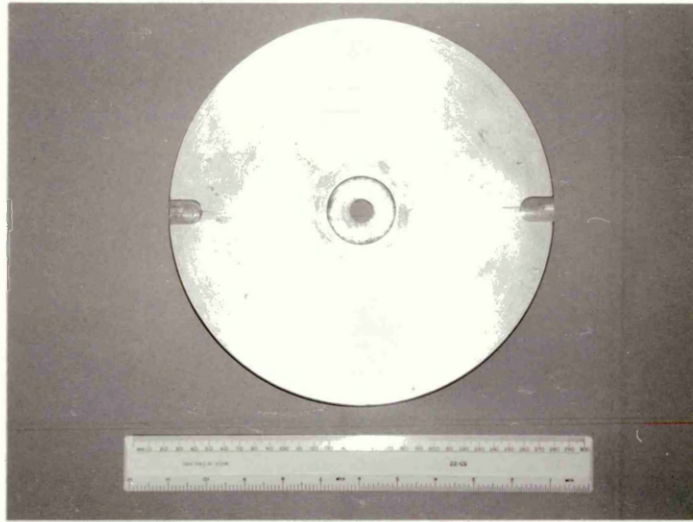
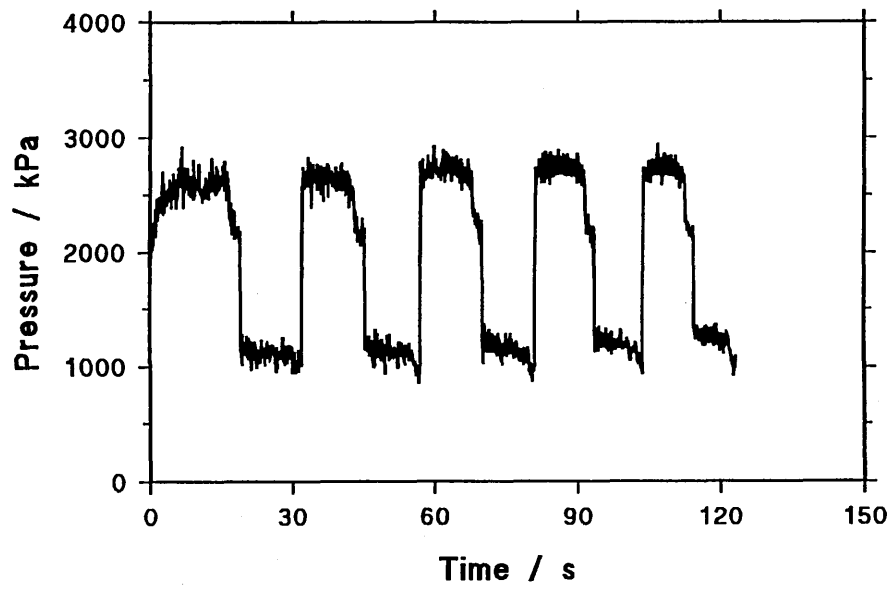
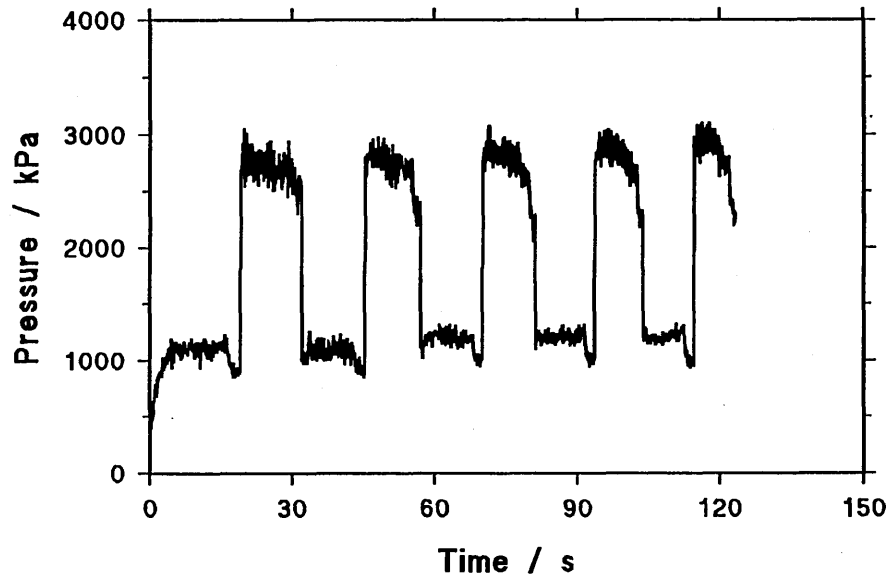


Figure 22 : The clamped 7A machine with tooling plates, die, and transducers in location.

Figure 23(a) : The upper transducer trace.

Figure 23(b) : The corresponding lower transducer trace.



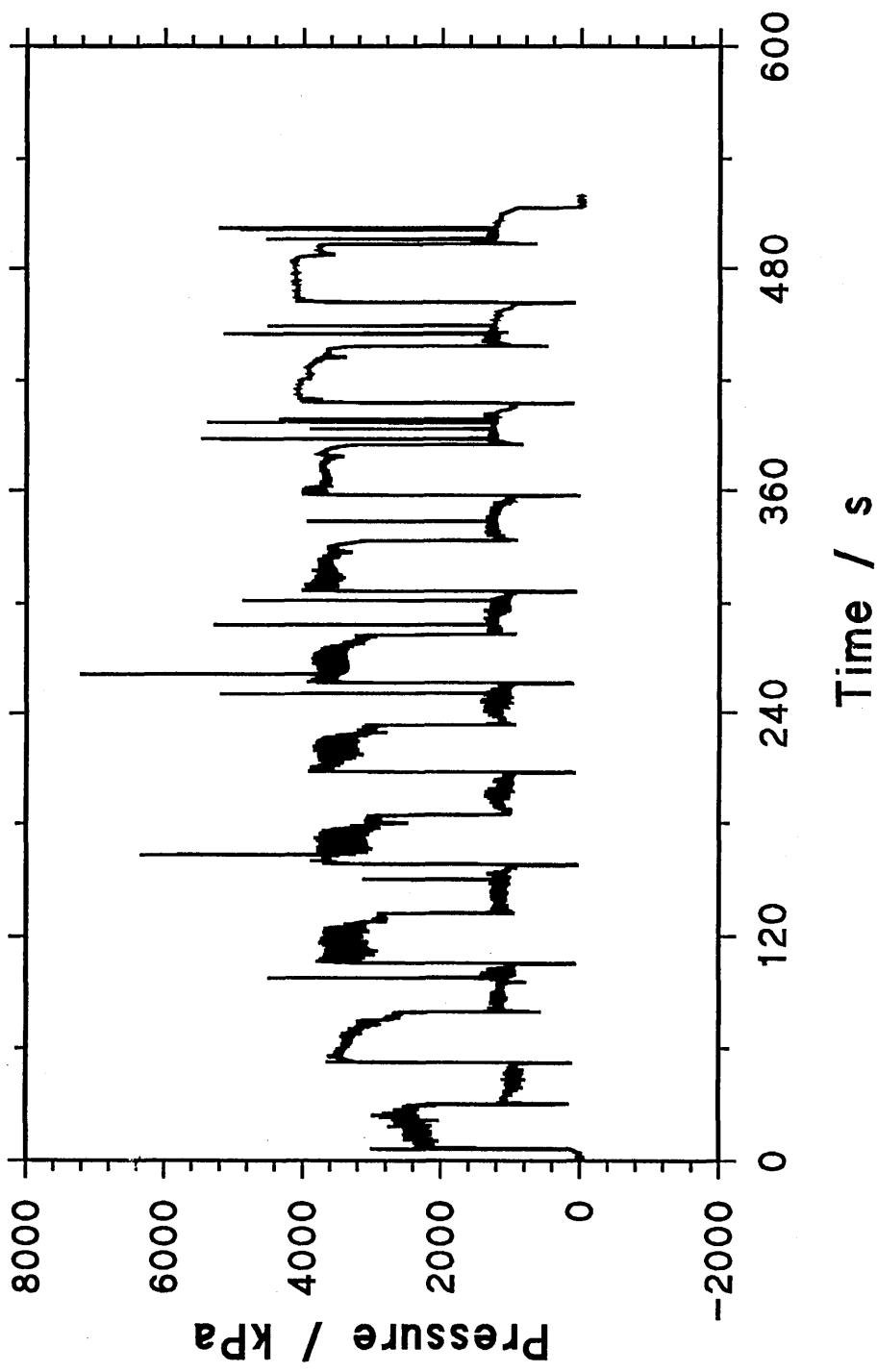


Figure 25(a) : Castle nut component - plan view.

x 1.8

Figure 25(b) : Castle nut component - side view.

x 1.8

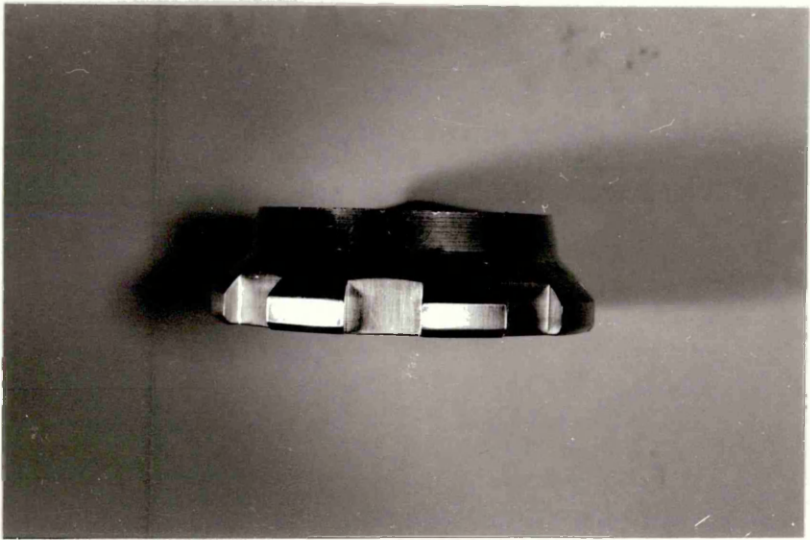


Figure 27(a) : The illustration of an inner spur corner of the castle nut component to show edge deburring.

x 70

Figure 27(b) : Illustration of the above feature at a greater magnification to show the effect of the grit particles and their direction of flow.

x 300

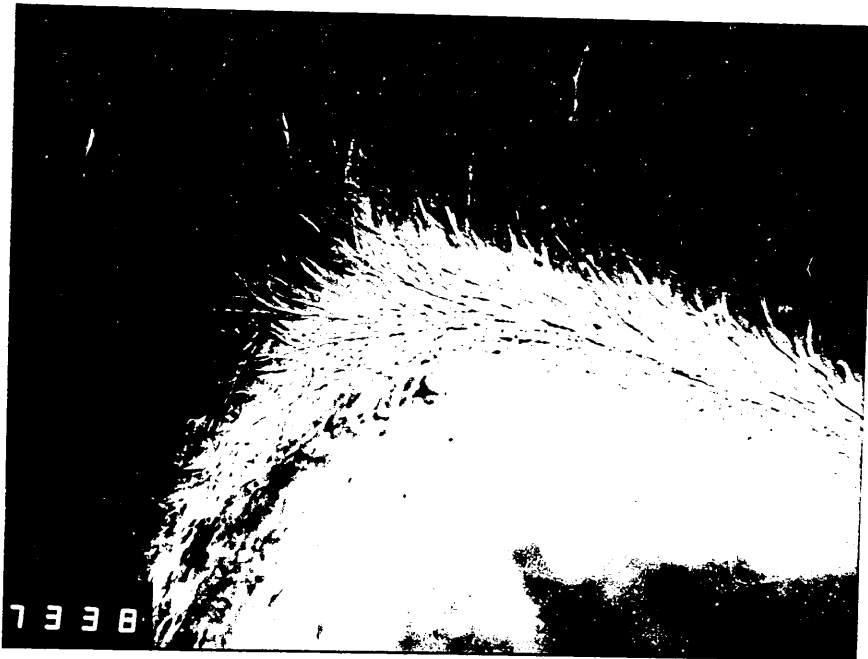
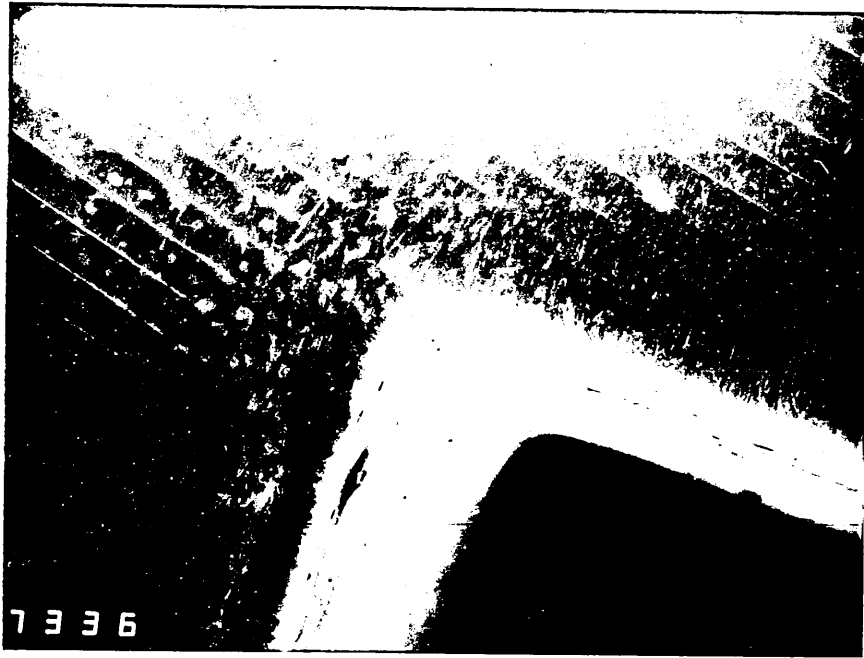


Figure 28(a)* : The illustration of an inclusion contained within the castle nut component after Abrasive Flow Machining has been performed.

x 300

Figure 28(b)* : The illustration of a void on the surface of the castle nut component after Abrasive Flow Machining has been performed.

x 300

* both features illustrated cannot be removed without significantly affecting the component's dimensions and therefore show the limitations of the AFM process.

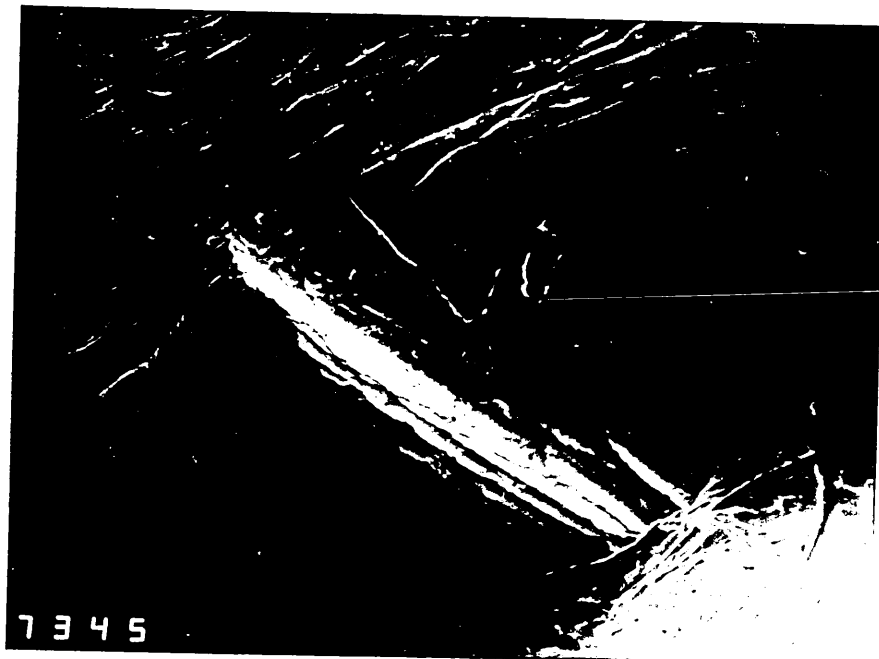


Figure 29(a) : The illustration of the conventional machining marks on an inner spur surface of the castle nut component.

x 170

Figure 29(b) : The illustration of the selective machining performed on the outer spur surface of the identical spur as shown in figure 29(a).

x 140

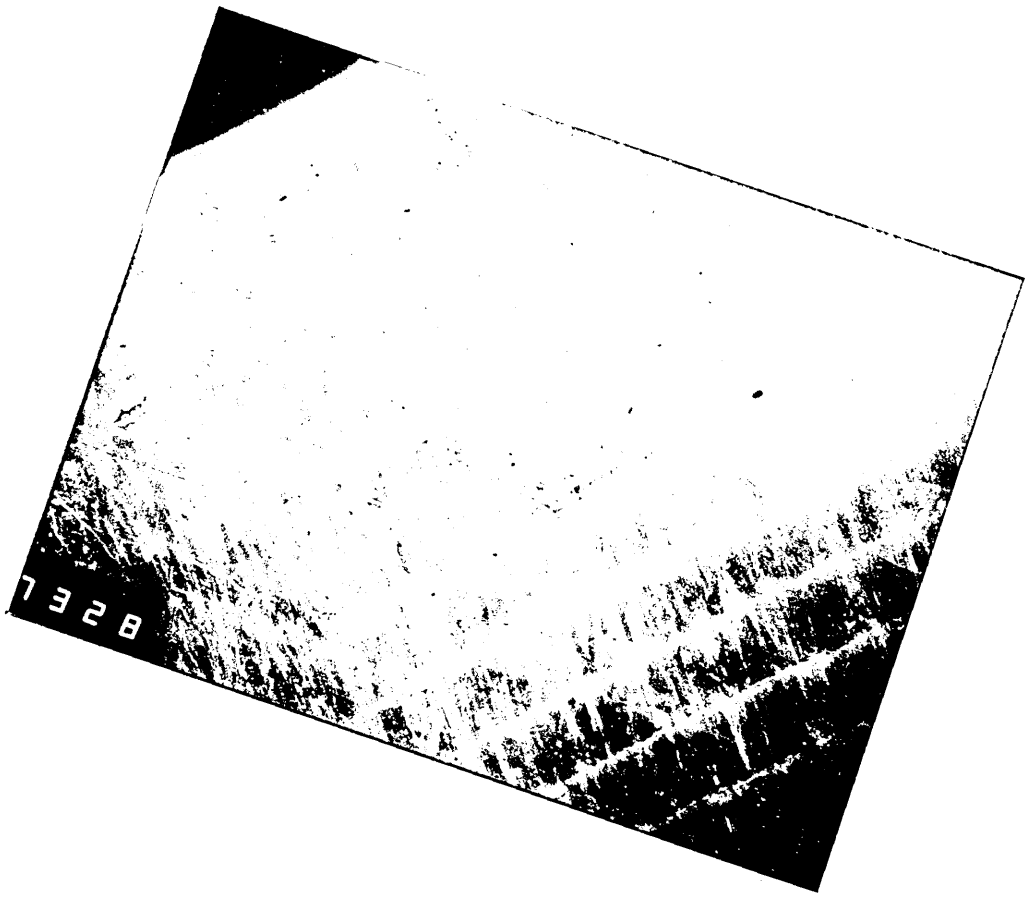
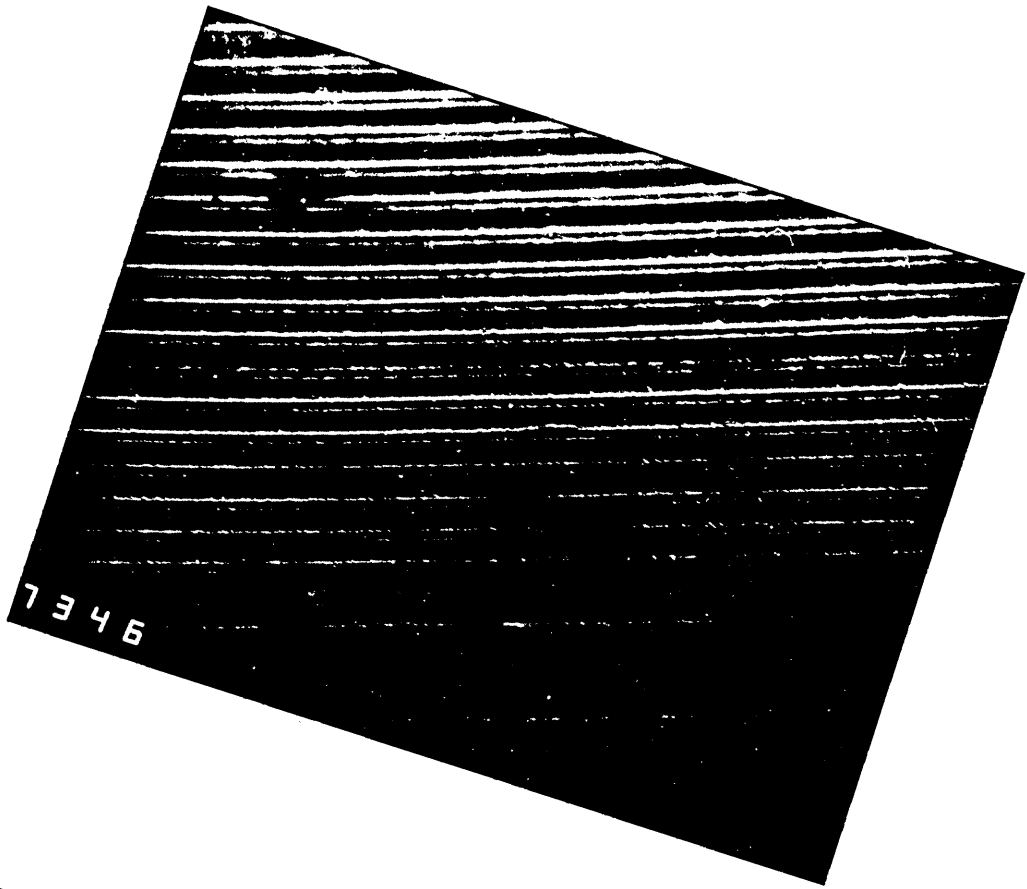


Figure 30 : The illustration of the ploughing effect of the grit particles.

x 560

Figure 31(a) : The illustration of the bearing component prior to AFM processing.

x 14.4

Figure 31(b) : The illustration of the bearing component after AFM processing.

x 12

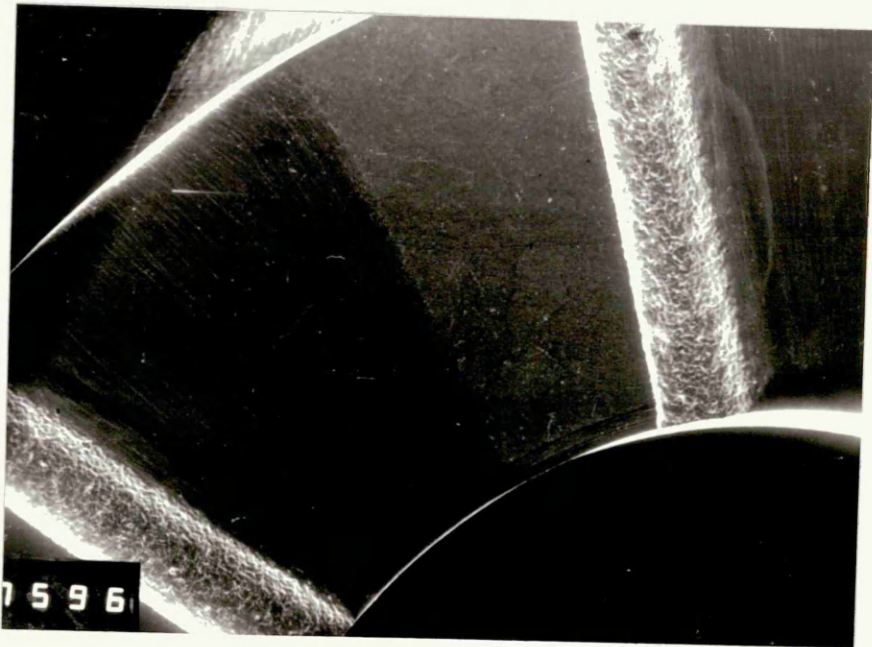
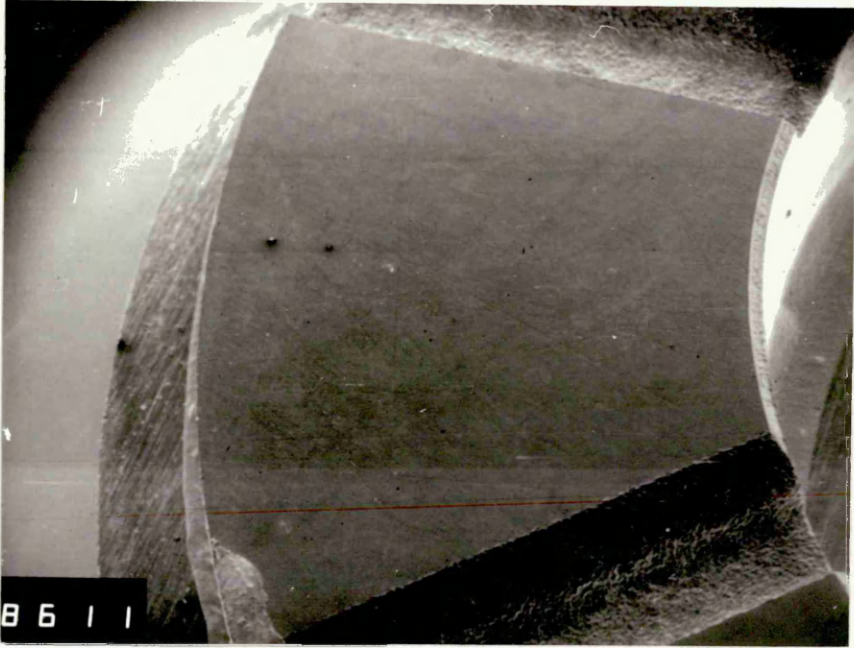


Figure 32(a) : The illustration of the bearing component surface prior to machining showing a random surface pattern.

x 120

Figure 32(b) : The illustration of the bearing component surface after machining showing the characteristic uni-directional surface pattern generated by the AFM process.

x 95

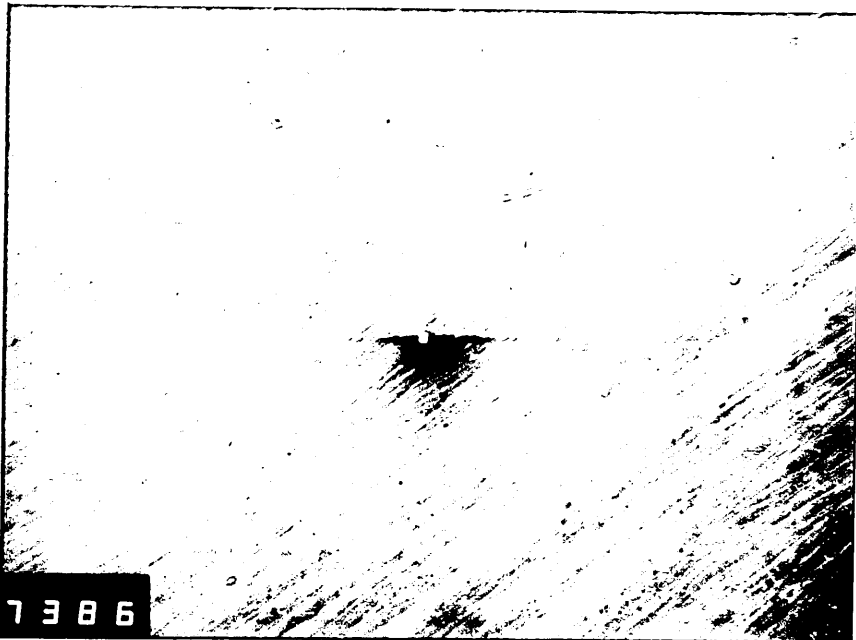
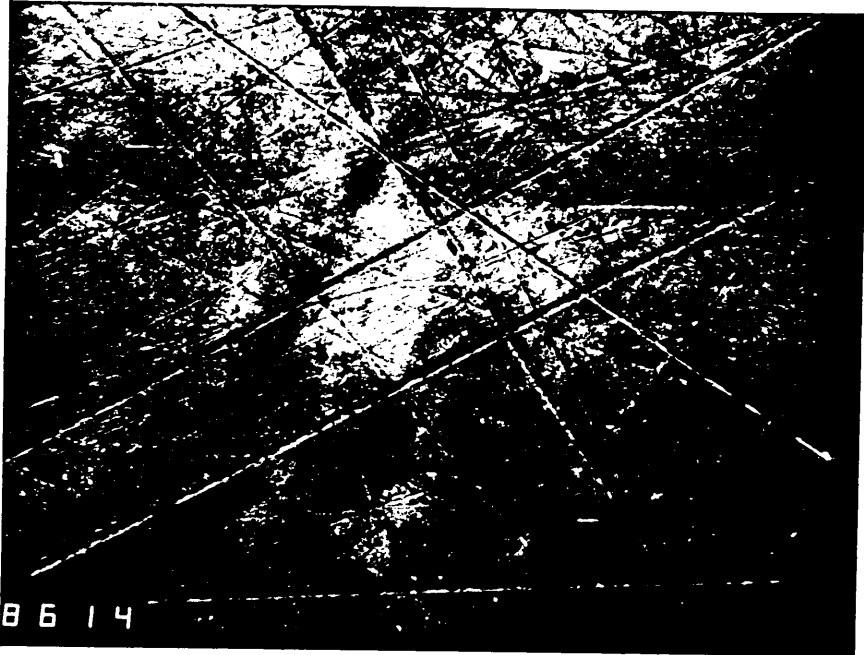


Figure 33 : The illustration of the surfaces on either side of the AFM generated apex on the bearing component showing the selective machining achieved by the tooling.

x 200

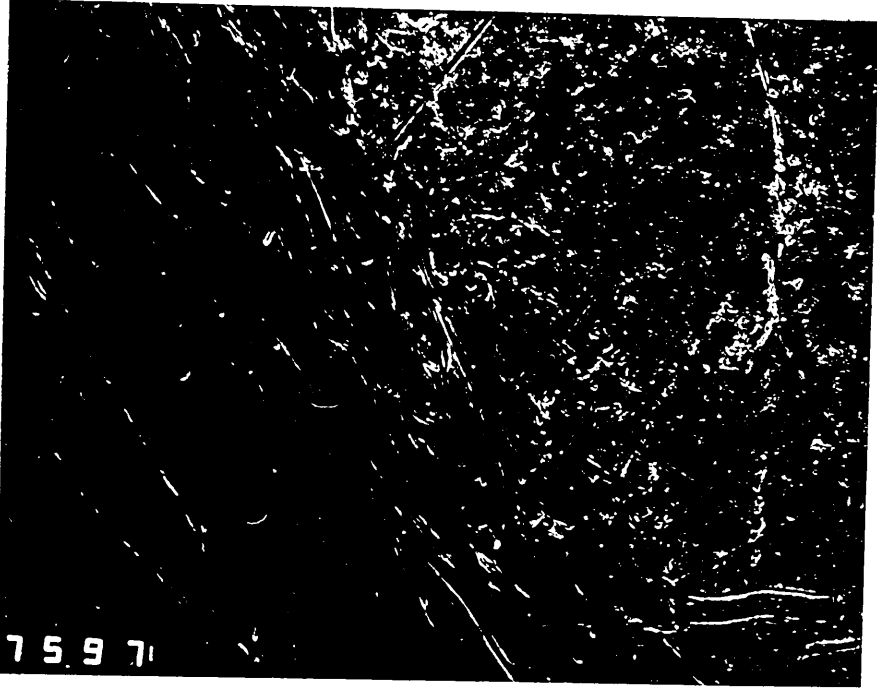


Figure 34(a) : The illustration of one of the bearing component's channels before processing.

x 60

Figure 34(b) : The illustration of one of the channels after machining showing once more the selective machining achieved by the tooling.

x 47.5

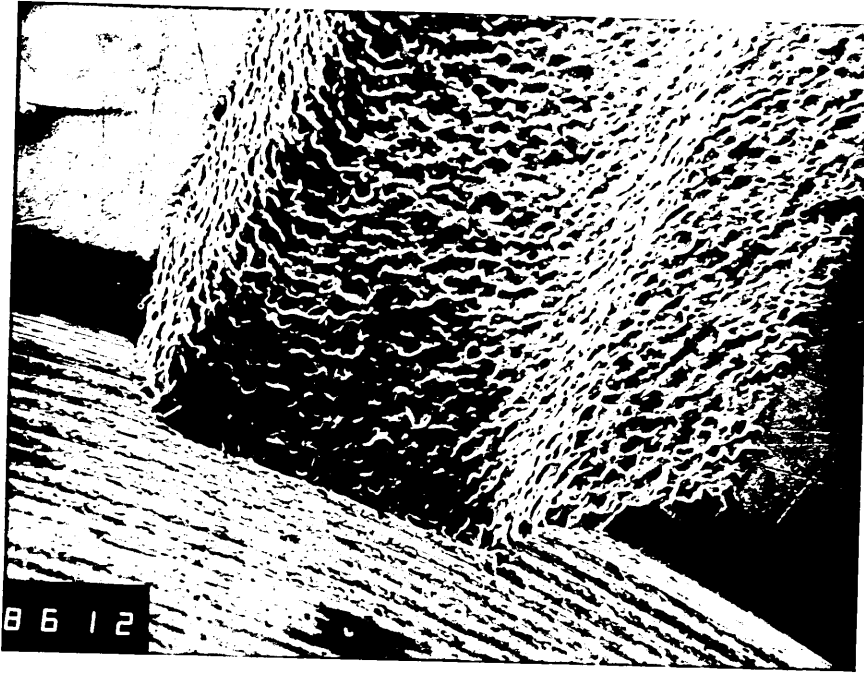


Figure 35 : The relationship between the number of extrusion cycles and the change in die diameter using LMV medium and 60 Mesh SiC grit. The relationship between the medium reuse and the change in die diameter is also shown.

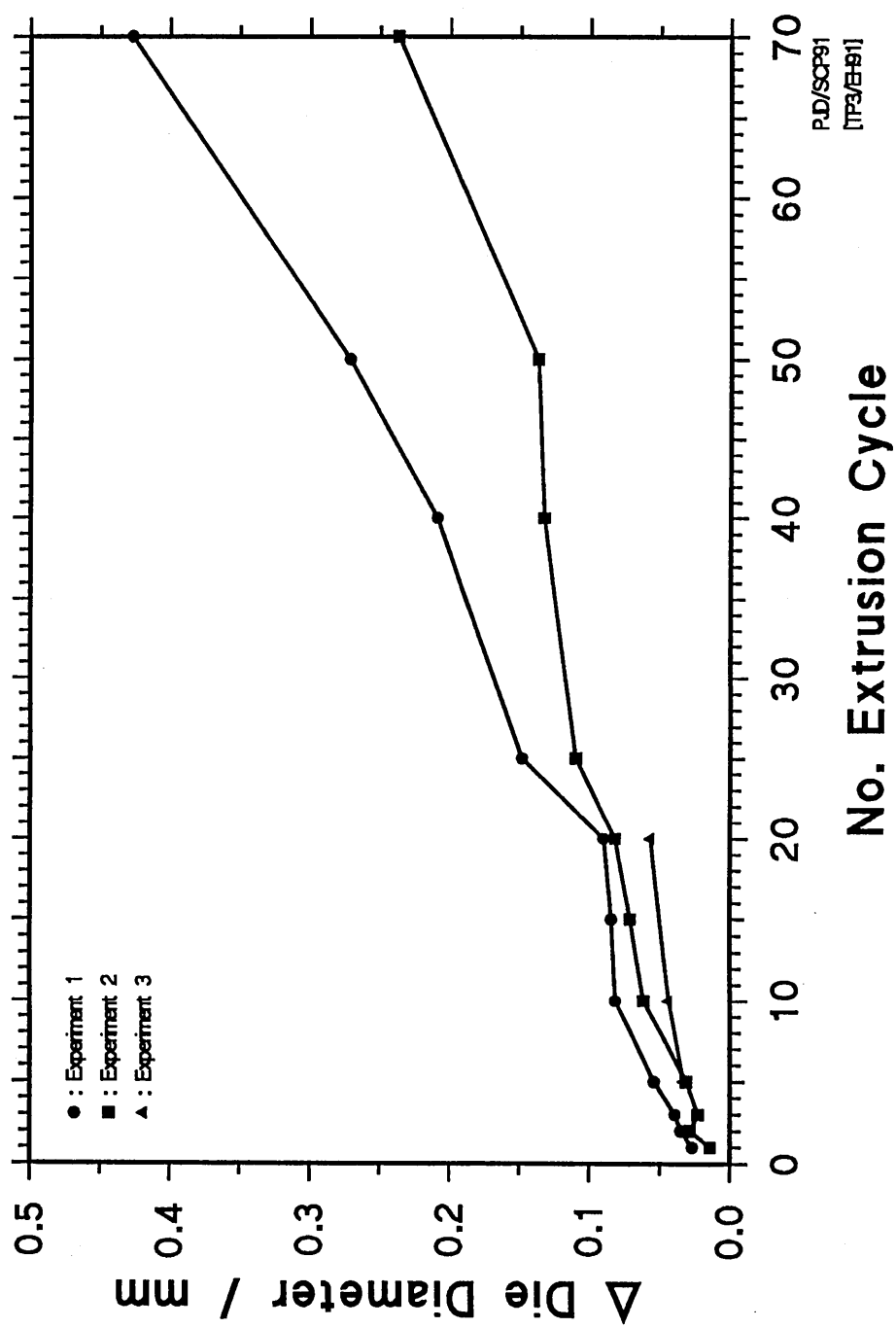


Figure 36 : The relationship between the number of extrusion cycles and the change in die mass using LMV medium and 60 Mesh SiC grit. The relationship between the medium reuse and the change in die mass is also shown.

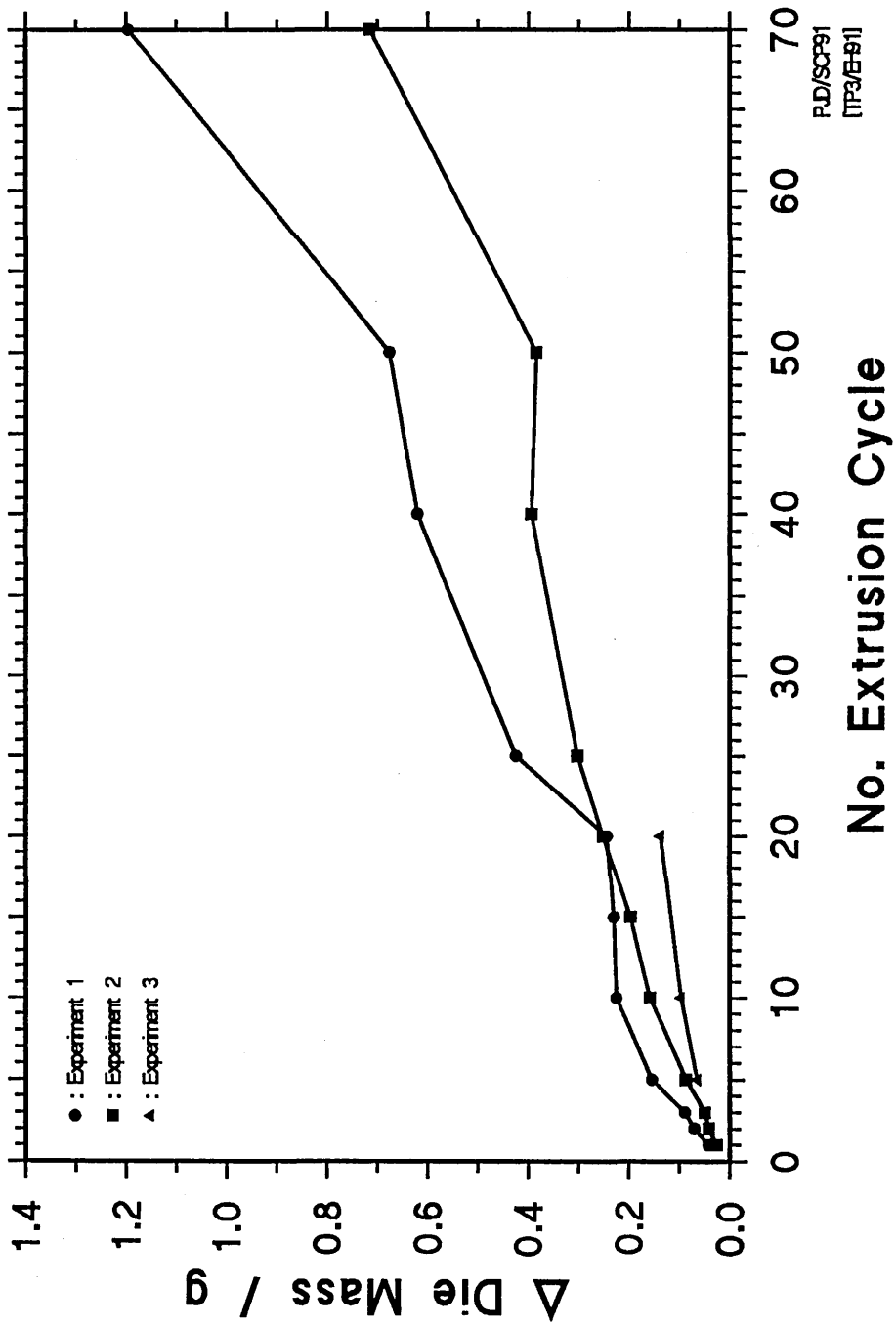


Figure 37 : The relationship between the number of extrusion cycles and the surface roughness improvement using LMV medium and 60 Mesh SiC grit. The relationship between the medium reuse and the change in surface roughness improvement is also shown.

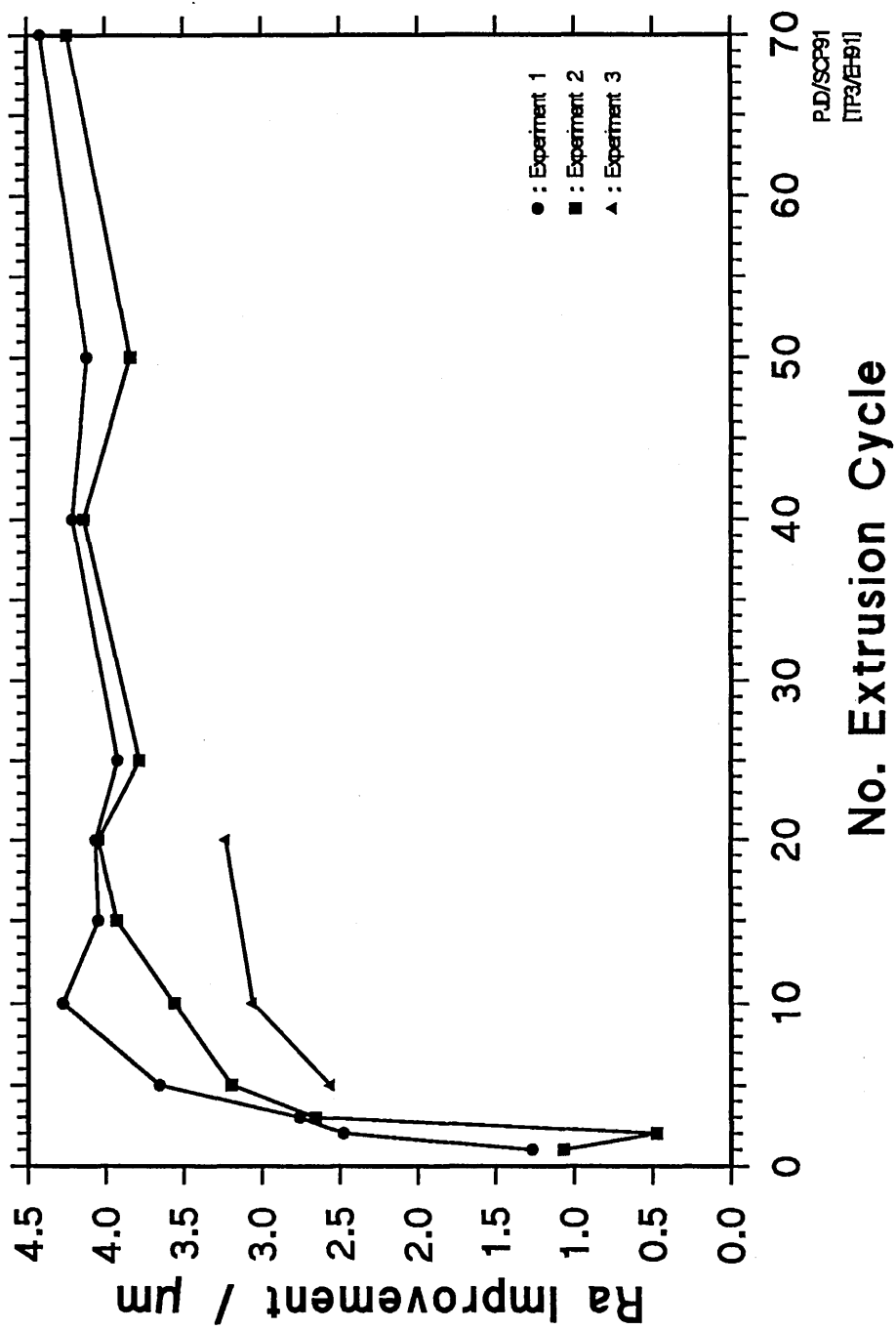


Figure 38(a) : Illustration of SiC grit that underwent 0 extrusion cycles.

x 16.25

Figure 38(b) : Illustration of SiC grit that underwent 1 extrusion cycle.

x 17.50



Figure 38(c) : Illustration of SiC grit that underwent 7 extrusion cycles.
x 18.75

Figure 38(d) : Illustration of SiC grit that underwent 21 extrusion cycles.
x 18.75

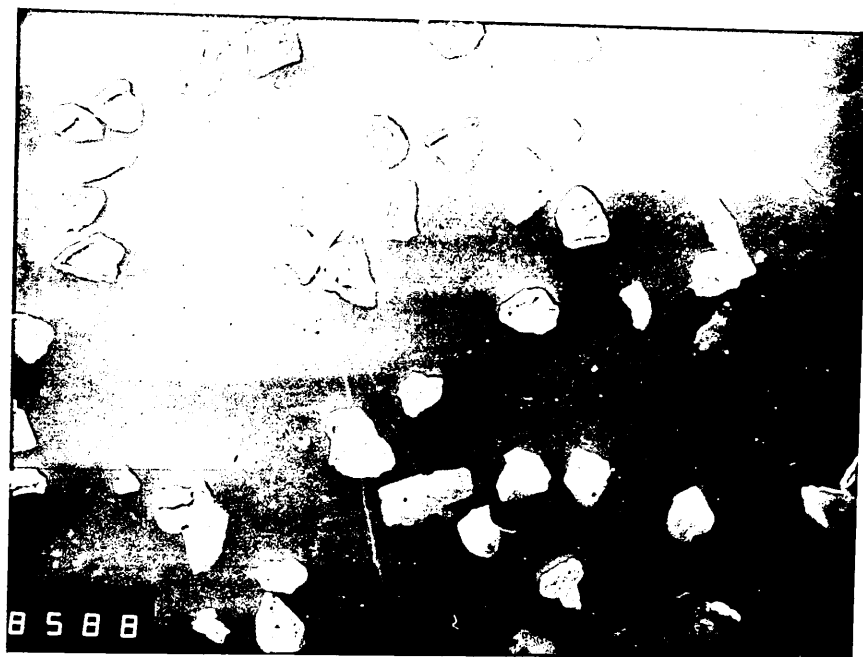


Figure 38(e) : Illustration of SiC grit that underwent 46 extrusion cycles.

x 18.75

Figure 38(f) : Illustration of SiC grit that underwent 91 extrusion cycles.

x 20

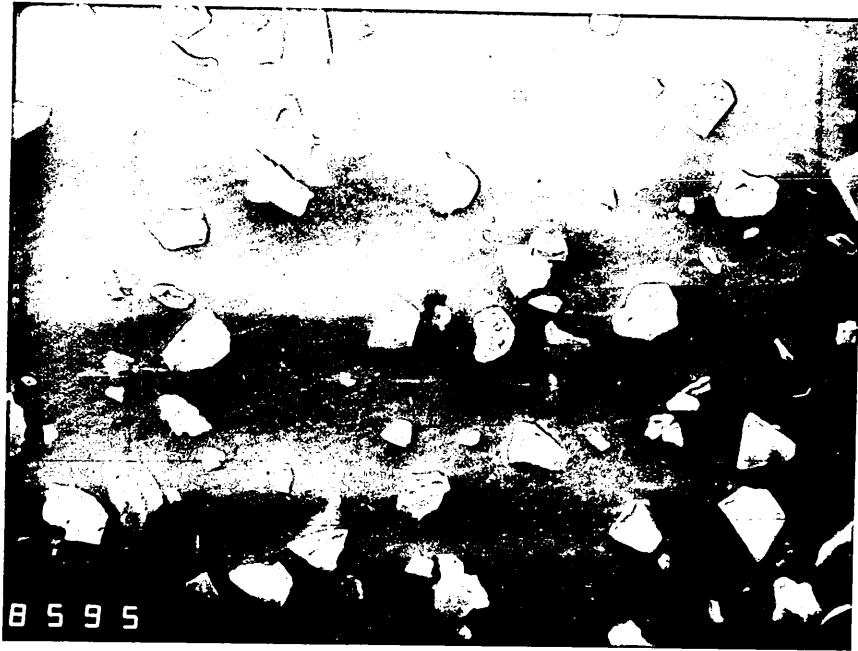


Figure 39 : A graph illustrating the results from the sieve analysis conducted on fresh and exhausted SiC grit.

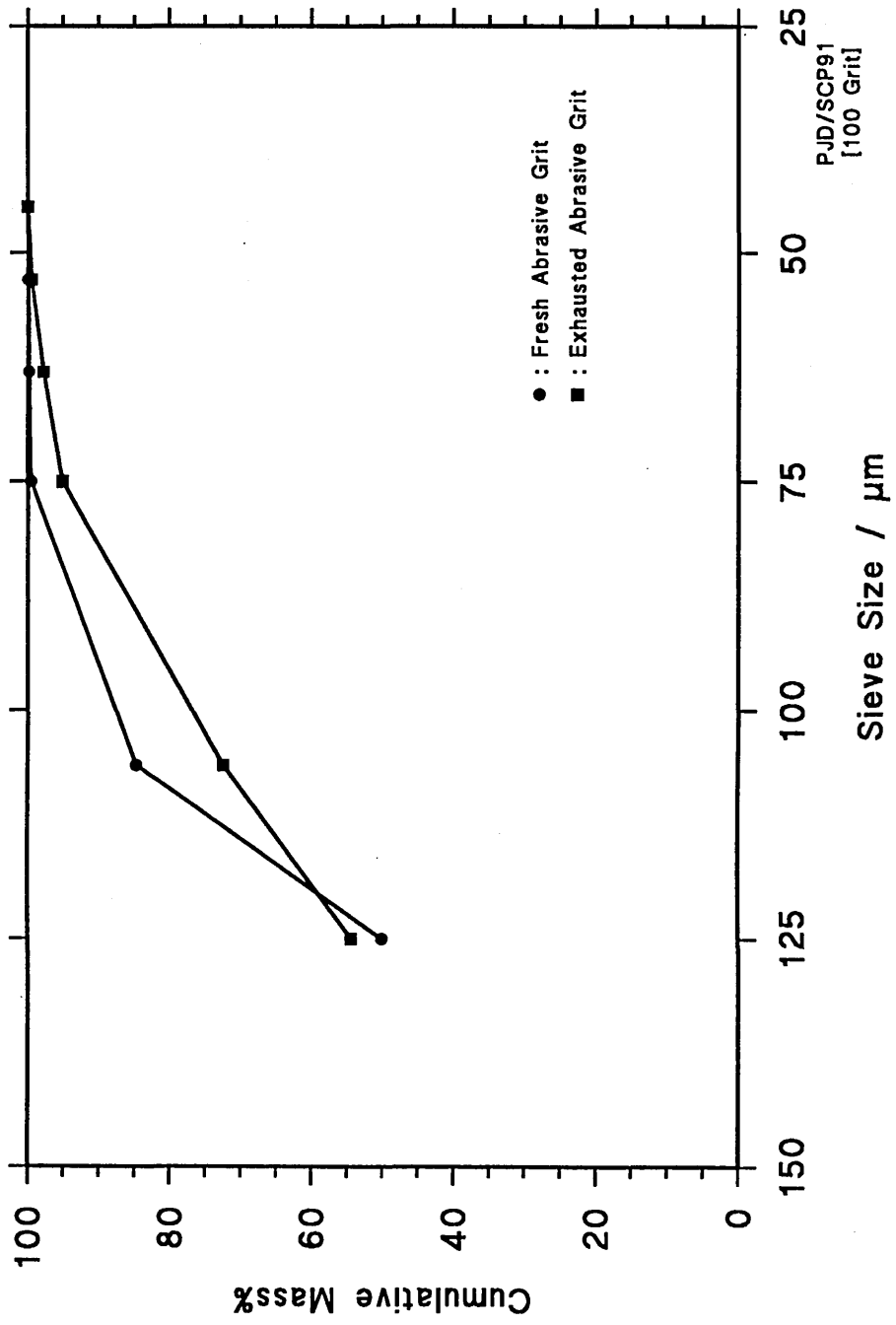


Figure 40(a) : The illustration of the grit particles retained on the 75 μ m sieve from the sieve analysis conducted on both the fresh and exhausted SiC grit.



Fresh Grit

x 75



Exhausted Grit

x 95

Figure 40(b) : The illustration of the grit particles retained on the $63\mu\text{m}$ sieve from the sieve analysis conducted on both the fresh and exhausted SiC grit.



Fresh Grit

x 75



Exhausted Grit

x 90

Figure 40(c) : The illustration of the grit particles retained on the 53 μ m sieve from the sieve analysis conducted on both the fresh and exhausted SiC grit.



Fresh Grit

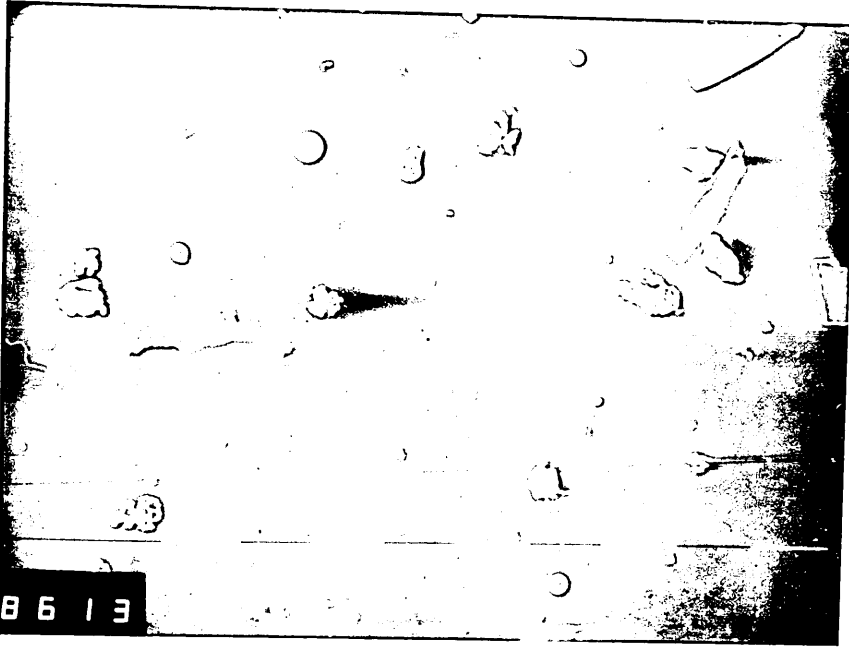
x 80



Exhausted Grit

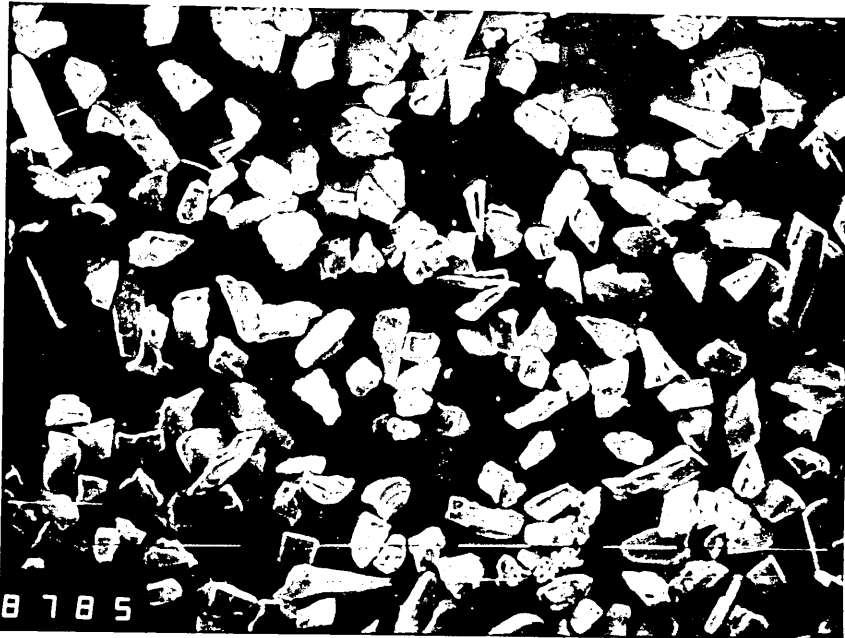
x 95

Figure 40(d) : The illustration of the grit particles retained on the 45 μ m sieve from the sieve analysis conducted on both the fresh and exhausted SiC grit.



Fresh Grit

x 80



Exhausted Grit

x 95

Figure 41 : The relationship between the number of extrusion cycles and the die diameter using LV medium and 60 Mesh grit with grit to polymer ratios of 0.5, 1 and 2.

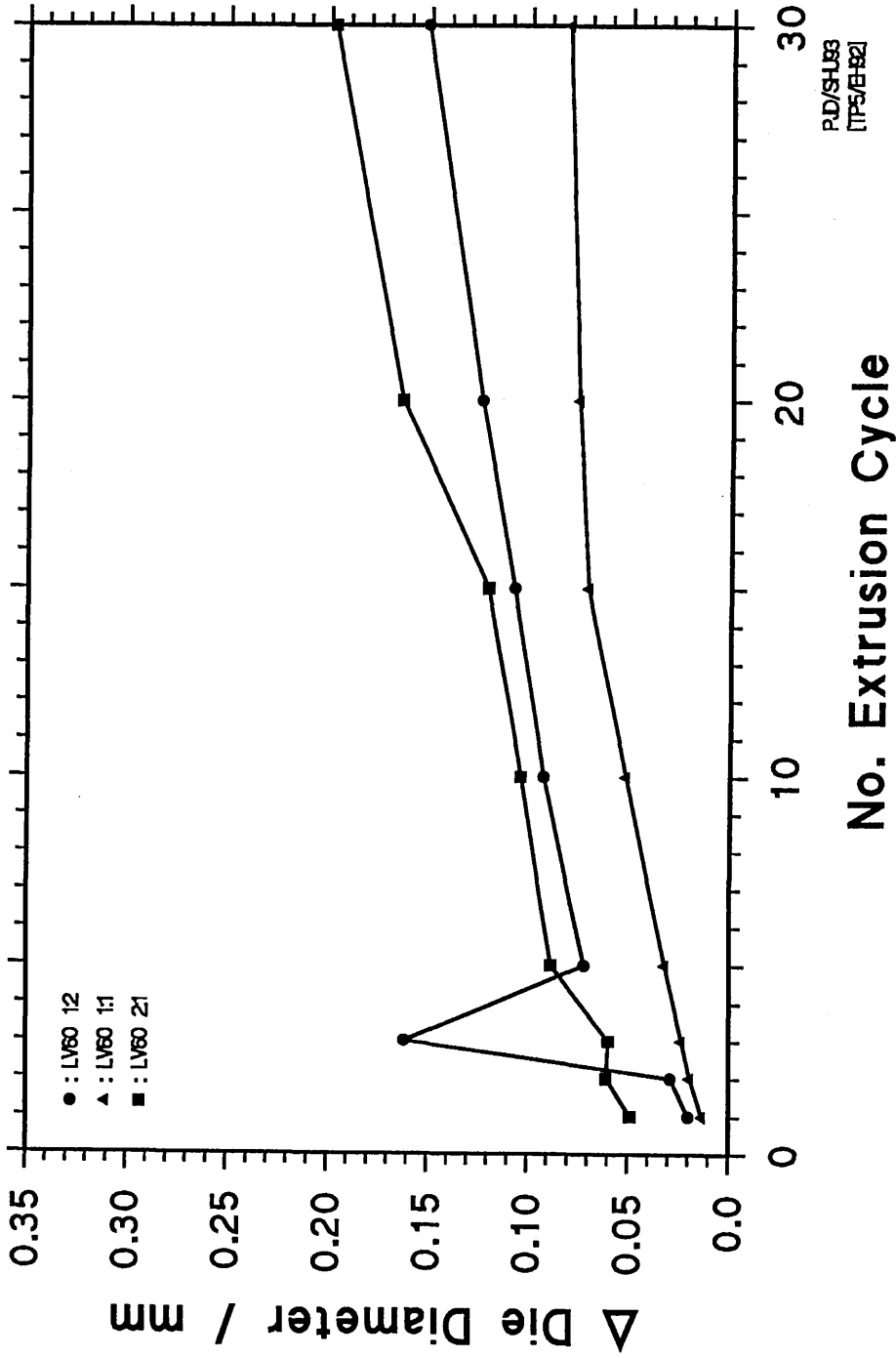


Figure 42 : The relationship between the number of extrusion cycles and the die diameter using LV medium and 100 Mesh grit with grit to polymer ratios of 0.5, 1 and 2.

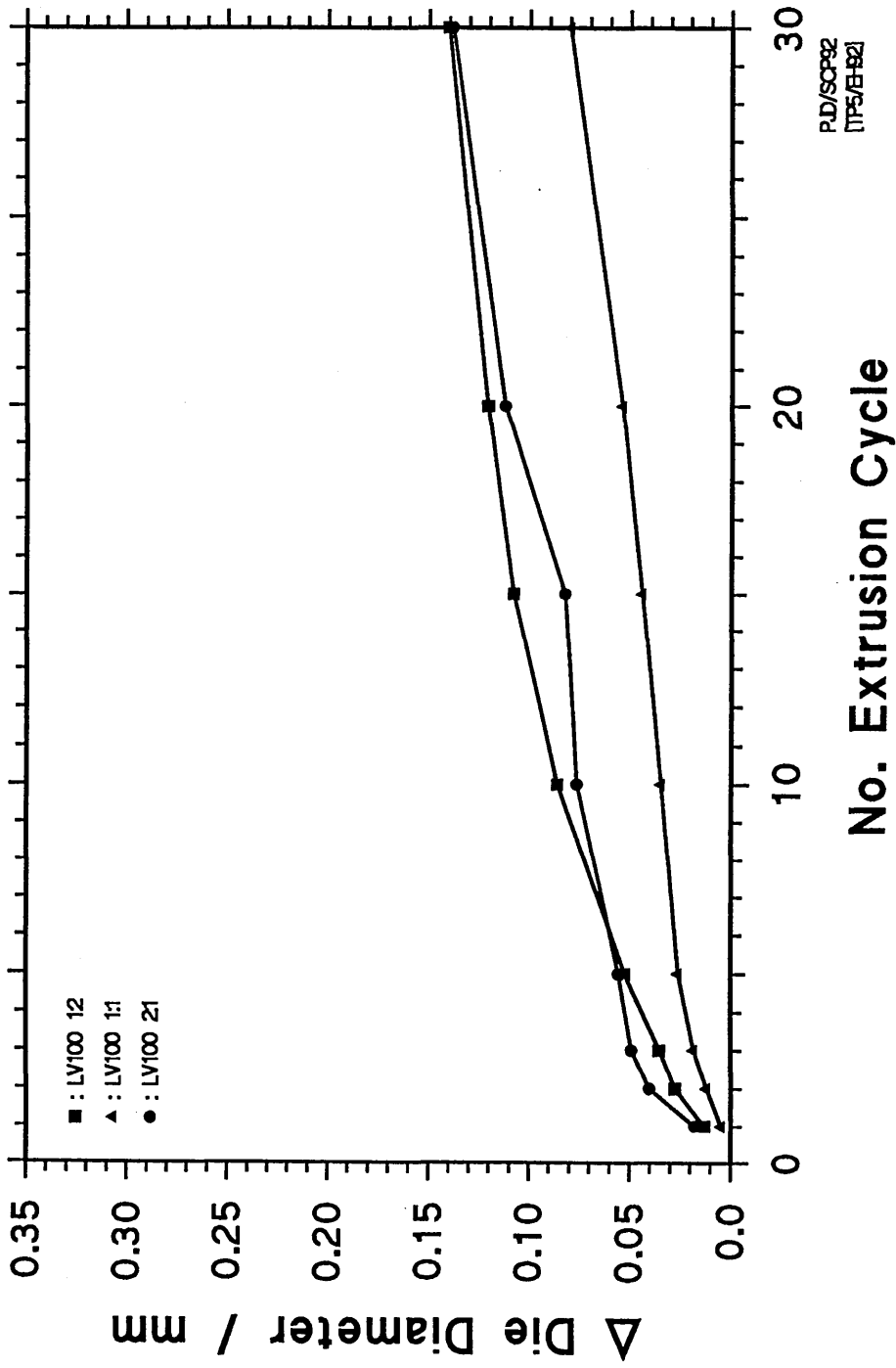
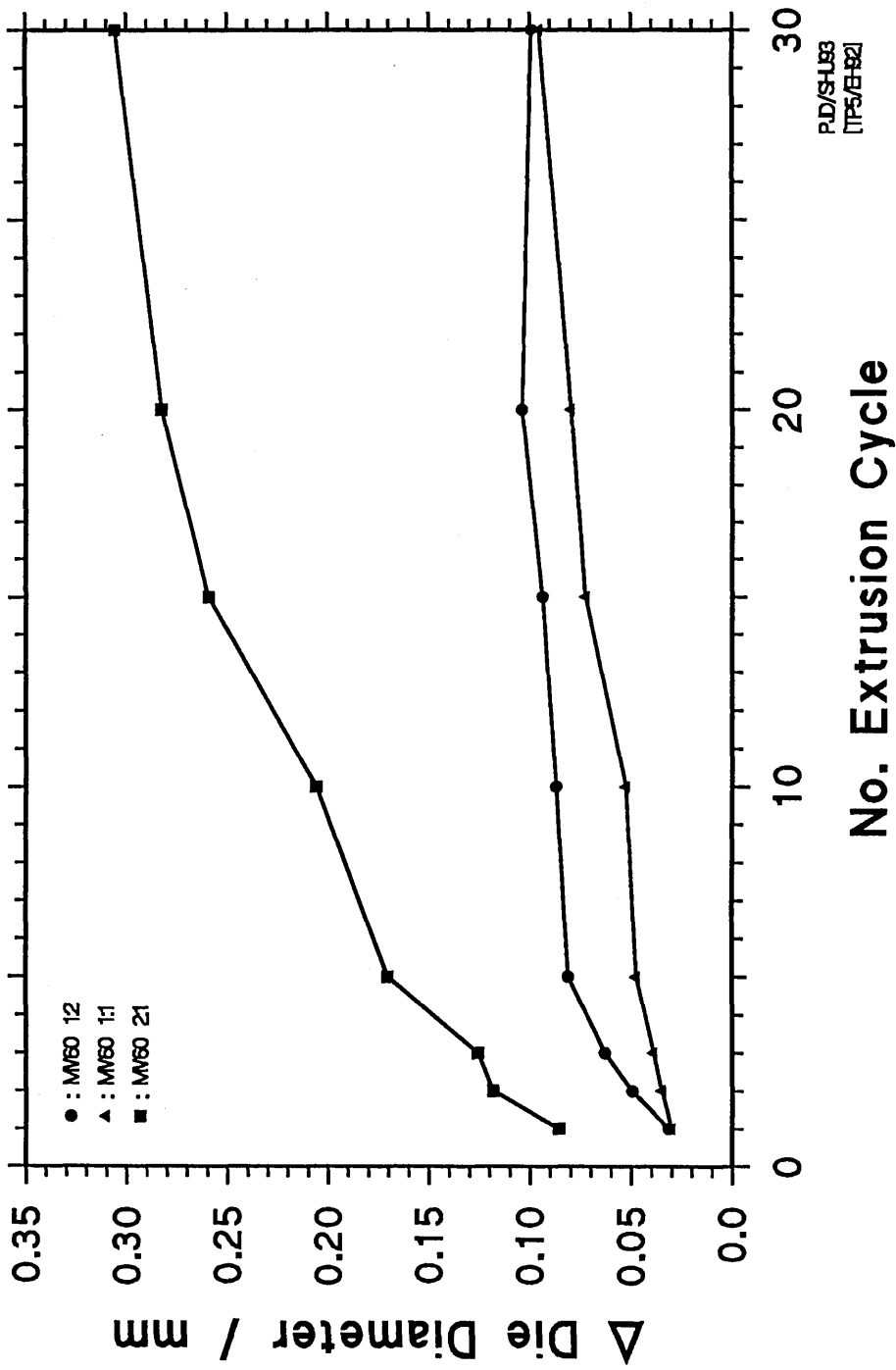


Figure 43 : The relationship between the number of extrusion cycles and the die diameter using MV medium and 60 Mesh grit with grit to polymer ratios of 0.5, 1 and 2.



P.D./S.H.188
[TP5/E-192]

Figure 44 : The relationship between the number of extrusion cycles and the die diameter using MV medium and 100 Mesh grit with grit to polymer ratios of 0.5, 1 and 2.

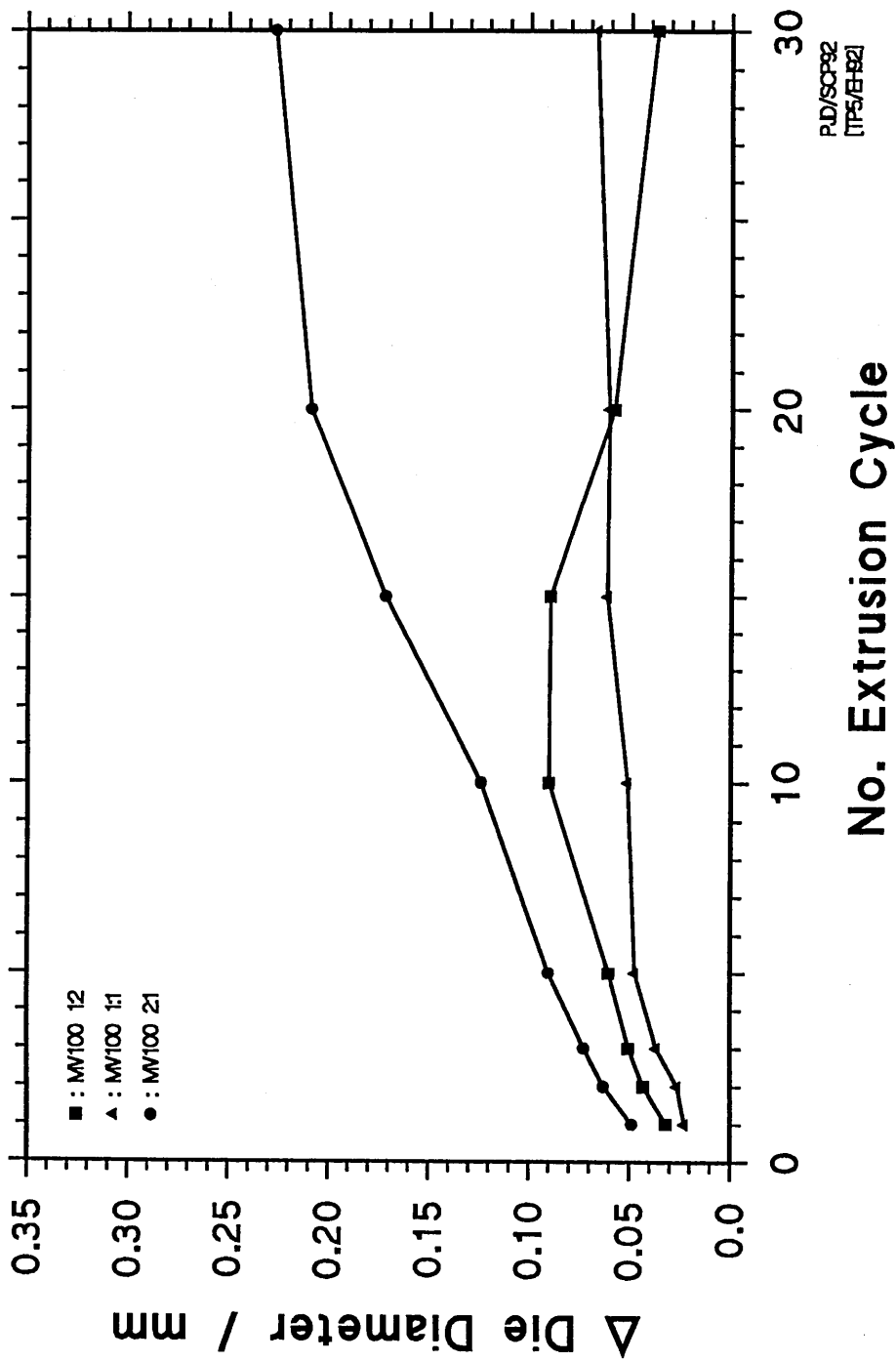
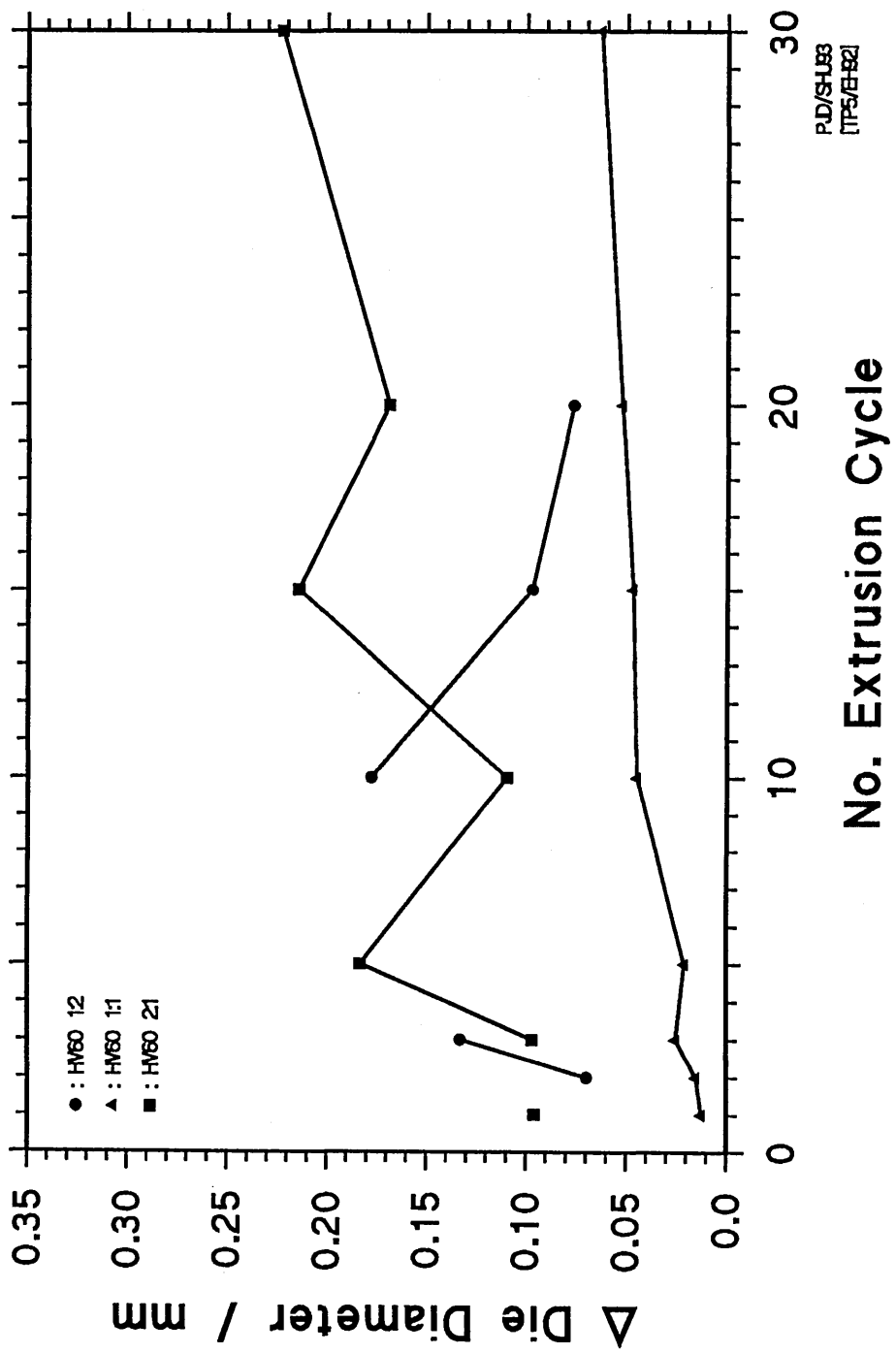


Figure 45 : The relationship between the number of extrusion cycles and the die diameter using HV medium and 60 Mesh grit with grit to polymer ratios of 0.5, 1 and 2.

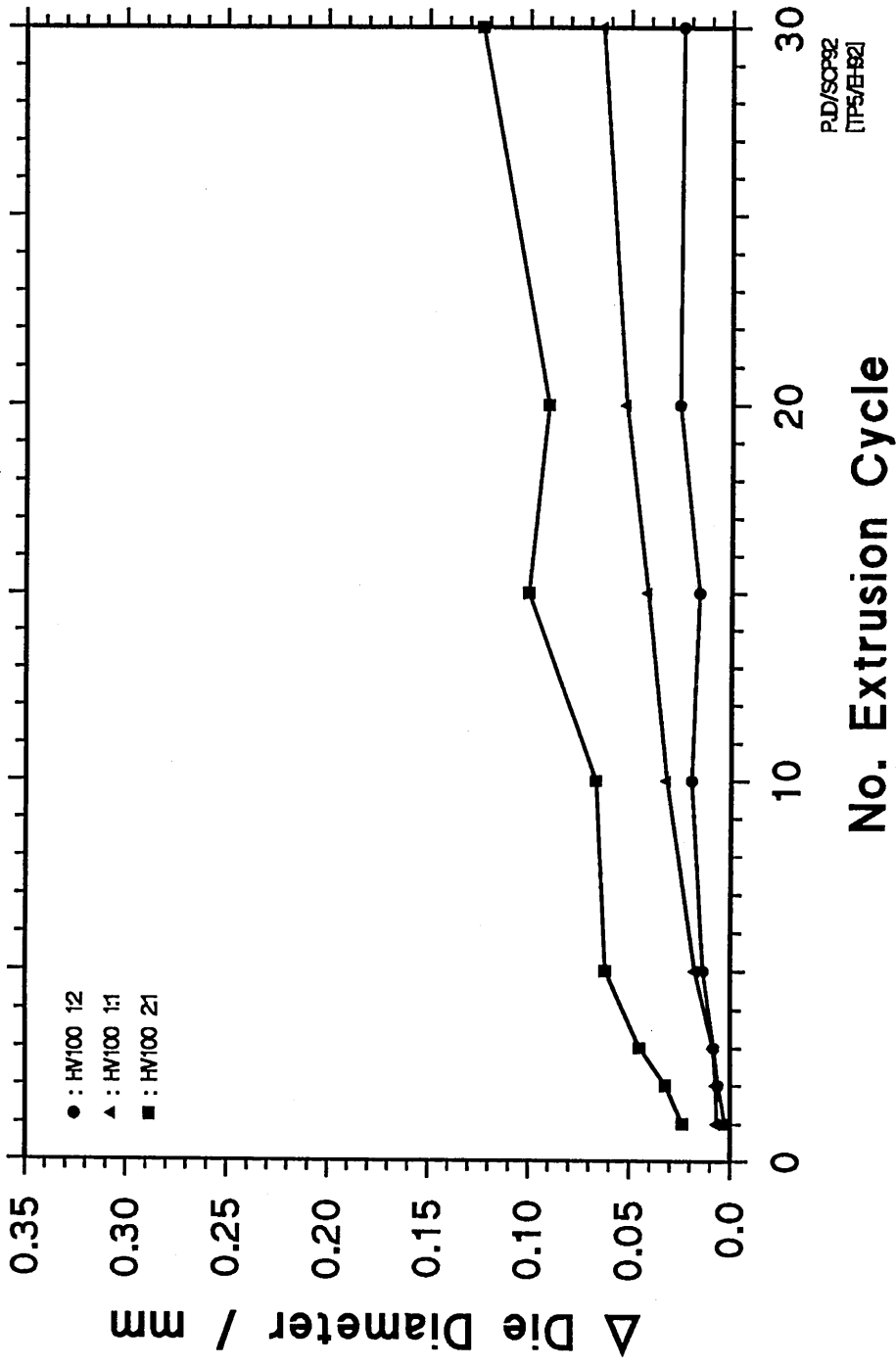


P.D./S+UBS
[TP5/E-B2]

No. Extrusion Cycle

Δ Die Diameter / mm

Figure 46 : The relationship between the number of extrusion cycles and the die diameter using HV medium and 100 Mesh grit with grit to polymer ratios of 0.5, 1 and 2.

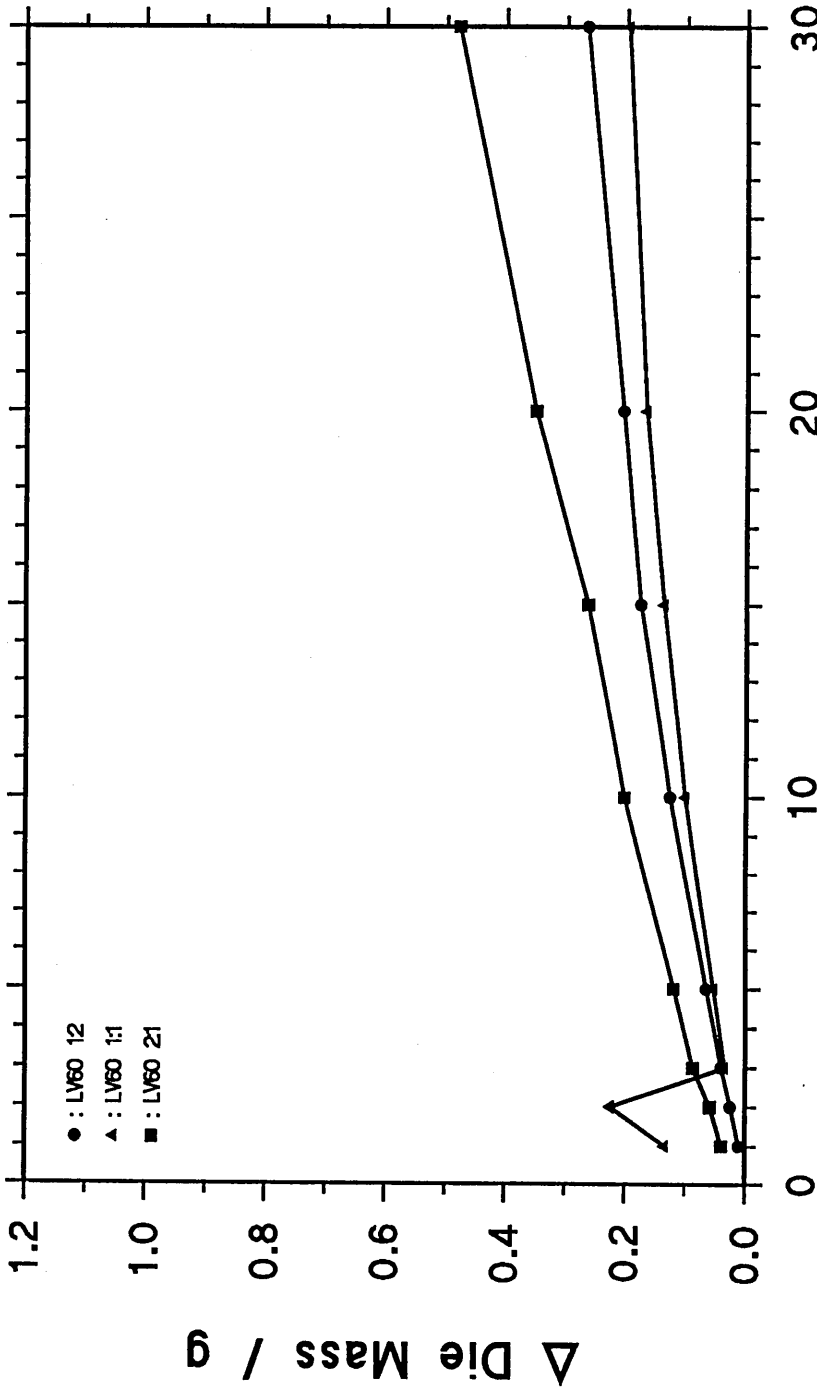


PJ.D/SCP92
[TP5/EH92]

No. Extrusion Cycle

△ Die Diameter / mm

Figure 47 : The relationship between the number of extrusion cycles and the die mass using LV medium and 60 Mesh grit with grit to polymer ratios of 0.5, 1 and 2.



R.D./S.H.U.88
[175/182]

No. Extrusion Cycle

Δ Die Mass / g

Figure 48 : The relationship between the number of extrusion cycles and the die mass using LV medium and 100 Mesh grit with grit to polymer ratios of 0.5, 1 and 2.

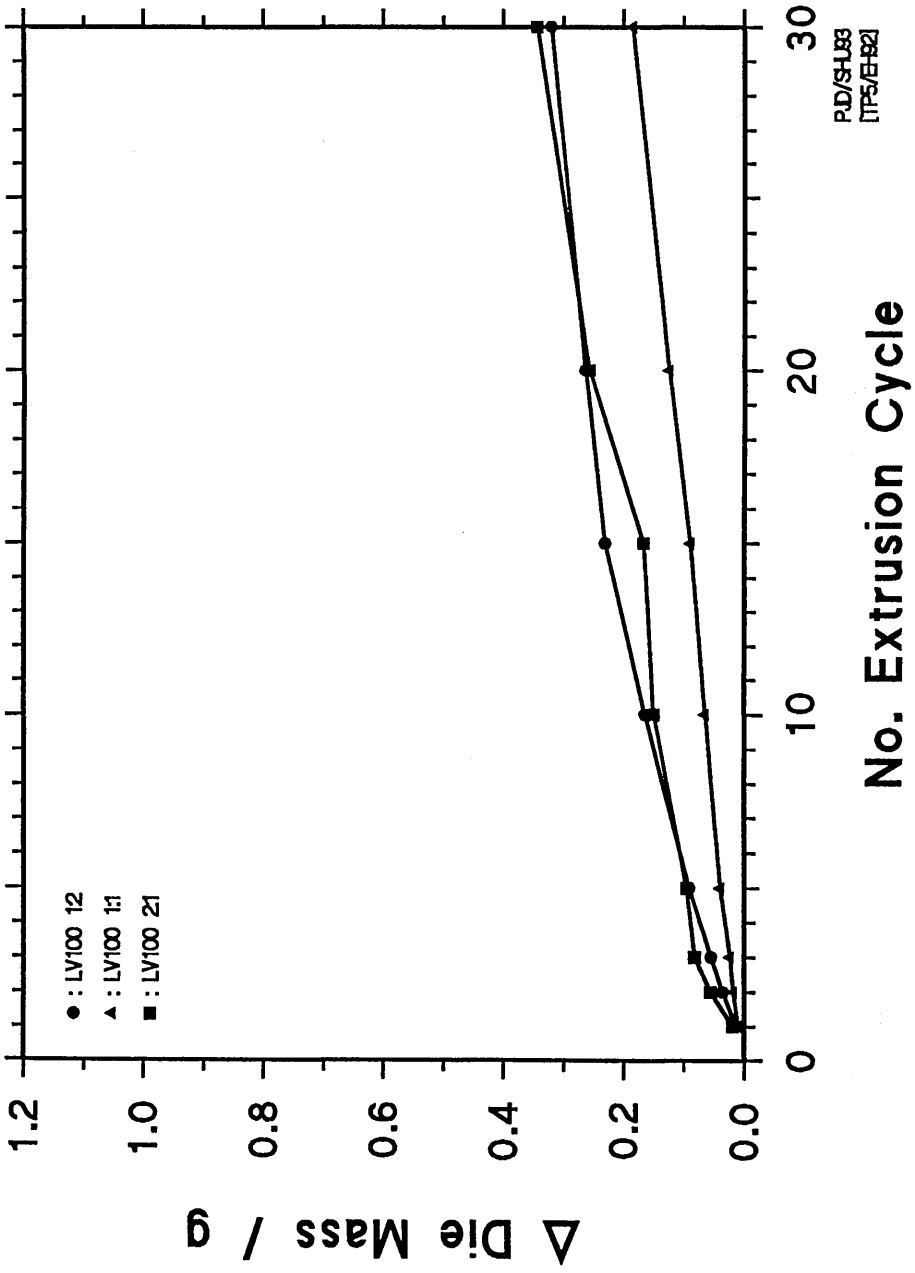
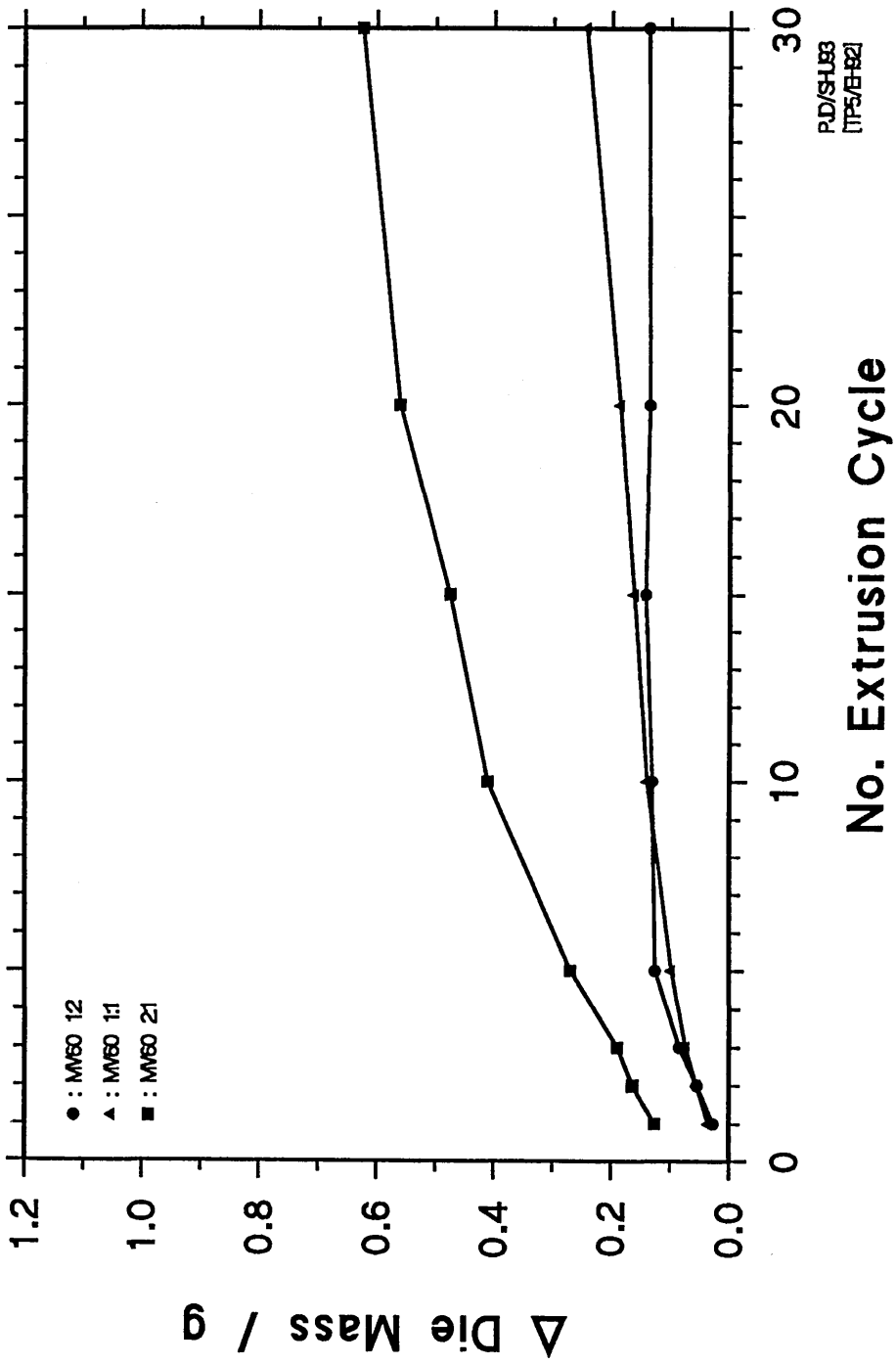


Figure 49 : The relationship between the number of extrusion cycles and the die mass using MV medium and 60 Mesh grit with grit to polymer ratios of 0.5, 1 and 2.



R.D./SHUB3
[TP5/B-62]

Figure 50 : The relationship between the number of extrusion cycles and the die mass using MV medium and 100 Mesh grit with grit to polymer ratios of 0.5, 1 and 2.

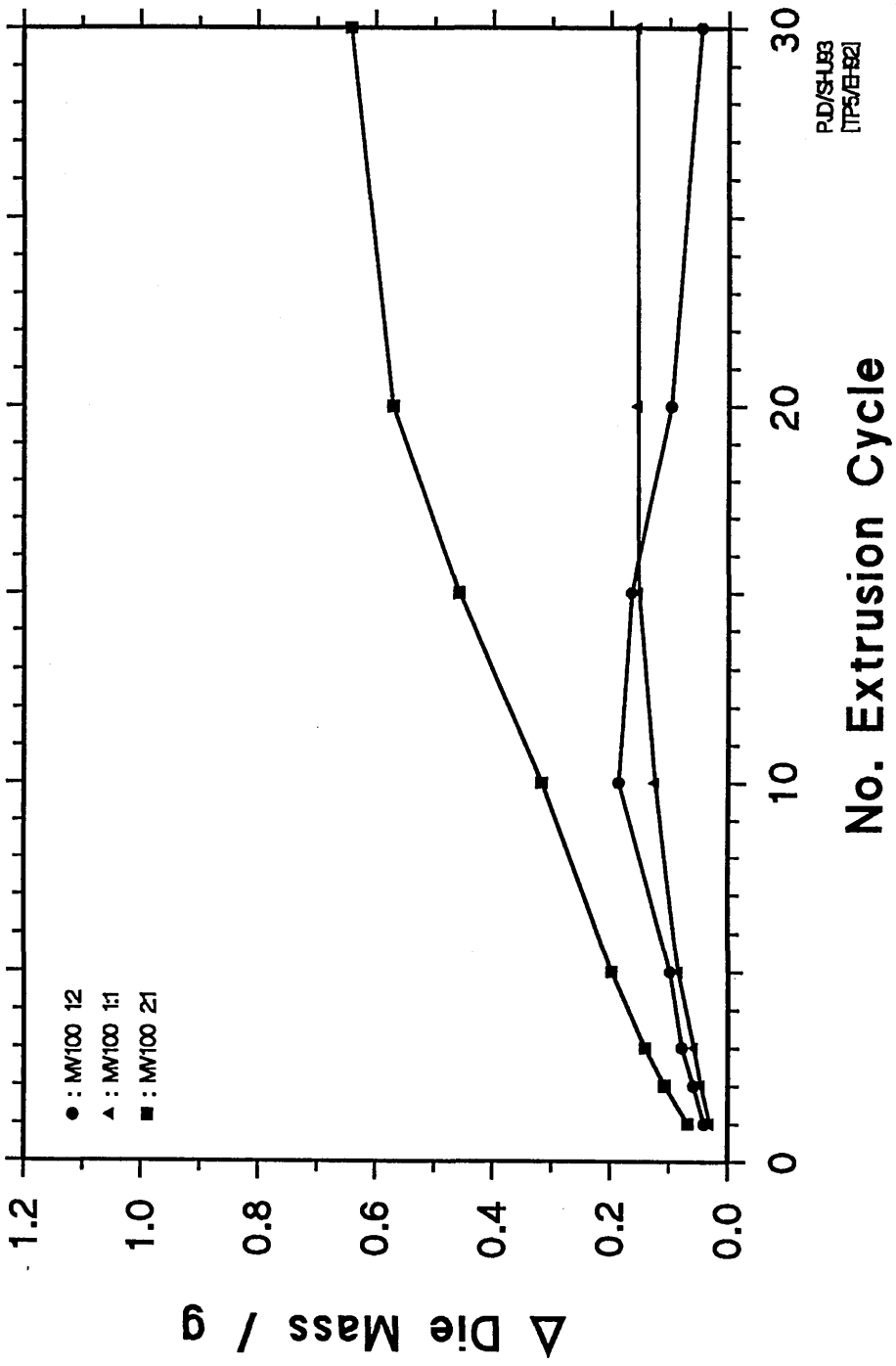
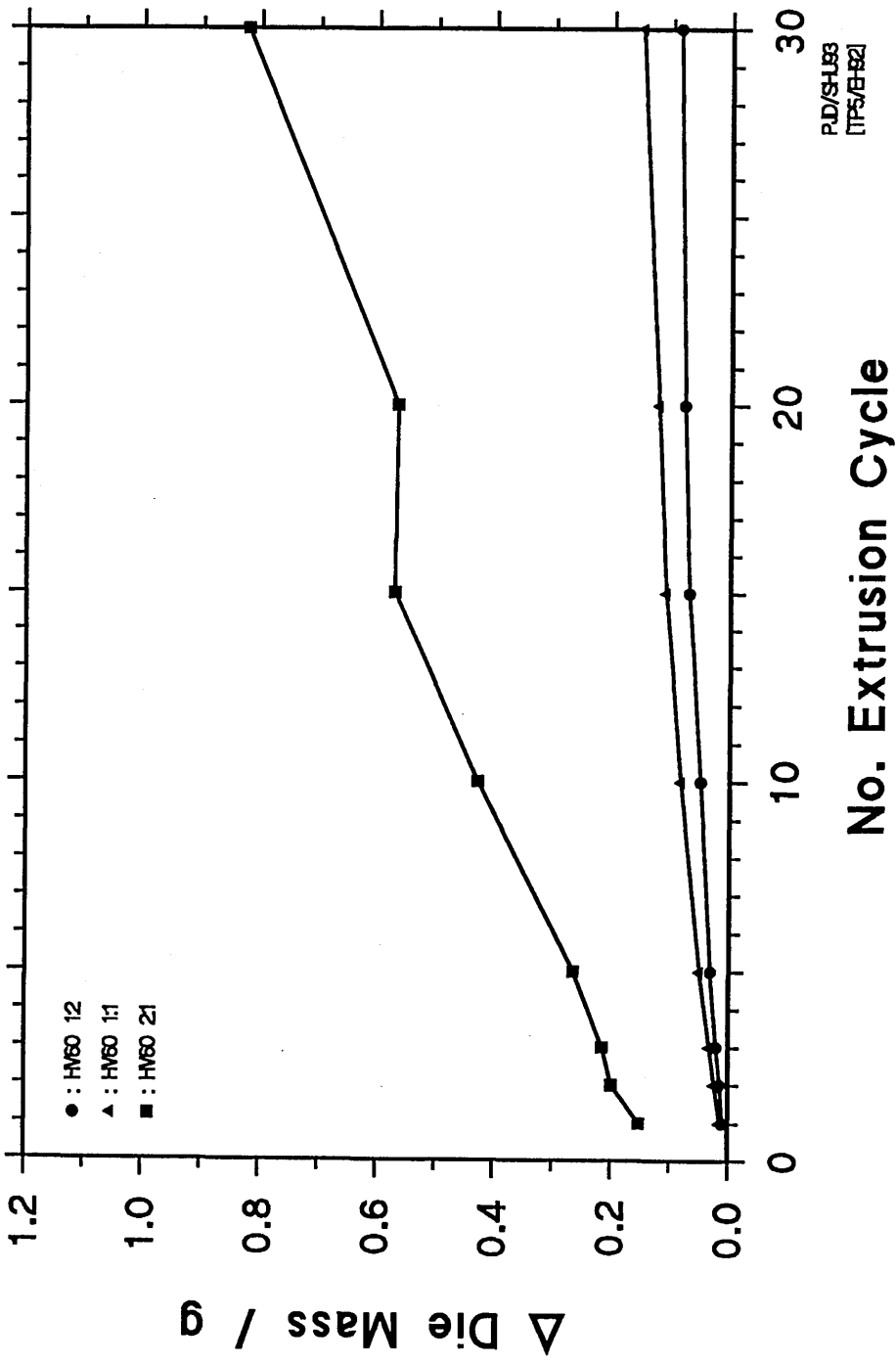


Figure 51 : The relationship between the number of extrusion cycles and the die mass using HV medium and 60 Mesh grit with grit to polymer ratios of 0.5, 1 and 2.



P.J.D./S.H.U.B.
[TFS/E/B2]

Figure 52 : The relationship between the number of extrusion cycles and the die mass using HV medium and 100 Mesh grit with grit to polymer ratios of 0.5, 1 and 2.

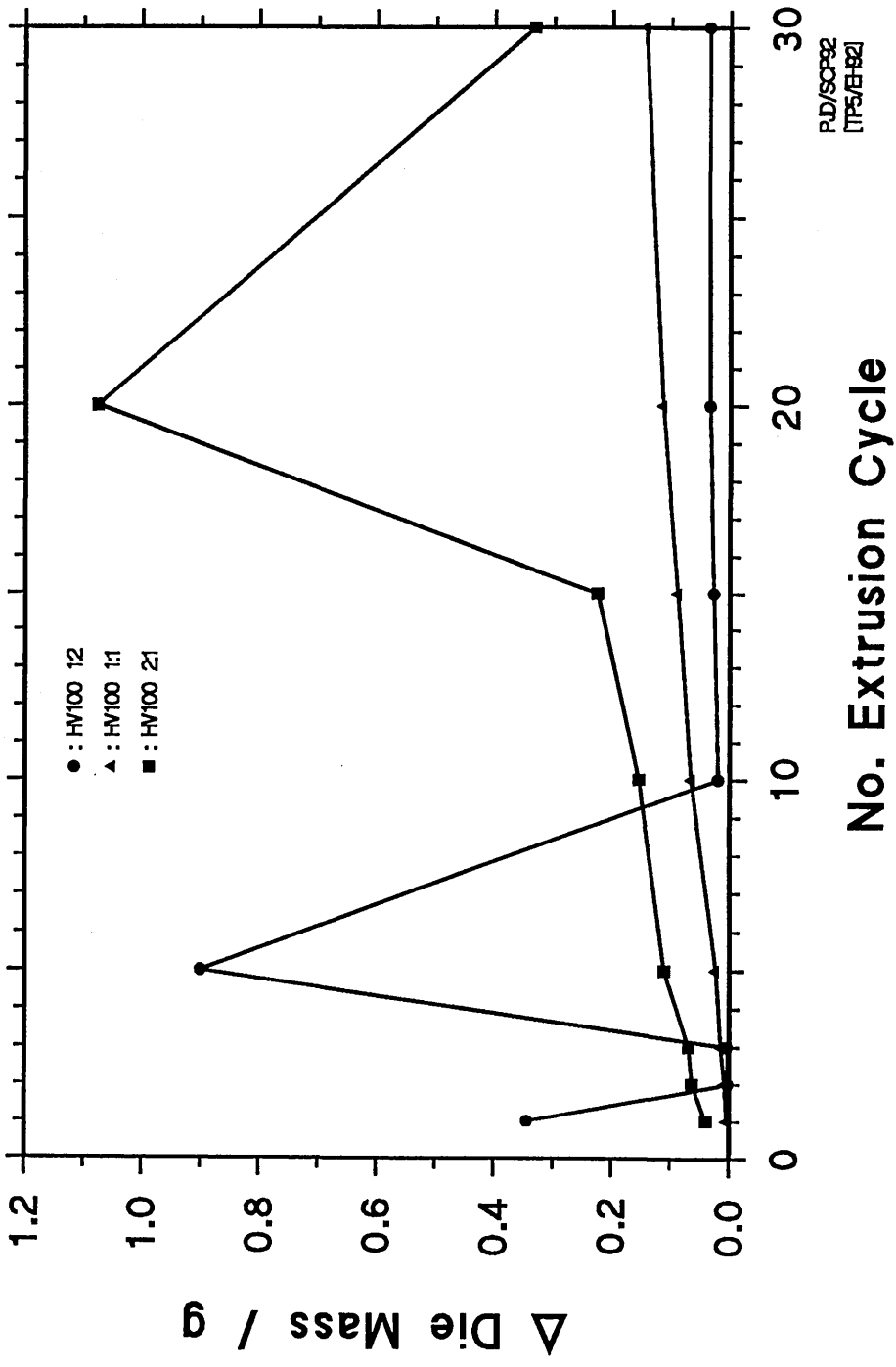
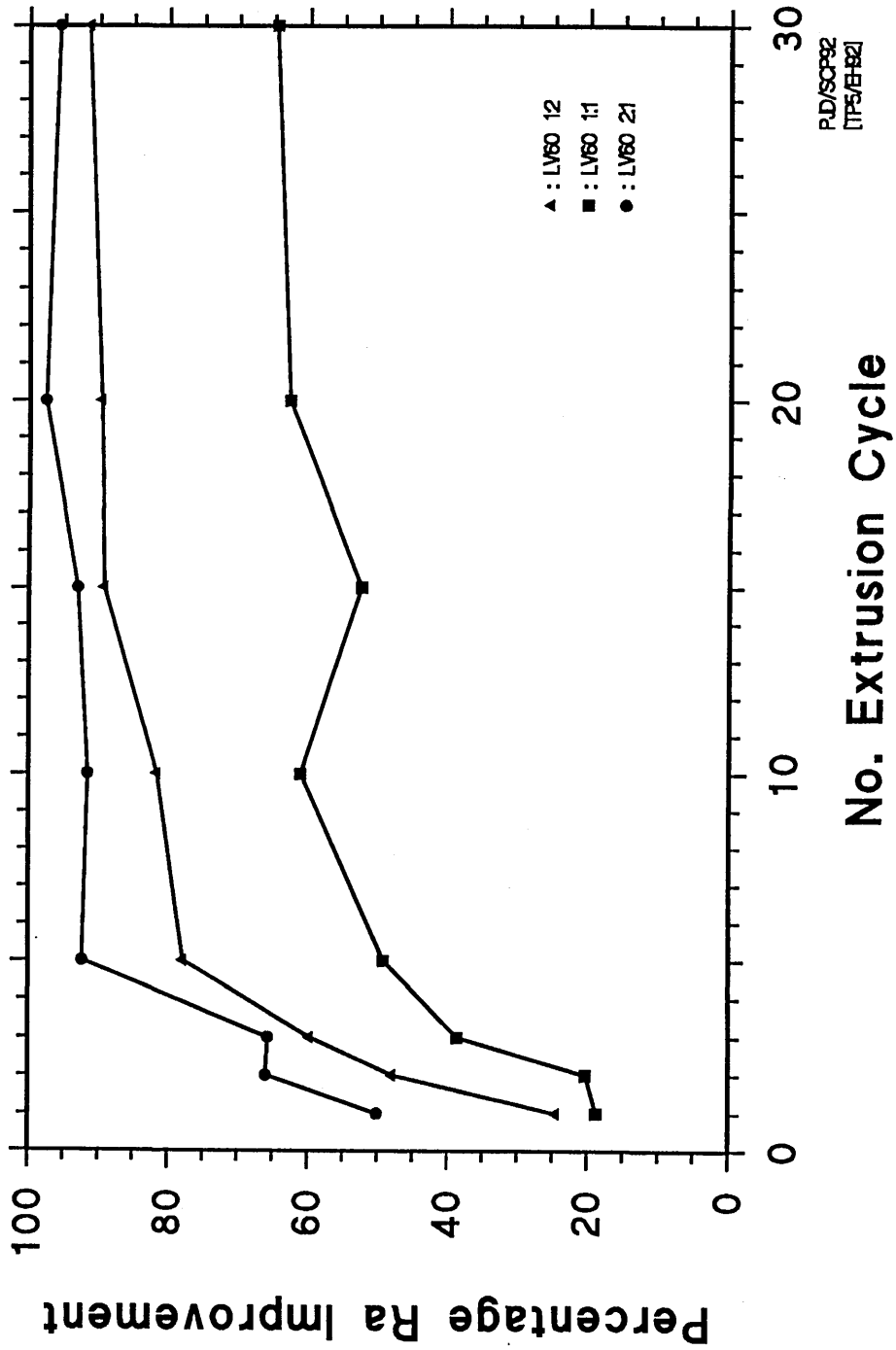
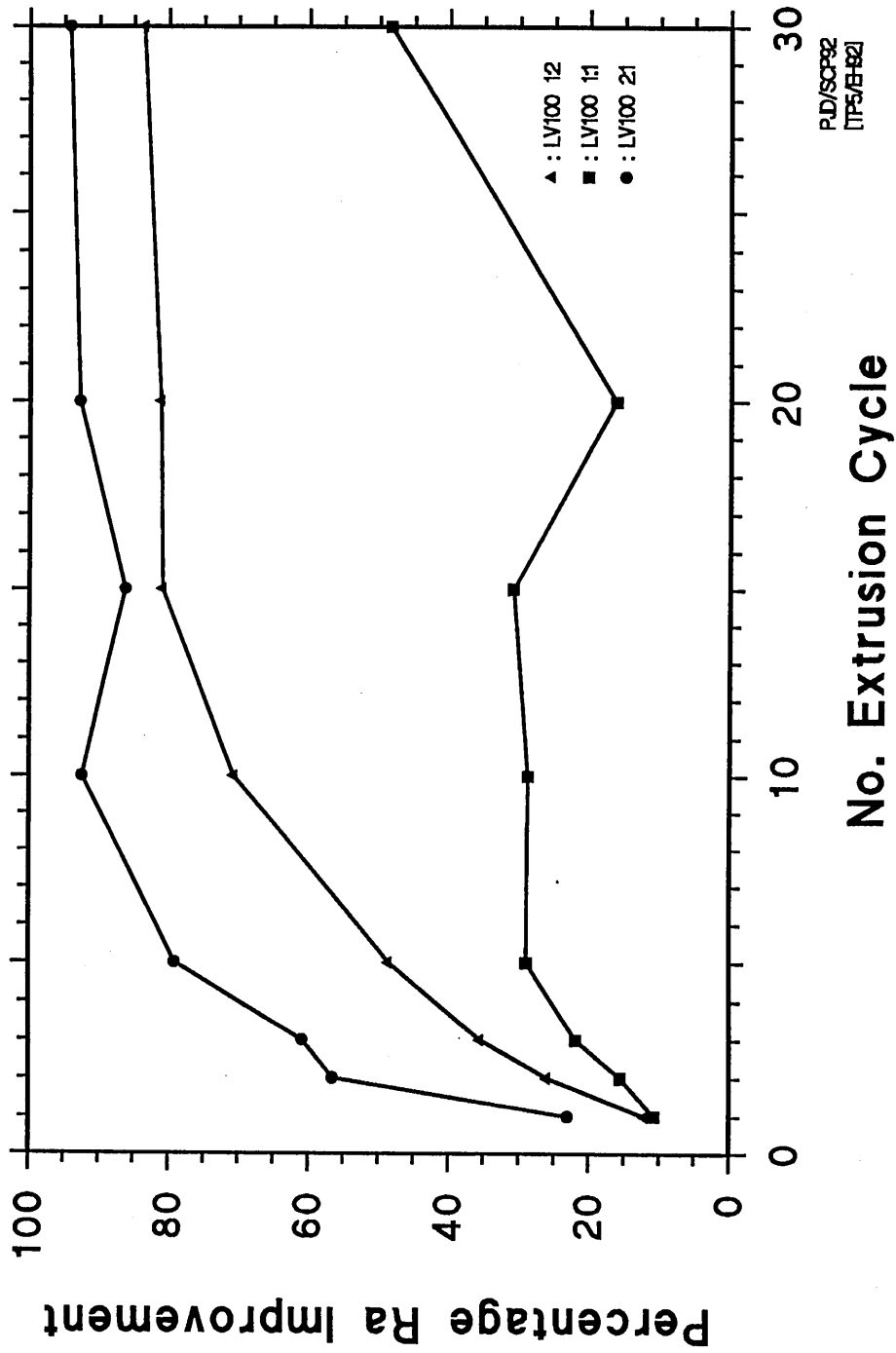


Figure 53 : The relationship between the number of extrusion cycles and the percentage surface roughness improvement using LV medium and 60 Mesh grit with grit to polymer ratios of 0.5, 1 and 2.



RJD/SCP92
[TP5/EH92]

Figure 54 : The relationship between the number of extrusion cycles and the percentage surface roughness improvement using LV medium and 100 Mesh grit with grit to polymer ratios of 0.5, 1 and 2.



P.D./SCF92
[TPS/EB92]

Figure 55 : The relationship between the number of extrusion cycles and the percentage surface roughness improvement using MV medium and 60 Mesh grit with grit to polymer ratios of 0.5, 1 and 2.

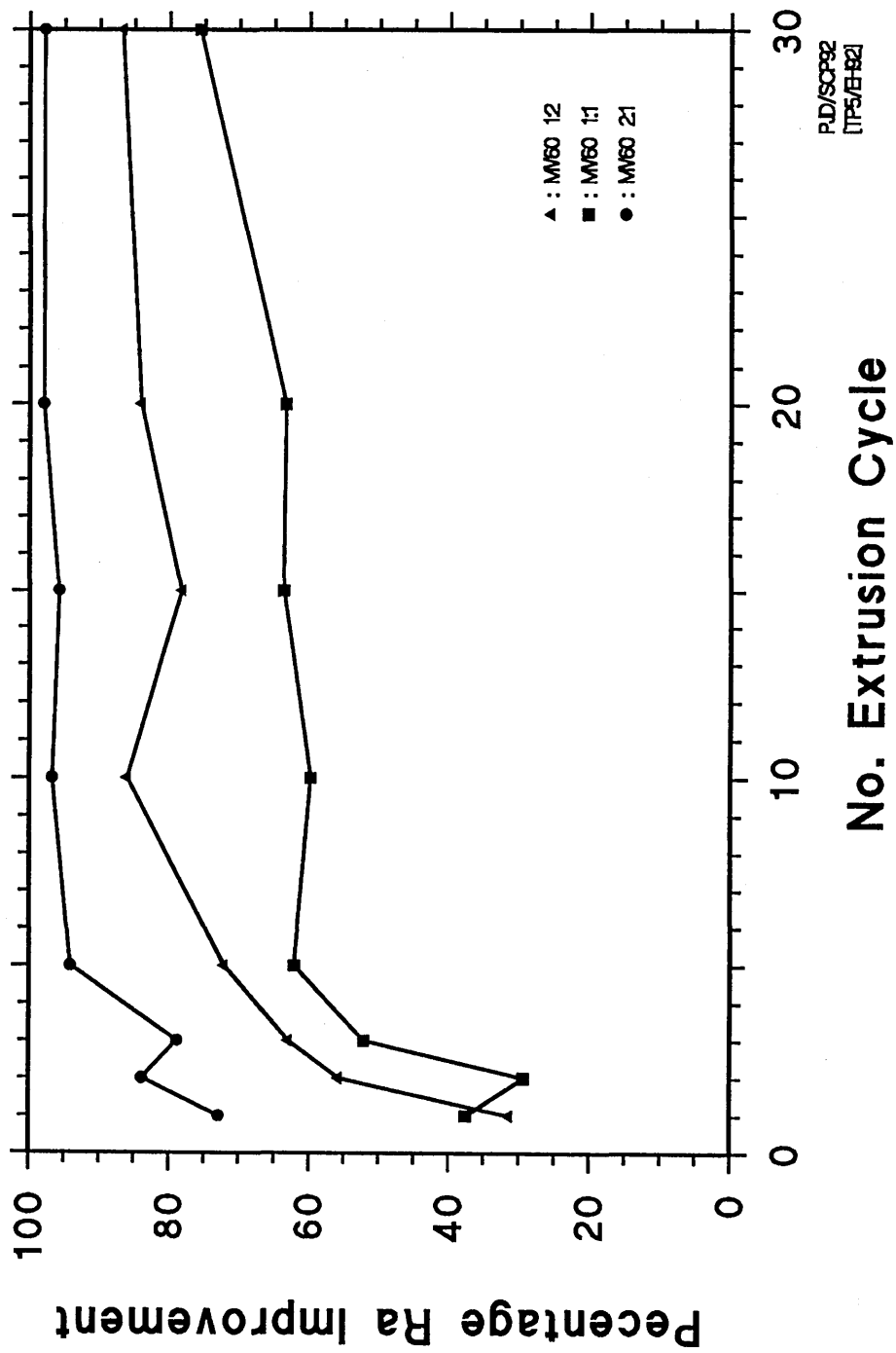
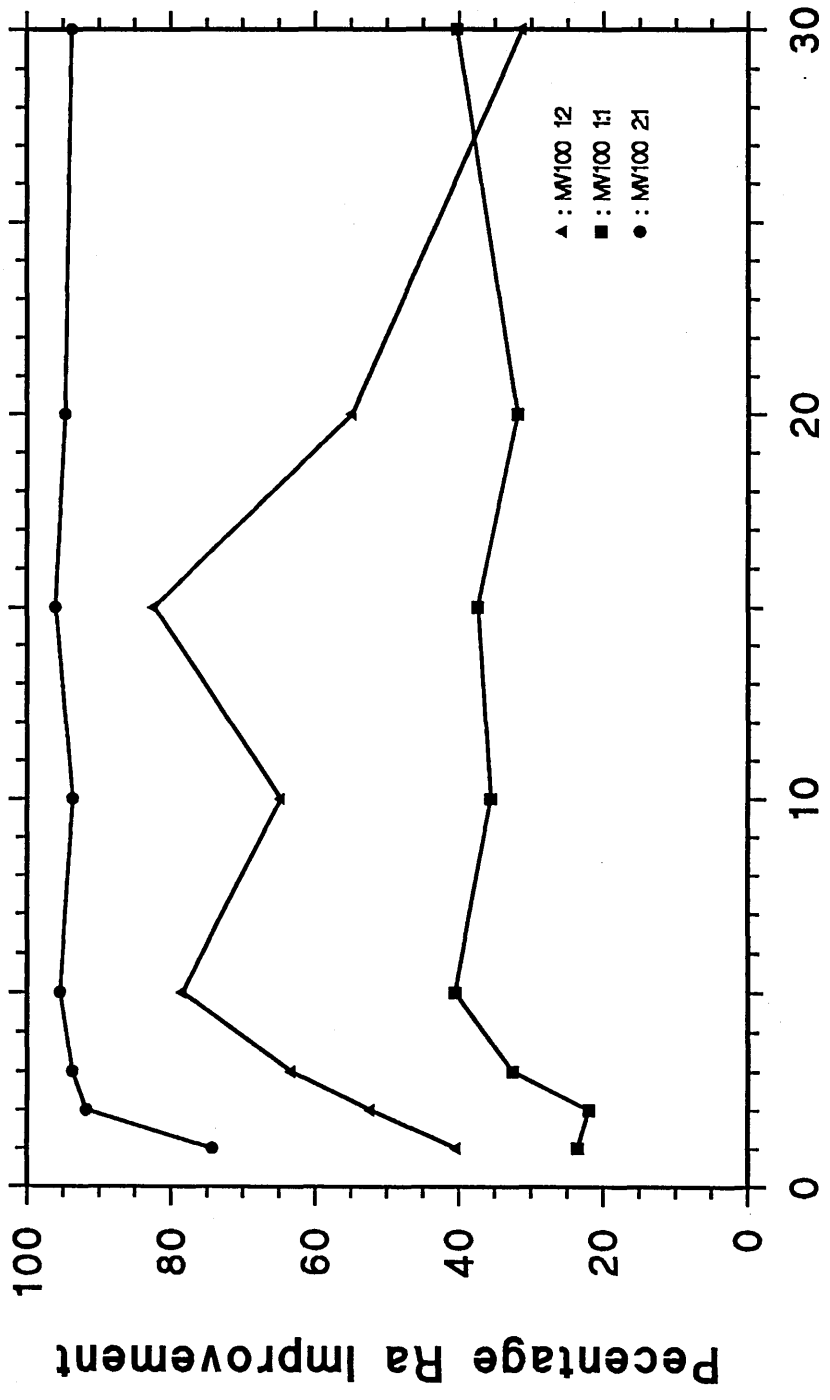


Figure 56 : The relationship between the number of extrusion cycles and the percentage surface roughness improvement using MV medium and 100 Mesh grit with grit to polymer ratios of 0.5, 1 and 2.



PJD/SCP92
[TP5/EH92]

No. Extrusion Cycle

Percentage Ra Improvement

Figure 57 : The relationship between the number of extrusion cycles and the percentage surface roughness improvement using HV medium and 60 Mesh grit with grit to polymer ratios of 0.5, 1 and 2.

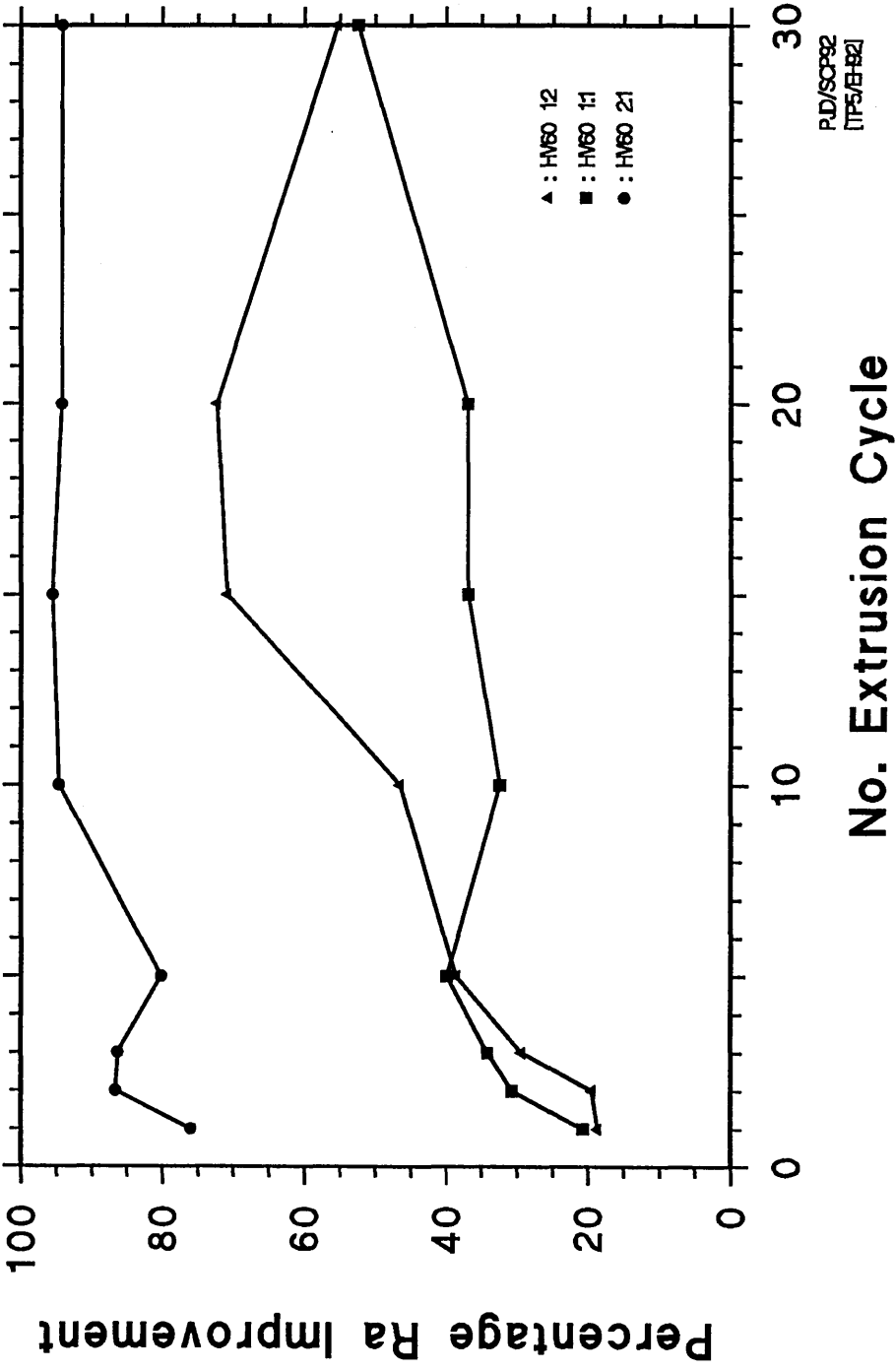


Figure 58 : The relationship between the number of extrusion cycles and the percentage surface roughness improvement using HV medium and 100 Mesh grit with grit to polymer ratios of 0.5, 1 and 2.

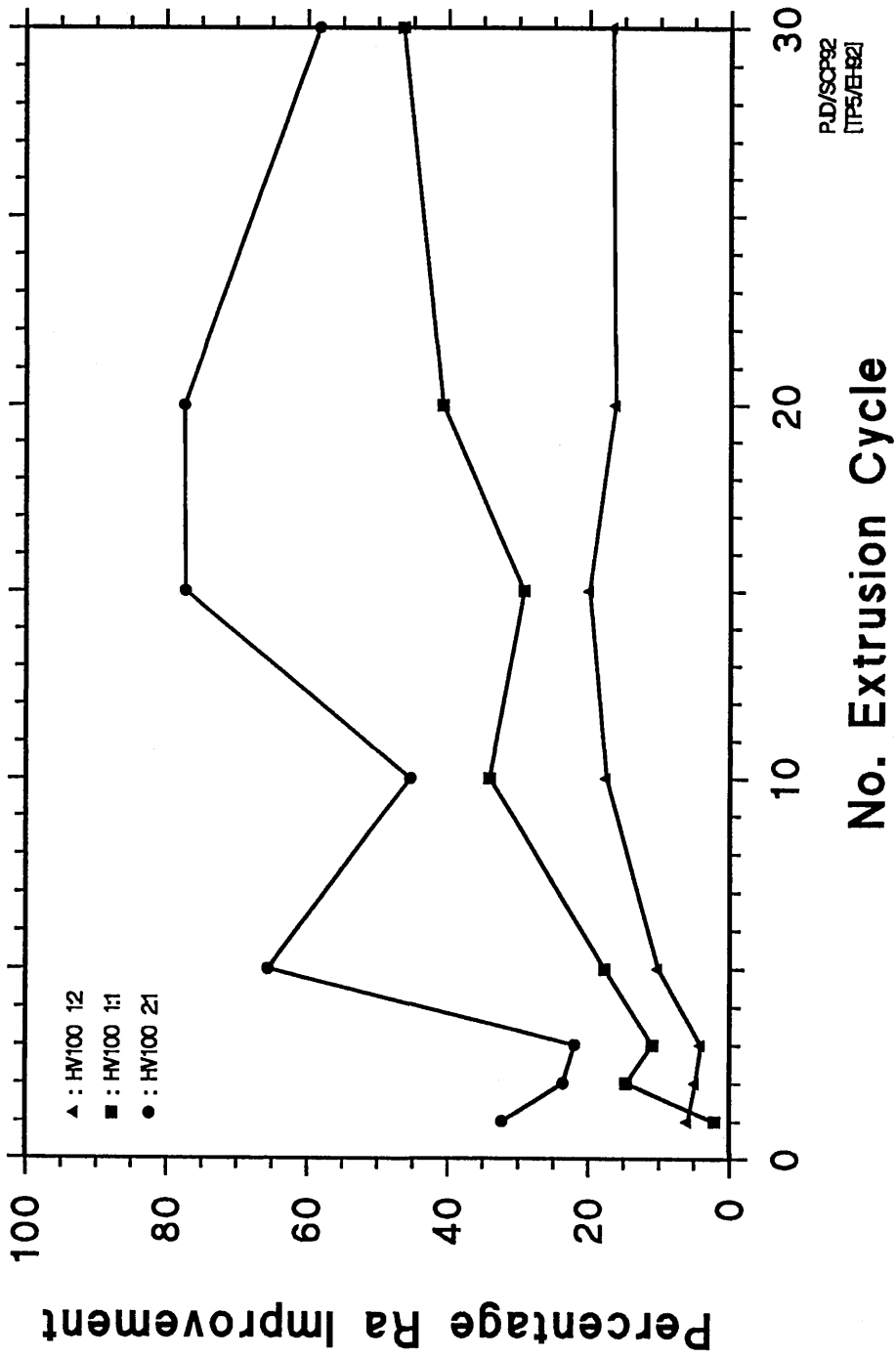


Figure 59(a) : Illustration of the die surface condition after 1 extrusion cycle using LV medium and 100 Mesh grit with a grit to polymer ratio of 1.

x 8

Figure 59(b) : Illustration of the die surface condition after 2 extrusion cycles using LV medium and 100 Mesh grit with a grit to polymer ratio of 1.

x 8

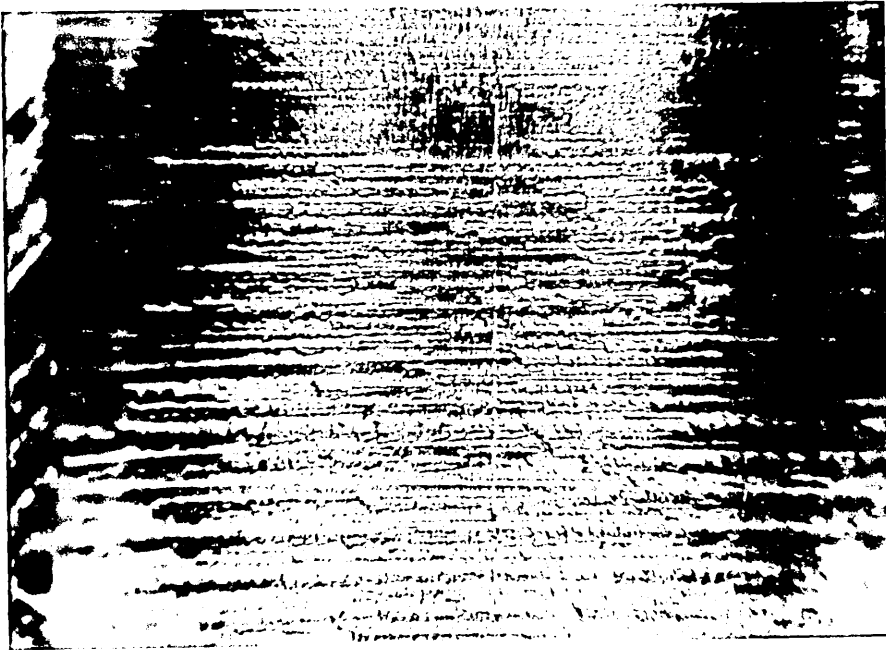
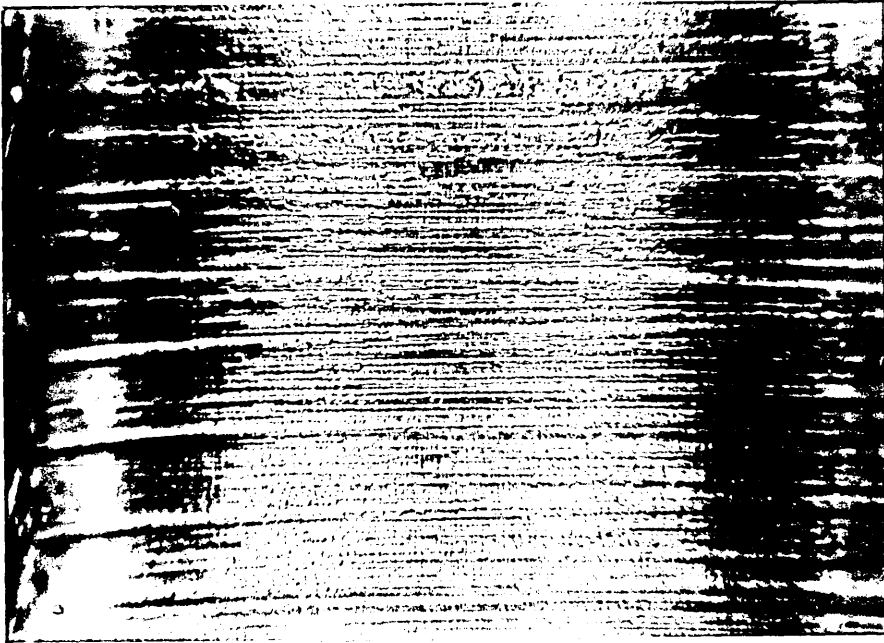


Figure 59(c) : Illustration of the die surface condition after 3 extrusion cycles using LV medium and 100 Mesh grit with a grit to polymer ratio of 1.

x 8

Figure 59(d) : Illustration of the die surface condition after 5 extrusion cycles using LV medium and 100 Mesh grit with a grit to polymer ratio of 1.

x 8

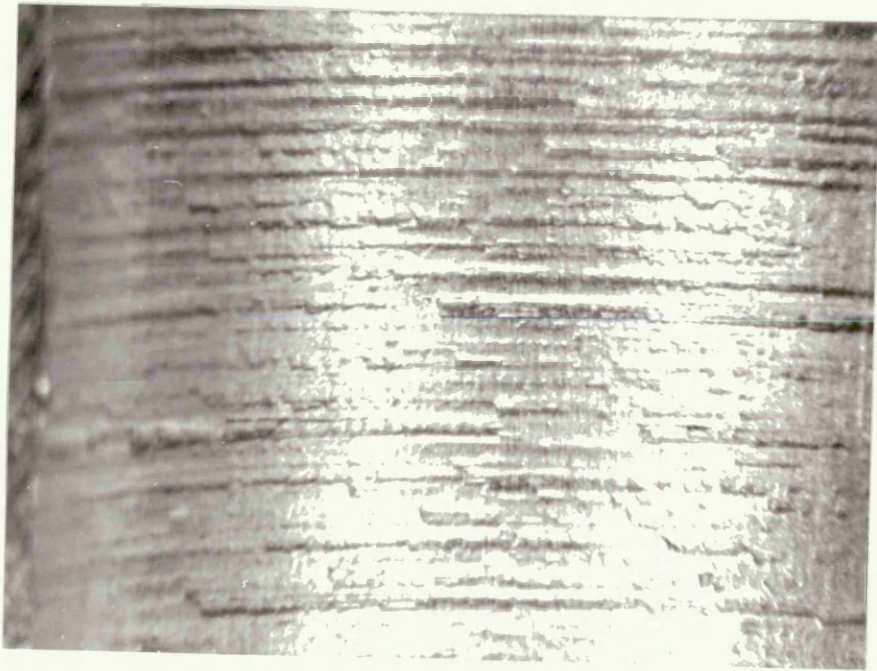
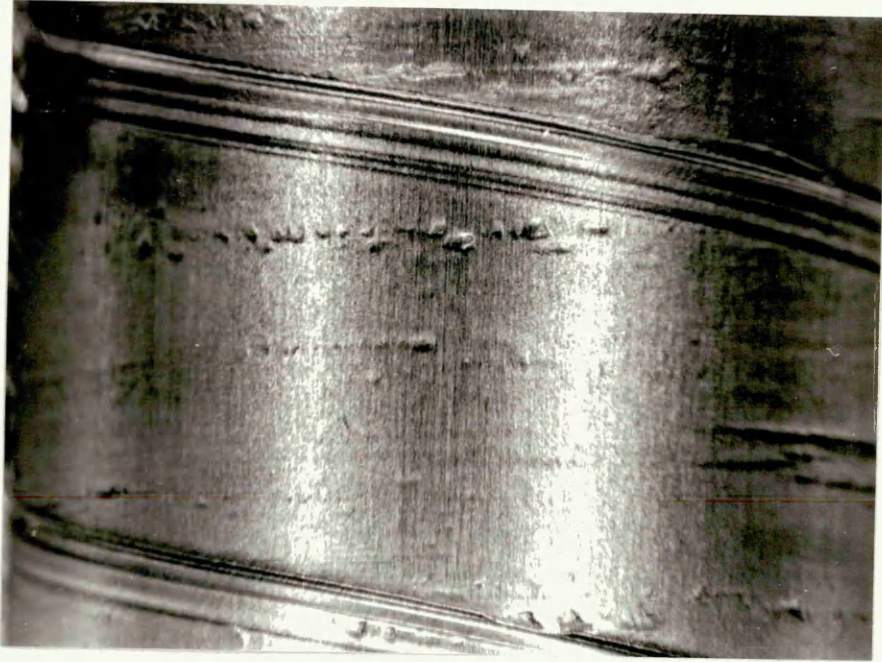


Figure 59(e) : Illustration of the die surface condition after 10 extrusion cycles using LV medium and 100 Mesh grit with a grit to polymer ratio of 1.

x 8

Figure 59(f) : Illustration of the die surface condition after 30 extrusion cycles using LV medium and 100 Mesh grit with a grit to polymer ratio of 1.

x 8

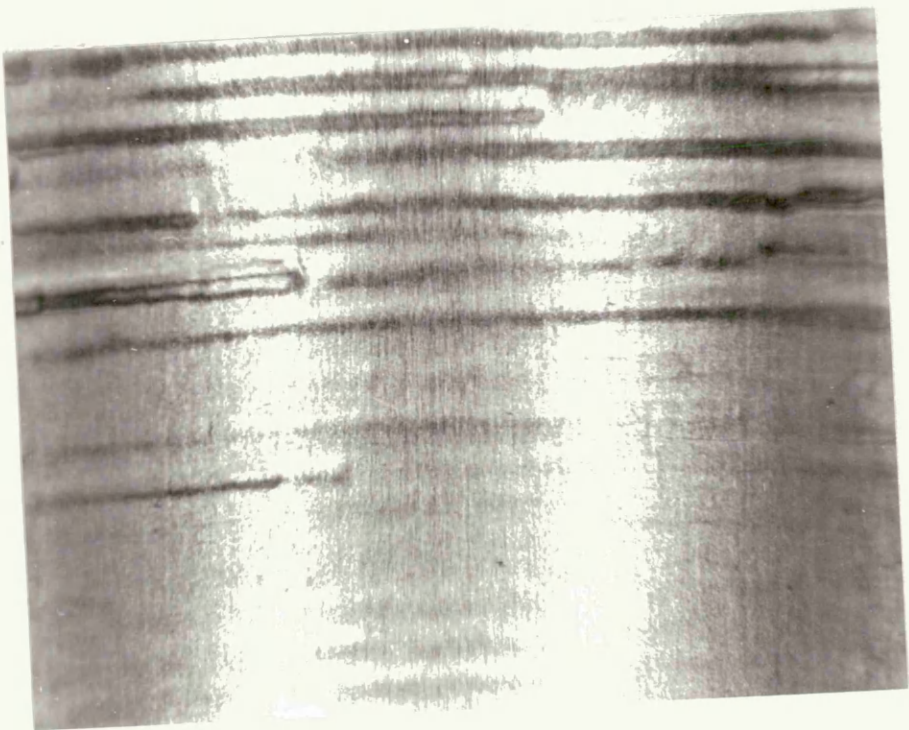
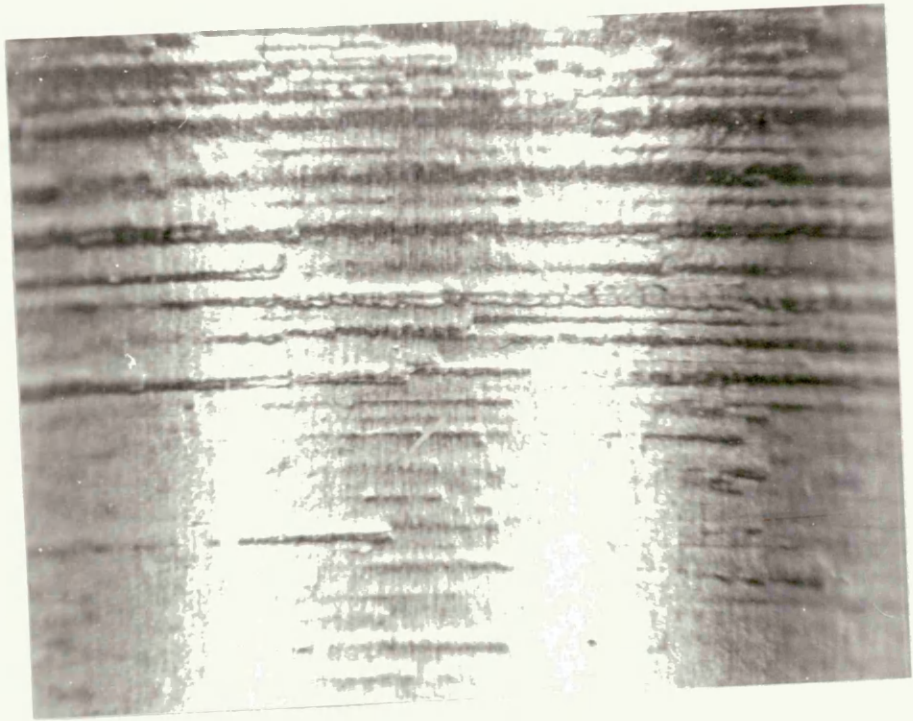


Figure 60(a) : Illustration of the die surface condition after 1 extrusion cycle using LV medium and 60 Mesh grit with a grit to polymer ratio of 1.

x 8

Figure 60(b) : Illustration of the die surface condition after 2 extrusion cycles using LV medium and 60 Mesh grit with a grit to polymer ratio of 1.

x 8

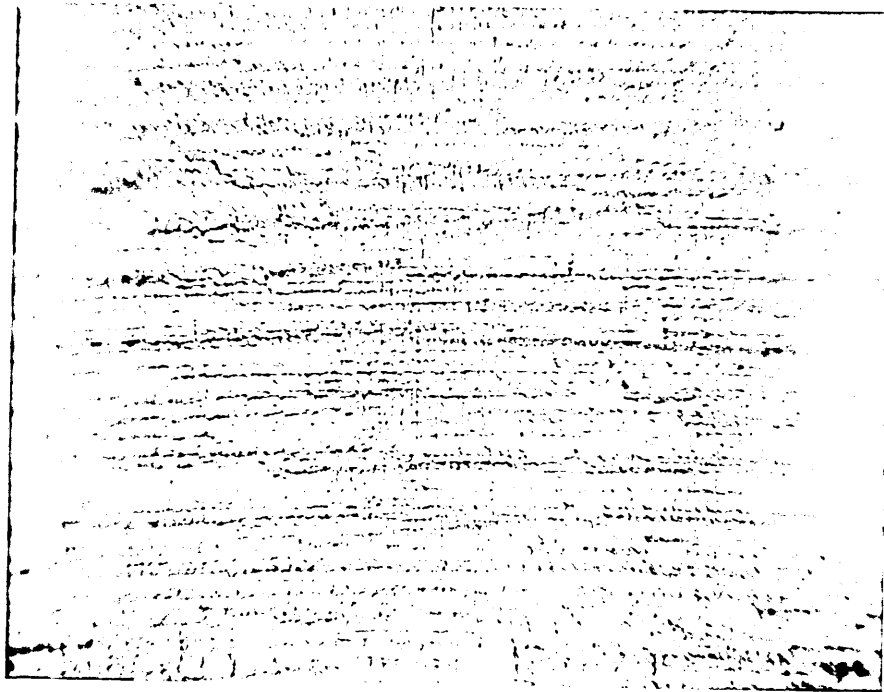


Figure 60(c) : Illustration of the die surface condition after 3 extrusion cycles using LV medium and 60 Mesh grit with a grit to polymer ratio of 1.

x 8

Figure 60(d) : Illustration of the die surface condition after 5 extrusion cycles using LV medium and 60 Mesh grit with a grit to polymer ratio of 1.

x 8

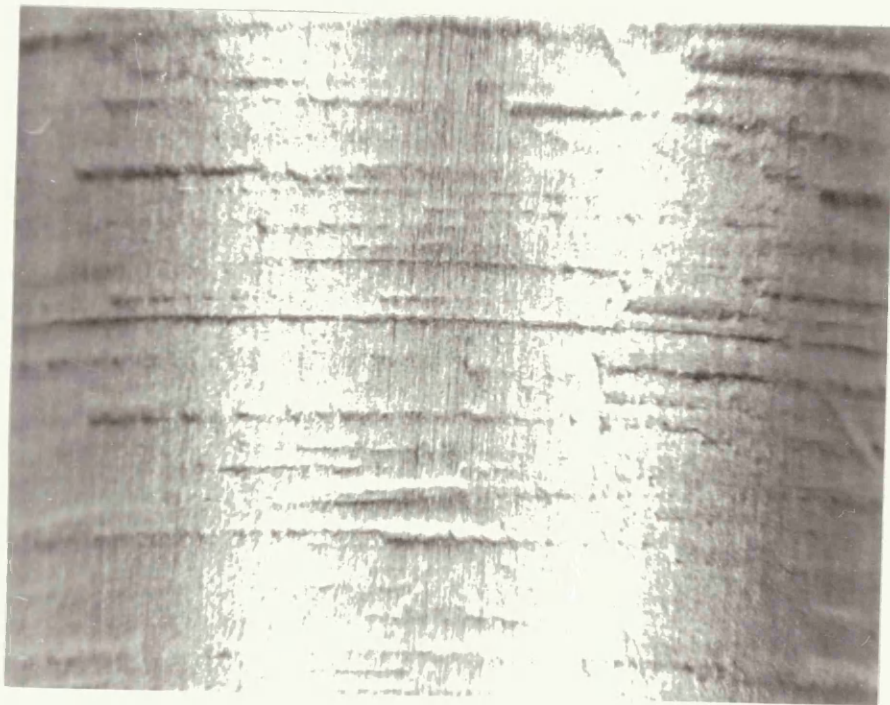
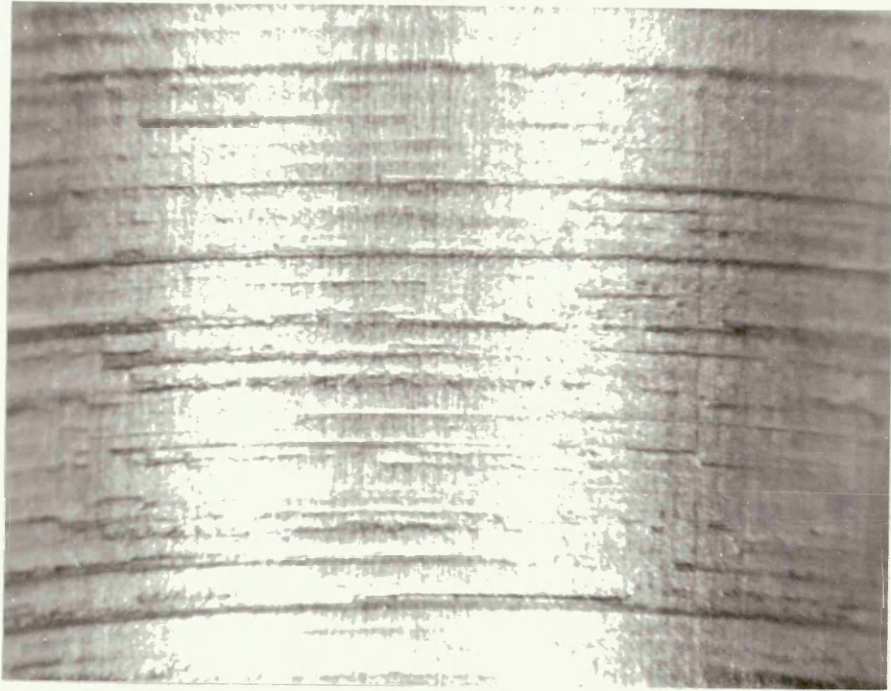


Figure 60(e) : Illustration of the die surface condition after 10 extrusion cycles using LV medium and 60 Mesh grit with a grit to polymer ratio of 1.

x 8

Figure 60(f) : Illustration of the die surface condition after 30 extrusion cycles using LV medium and 60 Mesh grit with a grit to polymer ratio of 1.

x 8

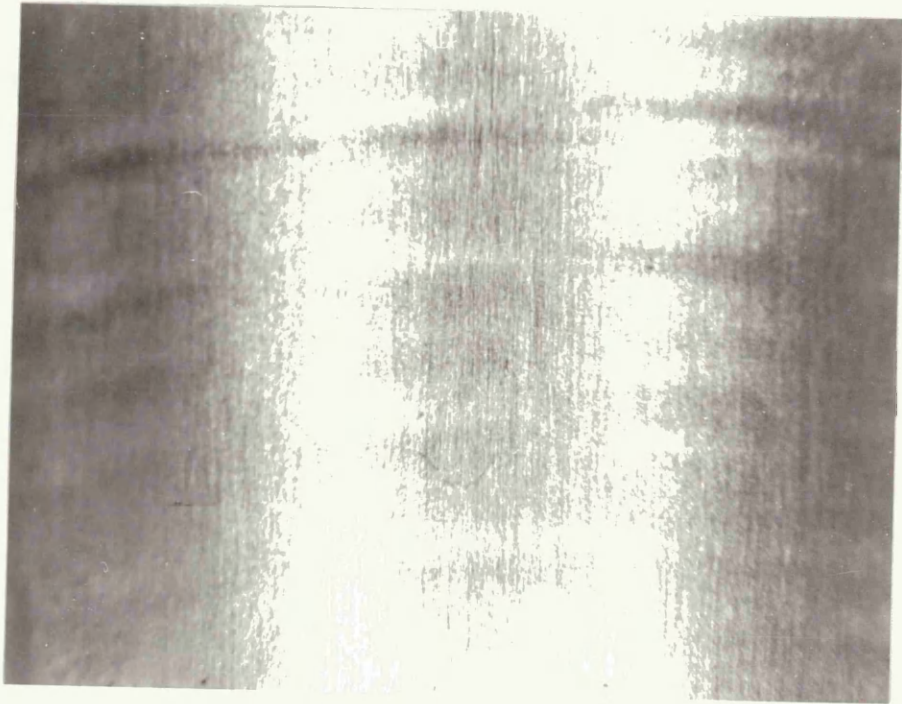
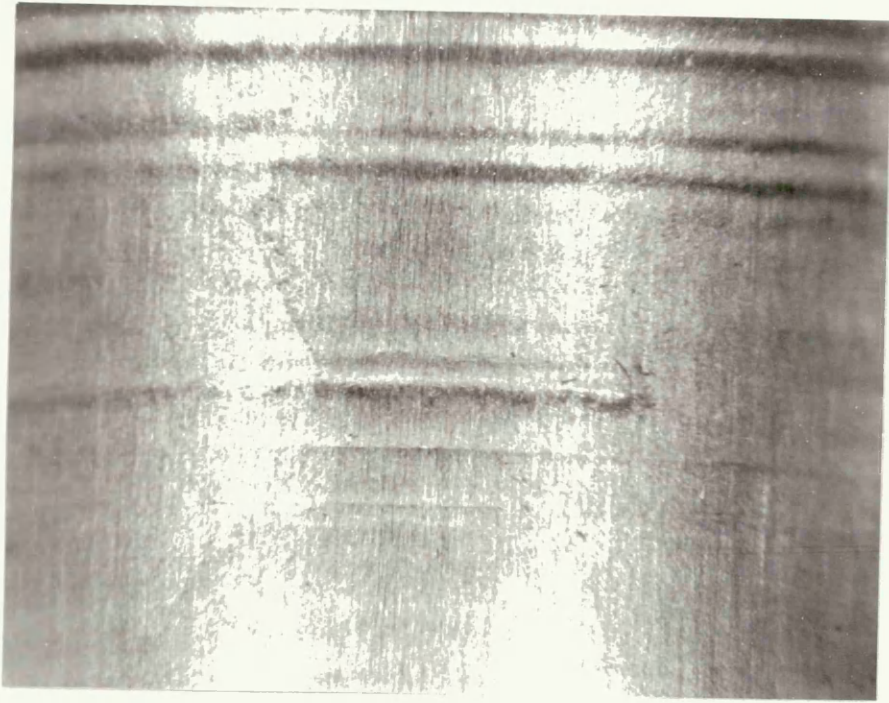


Figure 61(a) : Illustration of the die surface condition after 1
extrusion cycle using MV medium and 100 Mesh grit
with a grit to polymer ratio of 1.

x 8

Figure 61(b) : Illustration of the die surface condition after 2
extrusion cycles using MV medium and 100 Mesh grit
with a grit to polymer ratio of 1.

x 8

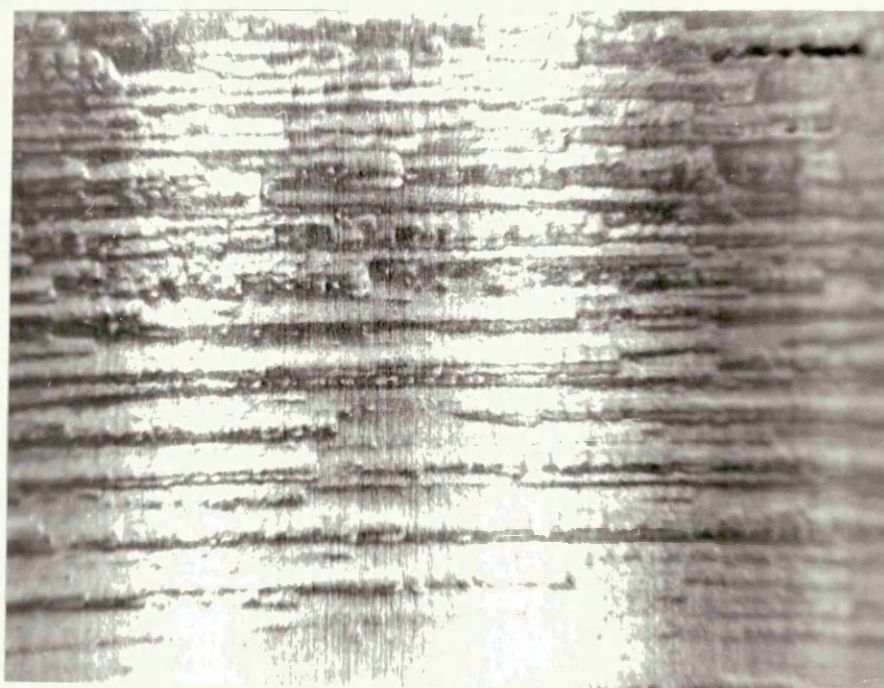
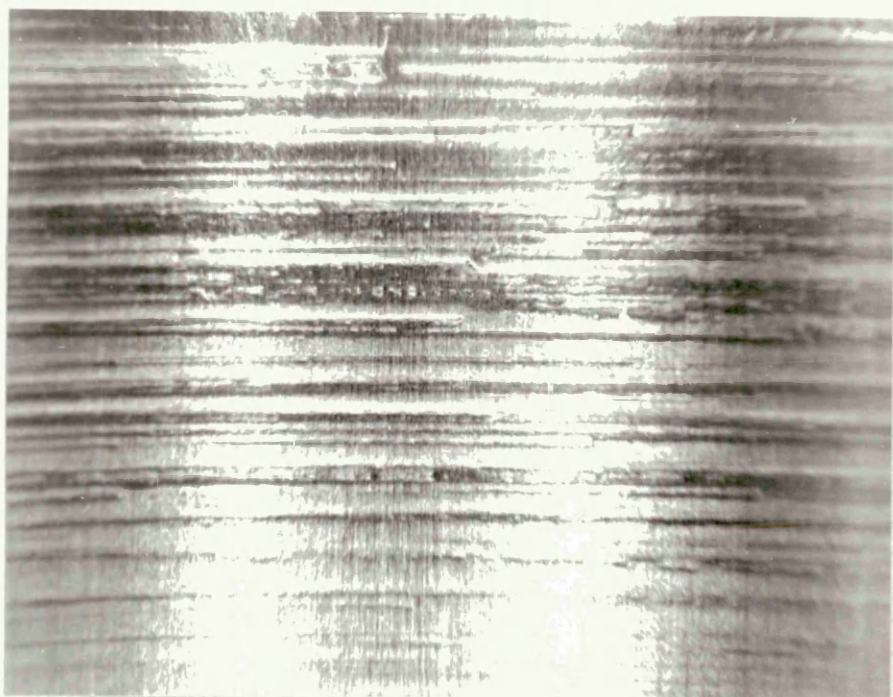


Figure 61(c) : Illustration of the die surface condition after 3 extrusion cycles using MV medium and 100 Mesh grit with a grit to polymer ratio of 1.

x 8

Figure 61(d) : Illustration of the die surface condition after 5 extrusion cycles using MV medium and 100 Mesh grit with a grit to polymer ratio of 1.

x 8

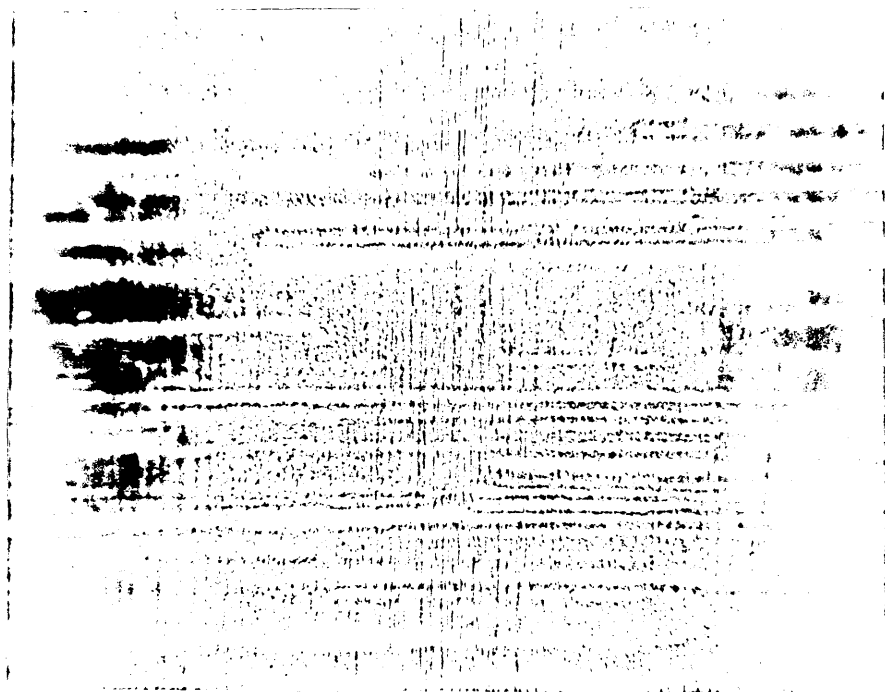
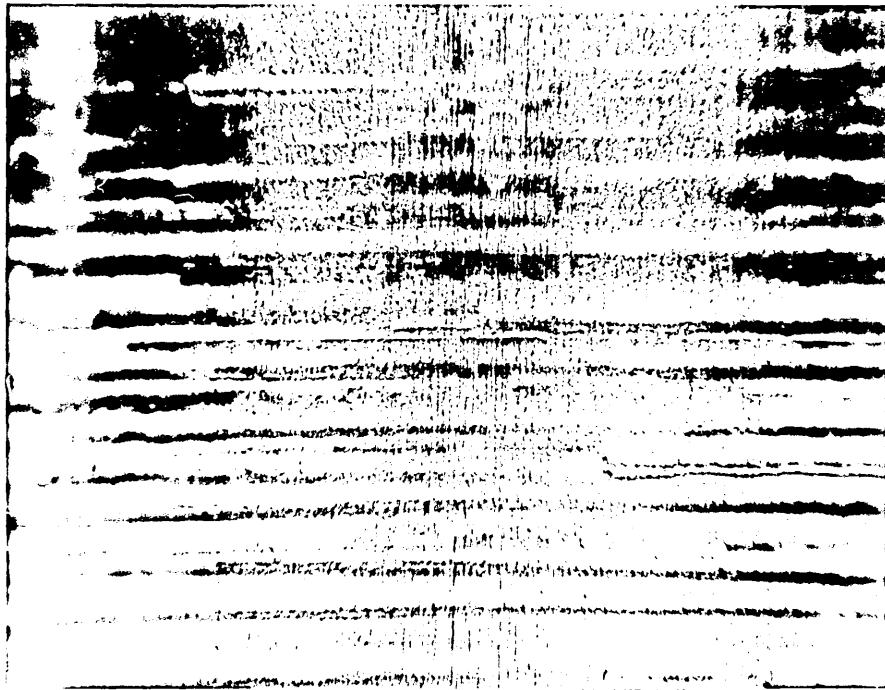


Figure 61(e) : Illustration of the die surface condition after 10 extrusion cycles using MV medium and 100 Mesh grit with a grit to polymer ratio of 1.

x 8

Figure 61(f) : Illustration of the die surface condition after 30 extrusion cycles using MV medium and 100 Mesh grit with a grit to polymer ratio of 1.

x 8

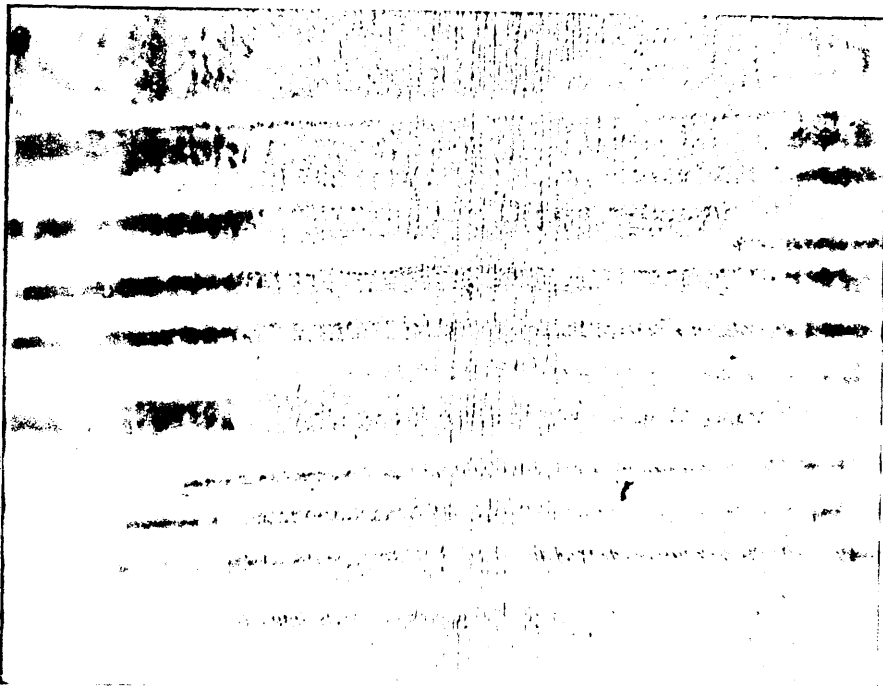
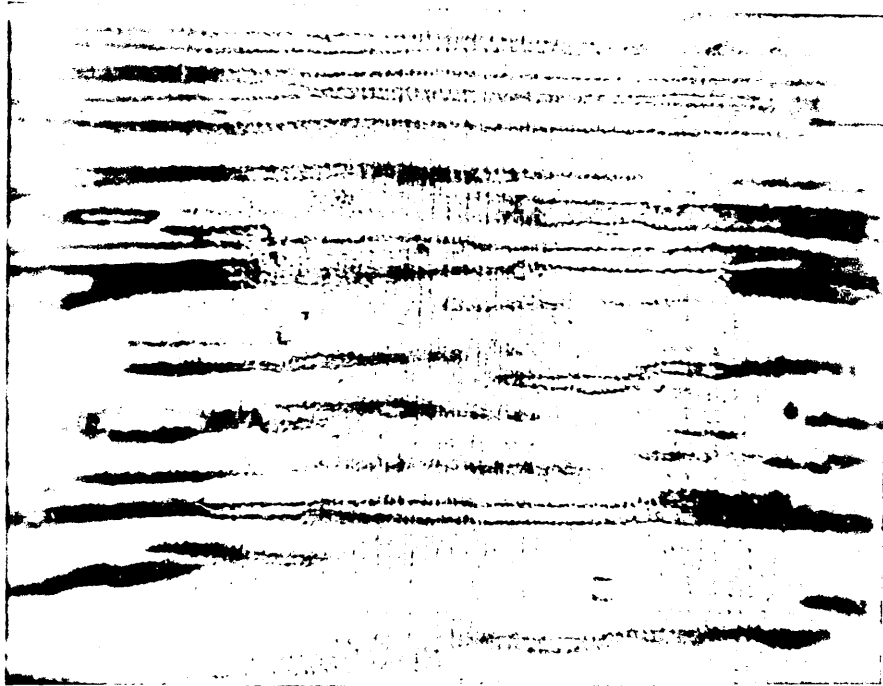


Figure 62(a) : Illustration of the die surface condition after 1 extrusion cycle using MV medium and 60 Mesh grit with a grit to polymer ratio of 1.

x 8

Figure 62(b) : Illustration of the die surface condition after 2 extrusion cycles using MV medium and 60 Mesh grit with a grit to polymer ratio of 1.

x 8

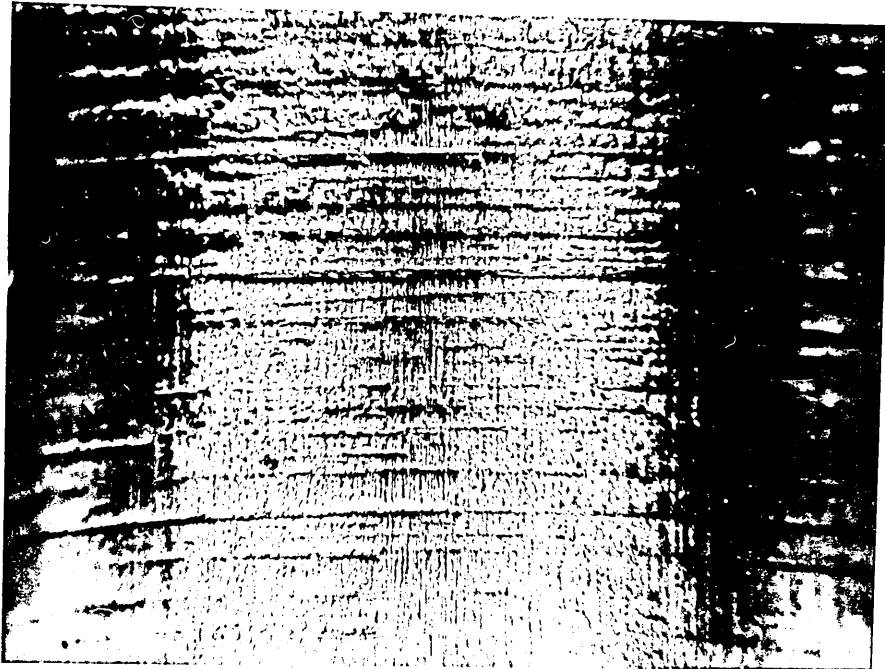
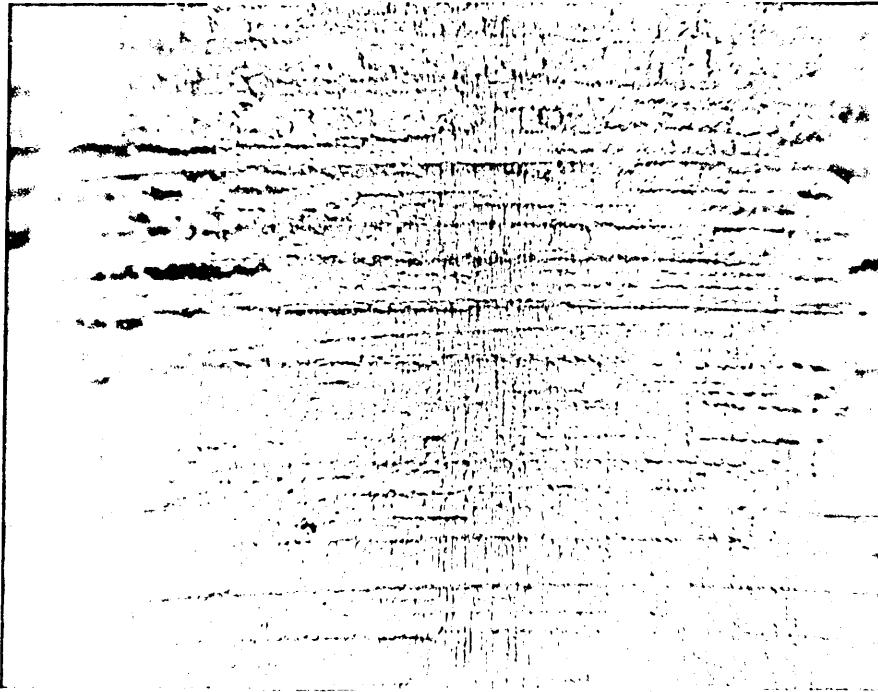


Figure 62(c) : Illustration of the die surface condition after 3 extrusion cycles using MV medium and 60 Mesh grit with a grit to polymer ratio of 1.

x 8

Figure 62(d) : Illustration of the die surface condition after 5 extrusion cycles using MV medium and 60 Mesh grit with a grit to polymer ratio of 1.

x 8

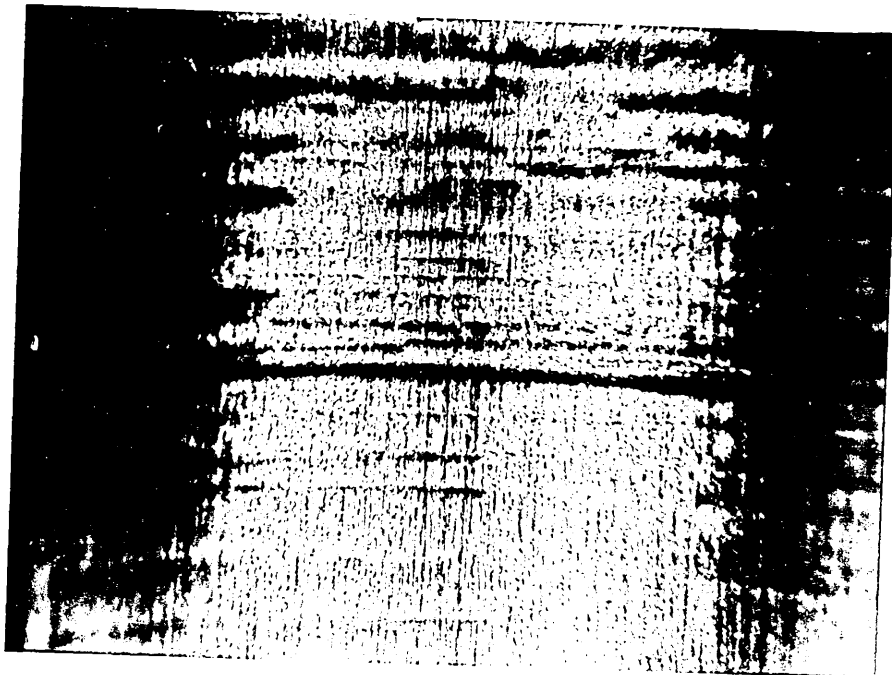
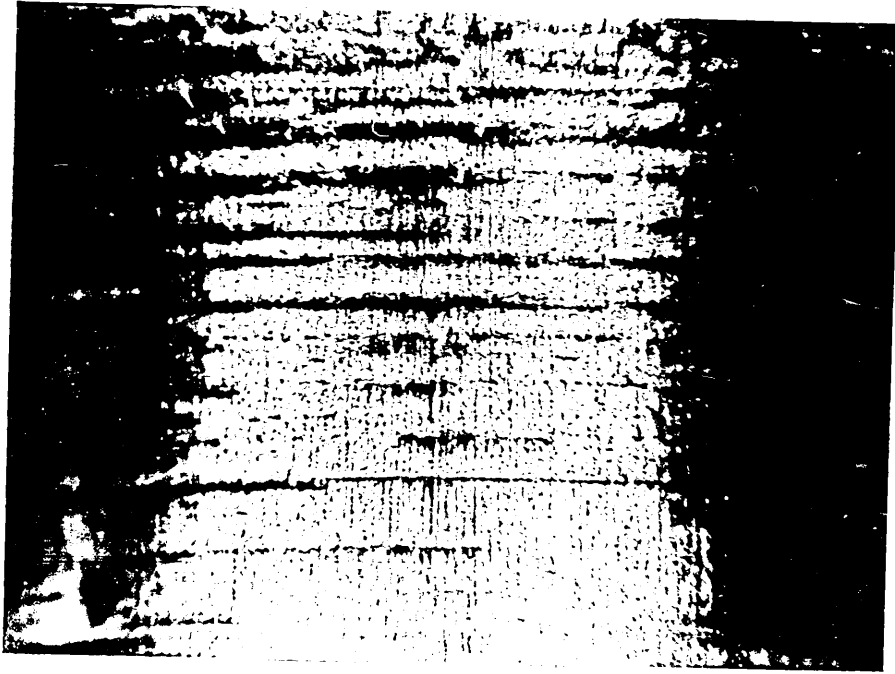


Figure 62(e) : Illustration of the die surface condition after 10 extrusion cycles using MV medium and 60 Mesh grit with a grit to polymer ratio of 1.

x 8

Figure 62(f) : Illustration of the die surface condition after 30 extrusion cycles using MV medium and 60 Mesh grit with a grit to polymer ratio of 1.

x 8

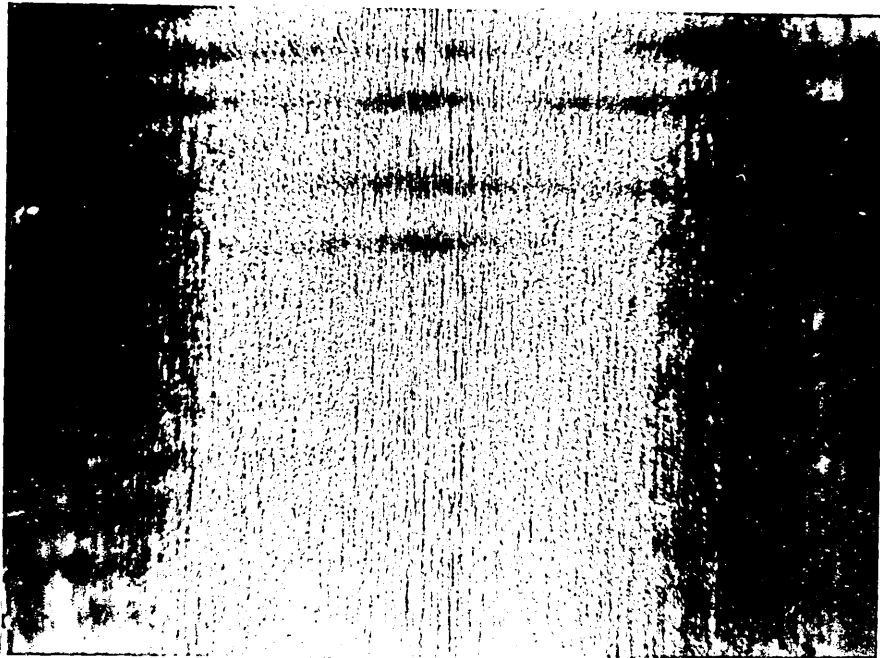
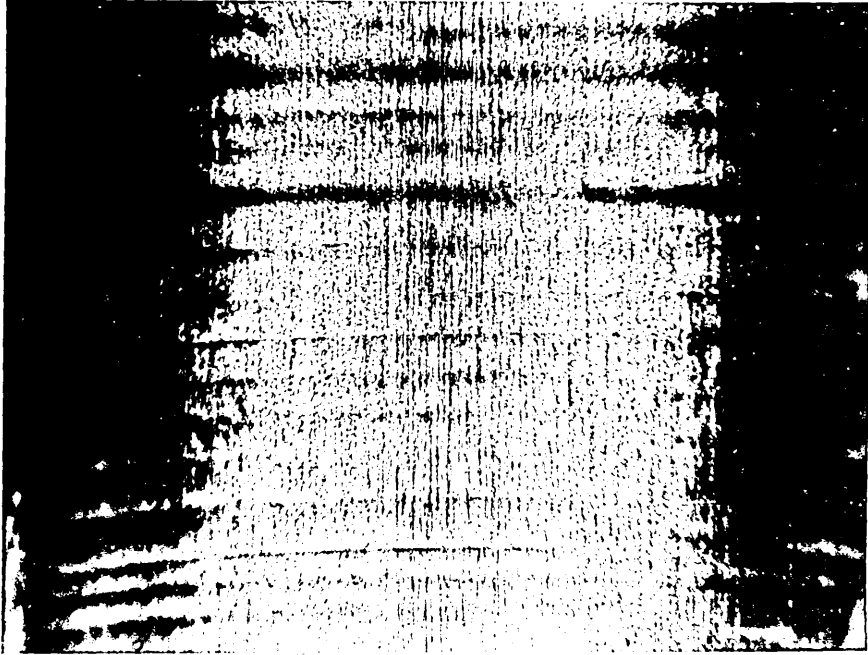


Figure 63(a) : Illustration of the die surface condition after 1
extrusion cycle using HV medium and 100 Mesh grit
with a grit to polymer ratio of 1.

x 8

Figure 63(b) : Illustration of the die surface condition after 2
extrusion cycles using HV medium and 100 Mesh grit
with a grit to polymer ratio of 1.

x 8

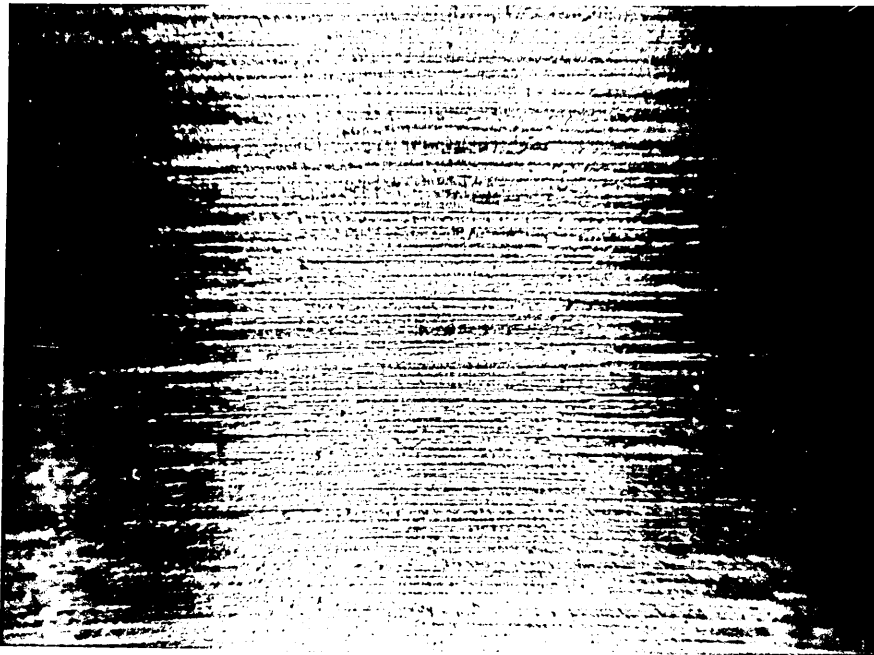
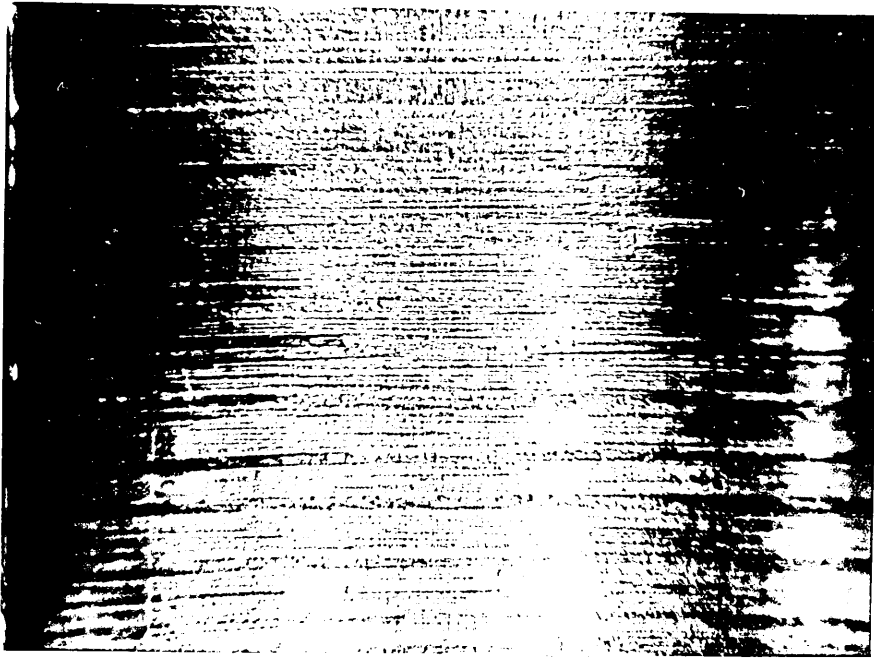


Figure 63(c) : Illustration of the die surface condition after 3 extrusion cycles using HV medium and 100 Mesh grit with a grit to polymer ratio of 1.

x 8

Figure 63(d) : Illustration of the die surface condition after 5 extrusion cycles using HV medium and 100 Mesh grit with a grit to polymer ratio of 1.

x 8

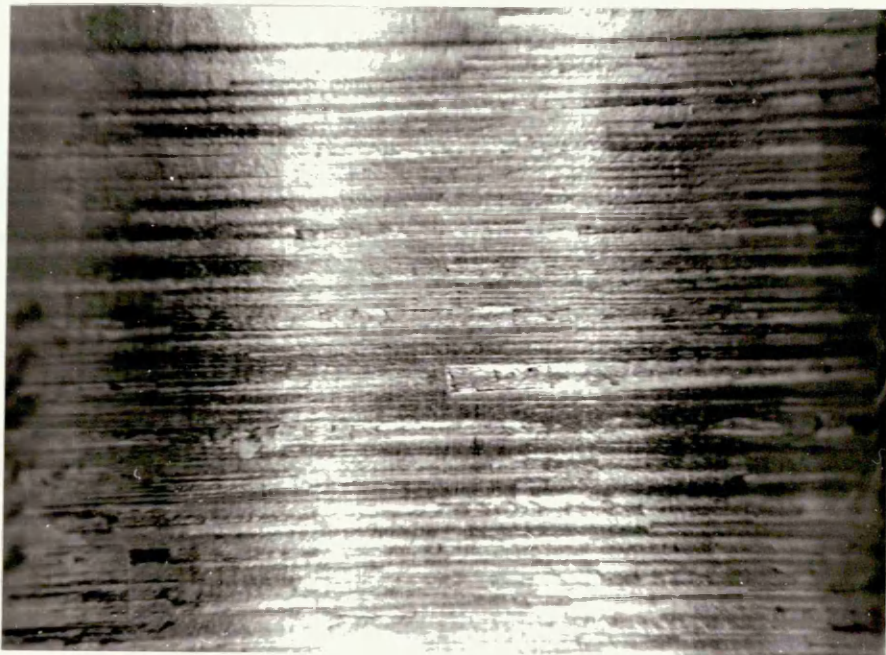
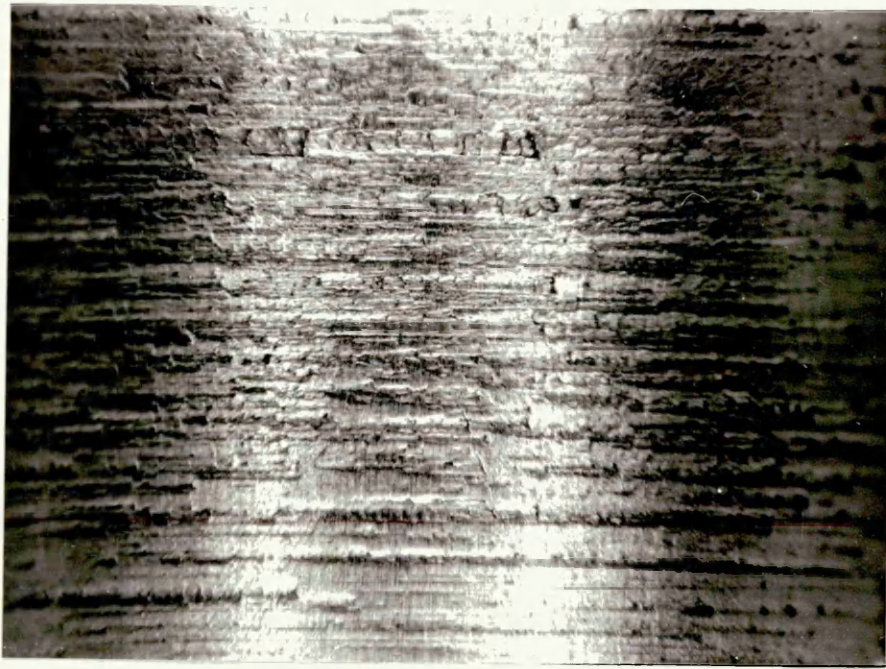


Figure 63(e) : Illustration of the die surface condition after 10 extrusion cycles using HV medium and 100 Mesh grit with a grit to polymer ratio of 1.

x 8

Figure 63(f) : Illustration of the die surface condition after 30 extrusion cycles using HV medium and 100 Mesh grit with a grit to polymer ratio of 1.

x 8

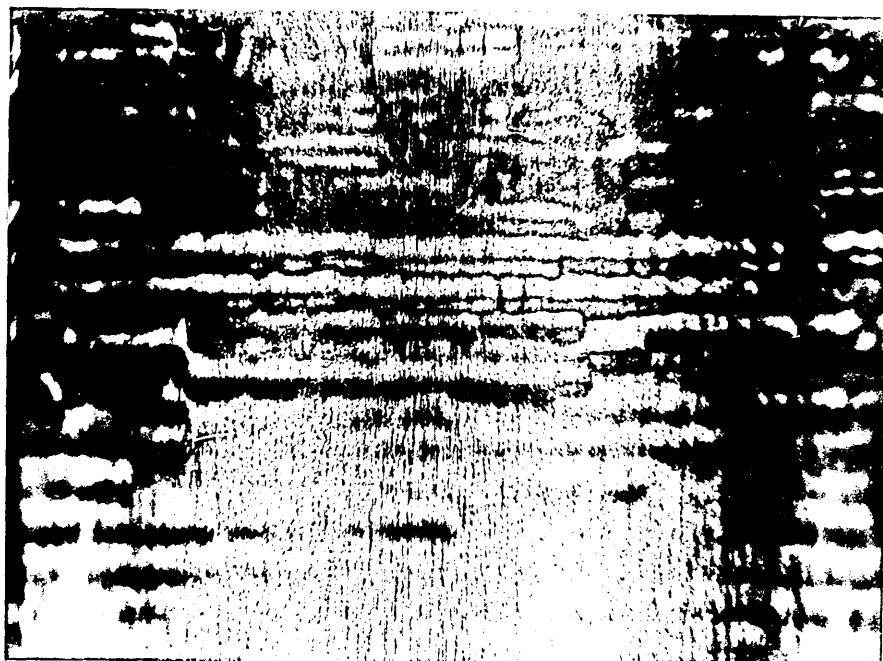
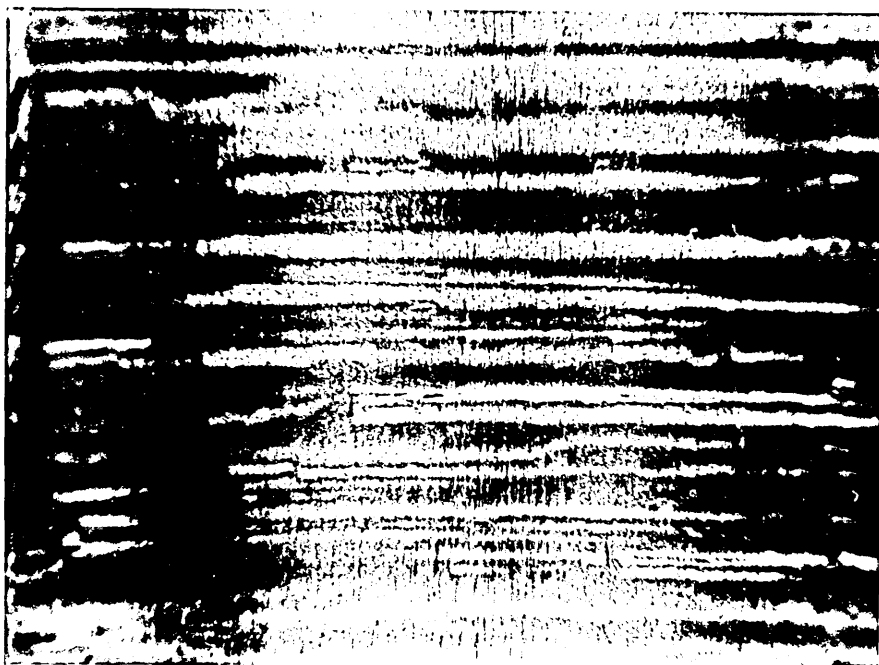


Figure 64(a) : Illustration of the die surface condition after 1
extrusion cycle using HV medium and 60 Mesh grit
with a grit to polymer ratio of 1.

x 8

Figure 64(b) : Illustration of the die surface condition after 2
extrusion cycles using HV medium and 60 Mesh grit
with a grit to polymer ratio of 1.

x 8

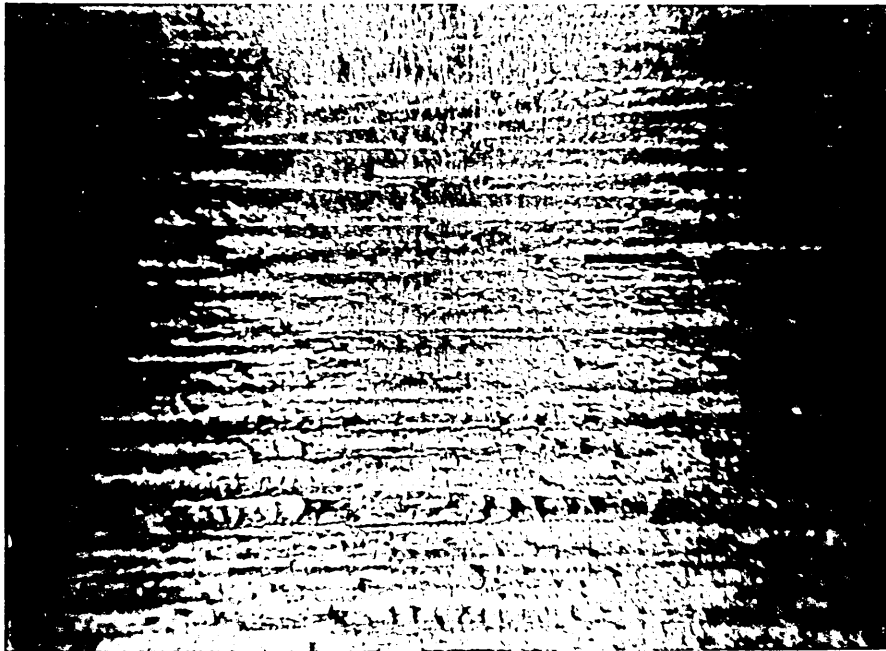
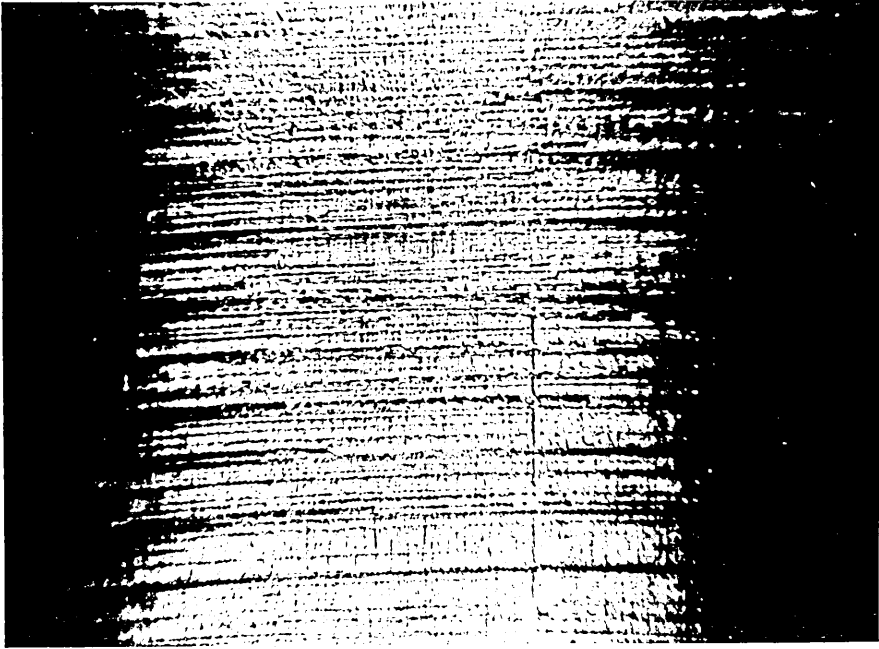


Figure 64(c) : Illustration of the die surface condition after 3 extrusion cycles using HV medium and 60 Mesh grit with a grit to polymer ratio of 1.

x 8

Figure 64(d) : Illustration of the die surface condition after 5 extrusion cycles using HV medium and 60 Mesh grit with a grit to polymer ratio of 1.

x 8

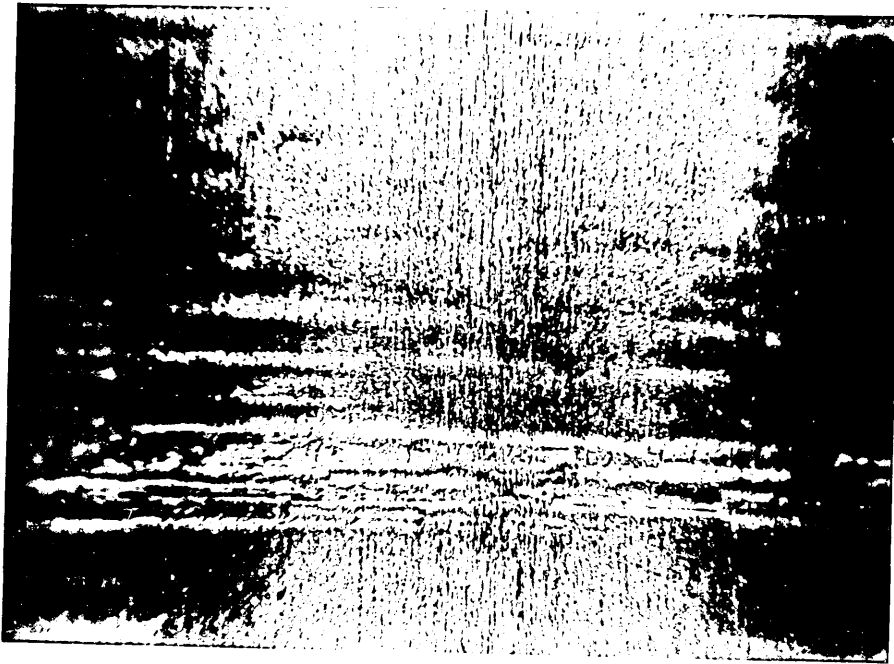
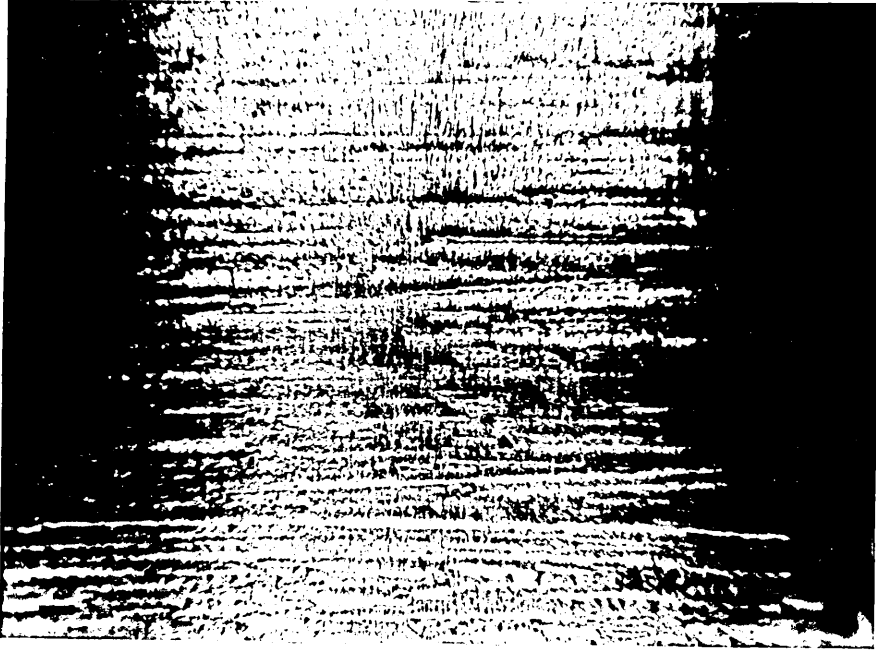


Figure 64(e) : Illustration of the die surface condition after 10 extrusion cycles using HV medium and 60 Mesh grit with a grit to polymer ratio of 1.

x 8

Figure 64(f) : Illustration of the die surface condition after 30 extrusion cycles using HV medium and 60 Mesh grit with a grit to polymer ratio of 1.

x 8

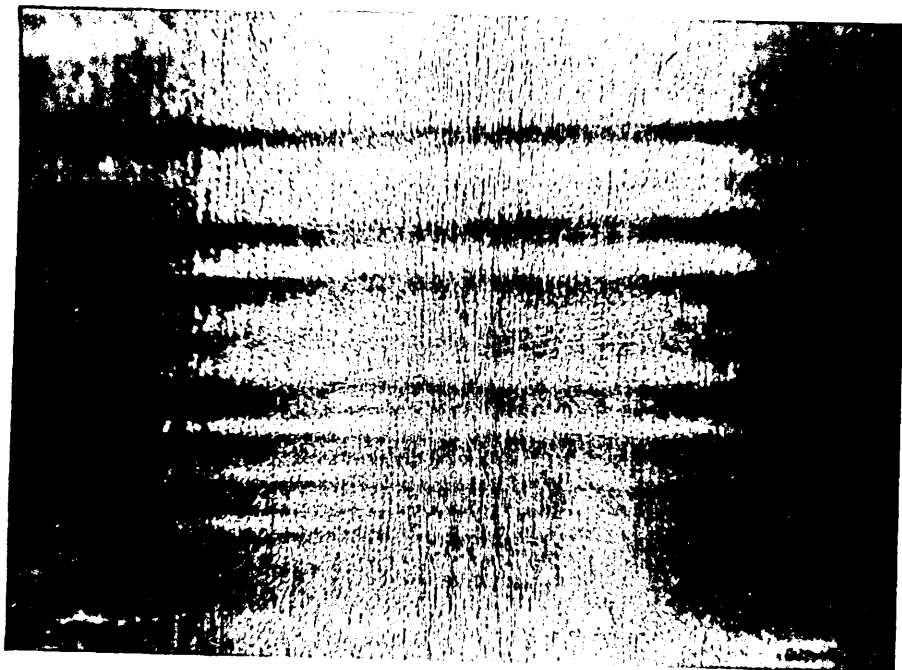
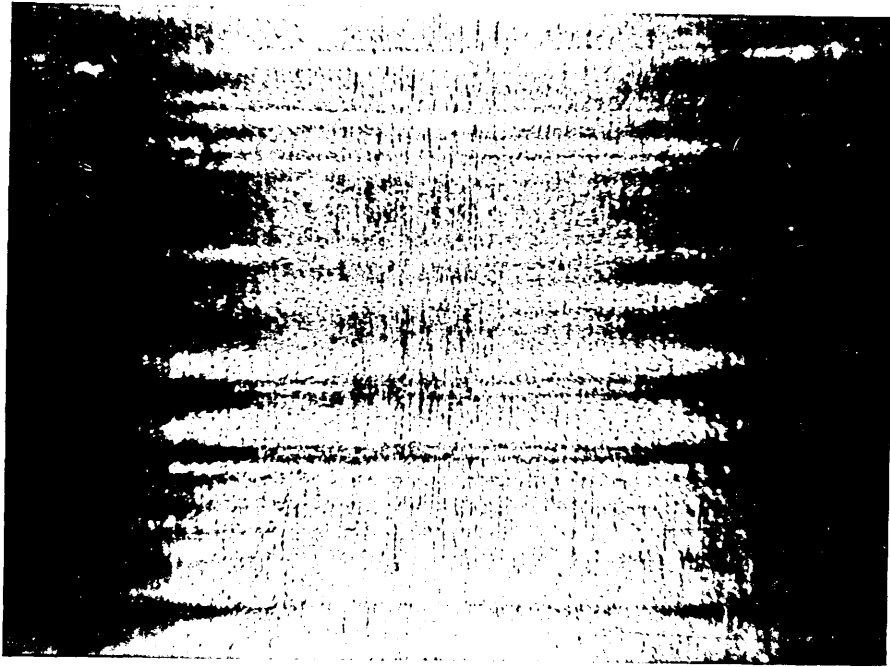
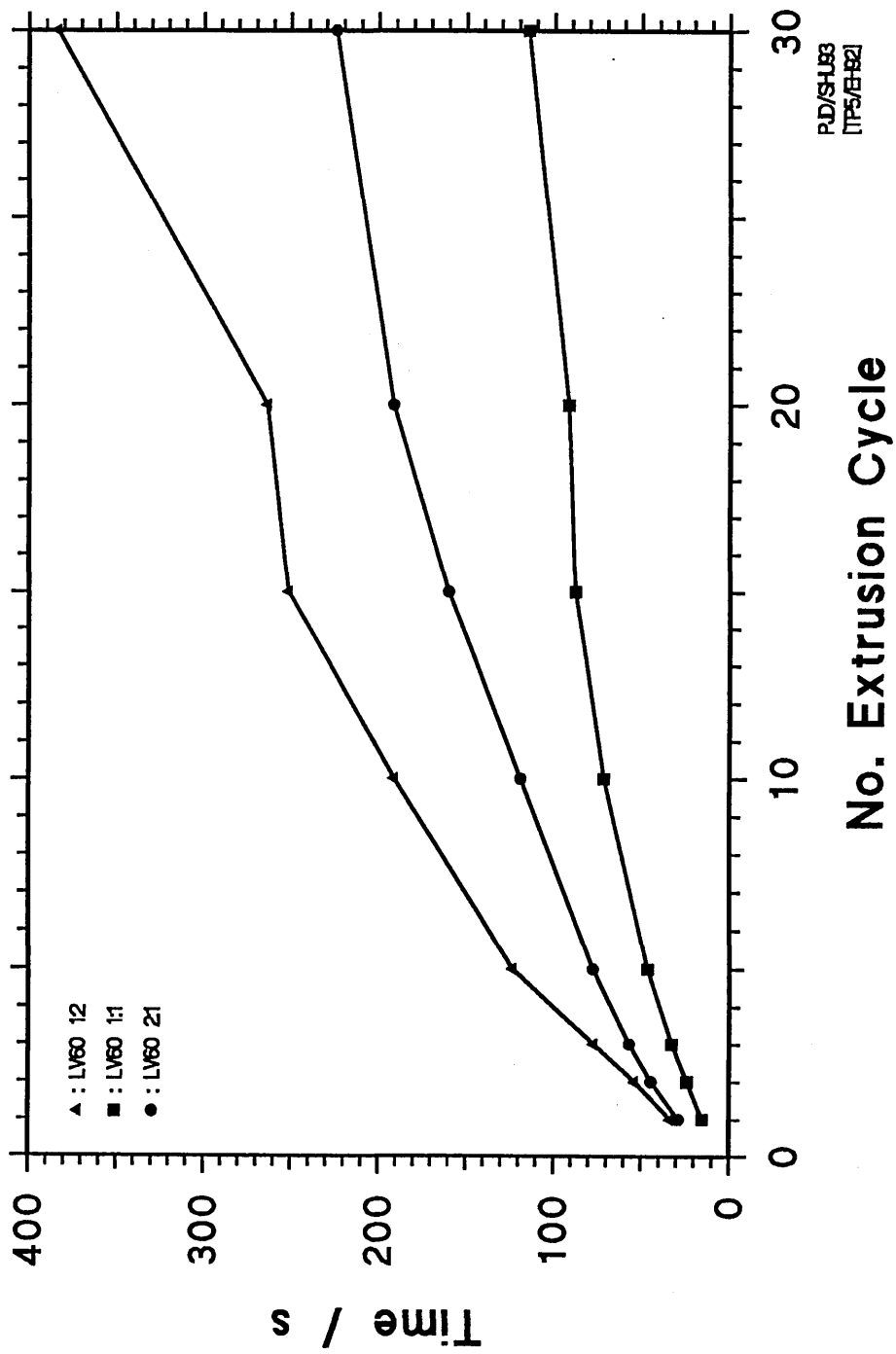


Figure 65 : The relationship between the number of extrusion cycles and the processing time required to complete machining using LV medium and 60 Mesh grit with grit to polymer ratios of 0.5, 1 and 2.

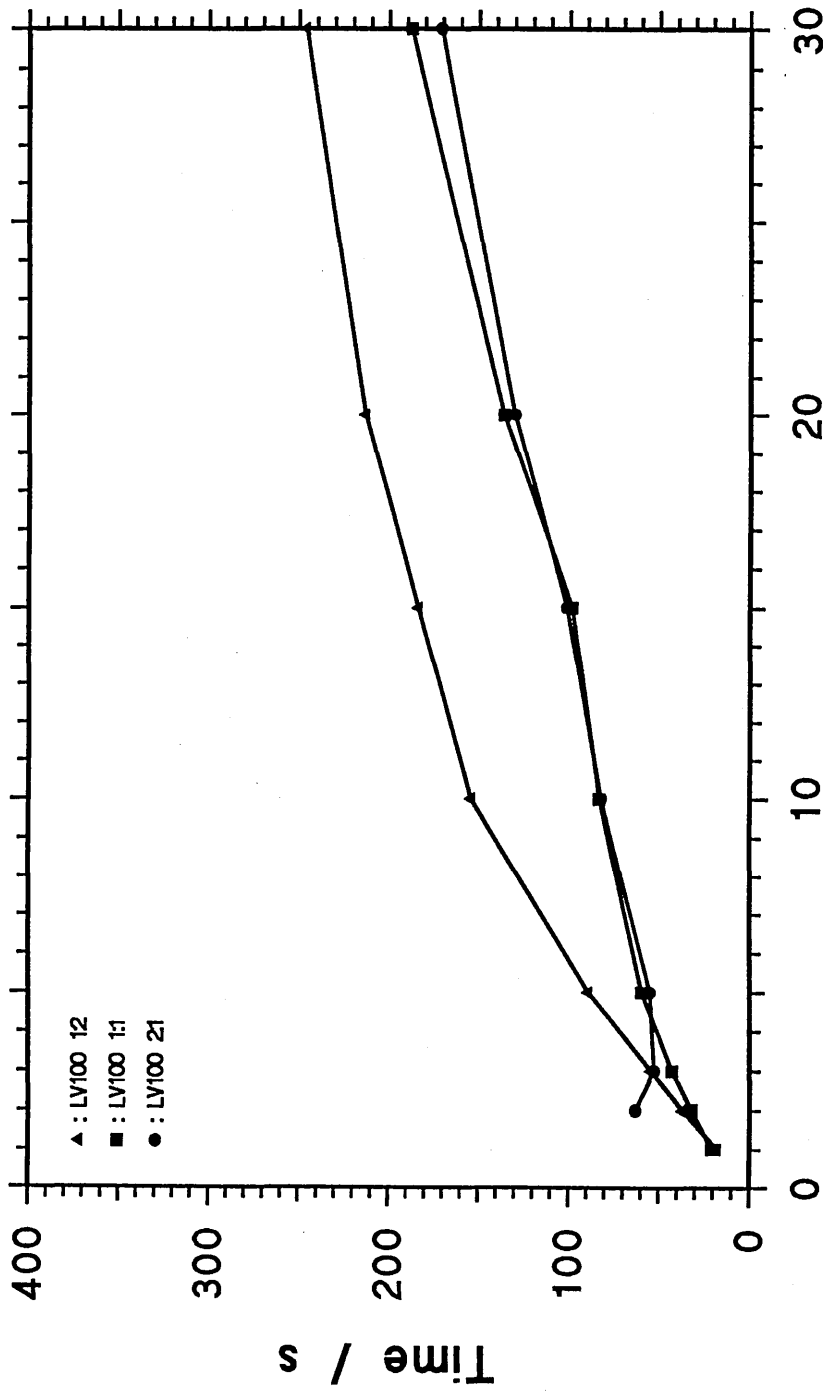


P.D./SHUBS
[TPS/E182]

No. Extrusion Cycle

Time / s

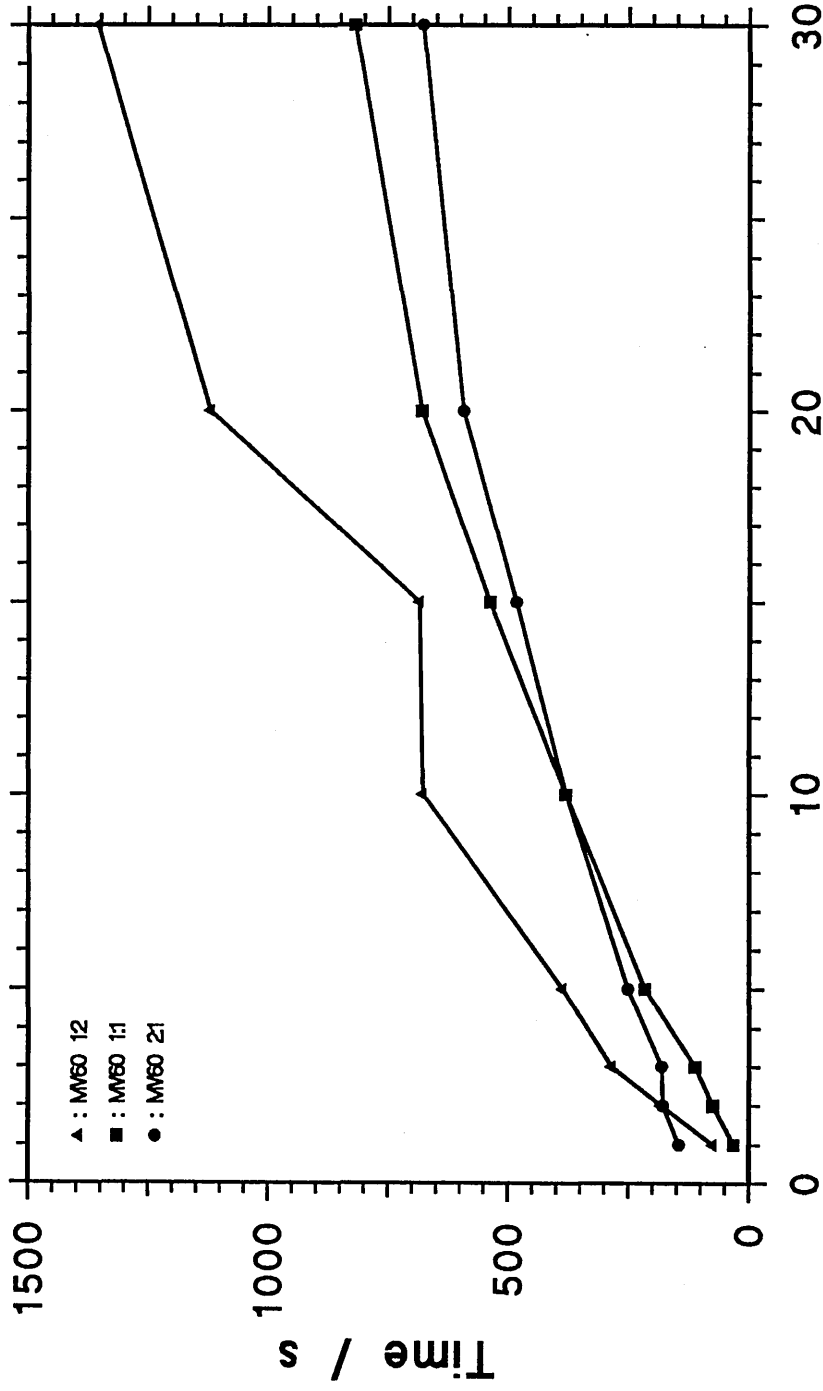
Figure 66 : The relationship between the number of extrusion cycles and the processing time required to complete machining using LV medium and 100 Mesh grit with grit to polymer ratios of 0.5, 1 and 2.



P.D./S.H.83
I.P.5/B-92

No. Extrusion Cycle

Figure 67 : The relationship between the number of extrusion cycles and the processing time required to complete machining using MV medium and 60 Mesh grit with grit to polymer ratios of 0.5, 1 and 2.



P.D./S.H.B3
[TP5/EH2]

No. Extrusion Cycle

Figure 68 : The relationship between the number of extrusion cycles and the processing time required to complete machining using MV medium and 100 Mesh grit with grit to polymer ratios of 0.5, 1 and 2.

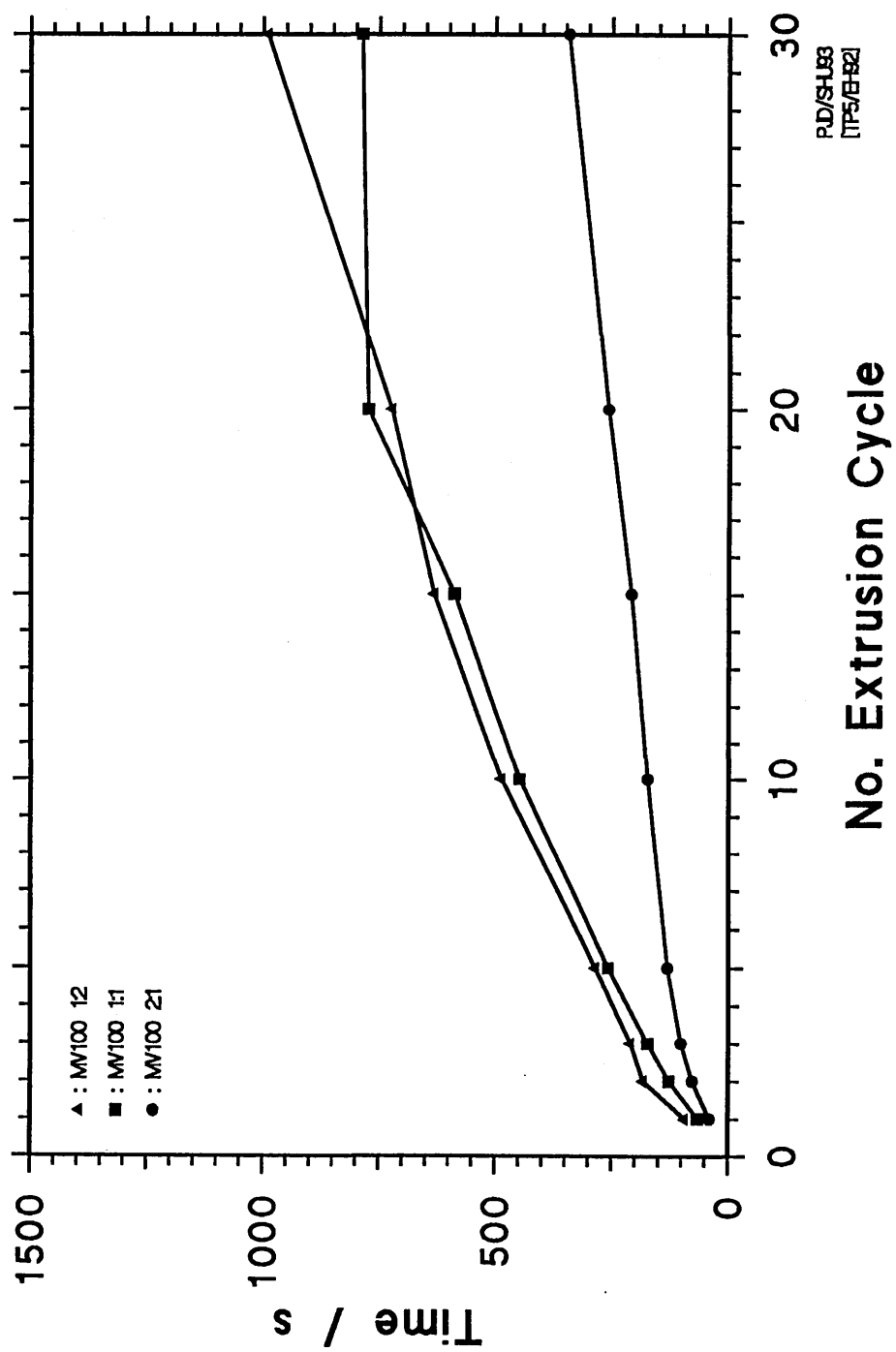


Figure 69 : The relationship between the number of extrusion cycles and the processing time required to complete machining using HV medium and 60 Mesh grit with grit to polymer ratios of 0.5, 1 and 2.

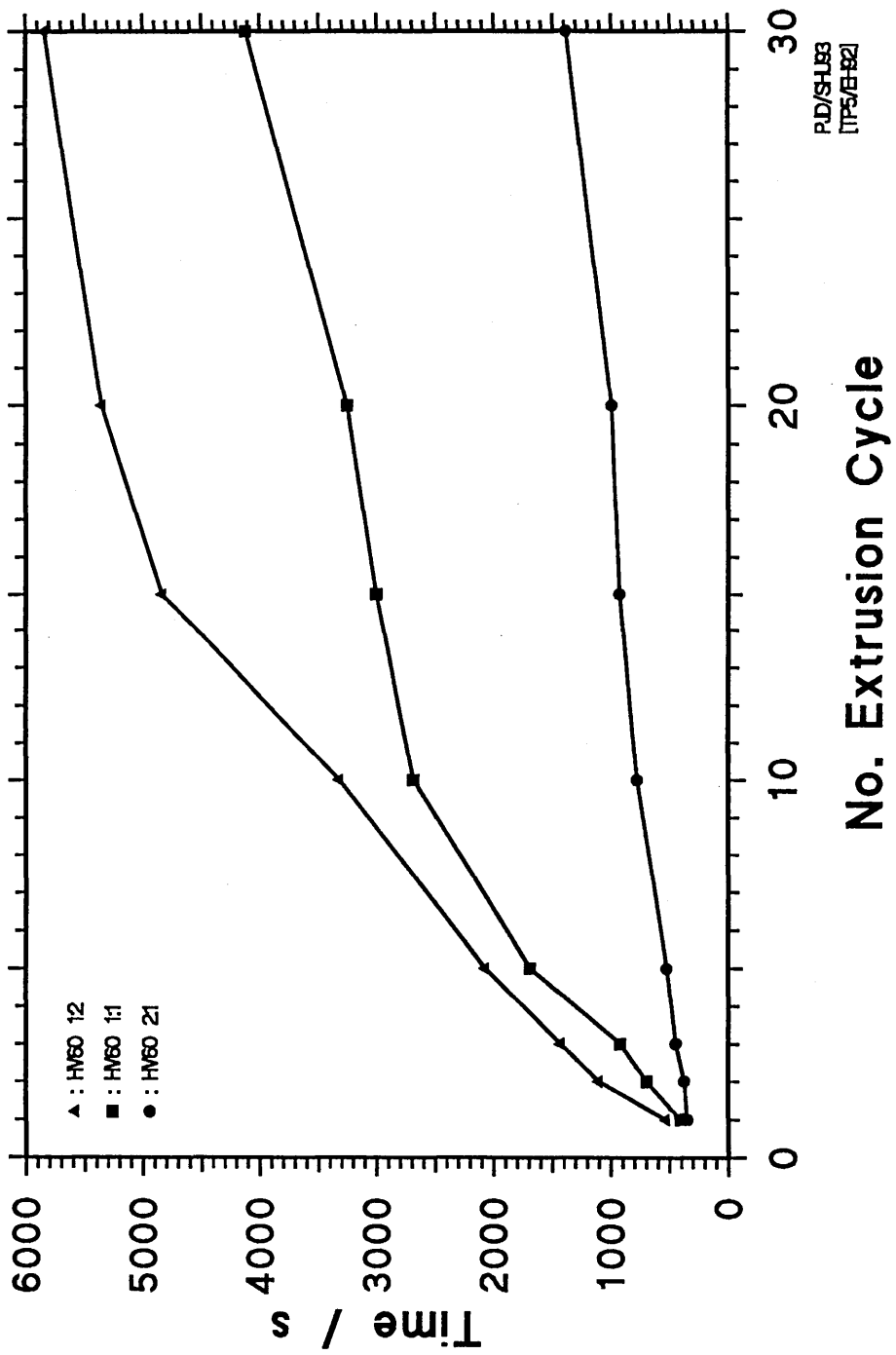


Figure 70 : The relationship between the number of extrusion cycles and the processing time required to complete machining using HV medium and 100 Mesh grit with grit to polymer ratios of 0.5, 1 and 2.

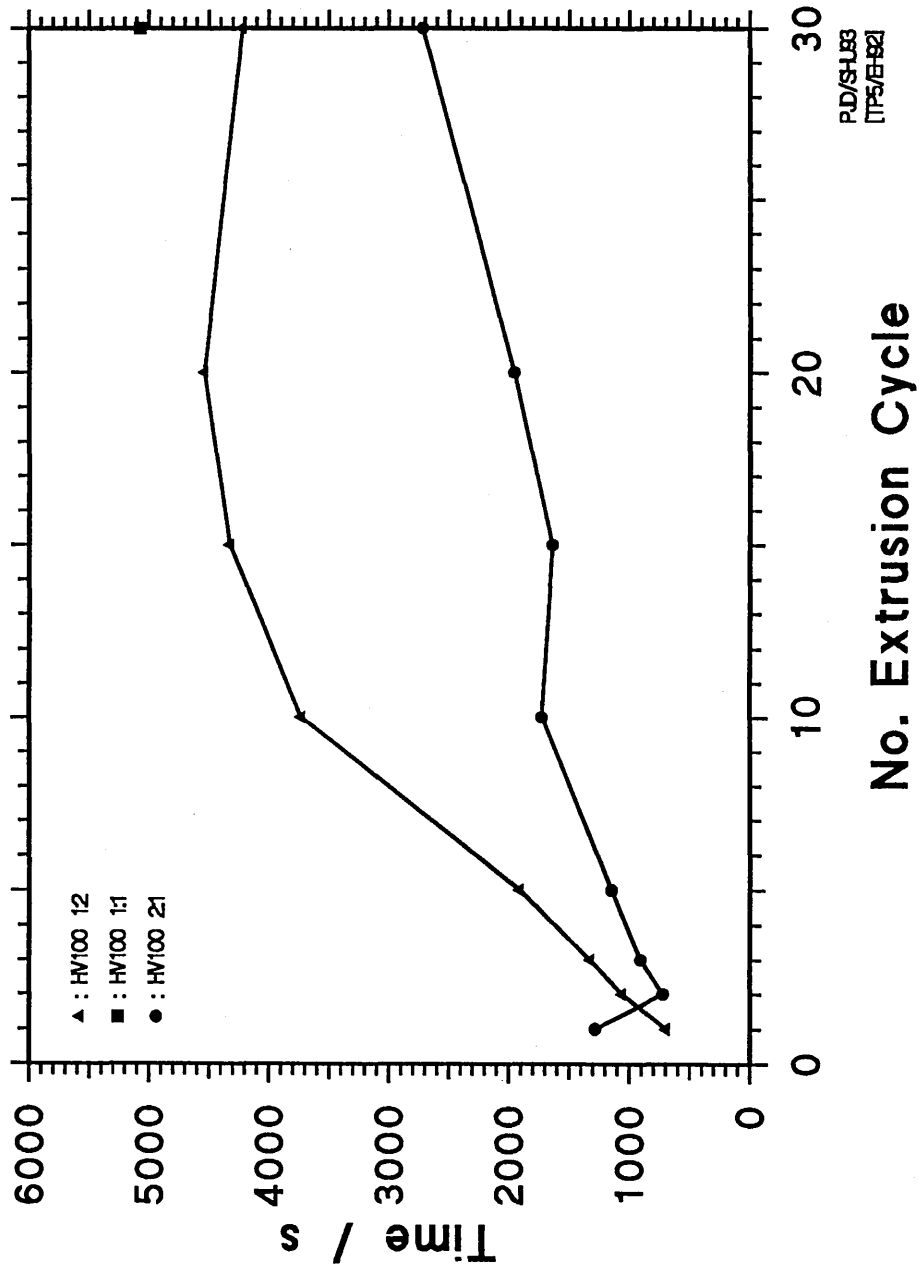


Figure 71(a) : The relationship between the number of extrusion cycles and the corresponding pressure drop across the die for pure LV medium.

Figure 71(b) : The relationship between the number of extrusion cycles and the corresponding pressure drop across the die for pure MV medium.

Figure 71(c) : The relationship between the number of extrusion cycles and the corresponding pressure drop across the die for pure HV medium.

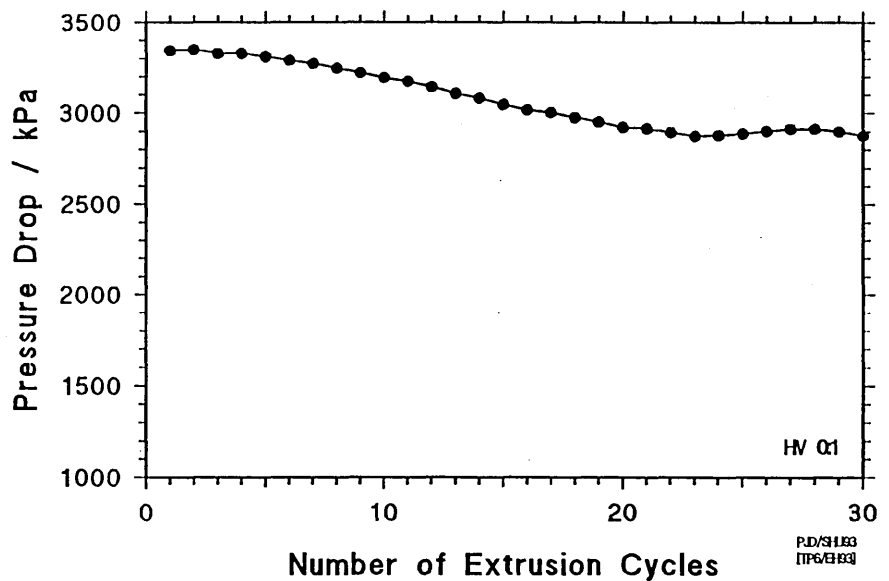
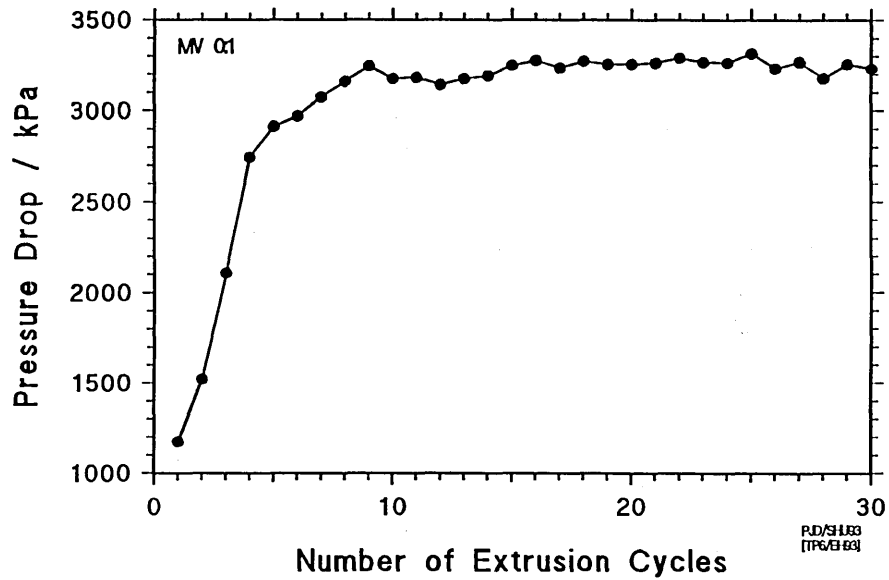
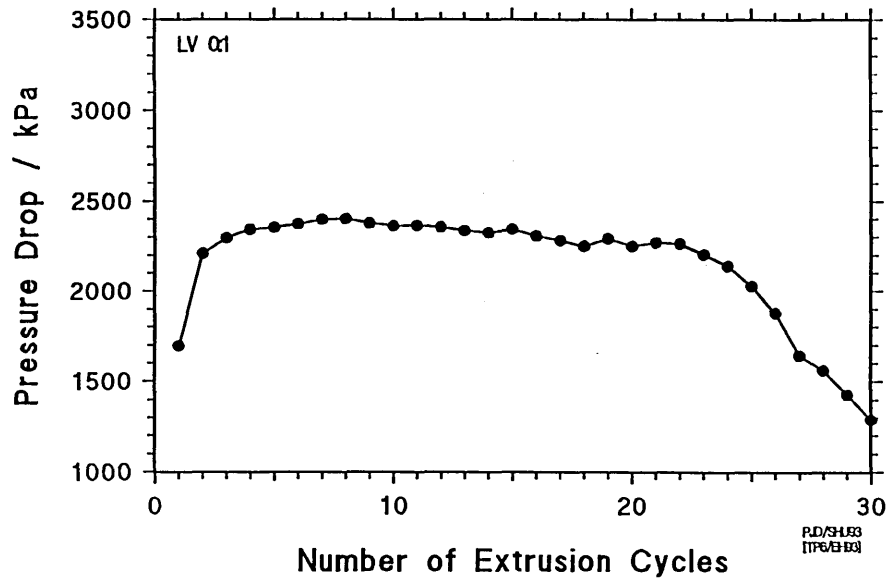


Figure 72(a) : The relationship between the number of extrusion cycles and the corresponding pressure drop across the die for all runs conducted using LV medium and 60 Mesh grit with a grit to polymer ratio of 0.5.

Figure 72(b) : The relationship between the number of extrusion cycles and the corresponding pressure drop across the die for all runs conducted using LV medium and 60 Mesh grit with a grit to polymer ratio of 1.

Figure 72(c) : The relationship between the number of extrusion cycles and the corresponding pressure drop across the die for all runs conducted using LV medium and 60 Mesh grit with a grit to polymer ratio of 2.

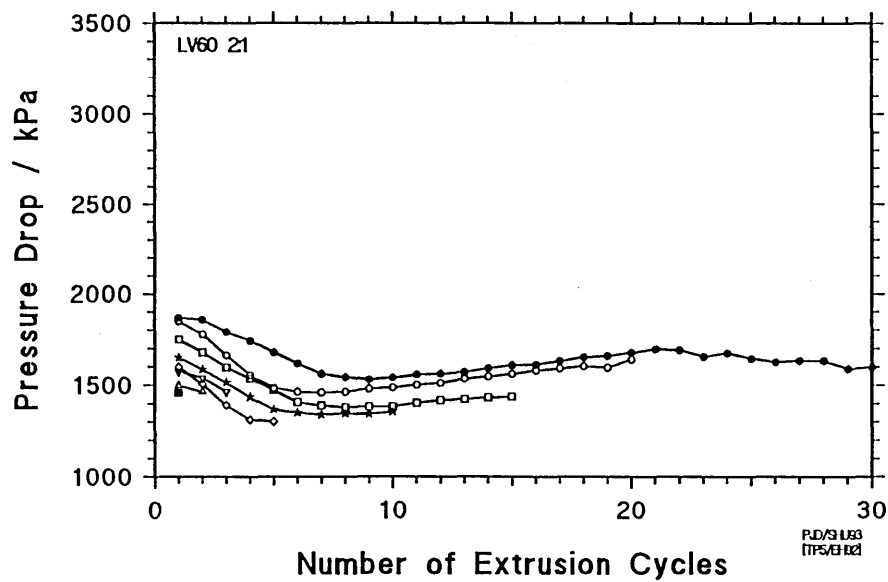
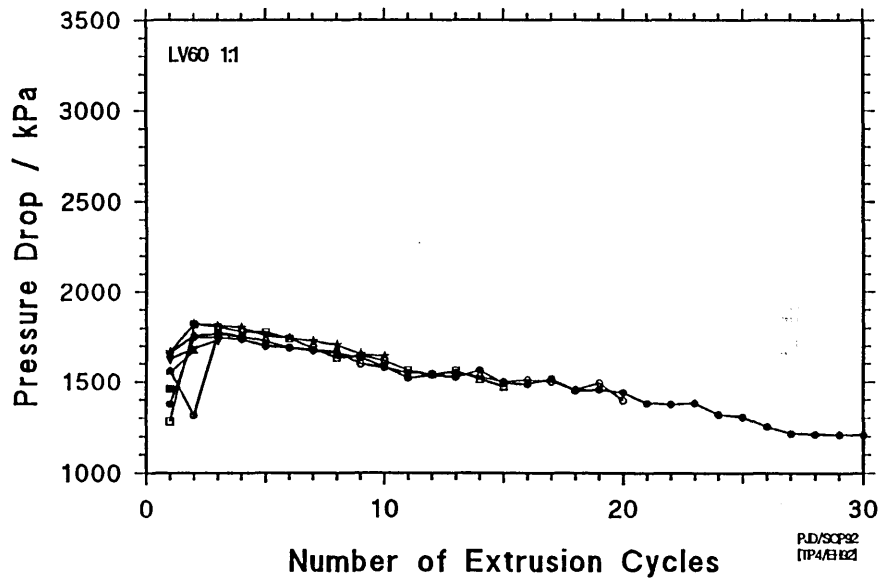
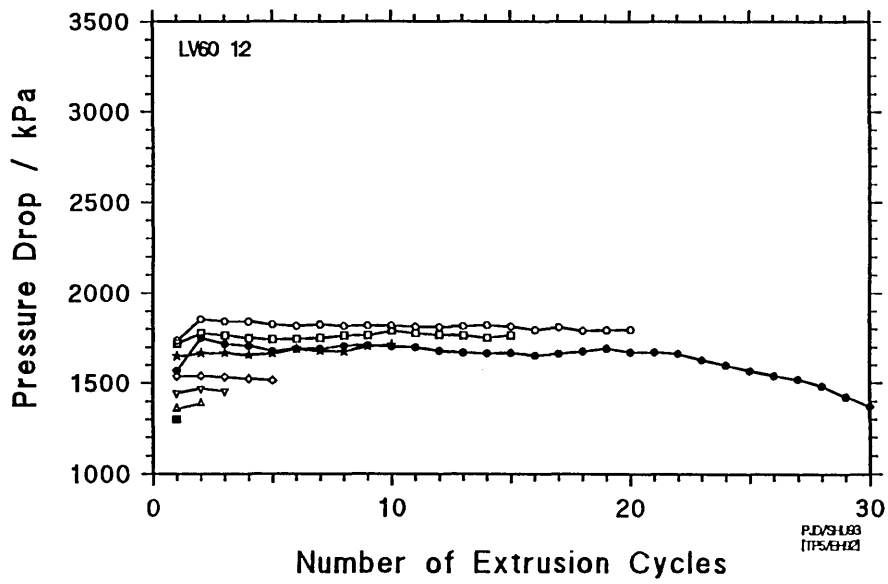


Figure 73(a) : The relationship between the number of extrusion cycles and the corresponding pressure drop across the die for all runs conducted using LV medium and 100 Mesh grit with a grit to polymer ratio of 0.5.

Figure 73(b) : The relationship between the number of extrusion cycles and the corresponding pressure drop across the die for all runs conducted using LV medium and 100 Mesh grit with a grit to polymer ratio of 1.

Figure 73(c) : The relationship between the number of extrusion cycles and the corresponding pressure drop across the die for all runs conducted using LV medium and 100 Mesh grit with a grit to polymer ratio of 2.

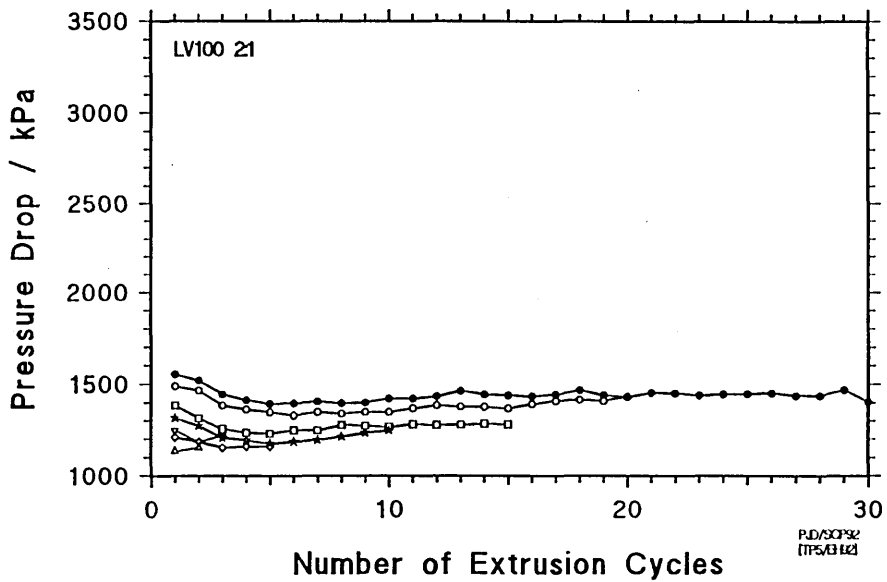
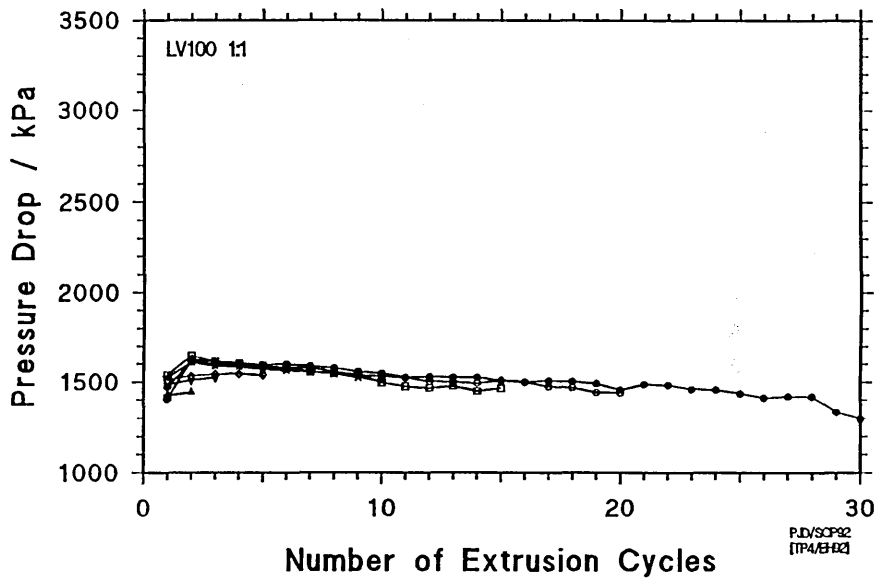
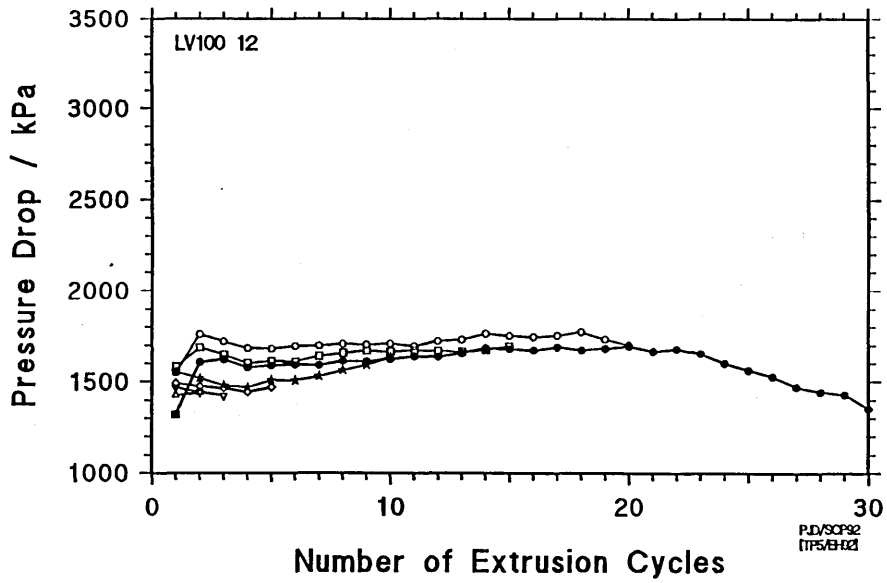


Figure 74(a) : The illustration of the relationship between the number of extrusion cycles and the pressure drop across the die for the 30 extrusion cycle run with respect to all LV medium and 60 Mesh grit mixtures utilised, as well as the pure LV medium.

Figure 74(b) : The illustration of the relationship between the number of extrusion cycles and the pressure drop across the die for the 30 extrusion cycle run with respect to all LV medium and 100 Mesh grit mixtures utilised, as well as the pure LV medium.

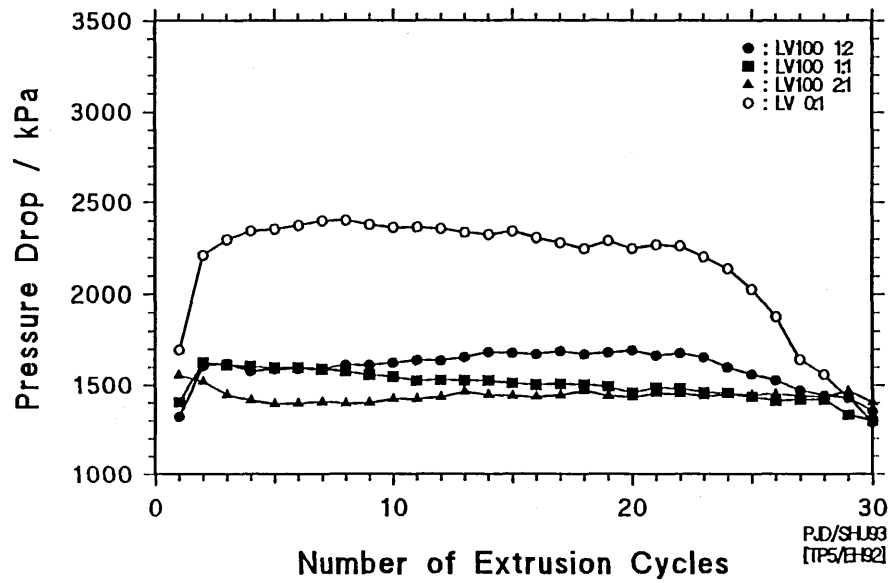
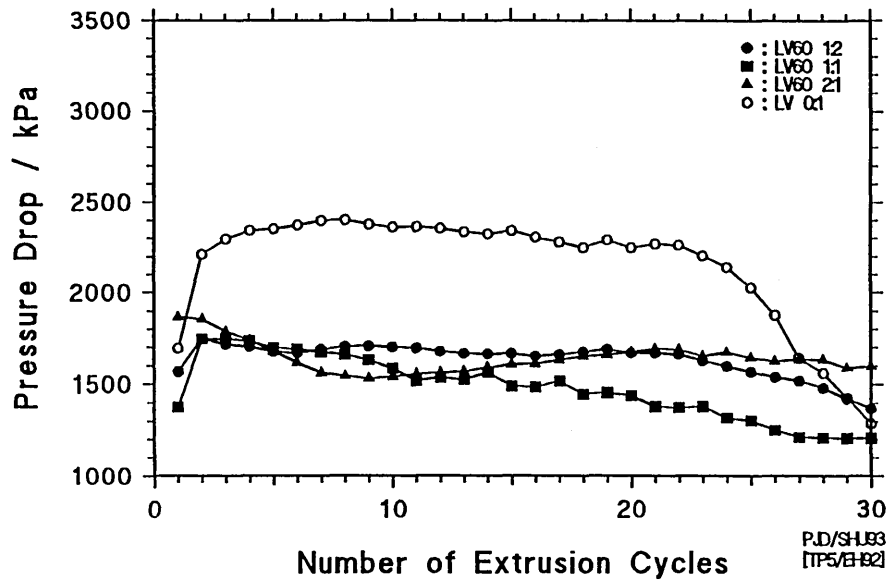


Figure 75(a) : The relationship between the number of extrusion cycles and the corresponding pressure drop across the die for all runs conducted using MV medium and 60 Mesh grit with a grit to polymer ratio of 0.5.

Figure 75(b) : The relationship between the number of extrusion cycles and the corresponding pressure drop across the die for all runs conducted using MV medium and 60 Mesh grit with a grit to polymer ratio of 1.

Figure 75(c) : The relationship between the number of extrusion cycles and the corresponding pressure drop across the die for all runs conducted using MV medium and 60 Mesh grit with a grit to polymer ratio of 2.

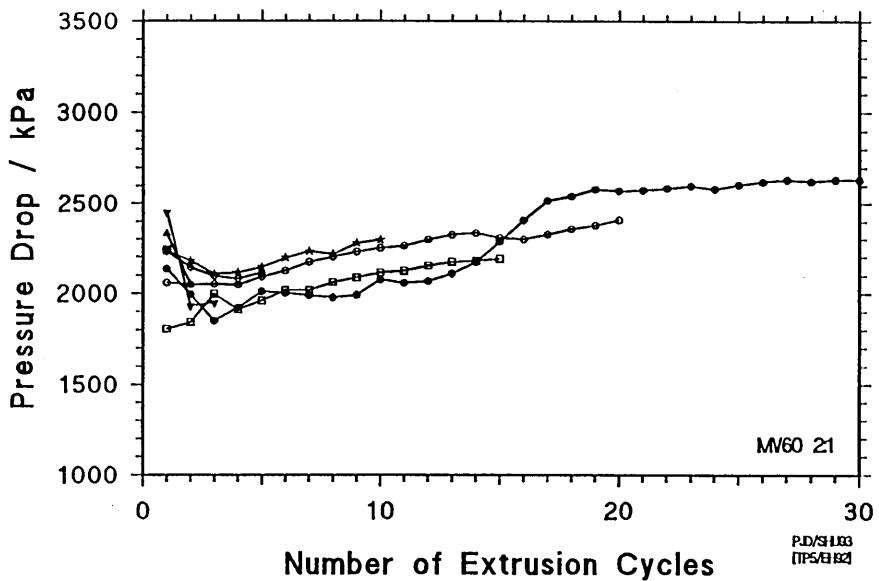
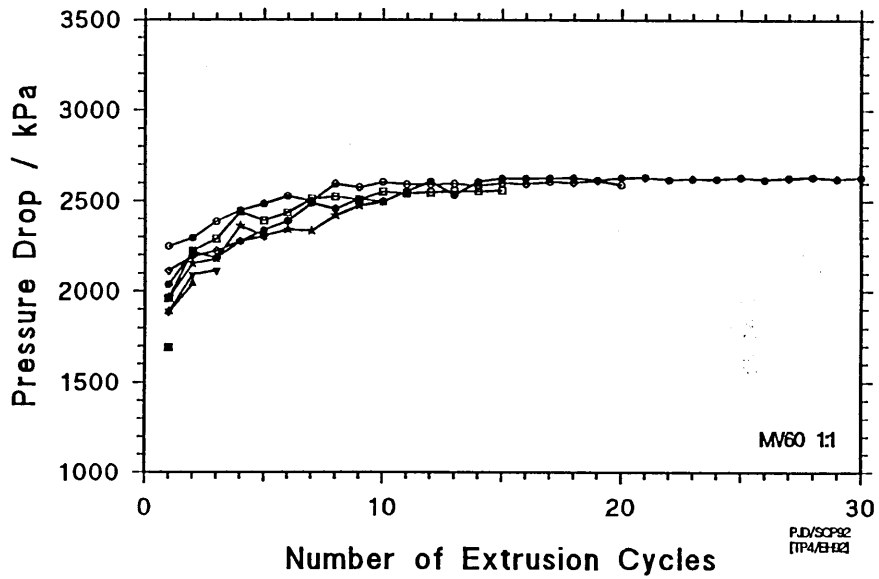
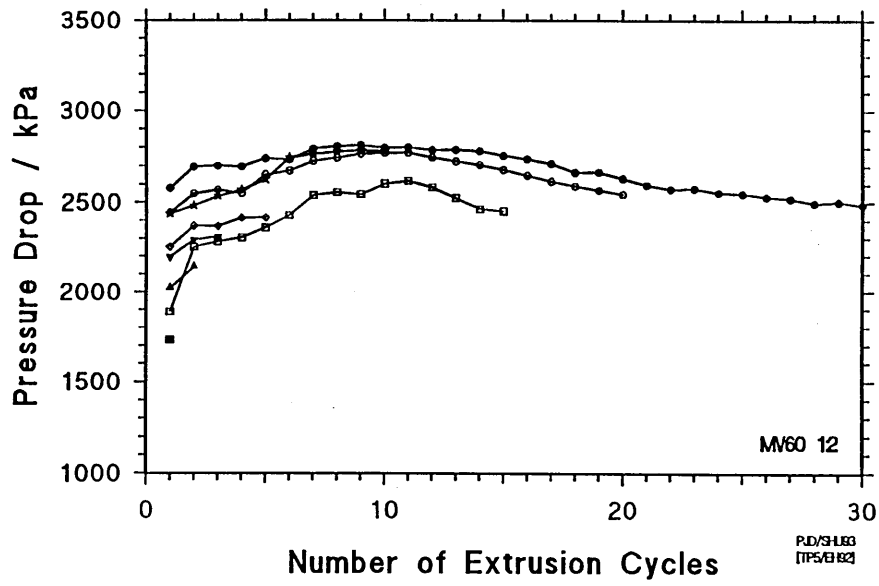


Figure 76(a) : The relationship between the number of extrusion cycles and the corresponding pressure drop across the die for all runs conducted using MV medium and 100 Mesh grit with a grit to polymer ratio of 0.5.

Figure 76(b) : The relationship between the number of extrusion cycles and the corresponding pressure drop across the die for all runs conducted using MV medium and 100 Mesh grit with a grit to polymer ratio of 1.

Figure 76(c) : The relationship between the number of extrusion cycles and the corresponding pressure drop across the die for all runs conducted using MV medium and 100 Mesh grit with a grit to polymer ratio of 2.

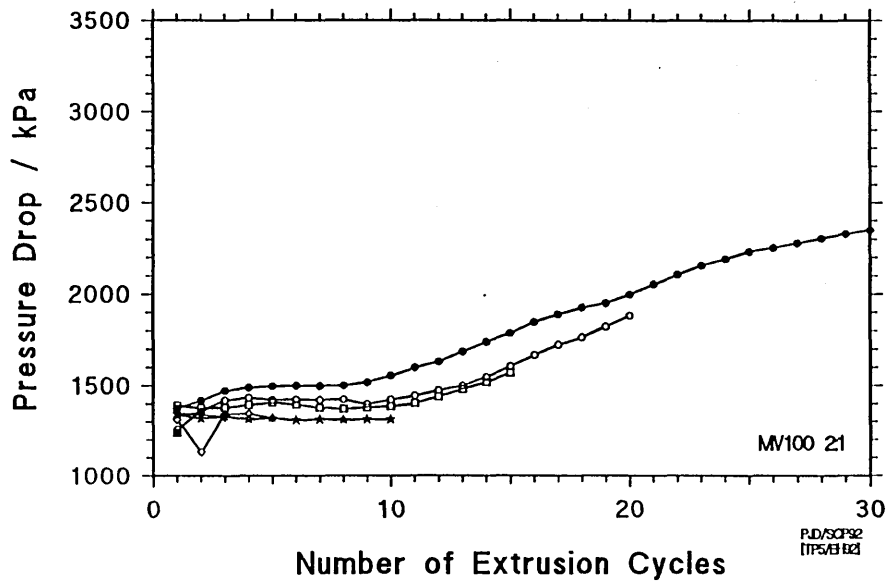
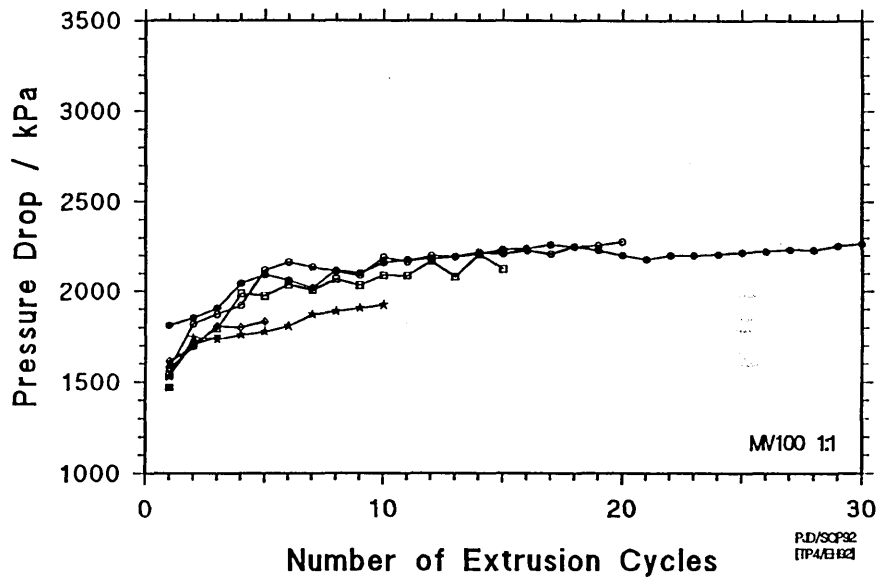
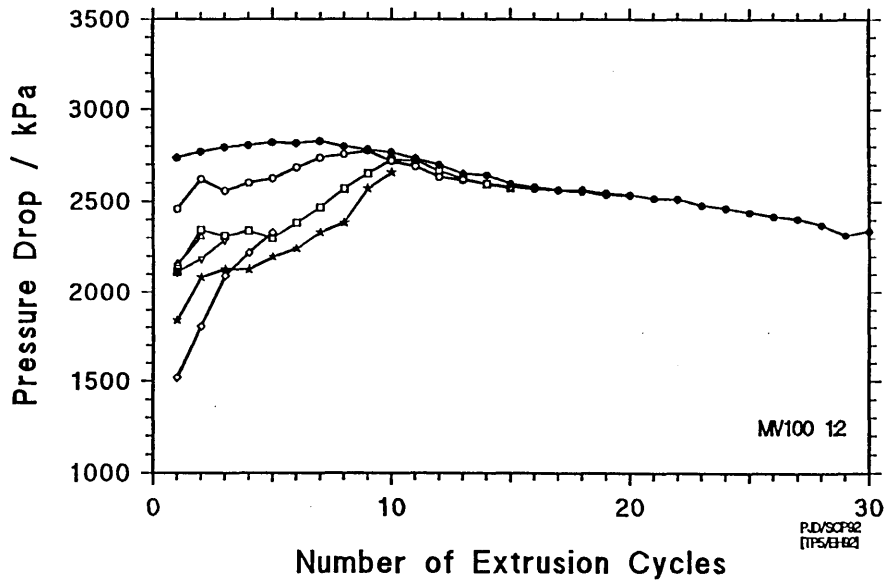


Figure 77(a) : The illustration of the relationship between the number of extrusion cycles and the pressure drop across the die for the 30 extrusion cycle run with respect to all MV medium and 60 Mesh grit mixtures utilised, as well as the pure MV medium.

Figure 77(b) : The illustration of the relationship between the number of extrusion cycles and the pressure drop across the die for the 30 extrusion cycle run with respect to all MV medium and 100 Mesh grit mixtures utilised, as well as the pure MV medium.

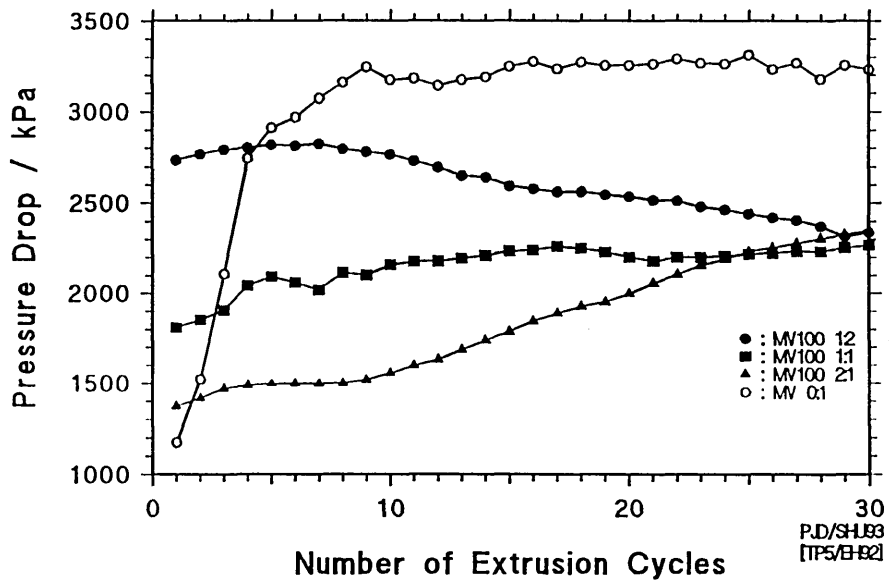
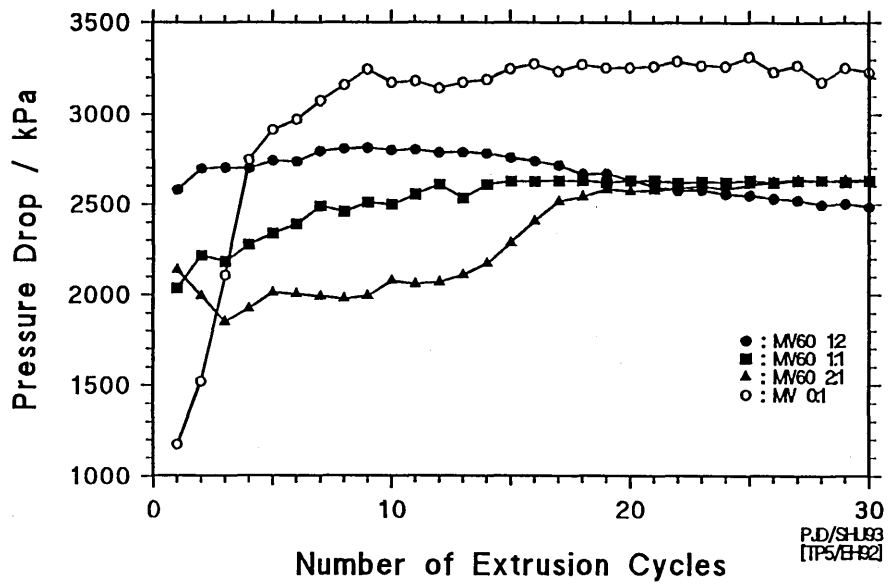


Figure 78(a) : The relationship between the number of extrusion cycles and the corresponding pressure drop across the die for all runs conducted using HV medium and 60 Mesh grit with a grit to polymer ratio of 0.5.

Figure 78(b) : The relationship between the number of extrusion cycles and the corresponding pressure drop across the die for all runs conducted using HV medium and 60 Mesh grit with a grit to polymer ratio of 1.

Figure 78(c) : The relationship between the number of extrusion cycles and the corresponding pressure drop across the die for all runs conducted using HV medium and 60 Mesh grit with a grit to polymer ratio of 2.

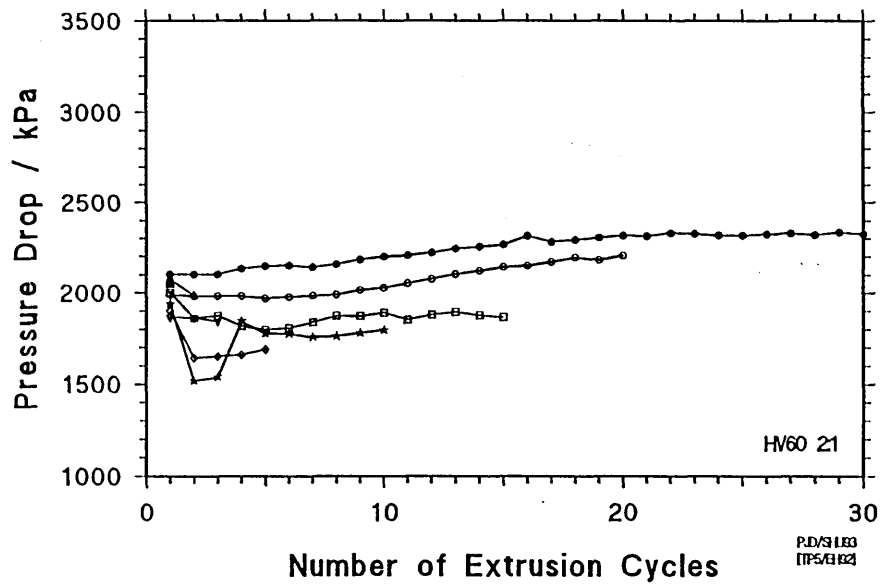
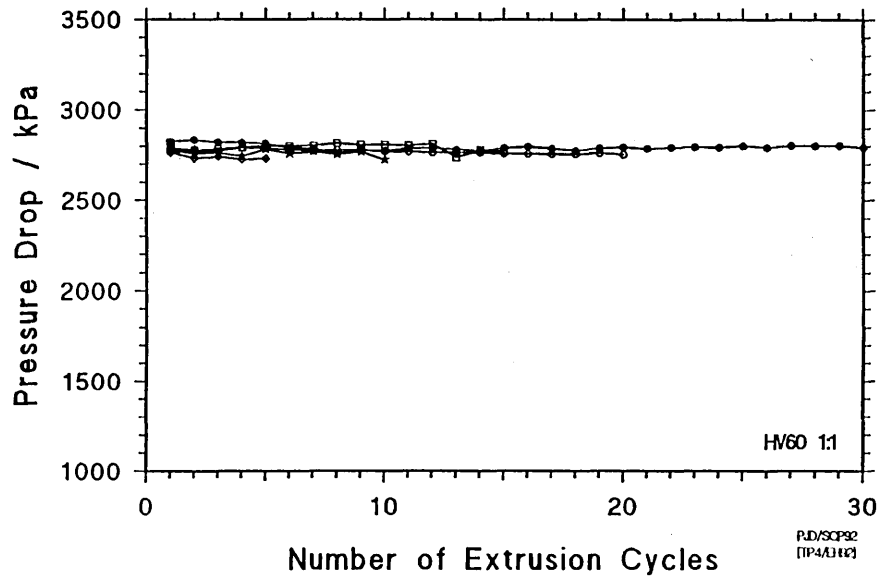
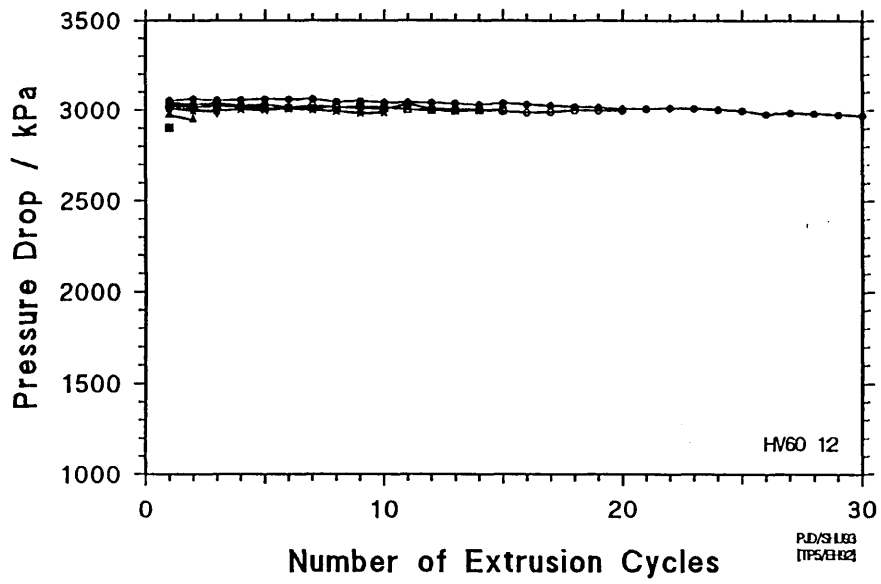


Figure 79(a) : The relationship between the number of extrusion cycles and the corresponding pressure drop across the die for all runs conducted using HV medium and 100 Mesh grit with a grit to polymer ratio of 0.5.

Figure 79(b) : The relationship between the number of extrusion cycles and the corresponding pressure drop across the die for all runs conducted using HV medium and 100 Mesh grit with a grit to polymer ratio of 1.

Figure 79(c) : The relationship between the number of extrusion cycles and the corresponding pressure drop across the die for all runs conducted using HV medium and 100 Mesh grit with a grit to polymer ratio of 2.

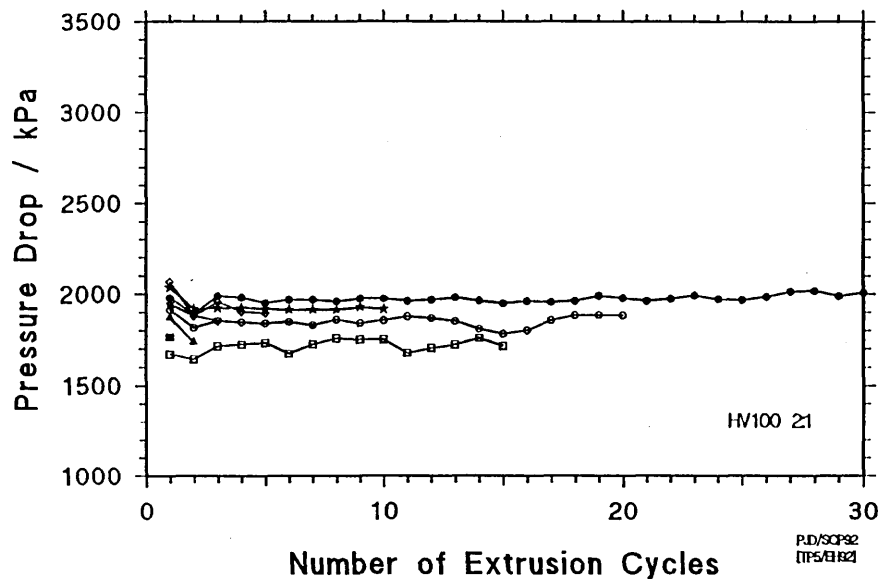
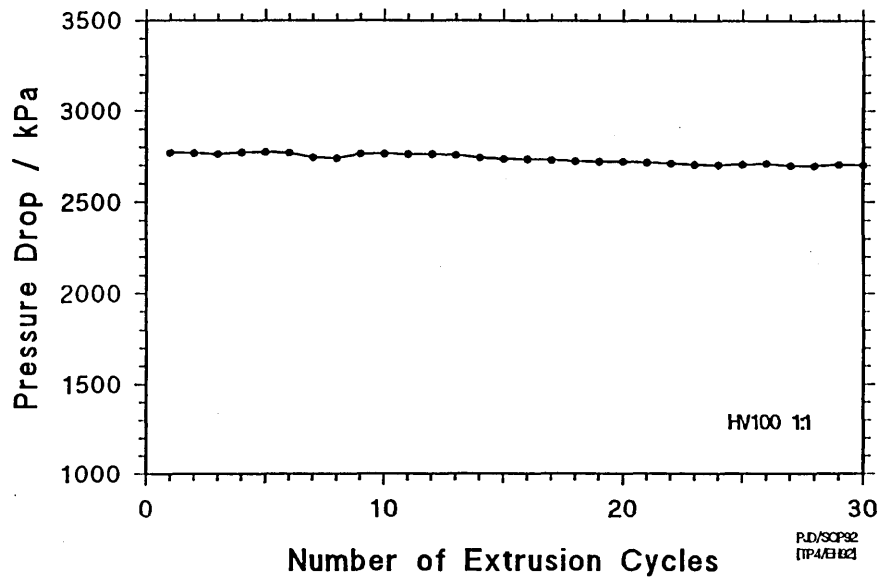
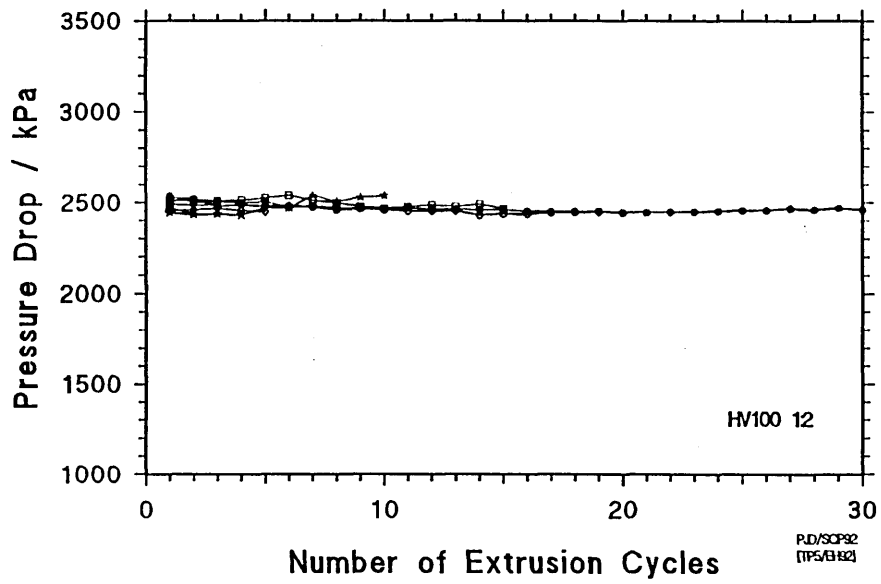


Figure 80(a) : The illustration of the relationship between the number of extrusion cycles and the pressure drop across the die for the 30 extrusion cycle run with respect to all HV medium and 60 Mesh grit mixtures utilised, as well as the pure HV medium.

Figure 80(b) : The illustration of the relationship between the number of extrusion cycles and the pressure drop across the die for the 30 extrusion cycle run with respect to all HV medium and 100 Mesh grit mixtures utilised, as well as the pure HV medium.

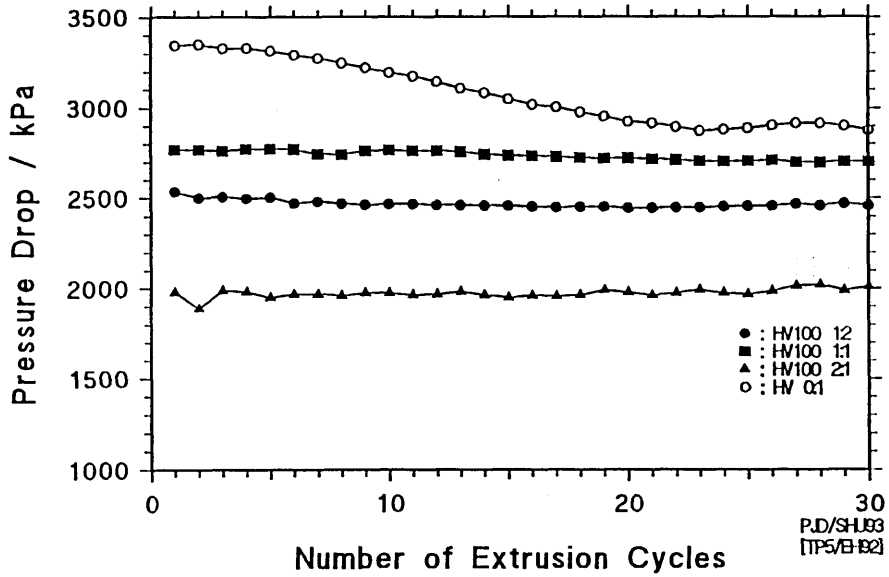
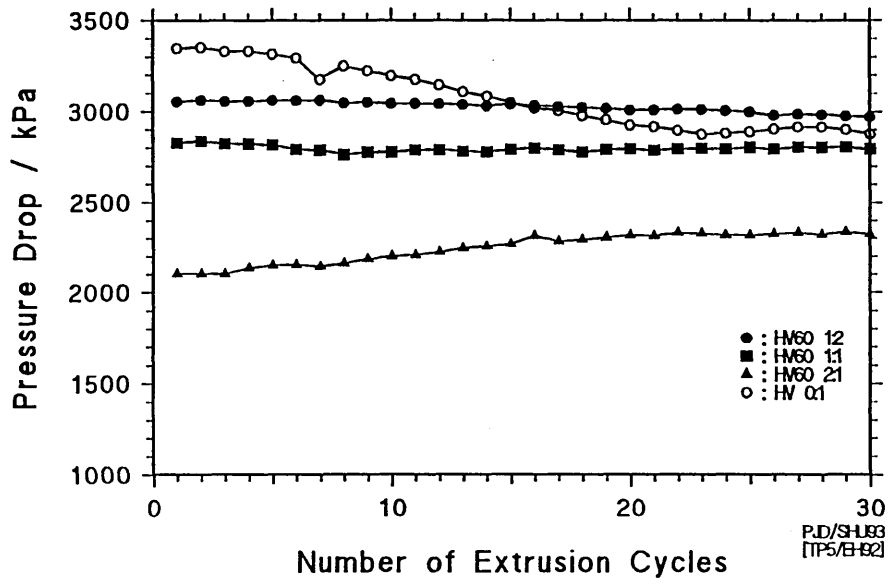


Figure 81 : The relationship between the number of extrusion cycles and the average pressure drops obtained in relation to all LV medium and 60 Mesh grit mixtures.

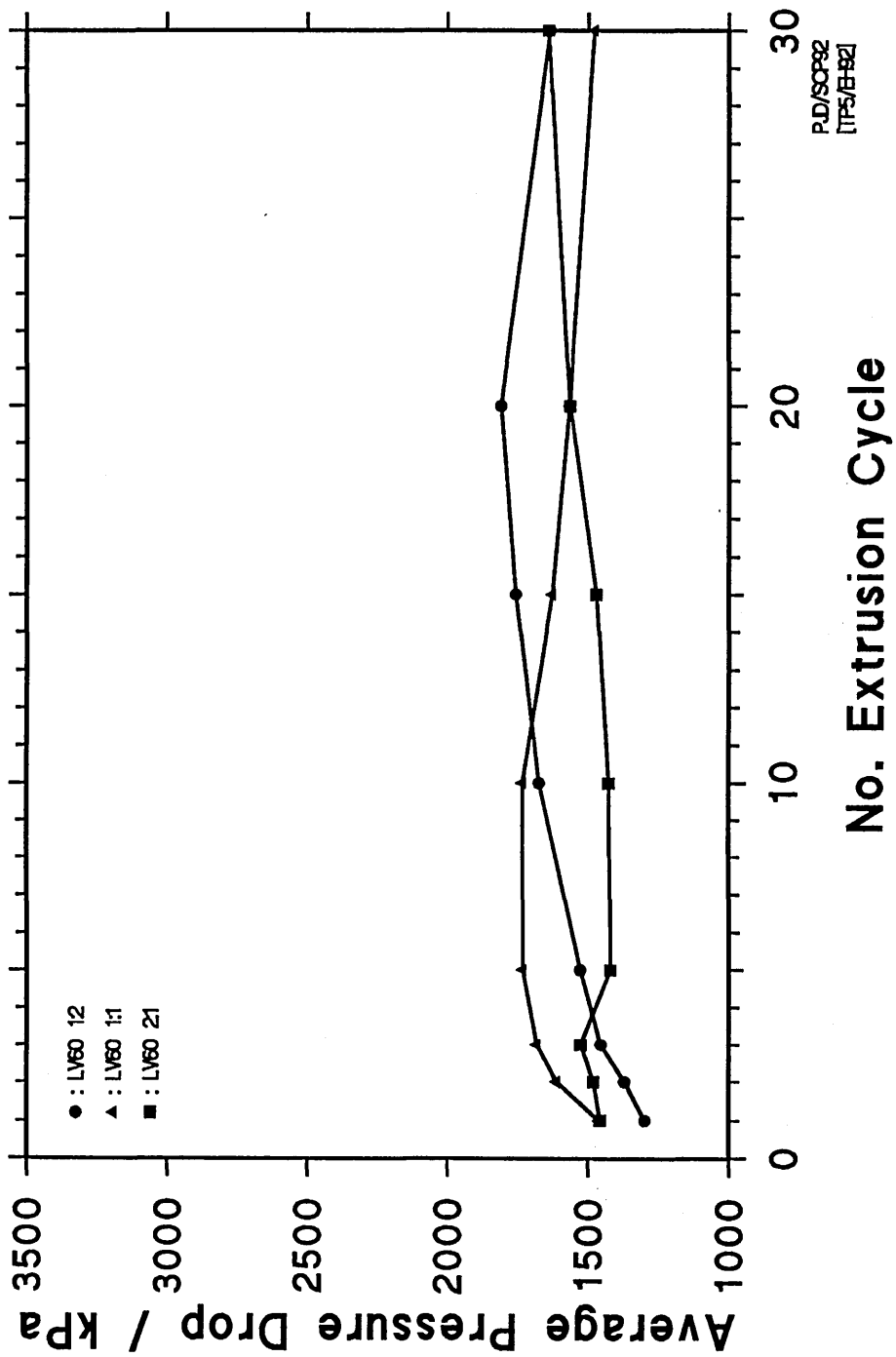
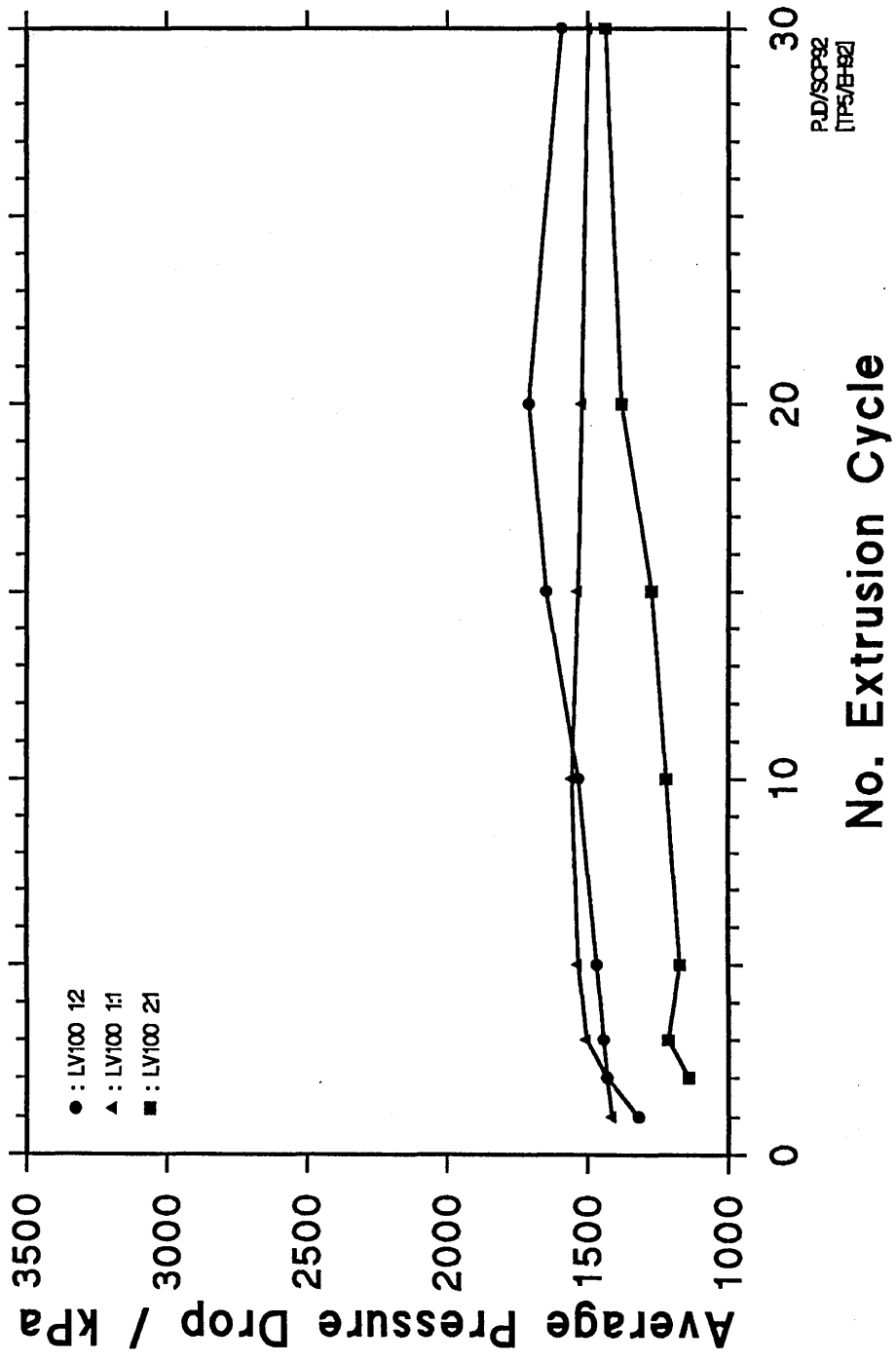


Figure 82 : The relationship between the number of extrusion cycles and the average pressure drops obtained in relation to all LV medium and 100 Mesh grit mixtures.



PJ/SCP82
[TP5/B-82]

No. Extrusion Cycle

Average Pressure Drop / kPa

● : LV100 12
▲ : LV100 11
■ : LV100 21

Figure 83 : The relationship between the number of extrusion cycles and the average pressure drops obtained in relation to all MV medium and 60 Mesh grit mixtures.

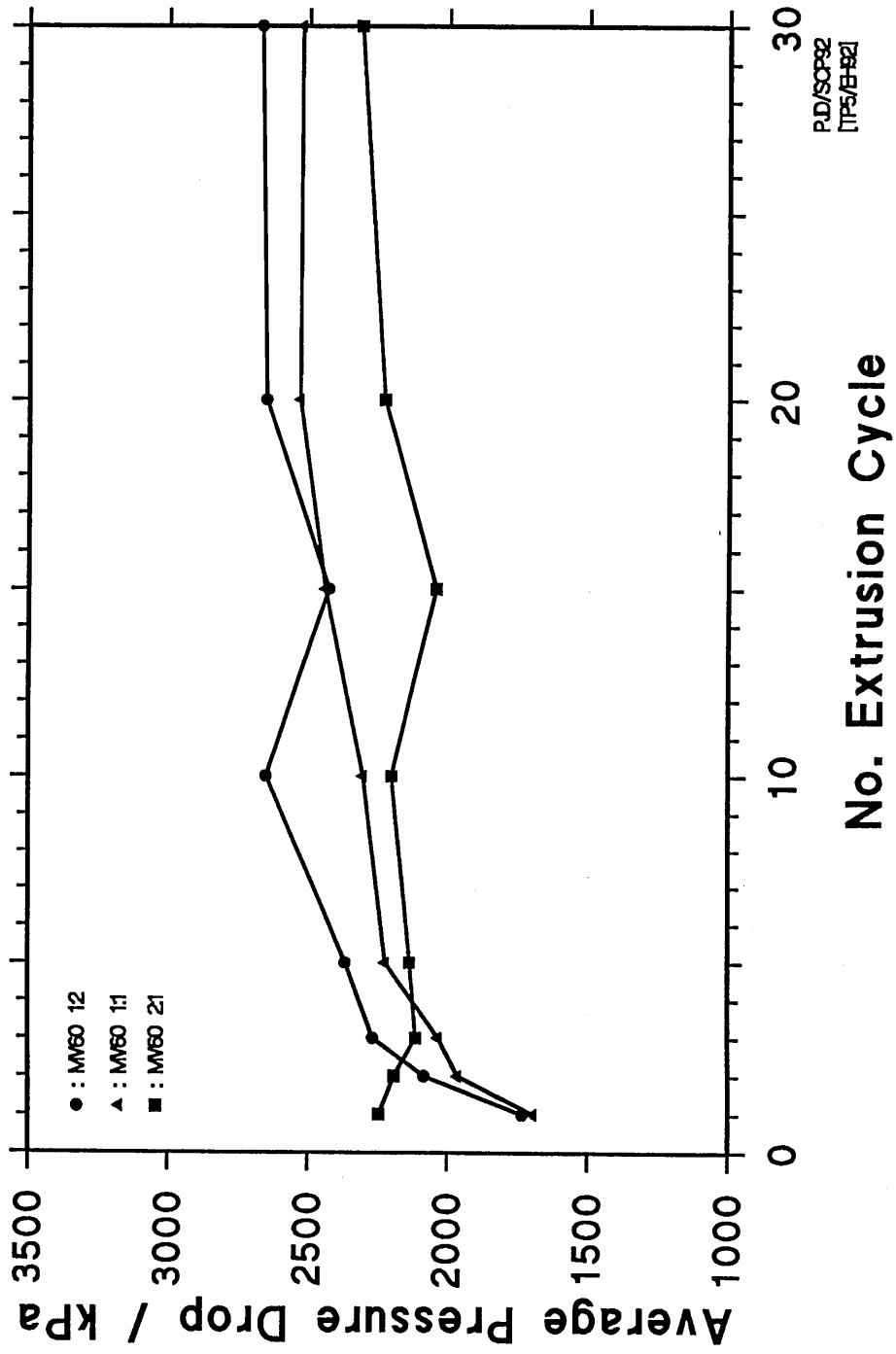


Figure 84 : The relationship between the number of extrusion cycles and the average pressure drops obtained in relation to all MV medium and 100 Mesh grit mixtures.

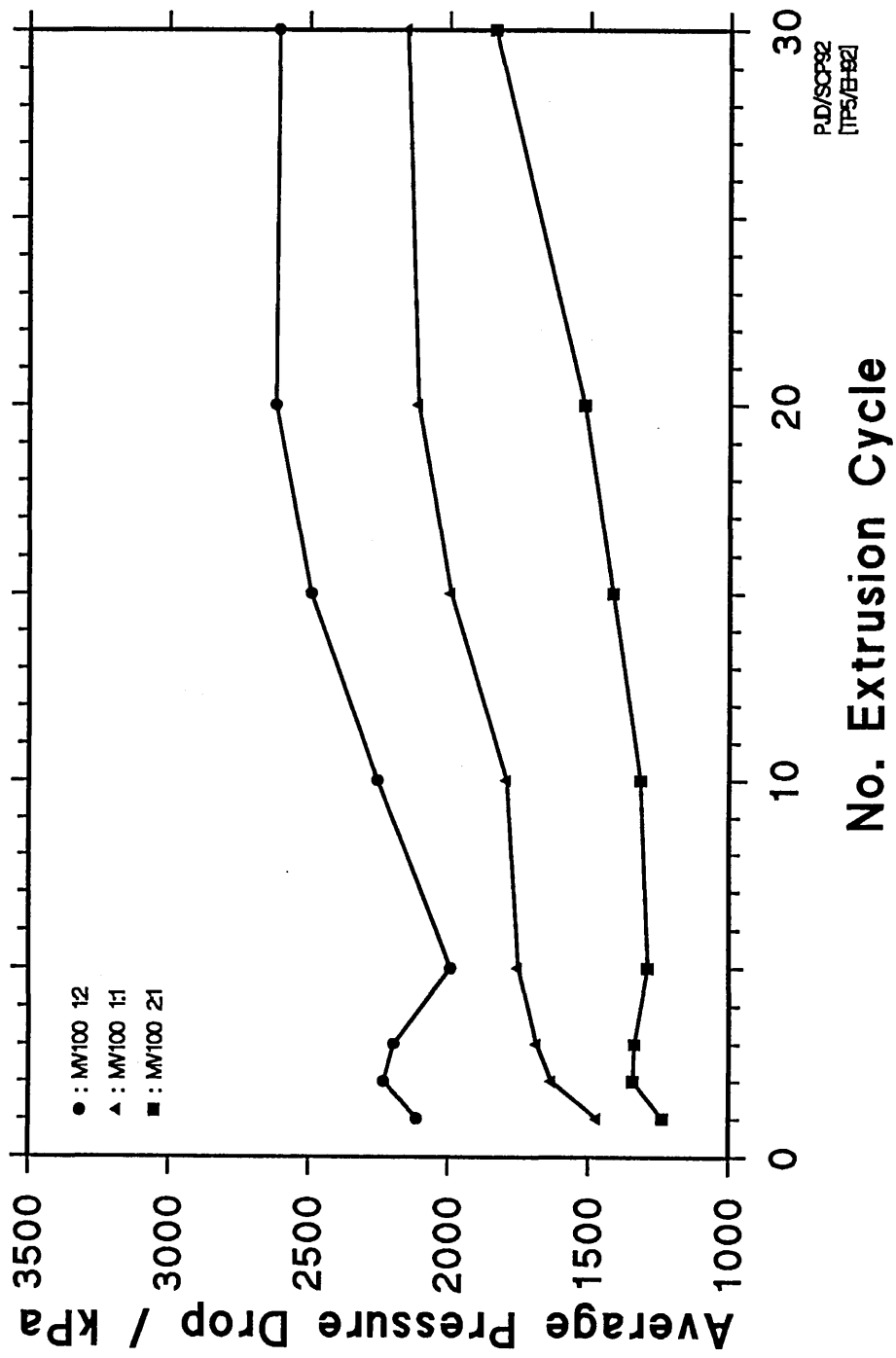


Figure 85 : The relationship between the number of extrusion cycles and the average pressure drops obtained in relation to all HV medium and 60 Mesh grit mixtures.

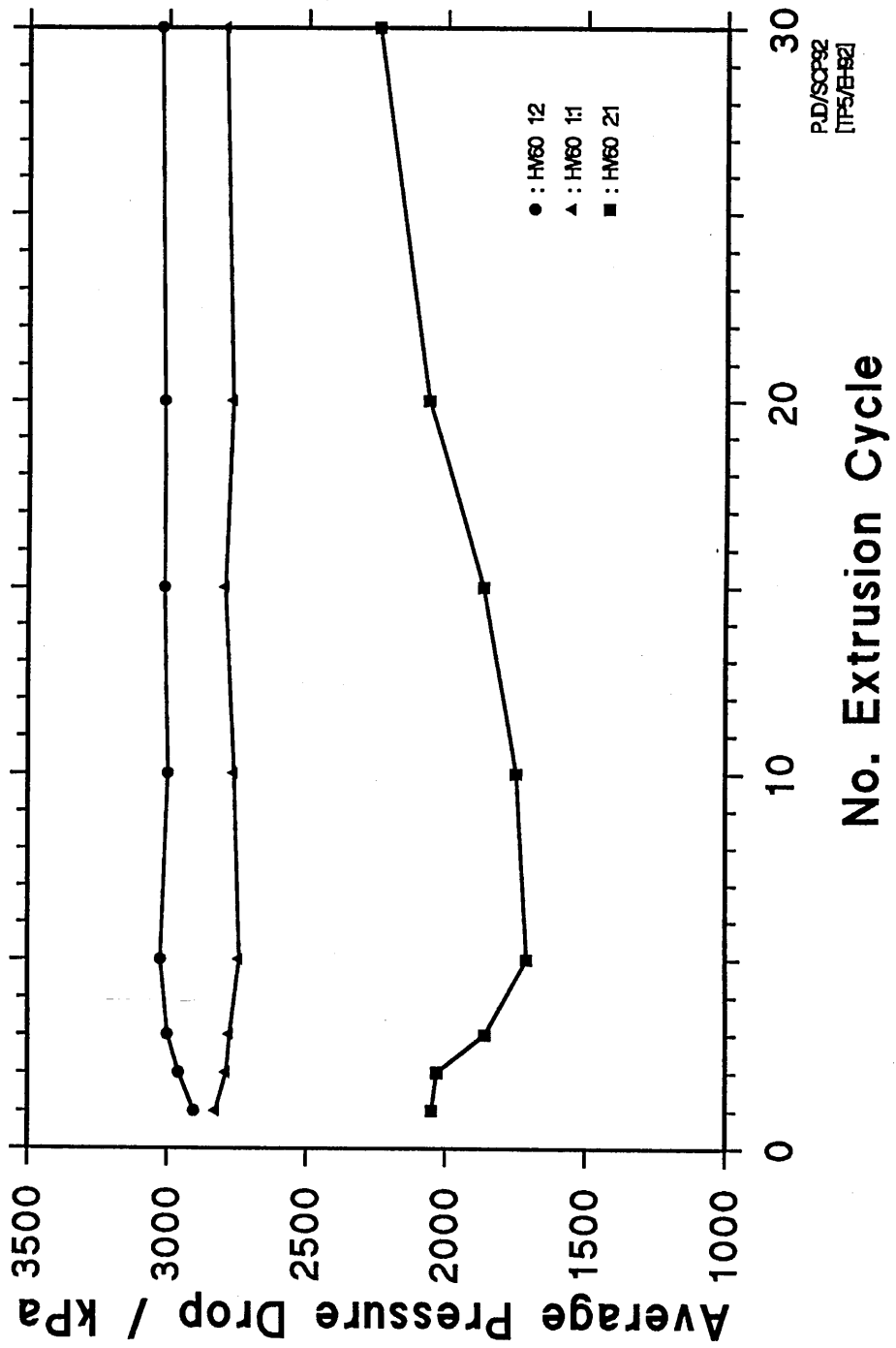


Figure 86 : The relationship between the number of extrusion cycles and the average pressure drops obtained in relation to all HV medium and 100 Mesh grit mixtures.

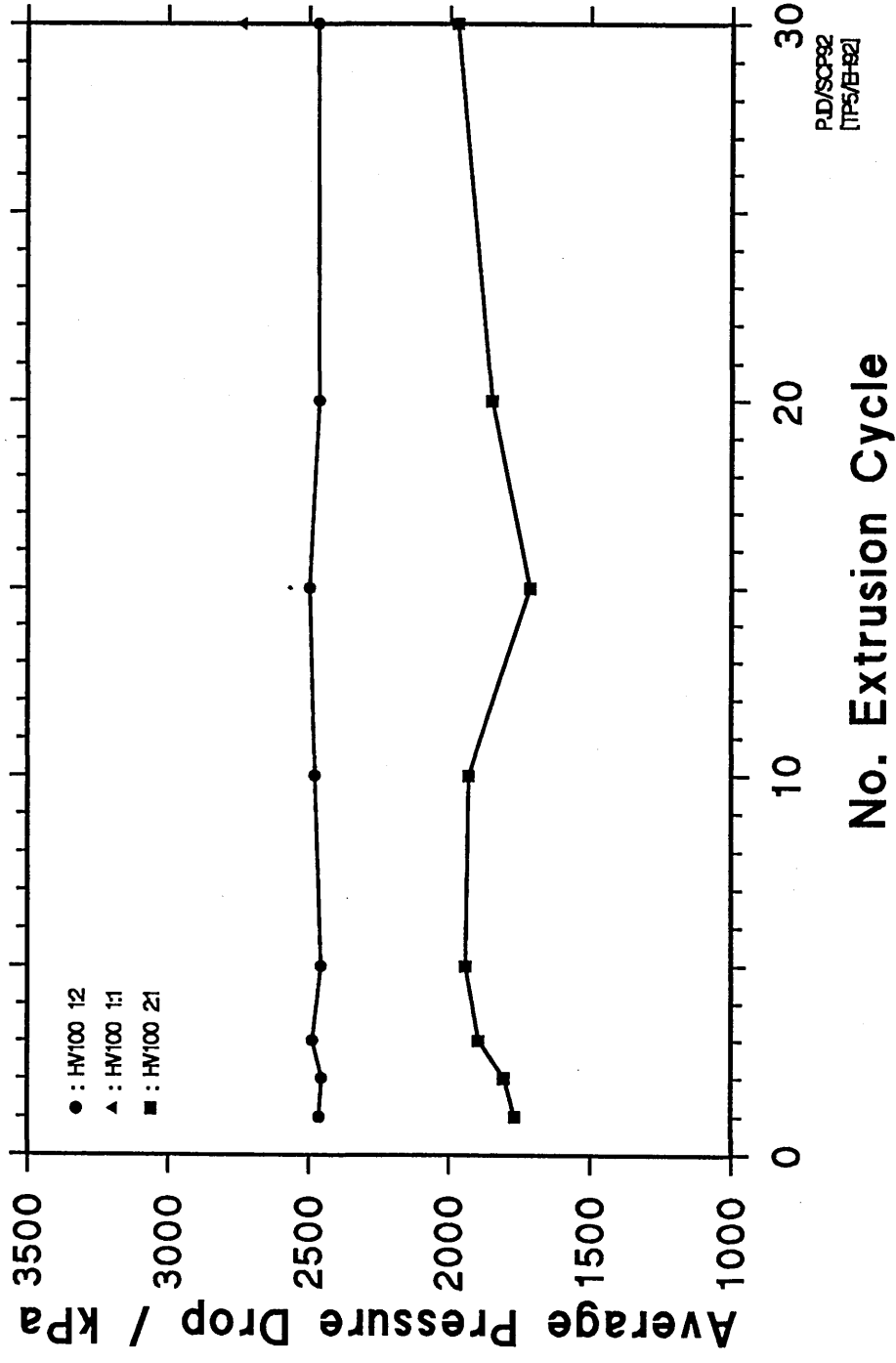
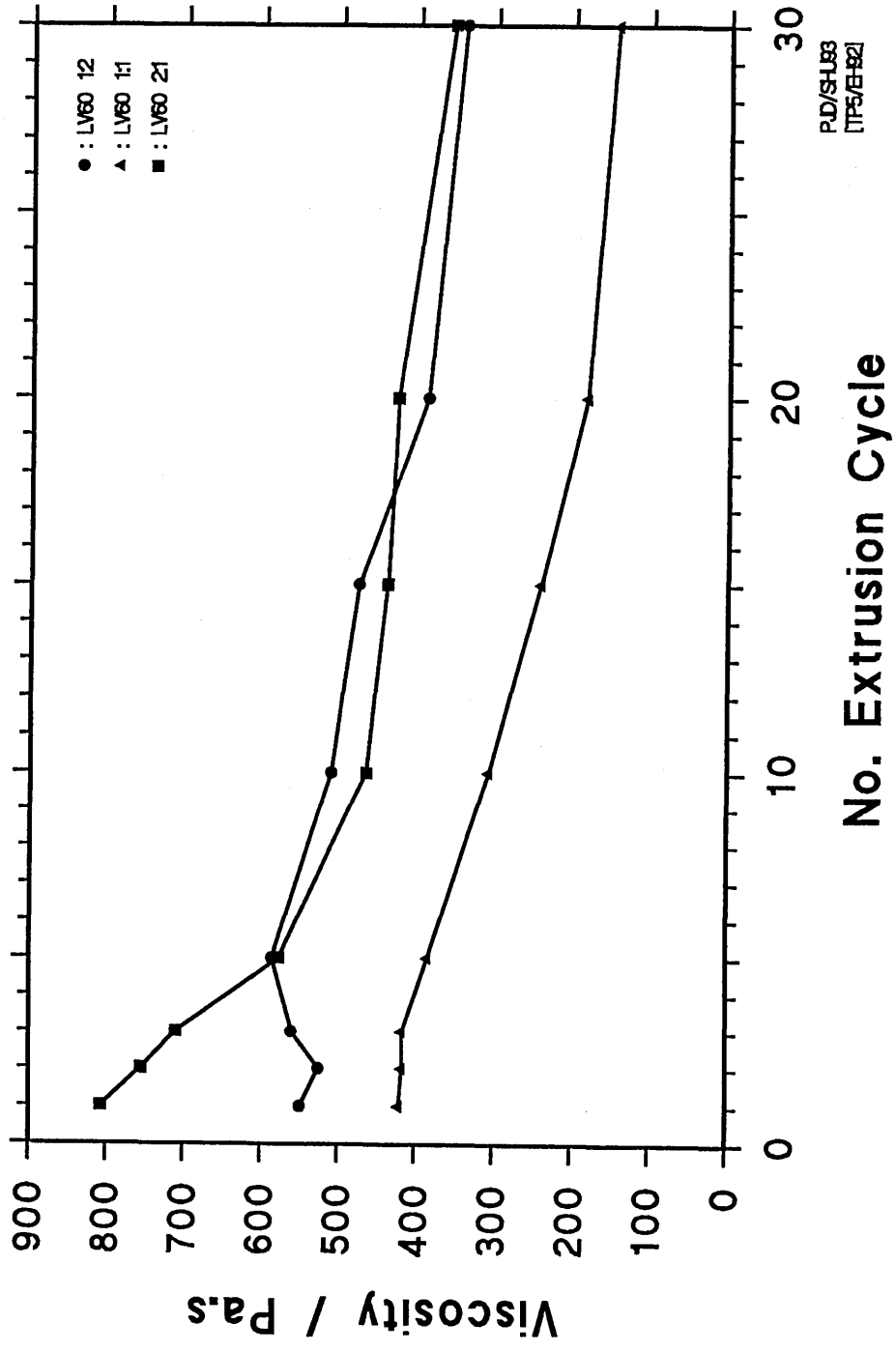


Figure 87 : The relationship between the number of extrusion cycles and the viscosity of the medium for all LV medium and 60 Mesh grit mixtures.



PJ/S/SHB3
[TFS/E/B2]

No. Extrusion Cycle

Figure 88 : The relationship between the number of extrusion cycles and the viscosity of the medium for all LV medium and 100 Mesh grit mixtures.

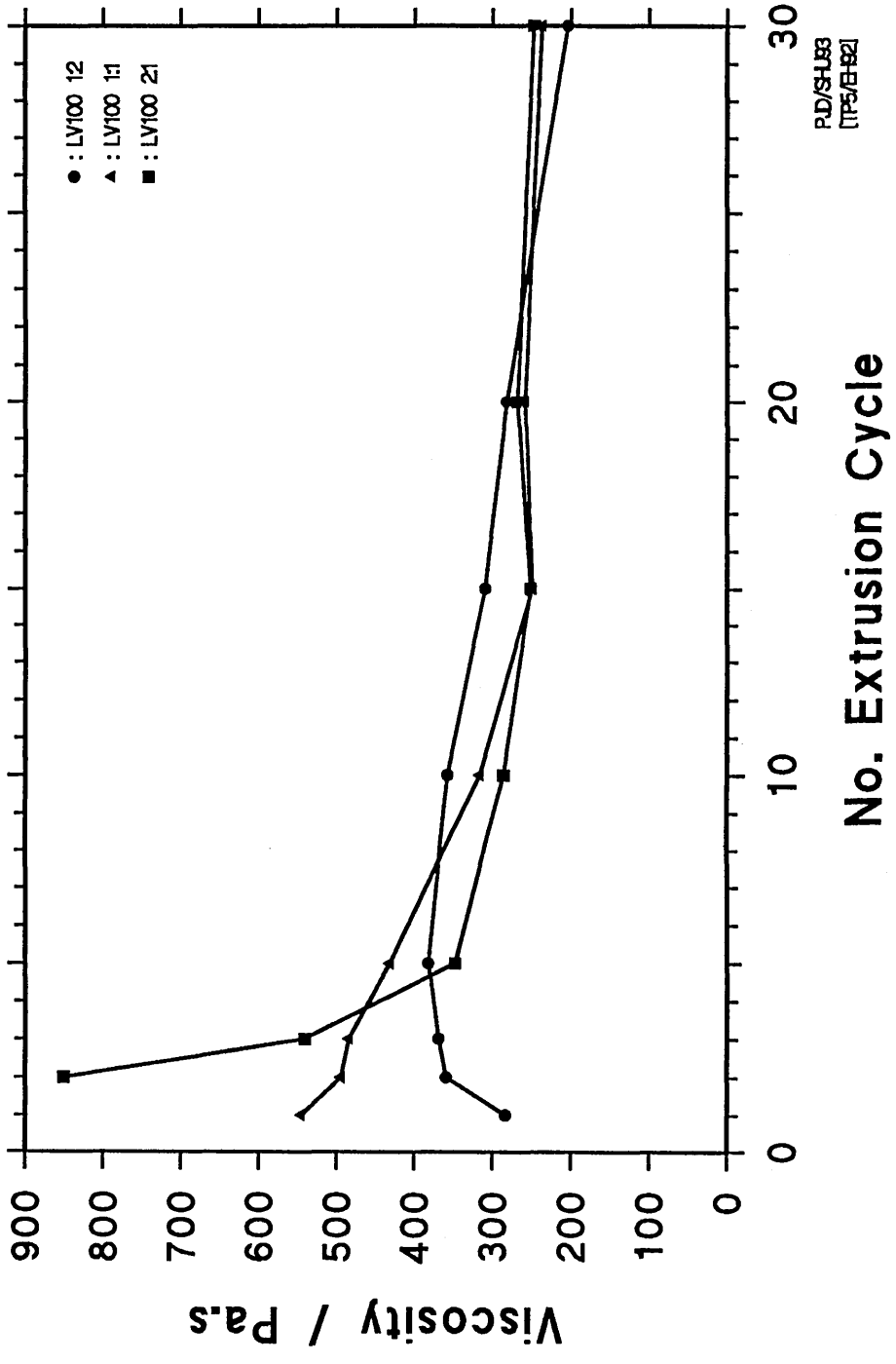


Figure 89 : The relationship between the number of extrusion cycles and the viscosity of the medium for all MV medium and 60 Mesh grit mixtures.

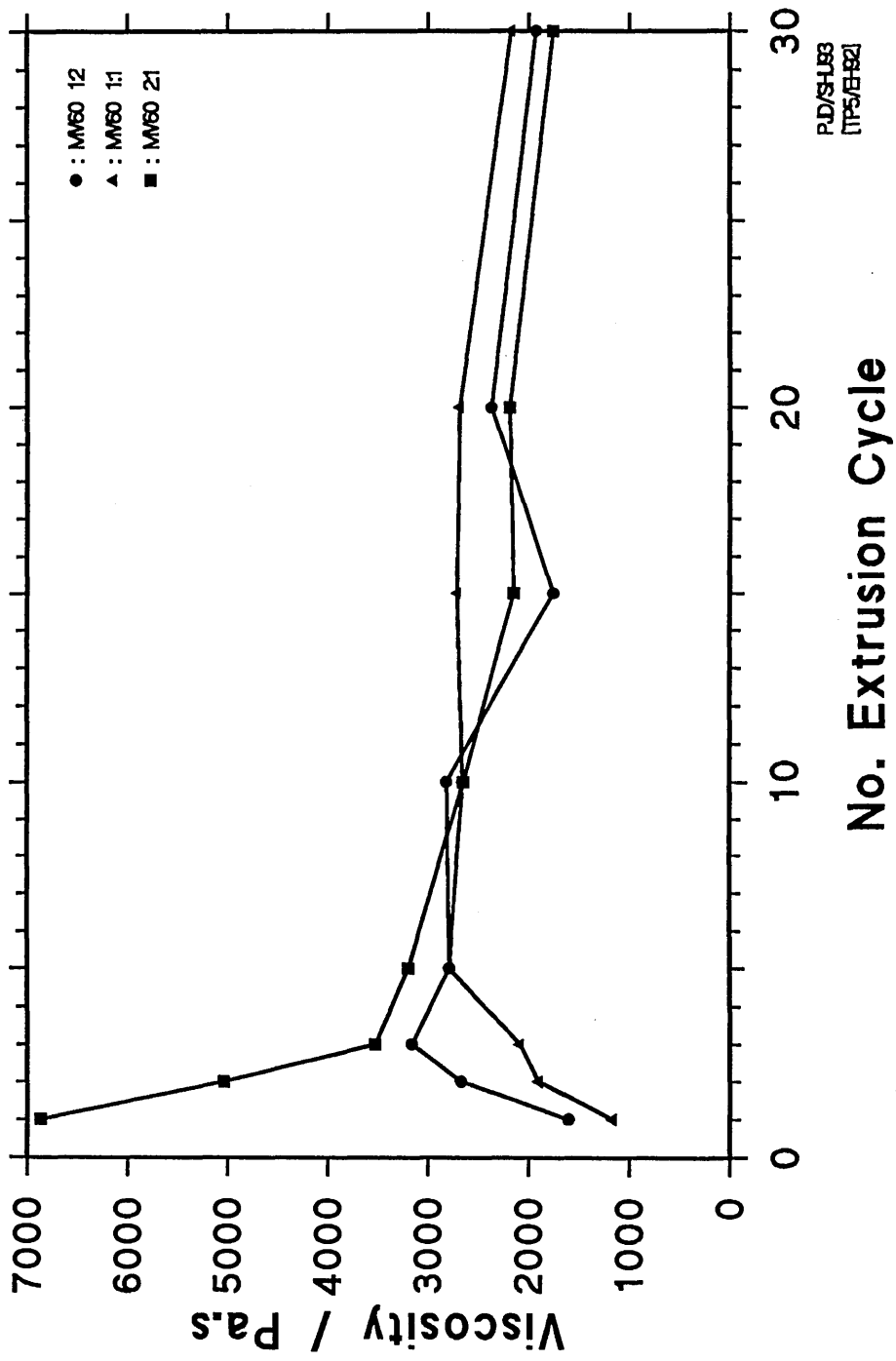


Figure 90 : The relationship between the number of extrusion cycles and the viscosity of the medium for all MV medium and 100 Mesh grit mixtures.

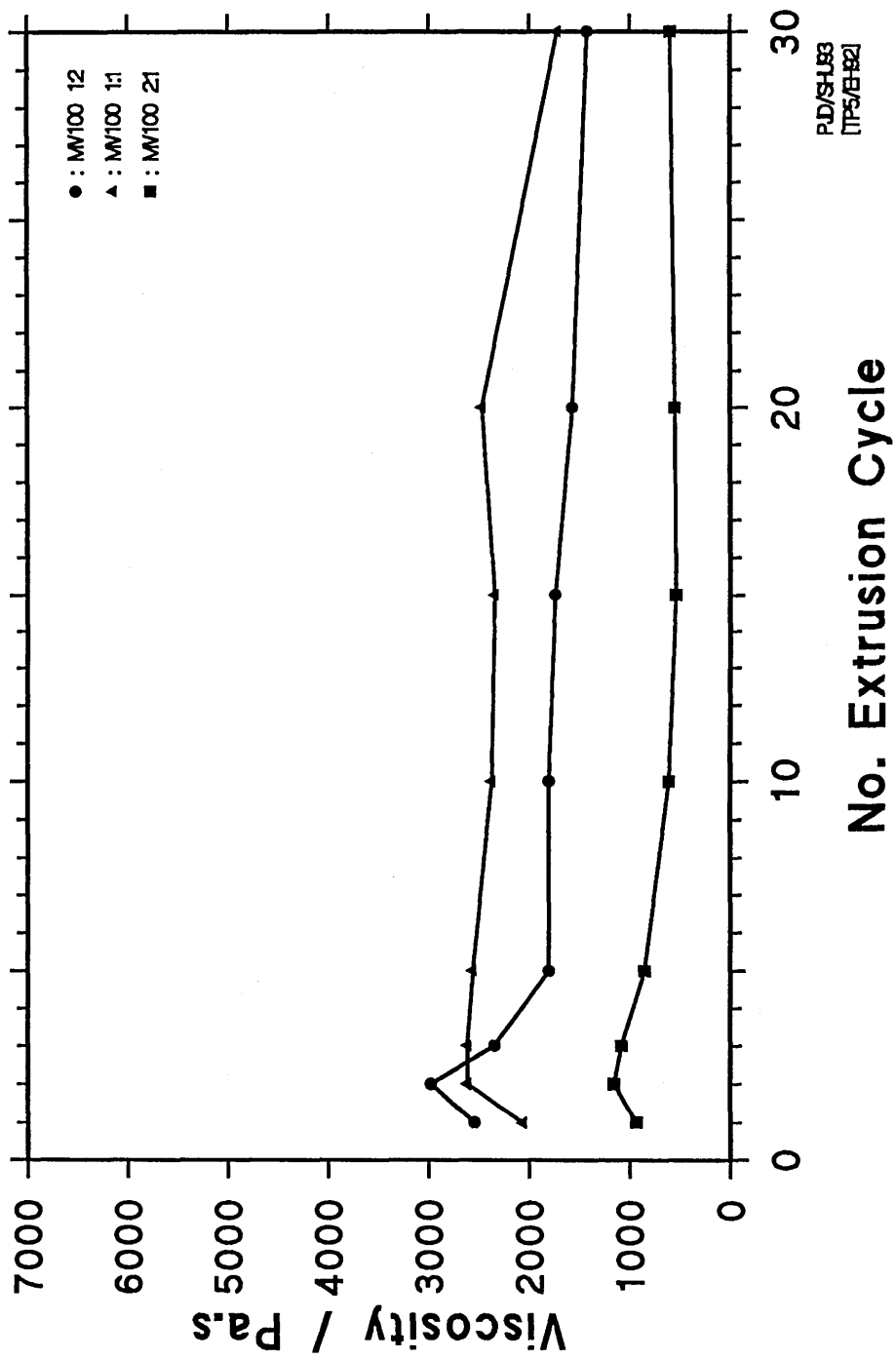
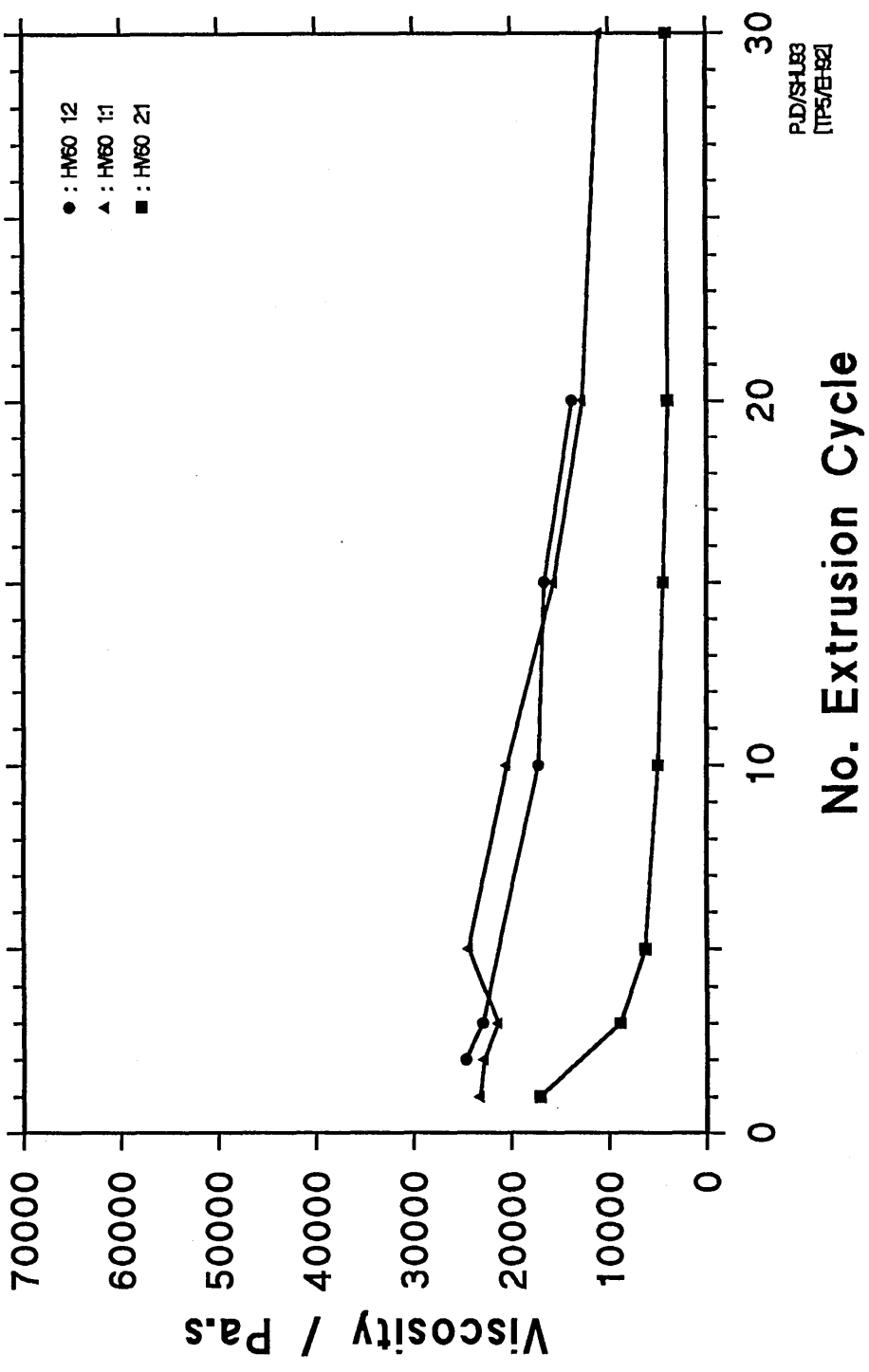


Figure 91 : The relationship between the number of extrusion cycles and the viscosity of the medium for all HV medium and 60 Mesh grit mixtures.



P.D./S.H.03
[TP5/E-92]

No. Extrusion Cycle

Figure 92 : The relationship between the number of extrusion cycles and the viscosity of the medium for all HV medium and 100 Mesh grit mixtures.

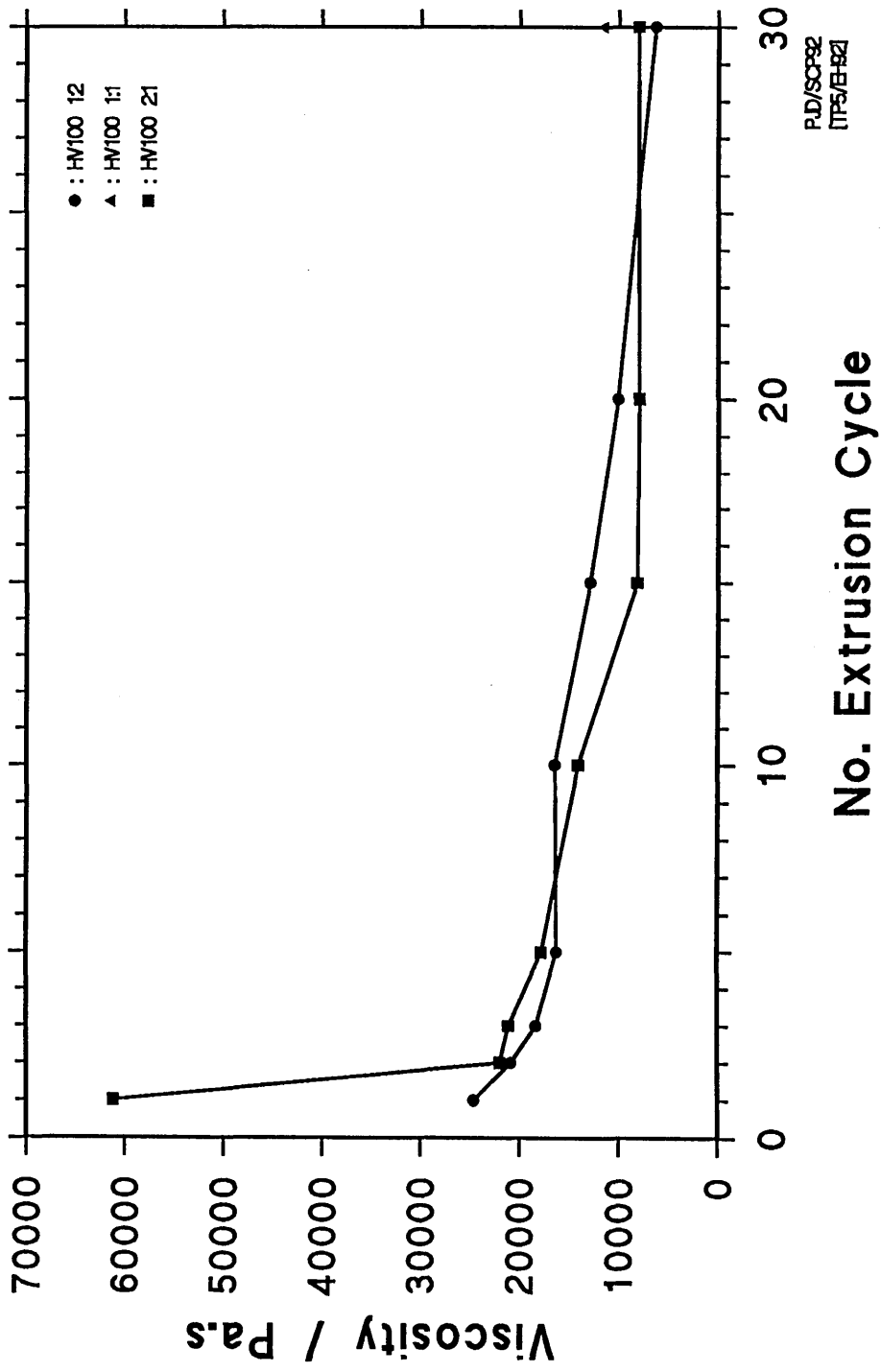


Figure 93(a) : The relationship between processing time and temperature of the pure LV medium.

Figure 93(b) : The relationship between processing time and temperature of the pure MV medium.

Figure 93(c) : The relationship between processing time and temperature of the pure HV medium.

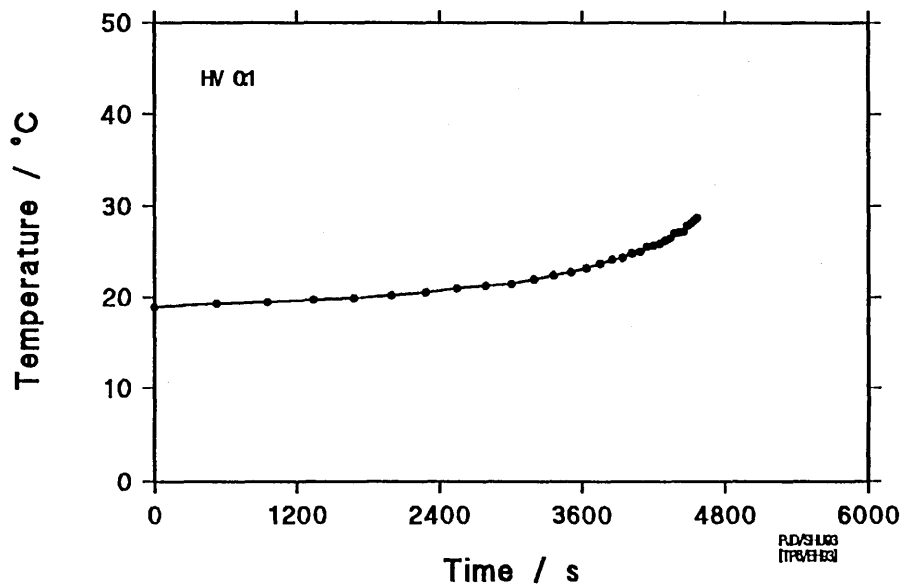
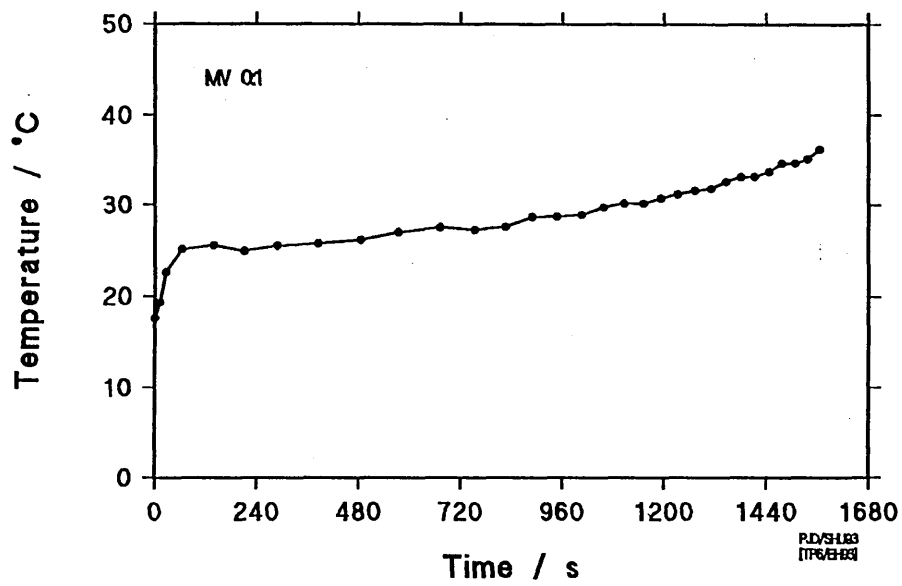
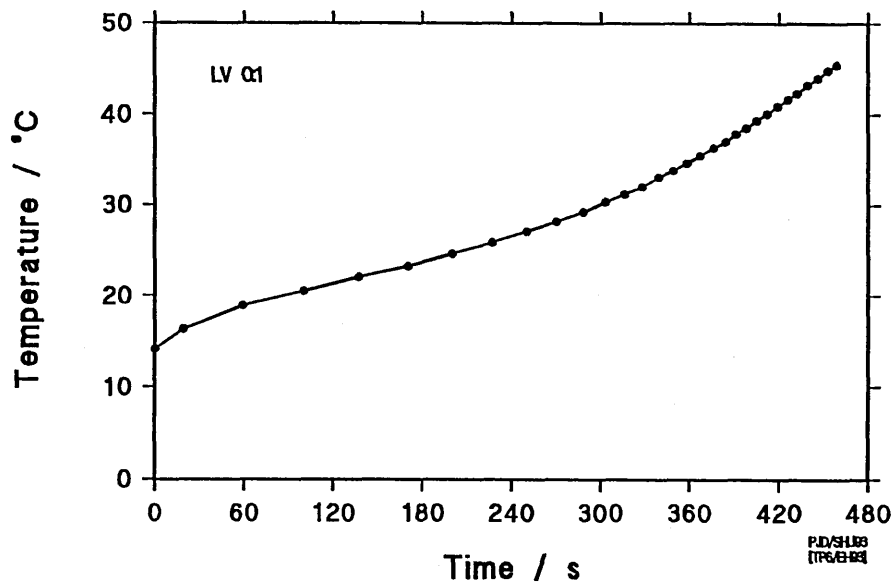


Figure 94(a) : The relationship between processing time and temperature for all runs conducted using LV medium and 60 Mesh grit with a grit to polymer ratio of 0.5.

Figure 94(b) : The relationship between processing time and temperature for all runs conducted using LV medium and 60 Mesh grit with a grit to polymer ratio of 1.

Figure 94(c) : The relationship between processing time and temperature for all runs conducted using LV medium and 60 Mesh grit with a grit to polymer ratio of 2.

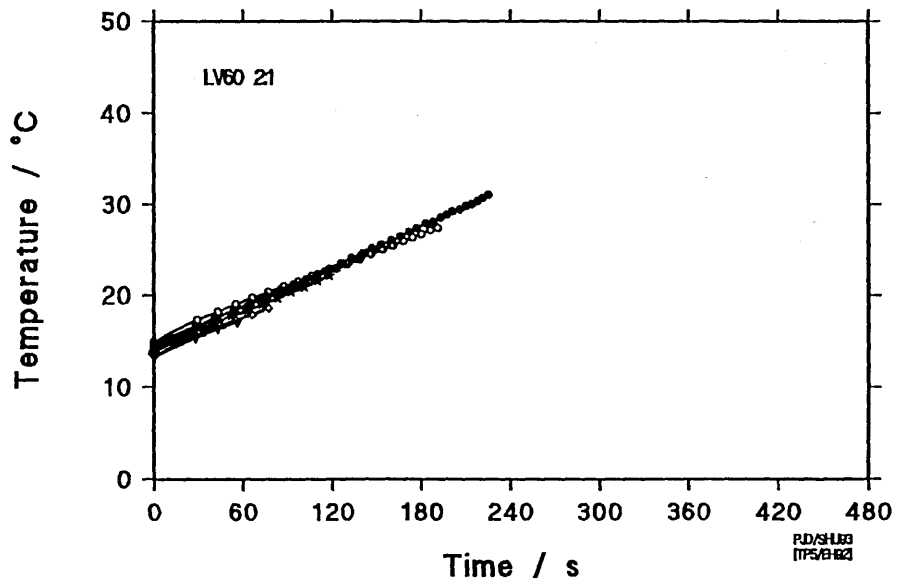
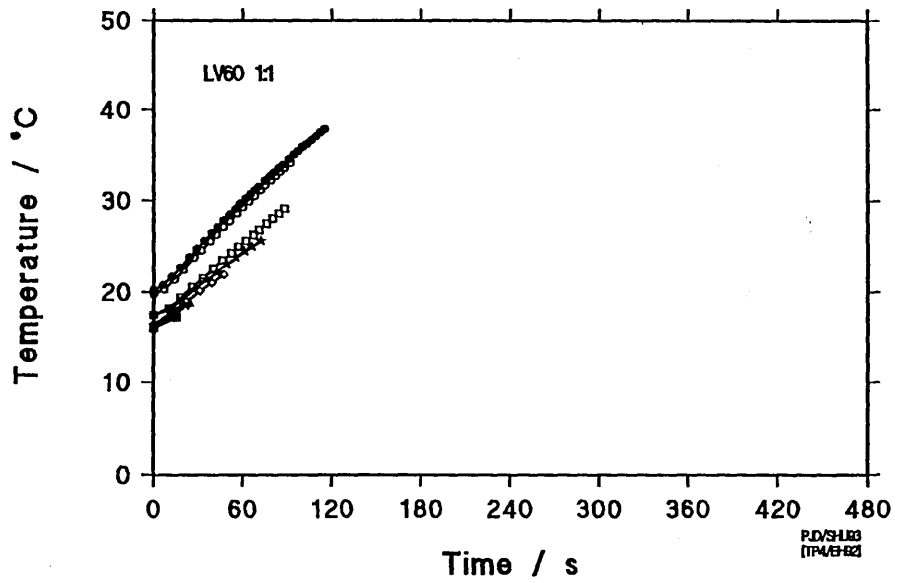
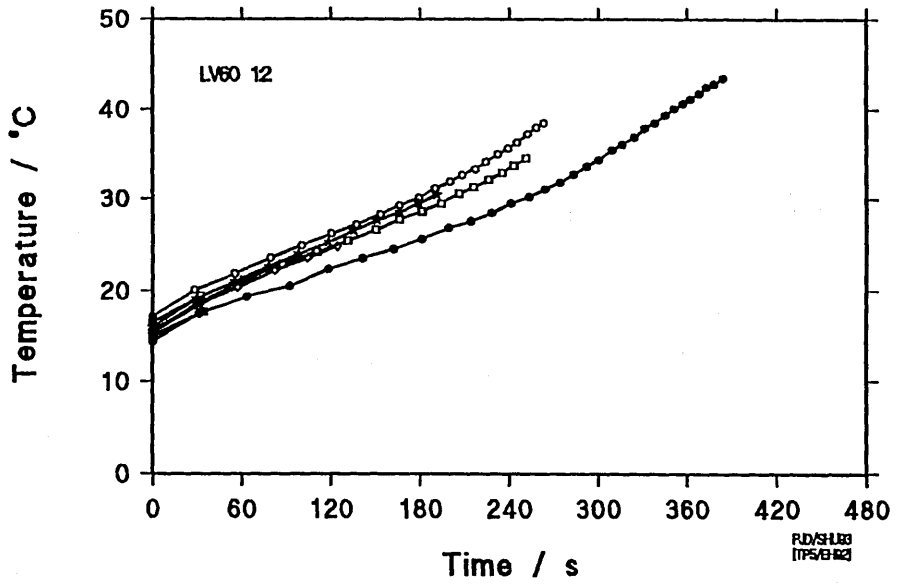


Figure 95(a) : The relationship between processing time and temperature for all runs conducted using LV medium and 100 Mesh grit with a grit to polymer ratio of 0.5.

Figure 95(b) : The relationship between processing time and temperature for all runs conducted using LV medium and 100 Mesh grit with a grit to polymer ratio of 1.

Figure 95(c) : The relationship between processing time and temperature for all runs conducted using LV medium and 100 Mesh grit with a grit to polymer ratio of 2.

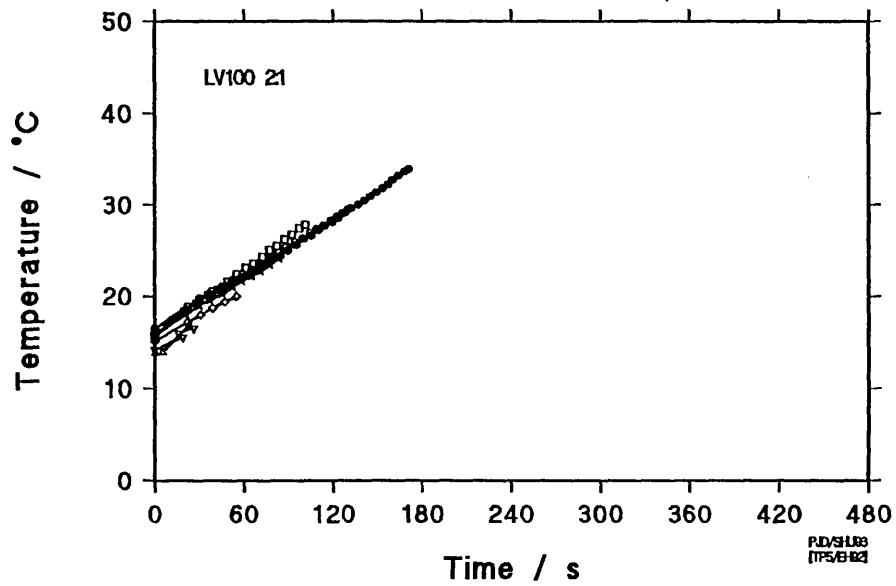
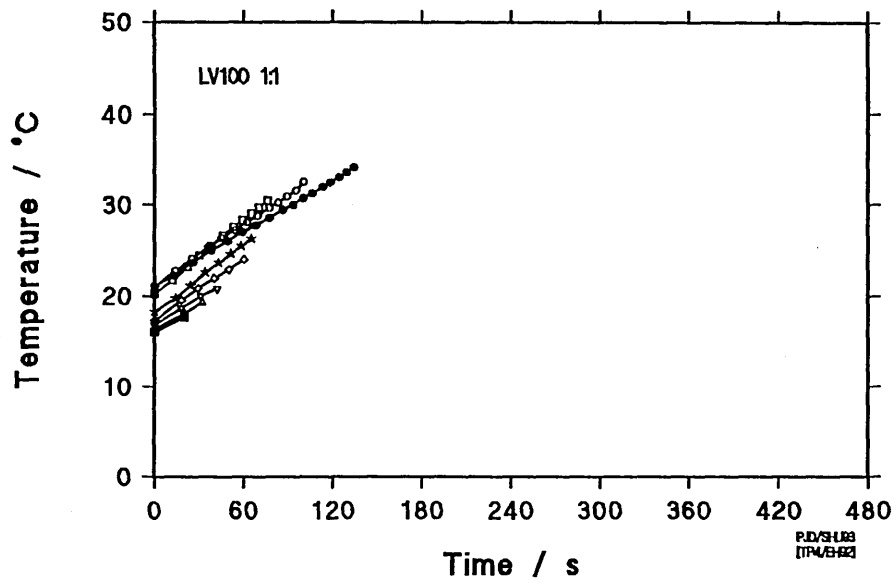
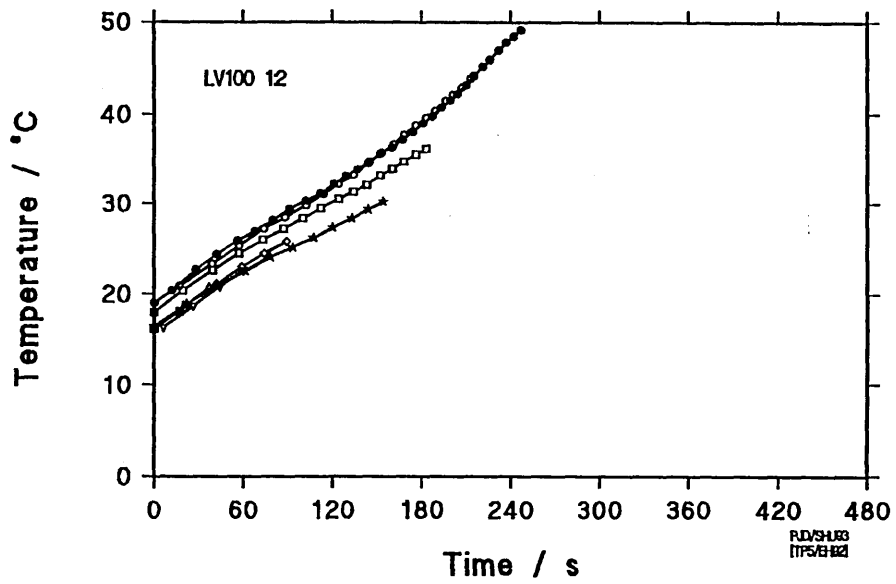


Figure 96(a) : The relationship between processing time and temperature for all runs conducted using MV medium and 60 Mesh grit with a grit to polymer ratio of 0.5.

Figure 96(b) : The relationship between processing time and temperature for all runs conducted using MV medium and 60 Mesh grit with a grit to polymer ratio of 1.

Figure 96(c) : The relationship between processing time and temperature for all runs conducted using MV medium and 60 Mesh grit with a grit to polymer ratio of 2.

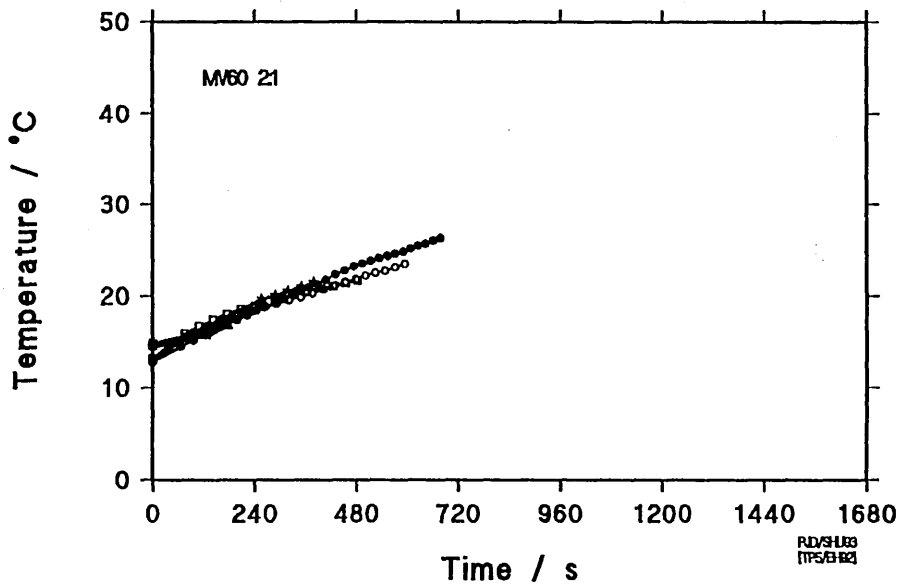
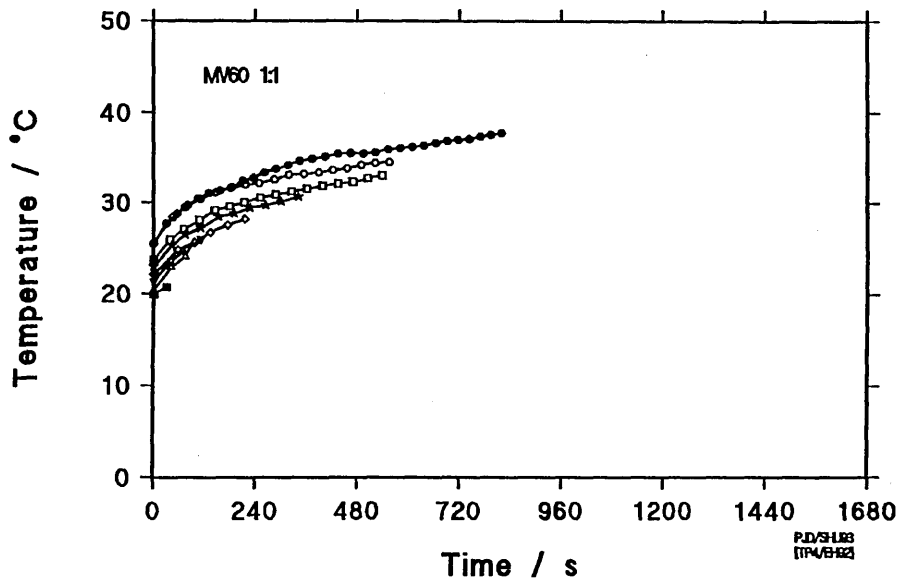
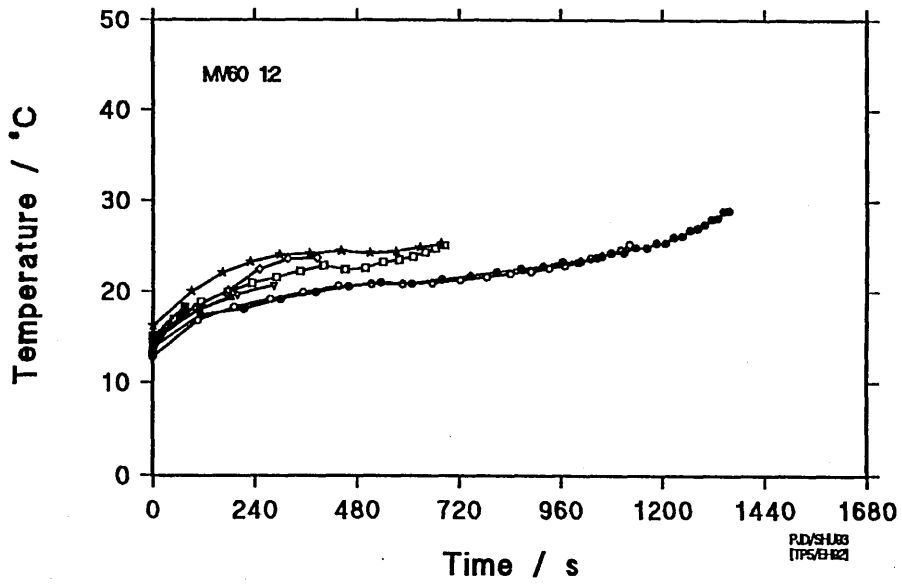


Figure 97(a) : The relationship between processing time and temperature for all runs conducted using MV medium and 100 Mesh grit with a grit to polymer ratio of 0.5.

Figure 97(b) : The relationship between processing time and temperature for all runs conducted using MV medium and 100 Mesh grit with a grit to polymer ratio of 1.

Figure 97(c) : The relationship between processing time and temperature for all runs conducted using MV medium and 100 Mesh grit with a grit to polymer ratio of 2.

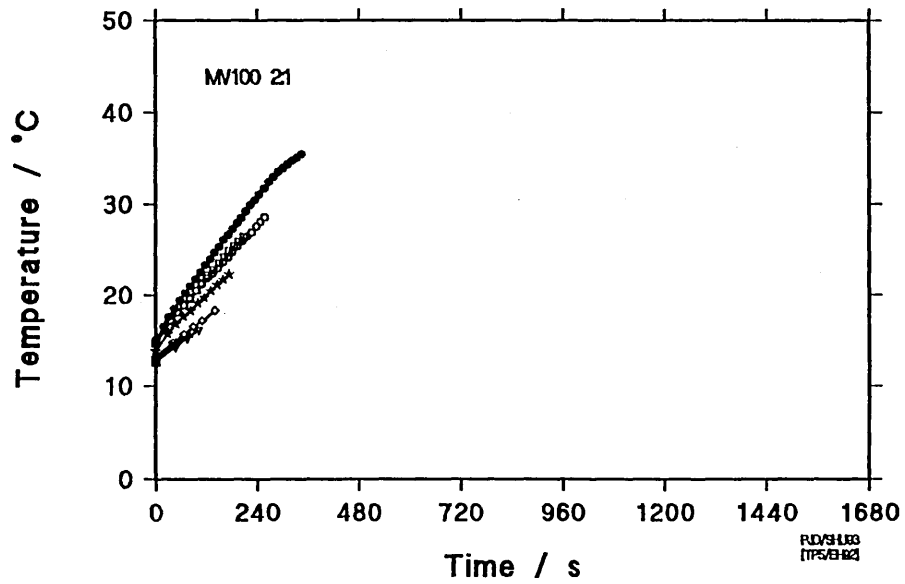
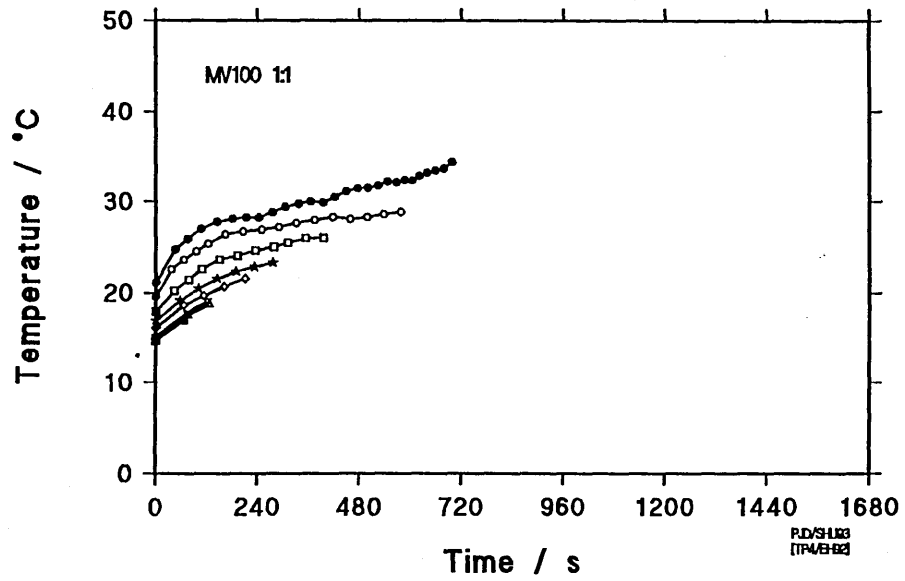
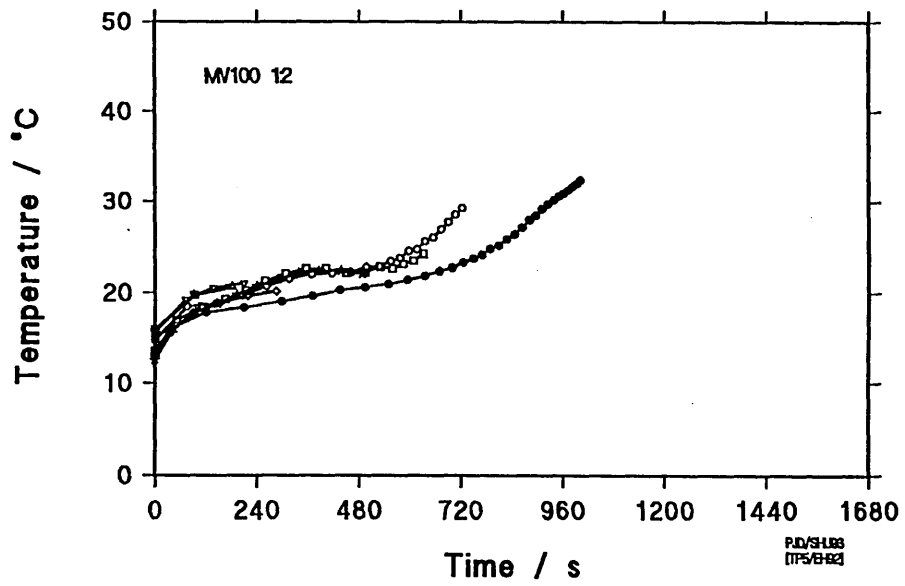


Figure 98(a) : The relationship between processing time and temperature for all runs conducted using HV medium and 60 Mesh grit with a grit to polymer ratio of 0.5.

Figure 98(b) : The relationship between processing time and temperature for all runs conducted using HV medium and 60 Mesh grit with a grit to polymer ratio of 1.

Figure 98(c) : The relationship between processing time and temperature for all runs conducted using HV medium and 60 Mesh grit with a grit to polymer ratio of 2.

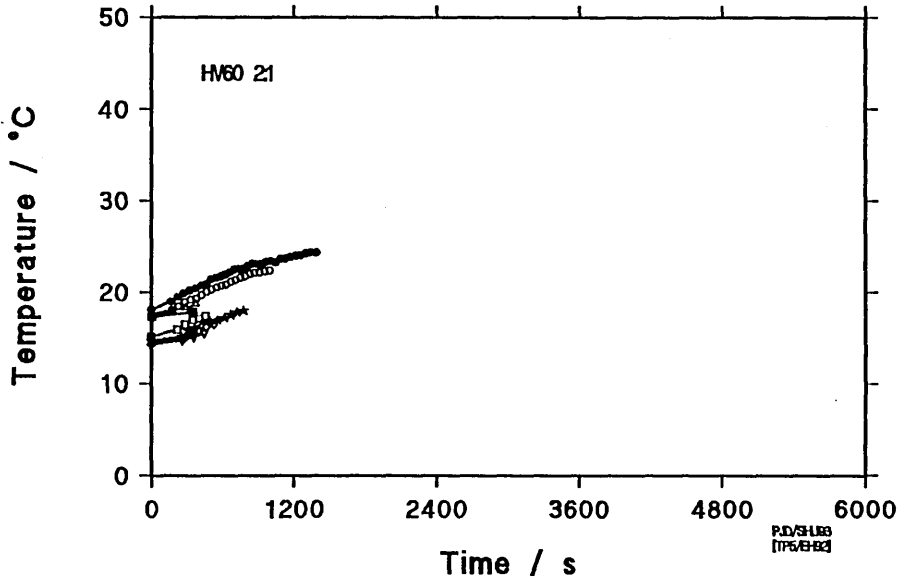
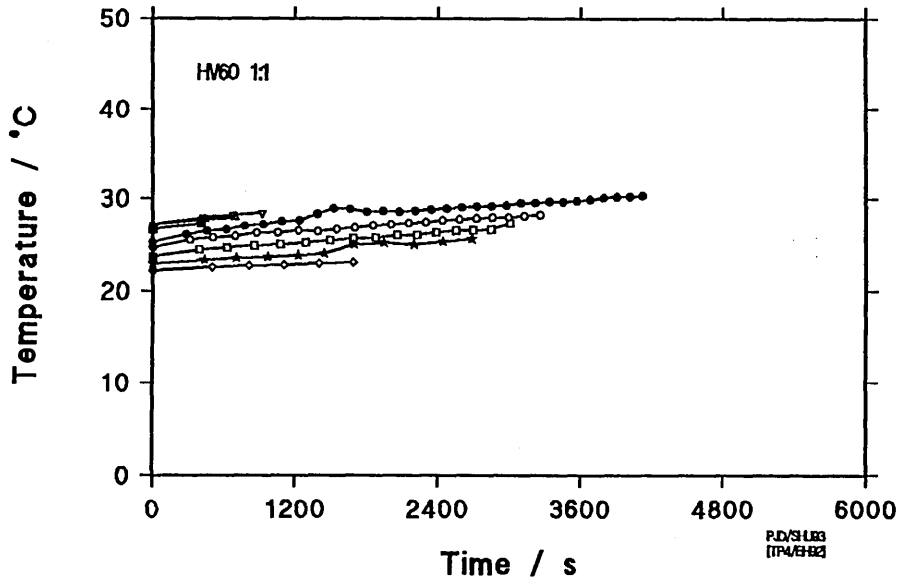
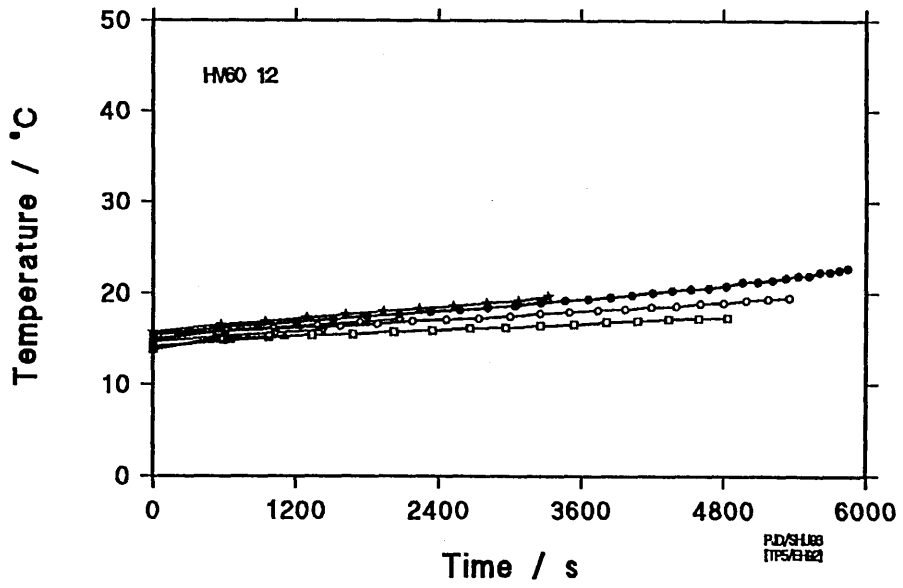


Figure 99(a) : The relationship between processing time and temperature for all runs conducted using HV medium and 100 Mesh grit with a grit to polymer ratio of 0.5.

Figure 99(b) : The relationship between processing time and temperature for all runs conducted using HV medium and 100 Mesh grit with a grit to polymer ratio of 1.

Figure 99(c) : The relationship between processing time and temperature for all runs conducted using HV medium and 100 Mesh grit with a grit to polymer ratio of 2.

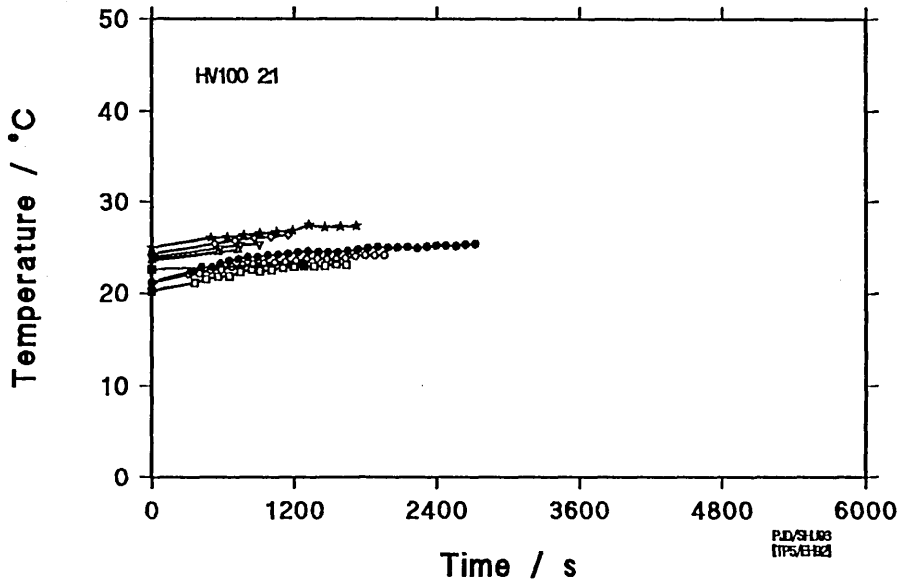
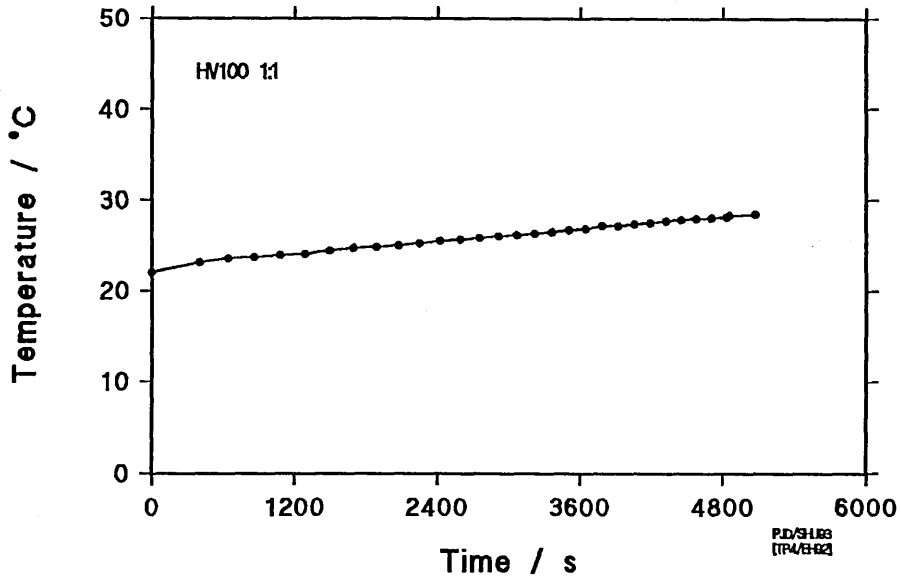
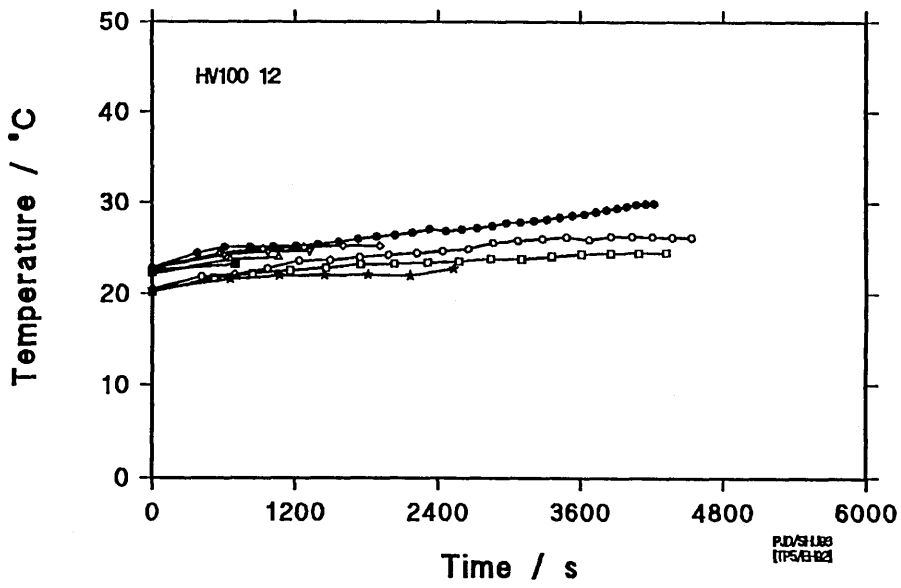


Figure 100(a) : The relationship between the number of extrusion cycles and the pressure drop across the die for all runs completed on day 1 (23/11/92) using LV medium and 60 Mesh grit with a grit to polymer ratio of 0.5.

Figure 100(b) : The relationship between the number of extrusion cycles and the pressure drop across the die for all runs completed on day 2 (24/11/92) using LV medium and 60 Mesh grit with a grit to polymer ratio of 0.5.

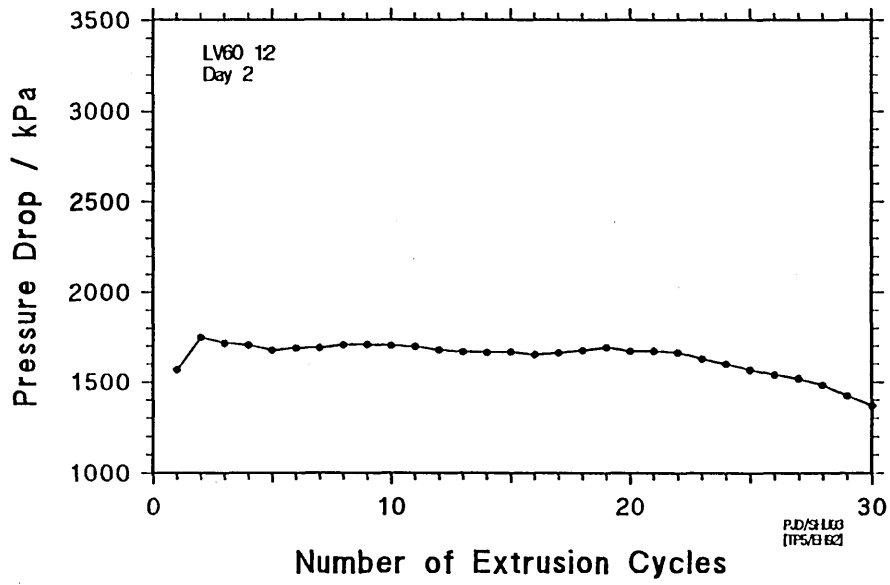
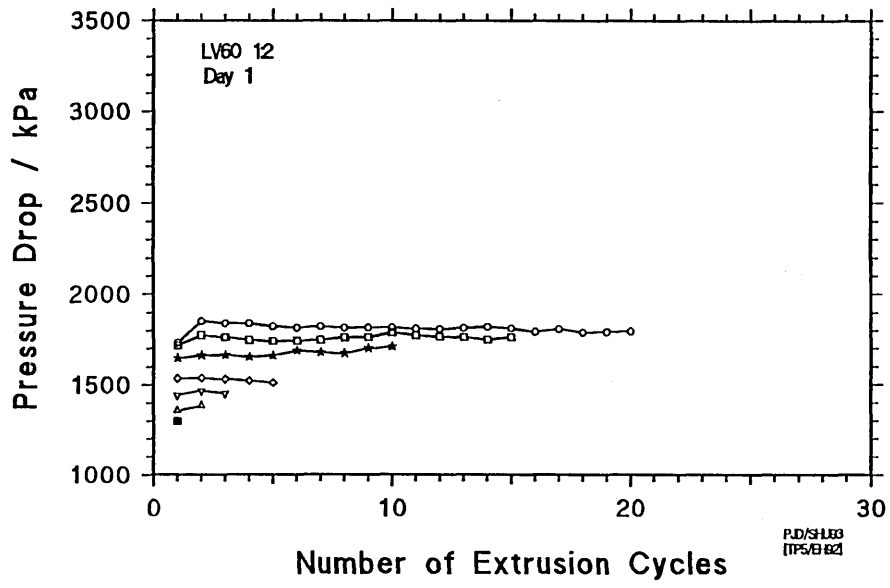


Figure 101(a) : The relationship between the number of extrusion cycles and the pressure drop across the die for all runs completed on day 1 (24/11/92) using MV medium and 60 Mesh grit with a grit to polymer ratio of 0.5.

Figure 101(b) : The relationship between the number of extrusion cycles and the pressure drop across the die for all runs completed on day 2 (25/11/92) using MV medium and 60 Mesh grit with a grit to polymer ratio of 0.5.

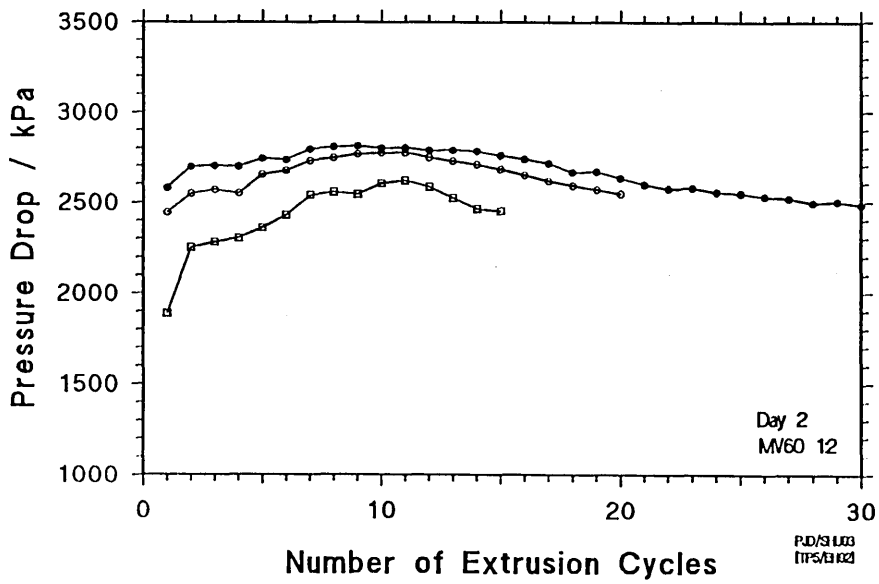
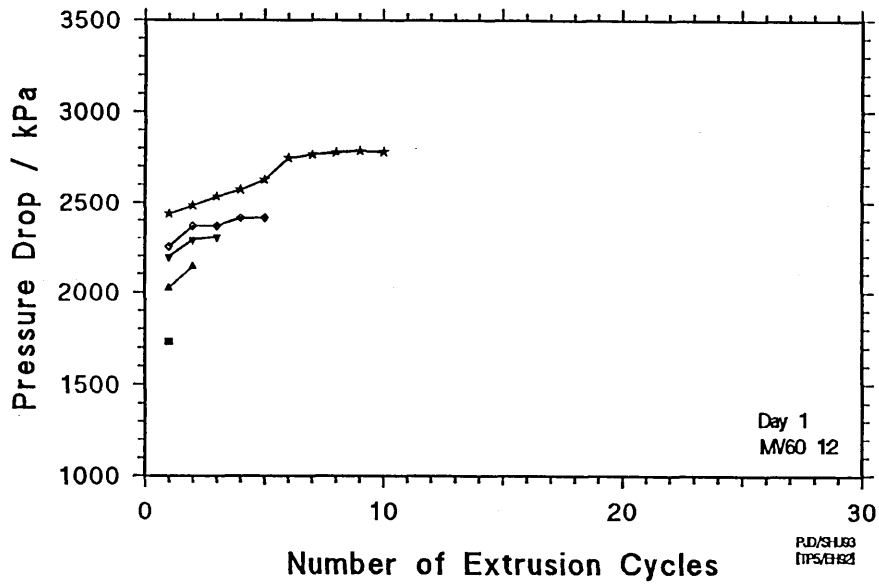


Figure 102(a) : The relationship between the number of extrusion cycles and the pressure drop across the die for all runs completed on day 1 (15/12/92) using HV medium and 60 Mesh grit with a grit to polymer ratio of 2.

Figure 102(b) : The relationship between the number of extrusion cycles and the pressure drop across the die for all runs completed on day 2 (16/12/92) using HV medium and 60 Mesh grit with a grit to polymer ratio of 2.

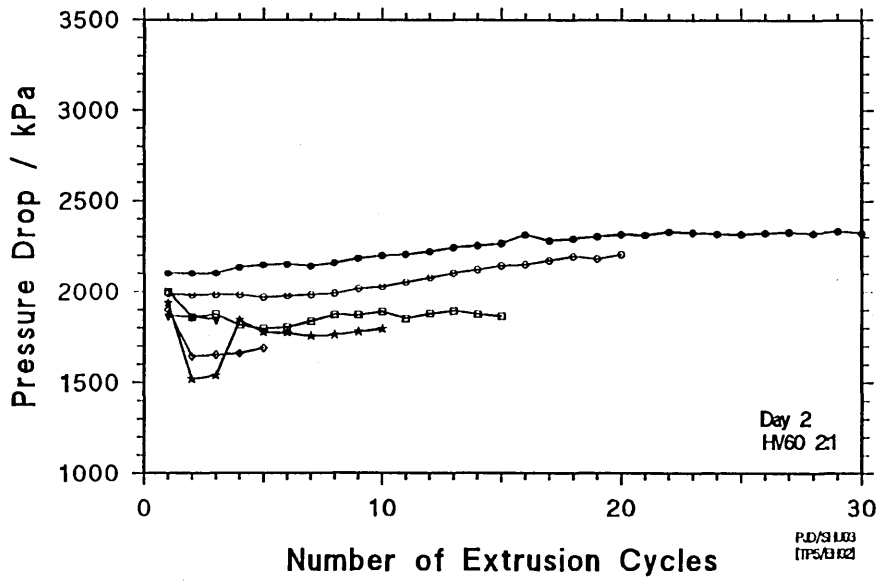
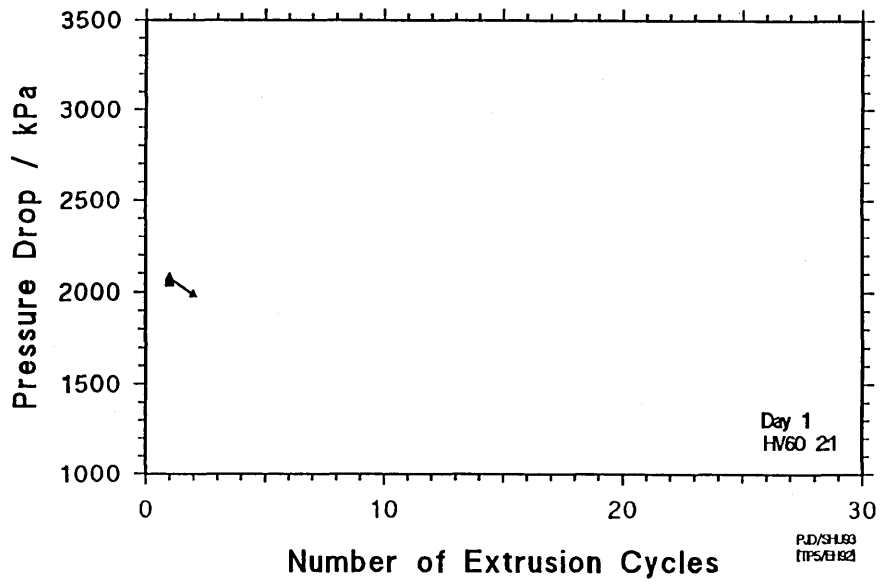


Figure 103(a) : The relationship between the increase in the number of extrusion cycles and the decrease in the rate of pressure drop increase for all runs completed on day 1 (03/11/92) using MV medium and 100 Mesh grit with a grit to polymer ratio of 0.5.

Figure 103(b) : The relationship between the increase in the number of extrusion cycles and the decrease in the rate of pressure drop increase for all runs completed on day 2 (04/11/92) using MV medium and 100 Mesh grit with a grit to polymer ratio of 0.5.

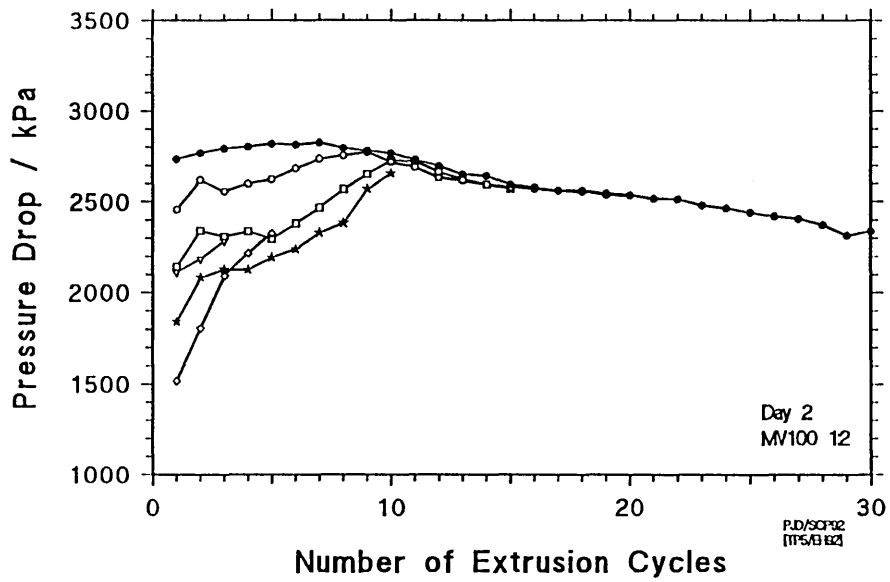
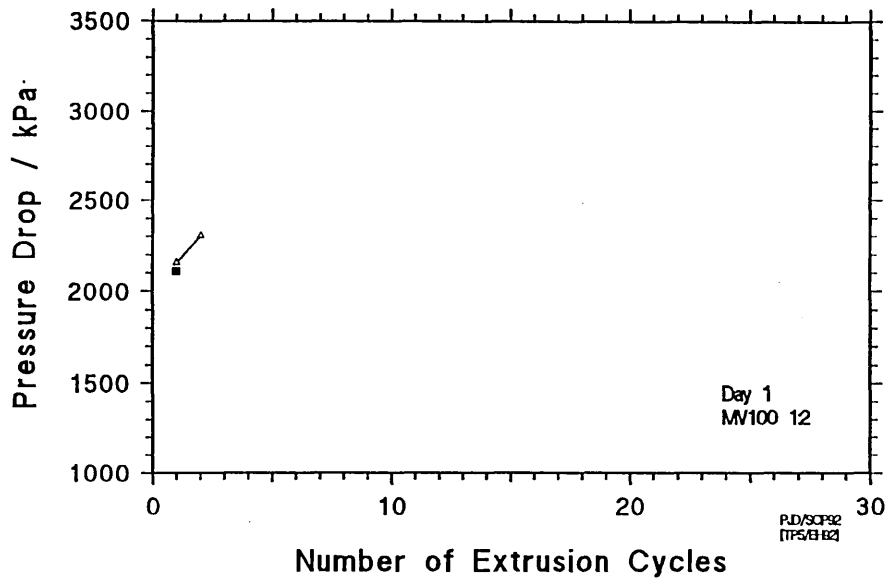


Figure 104(a) : The relationship between log shear rate and log shear stress obtained using LV medium and 60 Mesh grit with a grit to polymer ratio of 0.5.

Figure 104(b) : The relationship between log shear rate and log shear stress obtained using LV medium and 60 Mesh grit with a grit to polymer ratio of 1.

Figure 104(c) : The relationship between log shear rate and log shear stress obtained using LV medium and 60 Mesh grit with a grit to polymer ratio of 2.

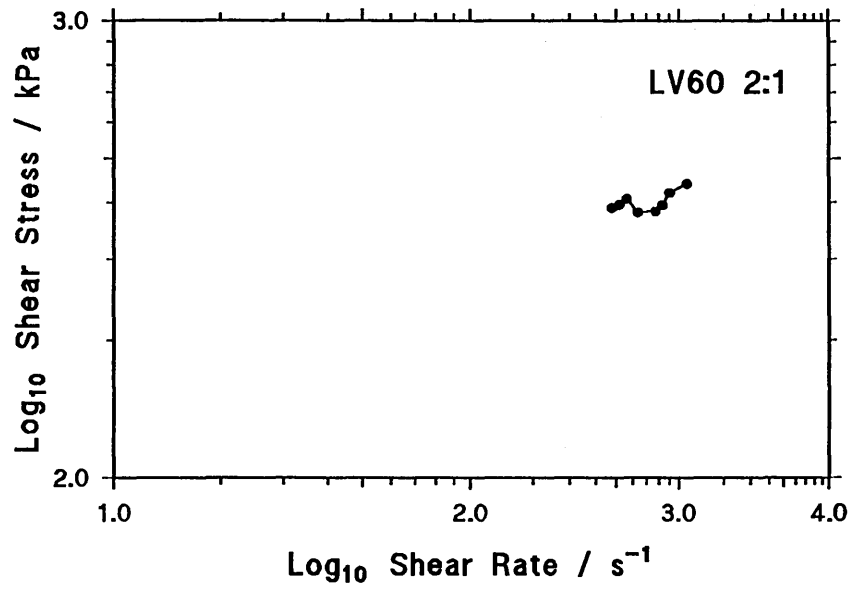
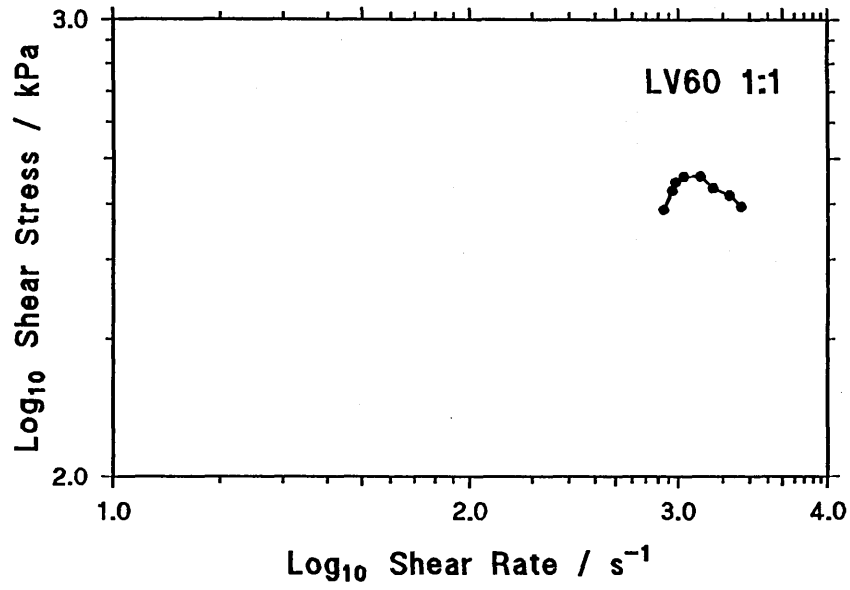
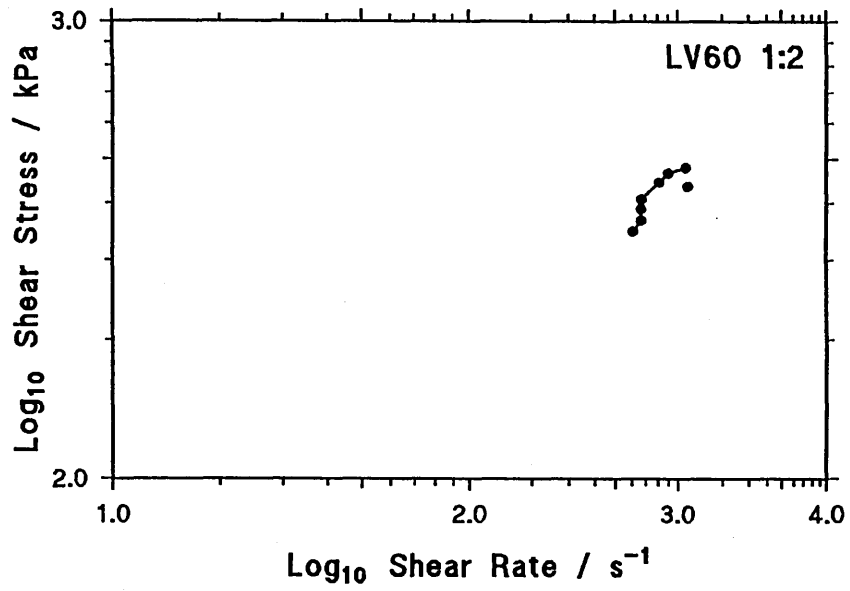


Figure 105(a) : The relationship between log shear rate and log shear stress obtained using LV medium and 100 Mesh grit with a grit to polymer ratio of 0.5.

Figure 105(b) : The relationship between log shear rate and log shear stress obtained using LV medium and 100 Mesh grit with a grit to polymer ratio of 1.

Figure 105(c) : The relationship between log shear rate and log shear stress obtained using LV medium and 100 Mesh grit with a grit to polymer ratio of 2.

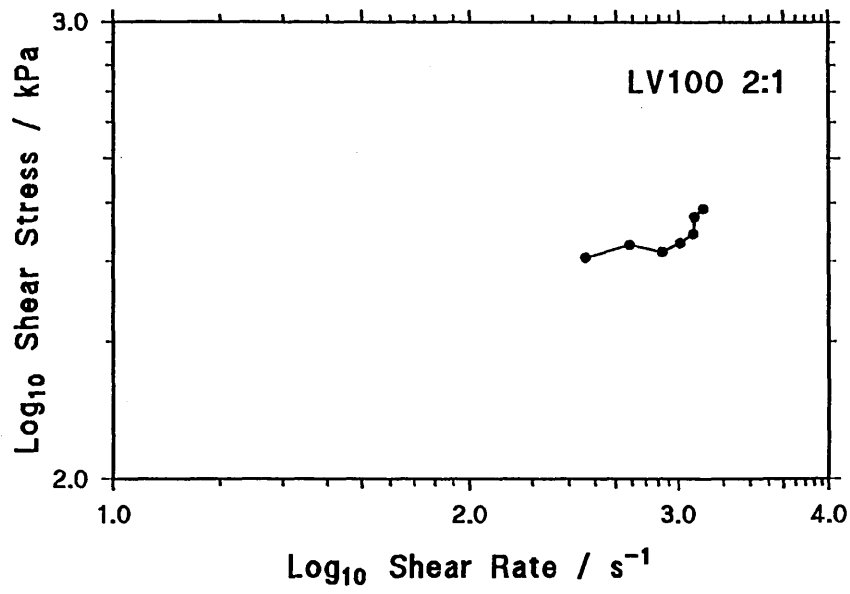
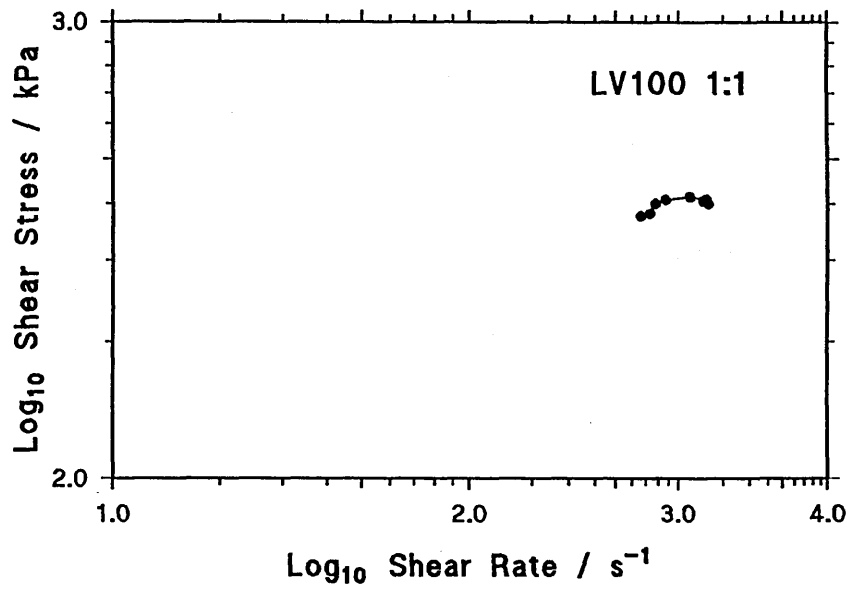
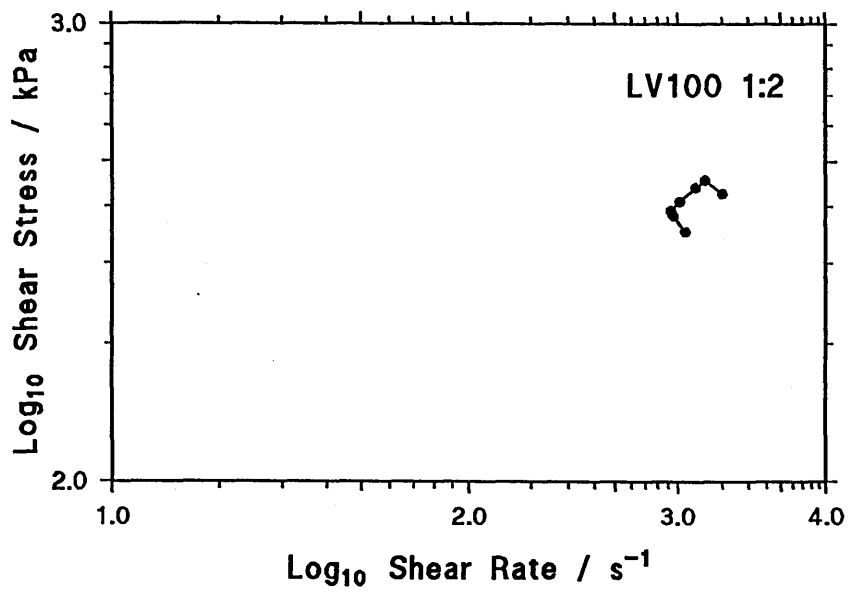


Figure 106(a) : The relationship between log shear rate and log shear stress obtained using MV medium and 60 Mesh grit with a grit to polymer ratio of 0.5.

Figure 106(b) : The relationship between log shear rate and log shear stress obtained using MV medium and 60 Mesh grit with a grit to polymer ratio of 1.

Figure 106(c) : The relationship between log shear rate and log shear stress obtained using MV medium and 60 Mesh grit with a grit to polymer ratio of 2.

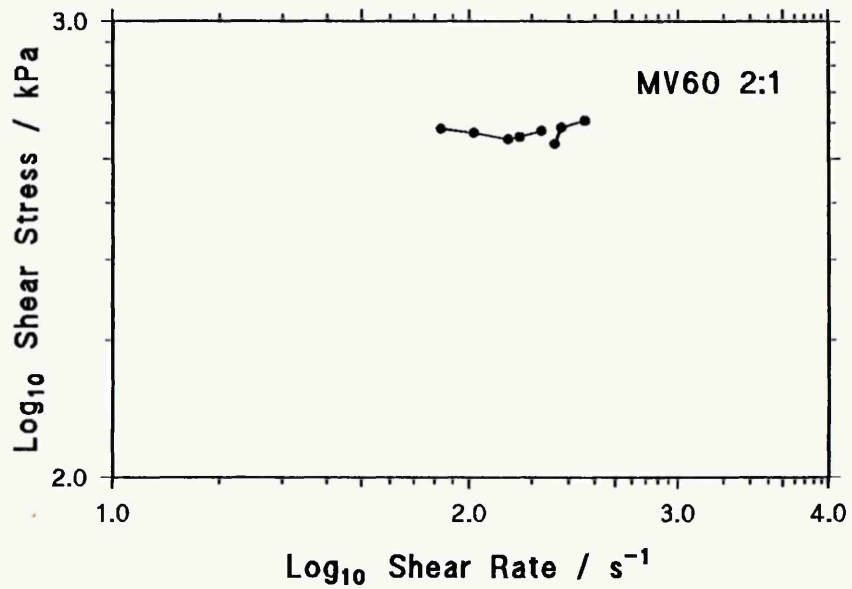
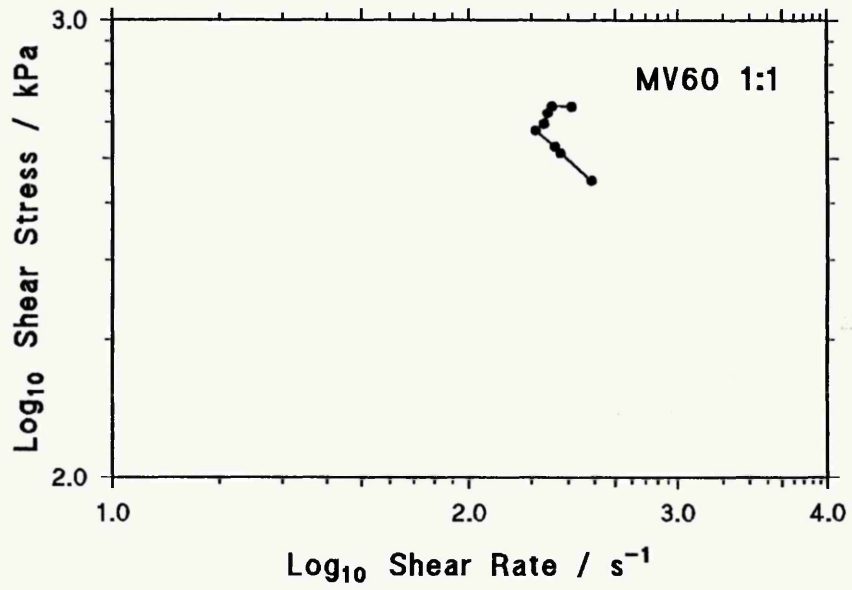
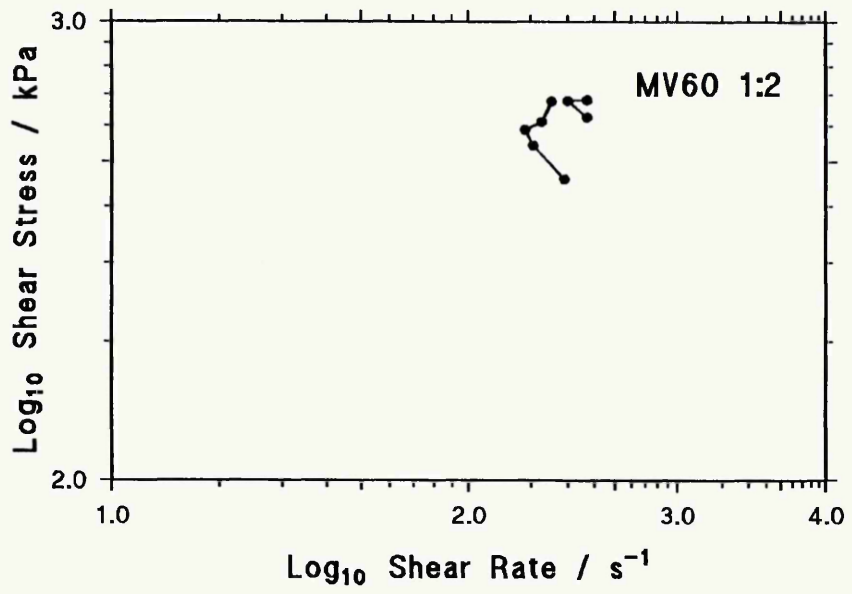


Figure 107(a) : The relationship between log shear rate and log shear stress obtained using MV medium and 100 Mesh grit with a grit to polymer ratio of 0.5.

Figure 107(b) : The relationship between log shear rate and log shear stress obtained using MV medium and 100 Mesh grit with a grit to polymer ratio of 1.

Figure 107(c) : The relationship between log shear rate and log shear stress obtained using MV medium and 100 Mesh grit with a grit to polymer ratio of 2.

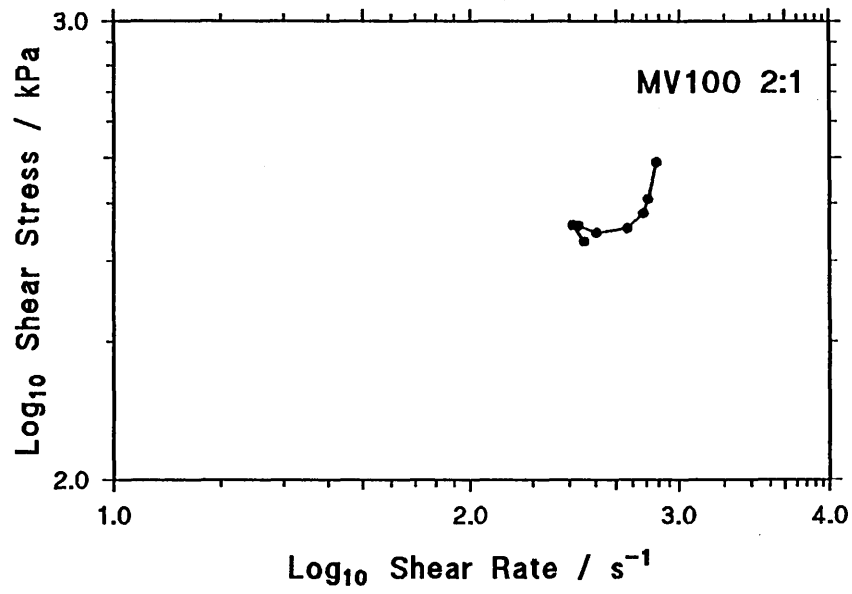
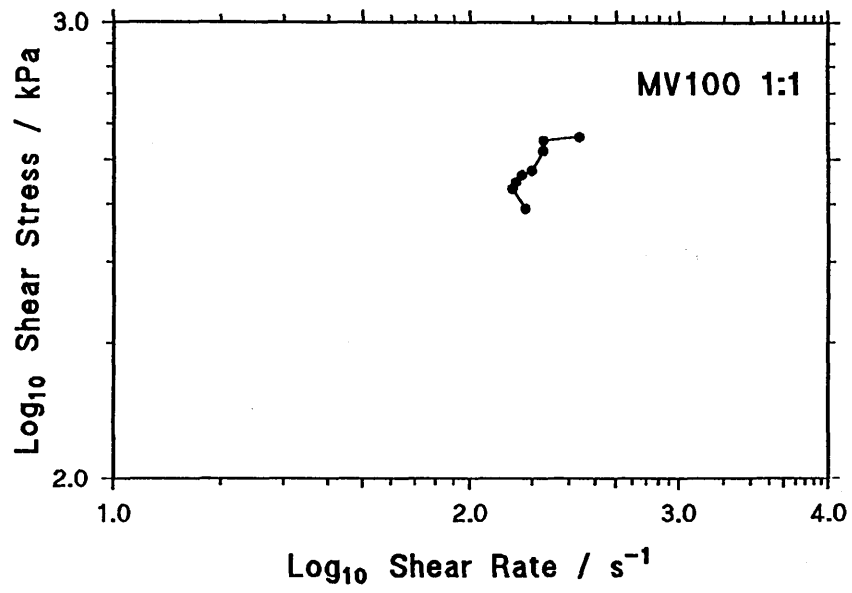
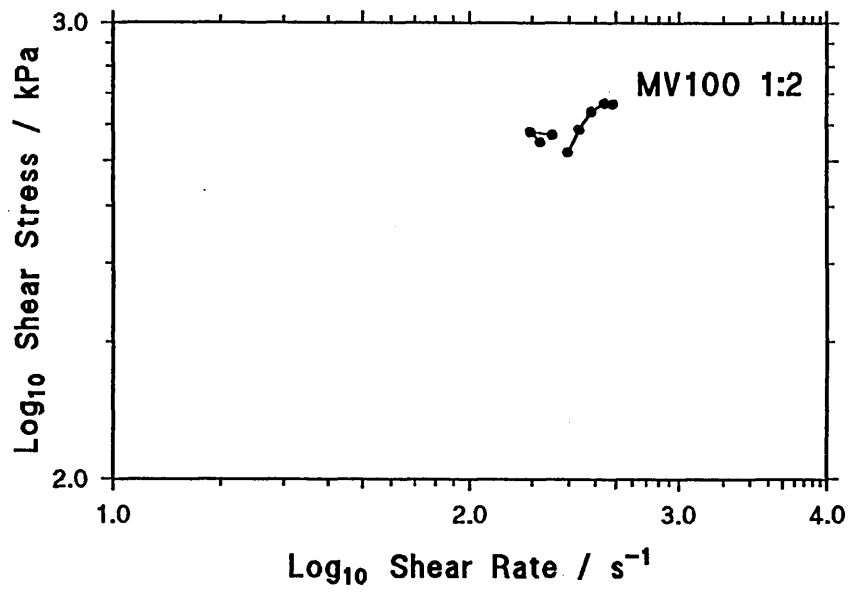


Figure 108(a) : The relationship between log shear rate and log shear stress obtained using HV medium and 60 Mesh grit with a grit to polymer ratio of 0.5.

Figure 108(b) : The relationship between log shear rate and log shear stress obtained using HV medium and 60 Mesh grit with a grit to polymer ratio of 1.

Figure 108(c) : The relationship between log shear rate and log shear stress obtained using HV medium and 60 Mesh grit with a grit to polymer ratio of 2.

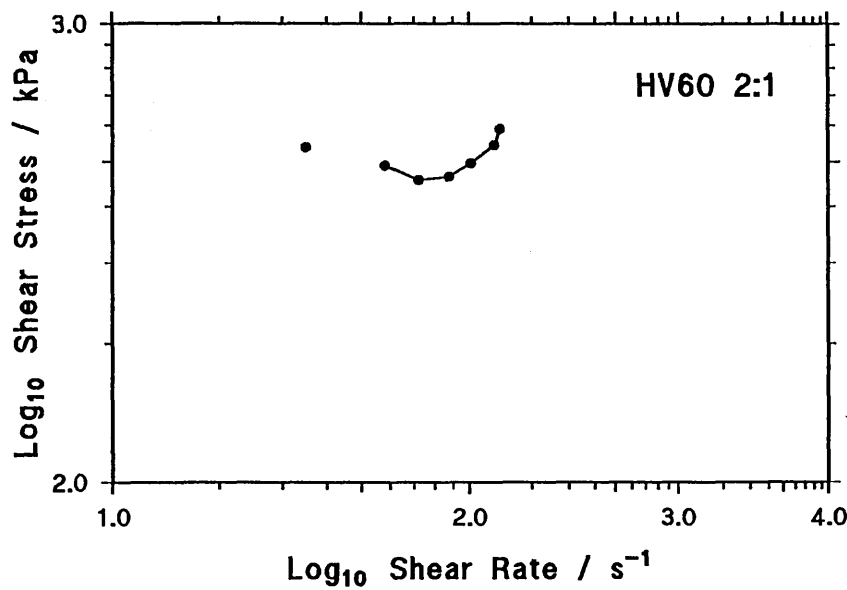
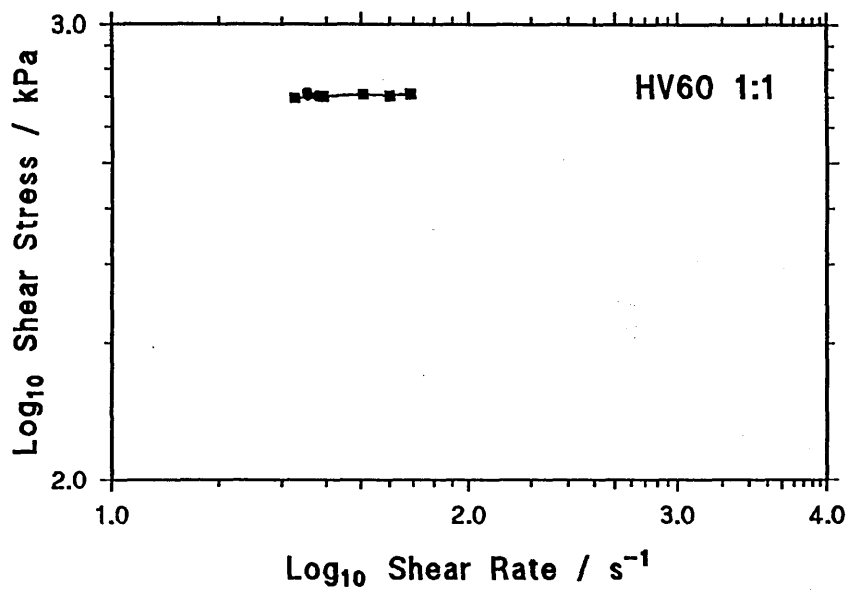
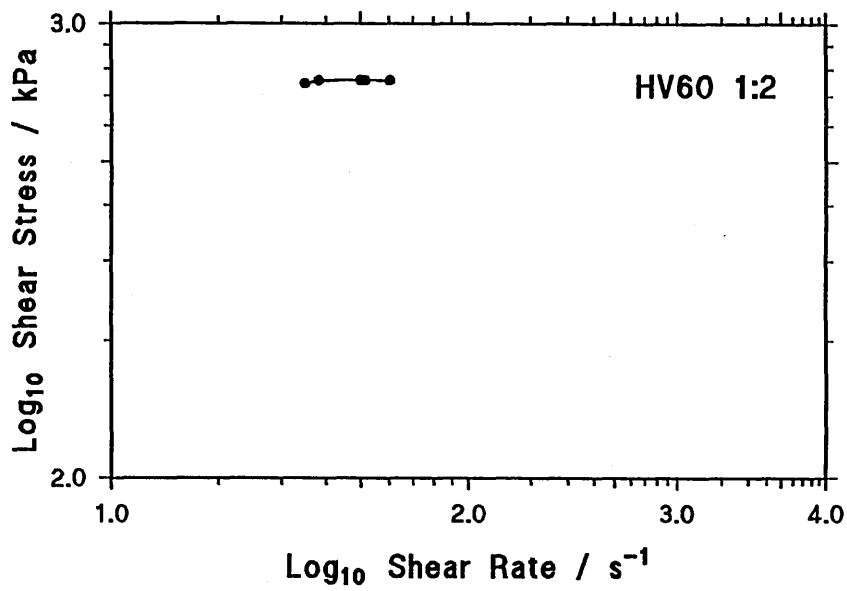


Figure 109(a) : The relationship between log shear rate and log shear stress obtained using HV medium and 100 Mesh grit with a grit to polymer ratio of 0.5.

Figure 109(b) : The relationship between log shear rate and log shear stress obtained using HV medium and 100 Mesh grit with a grit to polymer ratio of 2.

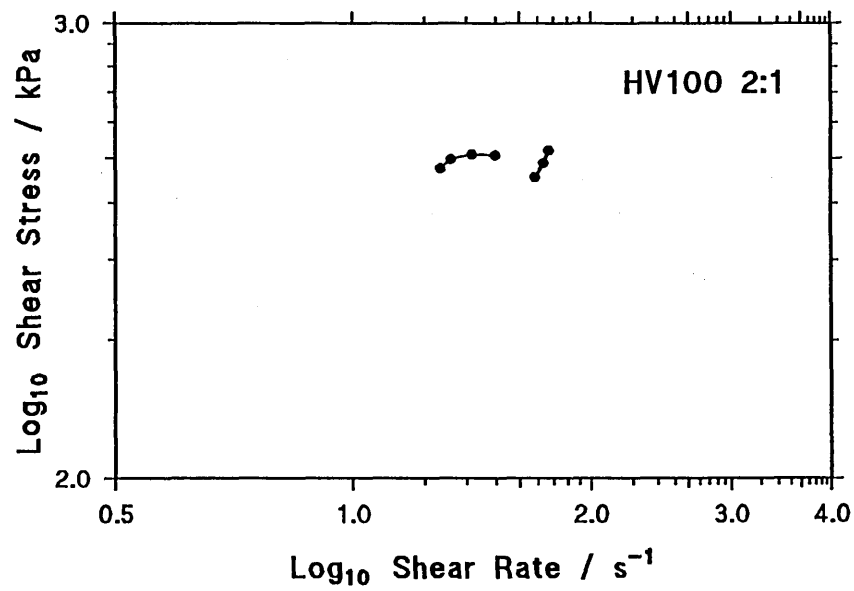
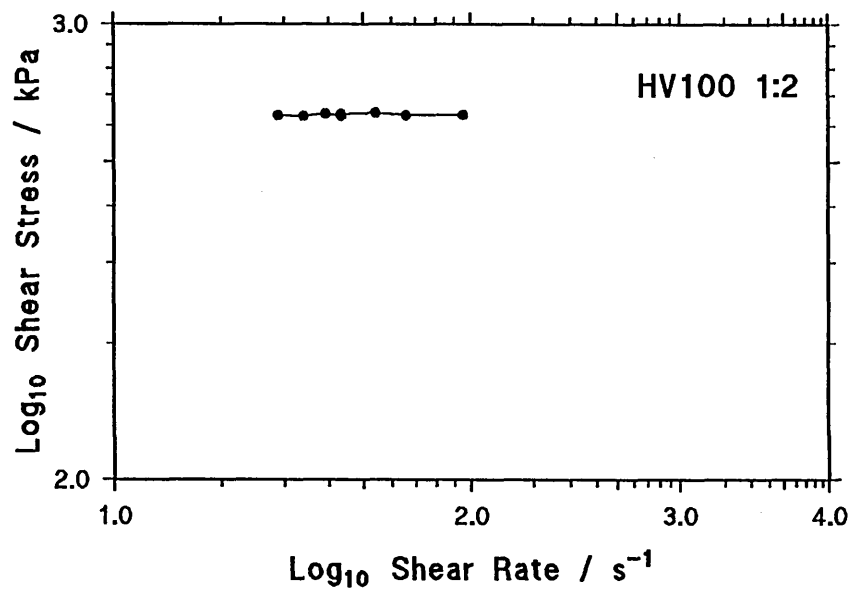


Figure 110(a) : The relationship between the number of extrusion cycles and (i) the mass change per cycle, (ii) the total mass change, and (iii) the percentage surface roughness improvement obtained using LV medium and 60 Mesh grit with a grit to polymer ratio of 0.5.

Figure 110(b) : The relationship between the number of extrusion cycles and (i) the mass change per cycle, (ii) the total mass change, and (iii) the percentage surface roughness improvement obtained using LV medium and 60 Mesh grit with a grit to polymer ratio of 1.

Figure 110(c) : The relationship between the number of extrusion cycles and (i) the mass change per cycle, (ii) the total mass change, and (iii) the percentage surface roughness improvement obtained using LV medium and 60 Mesh grit with a grit to polymer ratio of 2.

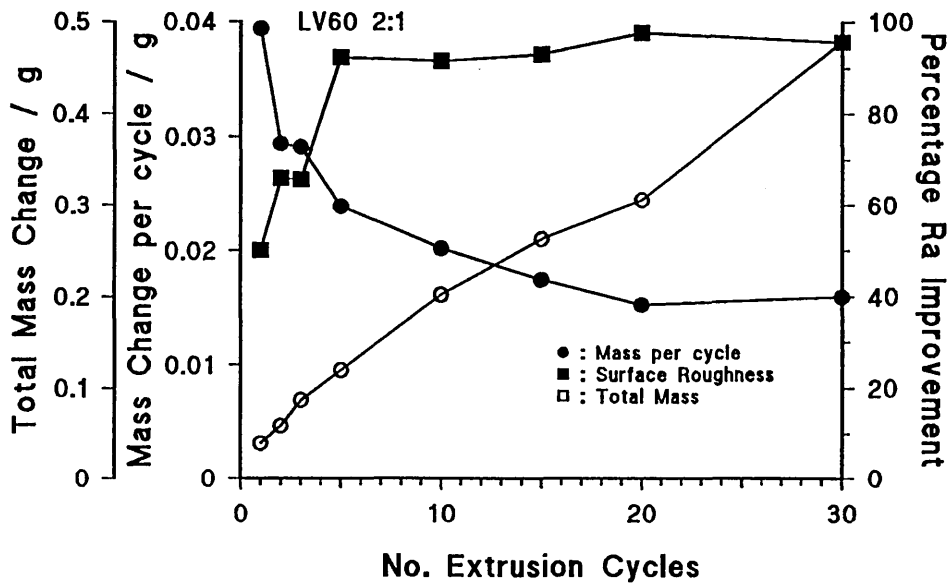
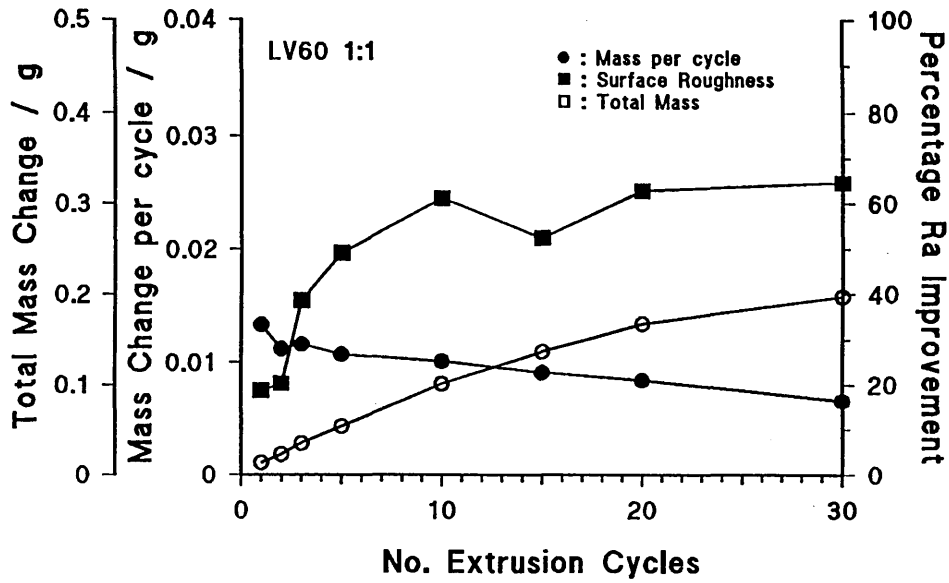
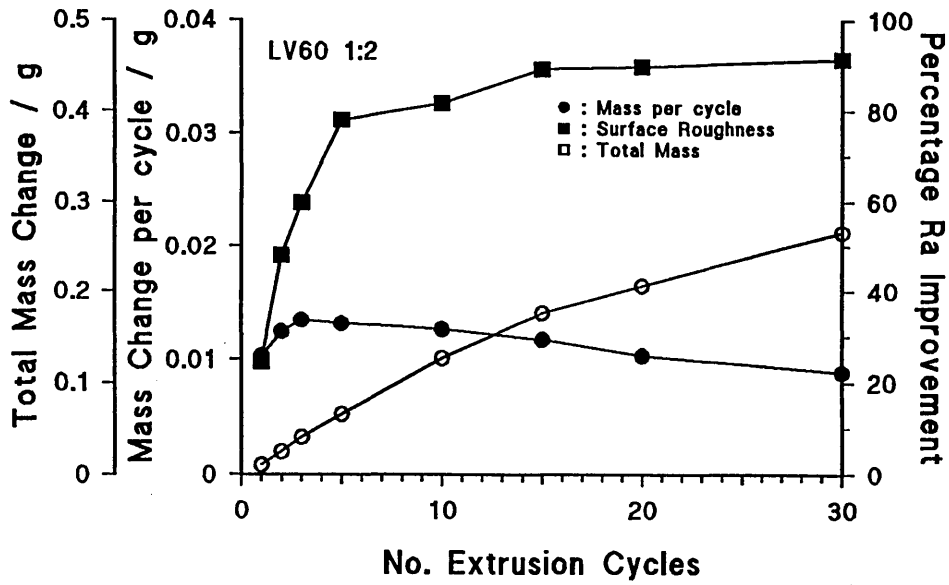


Figure 111(a) : The relationship between the number of extrusion cycles and (i) the mass change per cycle, (ii) the total mass change, and (iii) the percentage surface roughness improvement obtained using LV medium and 100 Mesh grit with a grit to polymer ratio of 0.5.

Figure 111(b) : The relationship between the number of extrusion cycles and (i) the mass change per cycle, (ii) the total mass change, and (iii) the percentage surface roughness improvement obtained using LV medium and 100 Mesh grit with a grit to polymer ratio of 1.

Figure 111(c) : The relationship between the number of extrusion cycles and (i) the mass change per cycle, (ii) the total mass change, and (iii) the percentage surface roughness improvement obtained using LV medium and 100 Mesh grit with a grit to polymer ratio of 2.

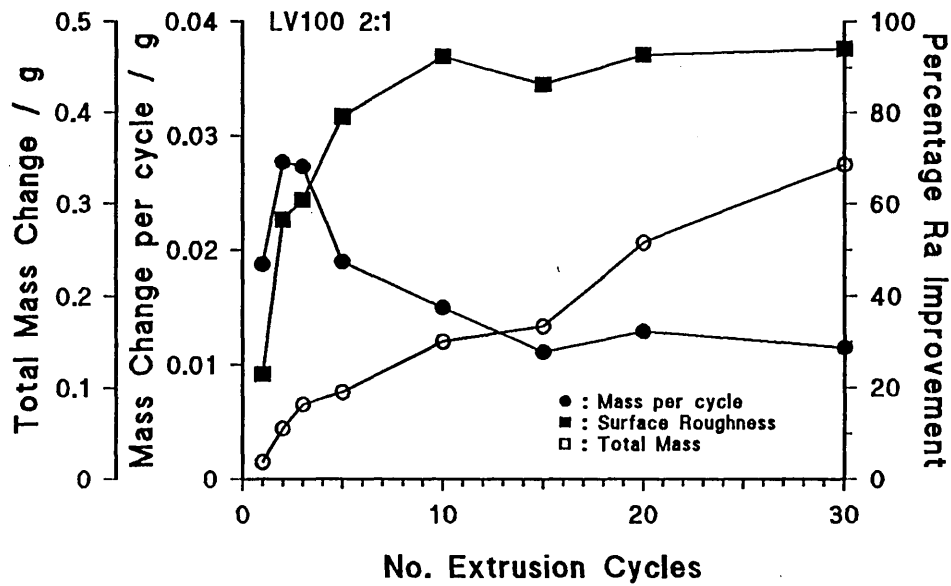
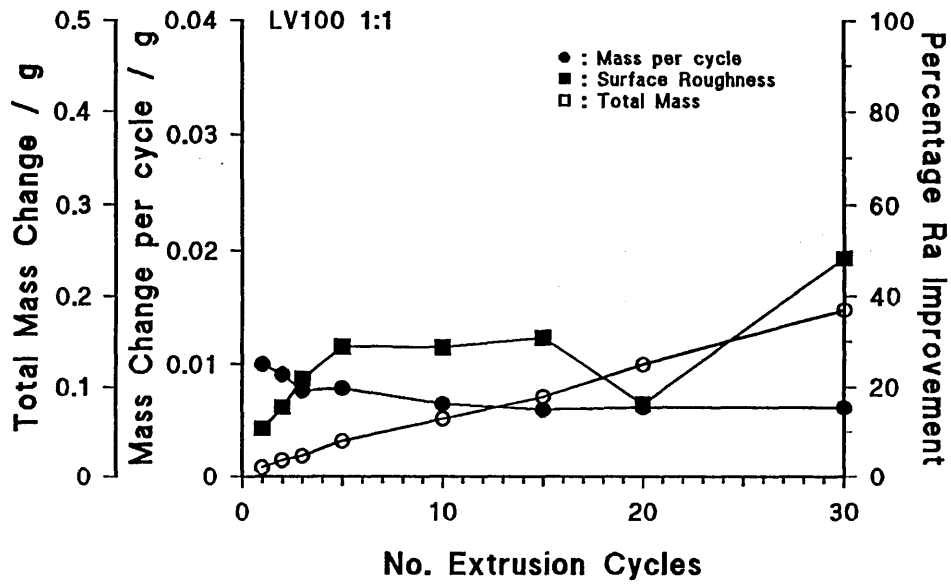
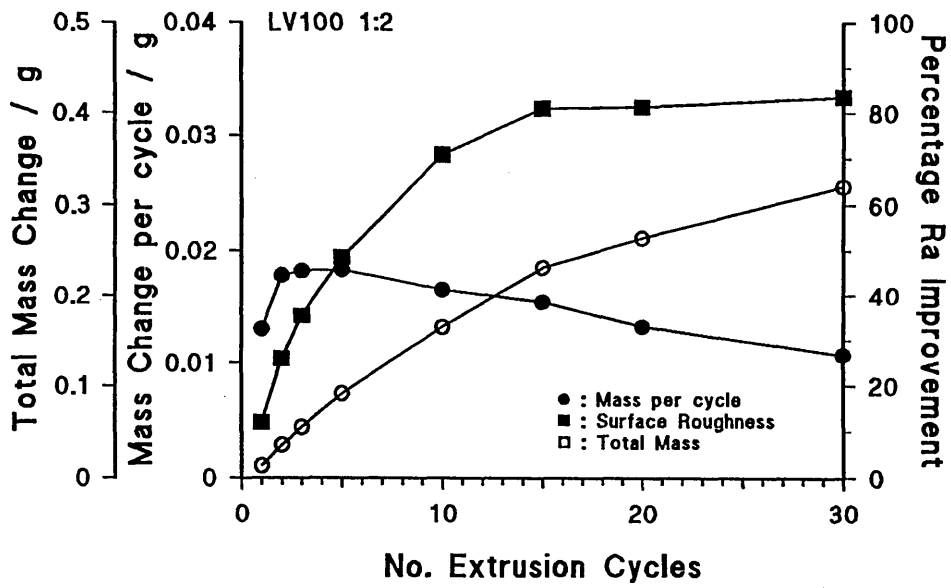


Figure 112(a) : The relationship between the number of extrusion cycles and (i) the mass change per cycle, (ii) the total mass change, and (iii) the percentage surface roughness improvement obtained using MV medium and 60 Mesh grit with a grit to polymer ratio of 0.5.

Figure 112(b) : The relationship between the number of extrusion cycles and (i) the mass change per cycle, (ii) the total mass change, and (iii) the percentage surface roughness improvement obtained using MV medium and 60 Mesh grit with a grit to polymer ratio of 1.

Figure 112(c) : The relationship between the number of extrusion cycles and (i) the mass change per cycle, (ii) the total mass change, and (iii) the percentage surface roughness improvement obtained using MV medium and 60 Mesh grit with a grit to polymer ratio of 2.

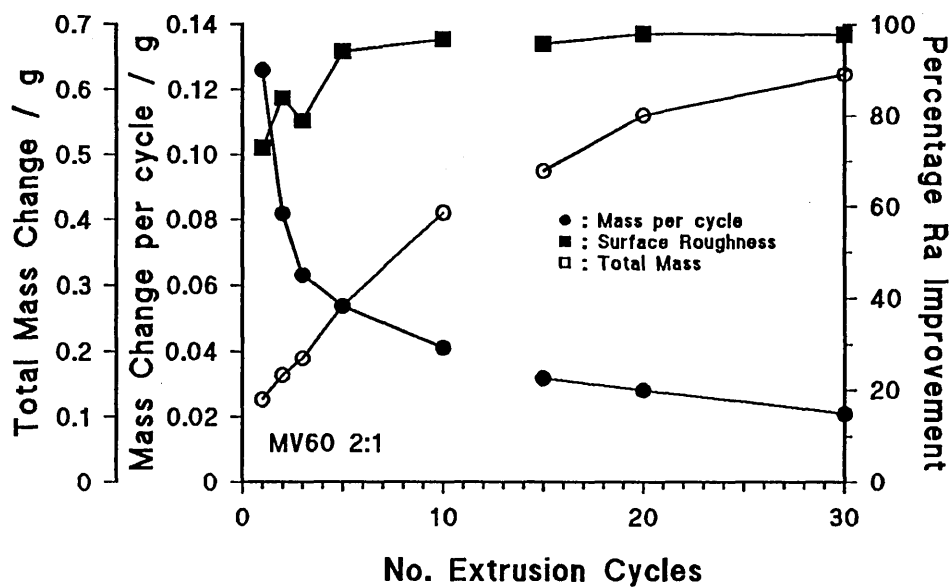
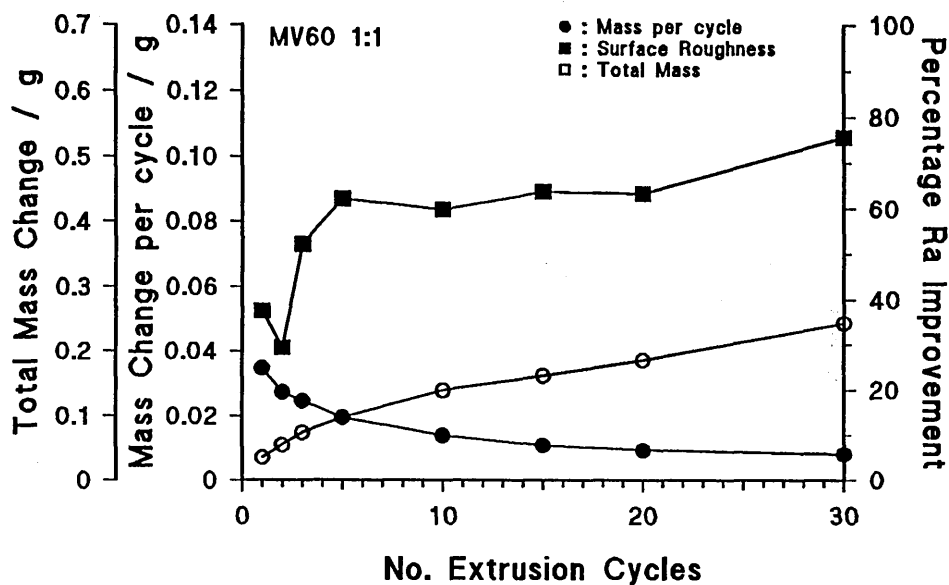
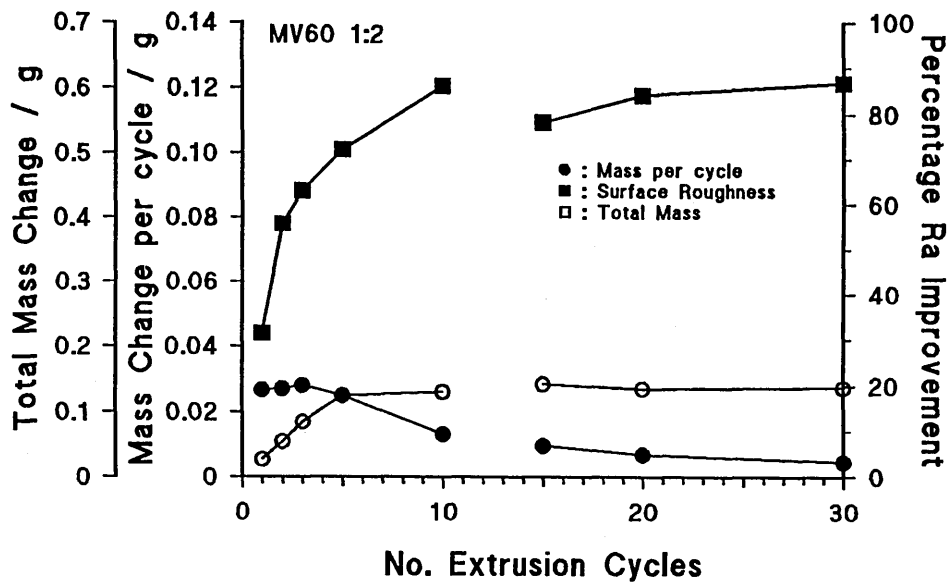


Figure 113(a) : The relationship between the number of extrusion cycles and (i) the mass change per cycle, (ii) the total mass change, and (iii) the percentage surface roughness improvement obtained using MV medium and 100 Mesh grit with a grit to polymer ratio of 0.5.

Figure 113(b) : The relationship between the number of extrusion cycles and (i) the mass change per cycle, (ii) the total mass change, and (iii) the percentage surface roughness improvement obtained using MV medium and 100 Mesh grit with a grit to polymer ratio of 1.

Figure 113(c) : The relationship between the number of extrusion cycles and (i) the mass change per cycle, (ii) the total mass change, and (iii) the percentage surface roughness improvement obtained using MV medium and 100 Mesh grit with a grit to polymer ratio of 2.

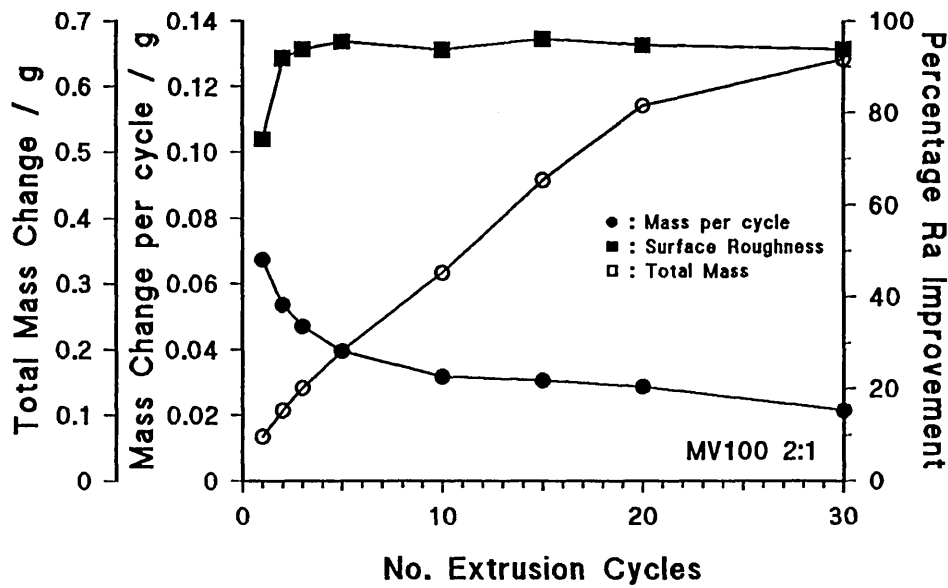
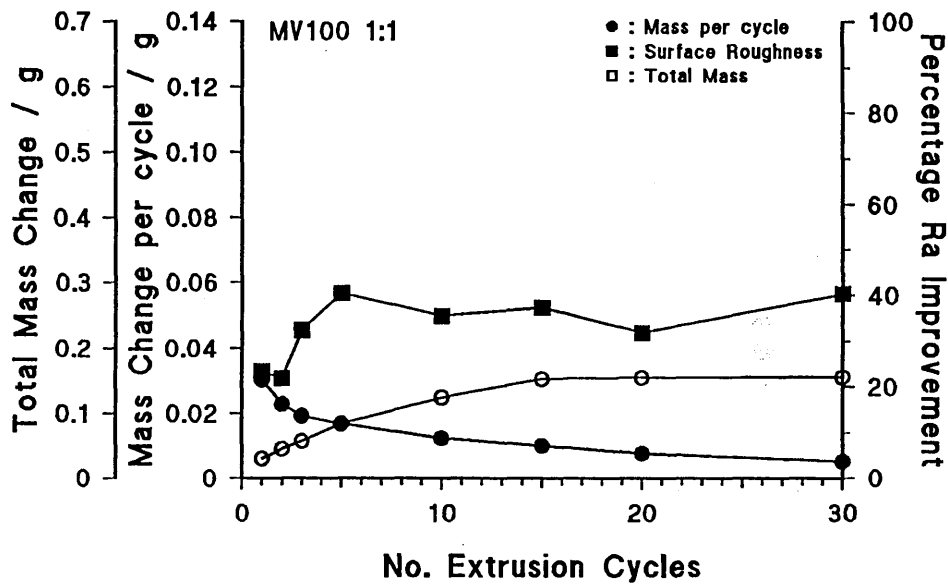
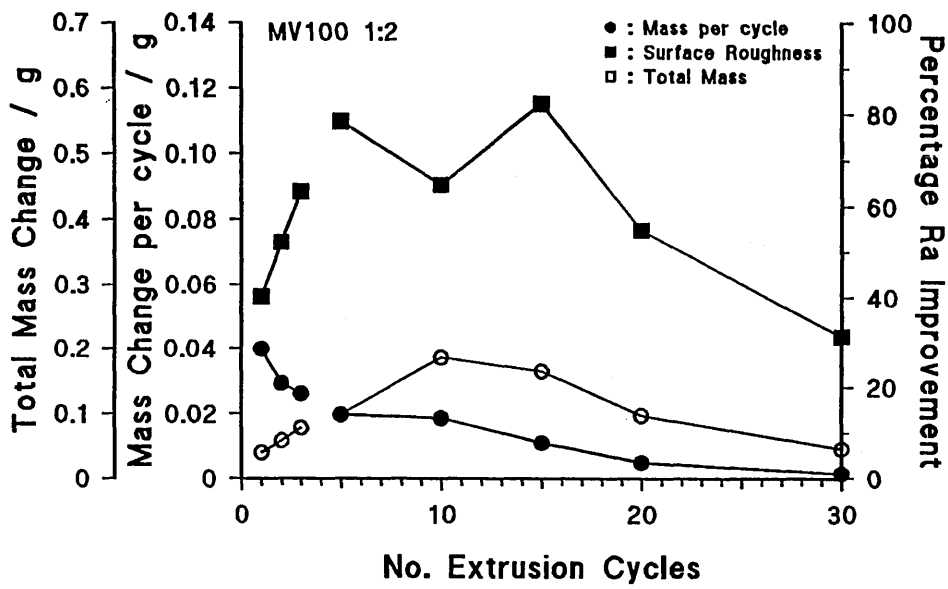


Figure 114(a) : The relationship between the number of extrusion cycles and (i) the mass change per cycle, (ii) the total mass change, and (iii) the percentage surface roughness improvement obtained using HV medium and 60 Mesh grit with a grit to polymer ratio of 0.5.

Figure 114(b) : The relationship between the number of extrusion cycles and (i) the mass change per cycle, (ii) the total mass change, and (iii) the percentage surface roughness improvement obtained using HV medium and 60 Mesh grit with a grit to polymer ratio of 1.

Figure 114(c) : The relationship between the number of extrusion cycles and (i) the mass change per cycle, (ii) the total mass change, and (iii) the percentage surface roughness improvement obtained using HV medium and 60 Mesh grit with a grit to polymer ratio of 2.

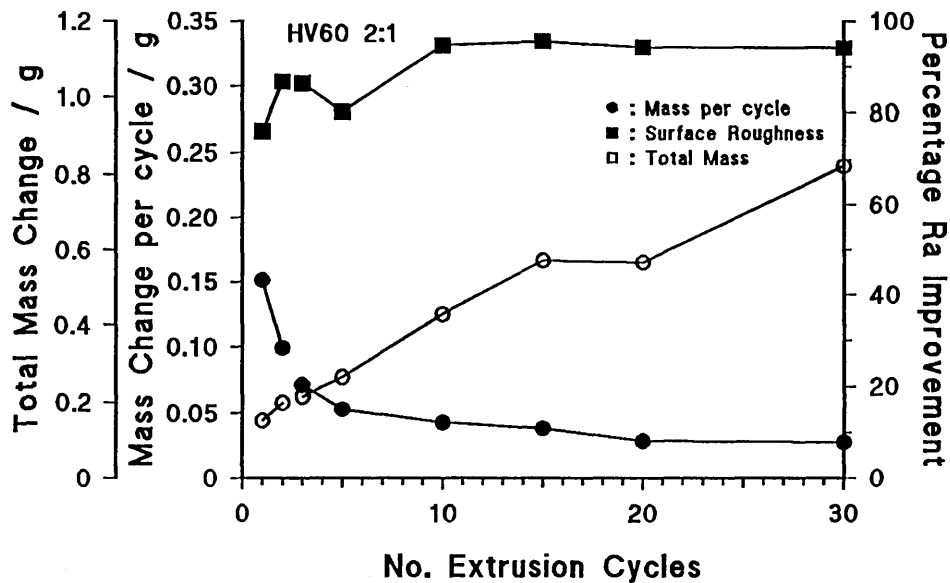
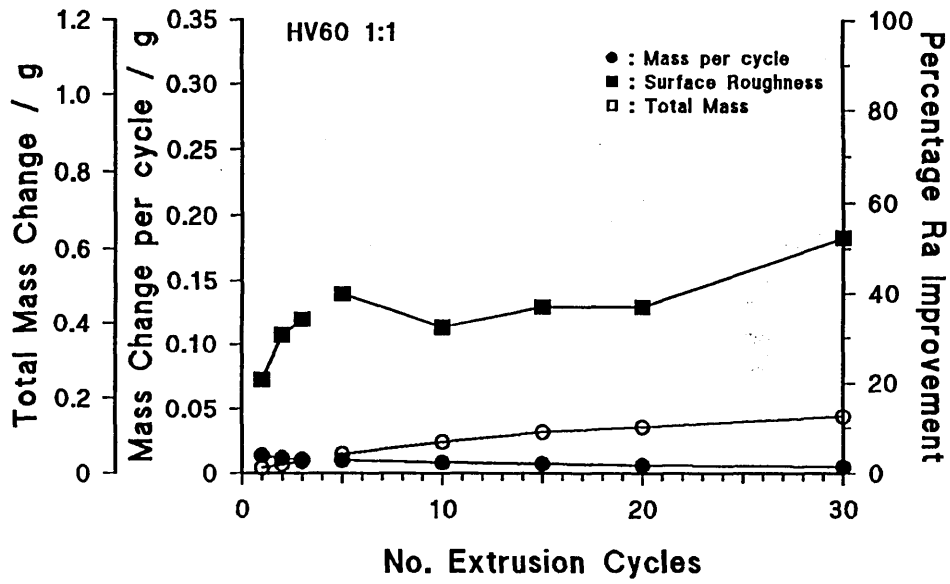
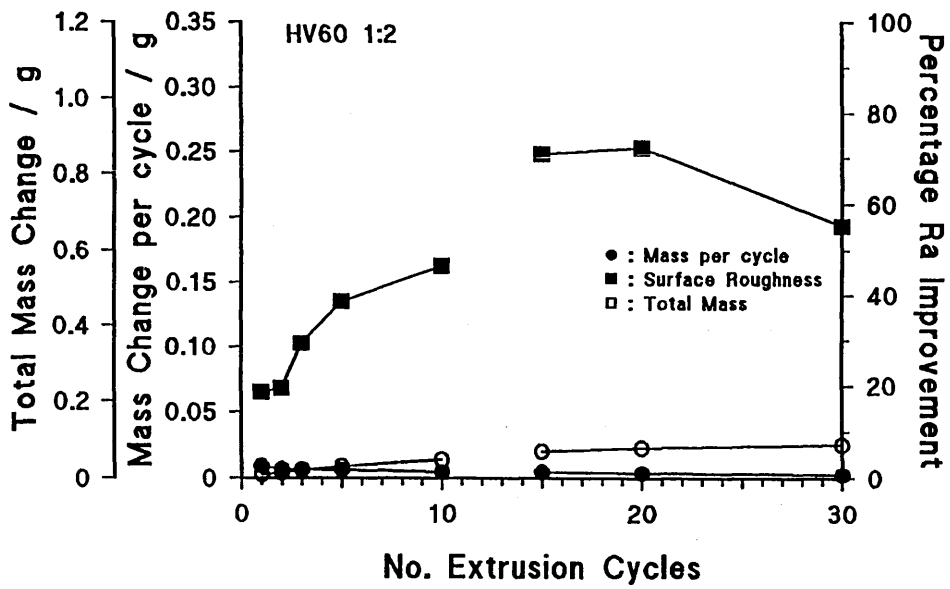


Figure 115(a) : The relationship between the number of extrusion cycles and (i) the mass change per cycle, (ii) the total mass change, and (iii) the percentage surface roughness improvement obtained using HV medium and 100 Mesh grit with a grit to polymer ratio of 0.5.

Figure 115(b) : The relationship between the number of extrusion cycles and (i) the mass change per cycle, (ii) the total mass change, and (iii) the percentage surface roughness improvement obtained using HV medium and 100 Mesh grit with a grit to polymer ratio of 1.

Figure 115(c) : The relationship between the number of extrusion cycles and (i) the mass change per cycle, (ii) the total mass change, and (iii) the percentage surface roughness improvement obtained using HV medium and 100 Mesh grit with a grit to polymer ratio of 2.

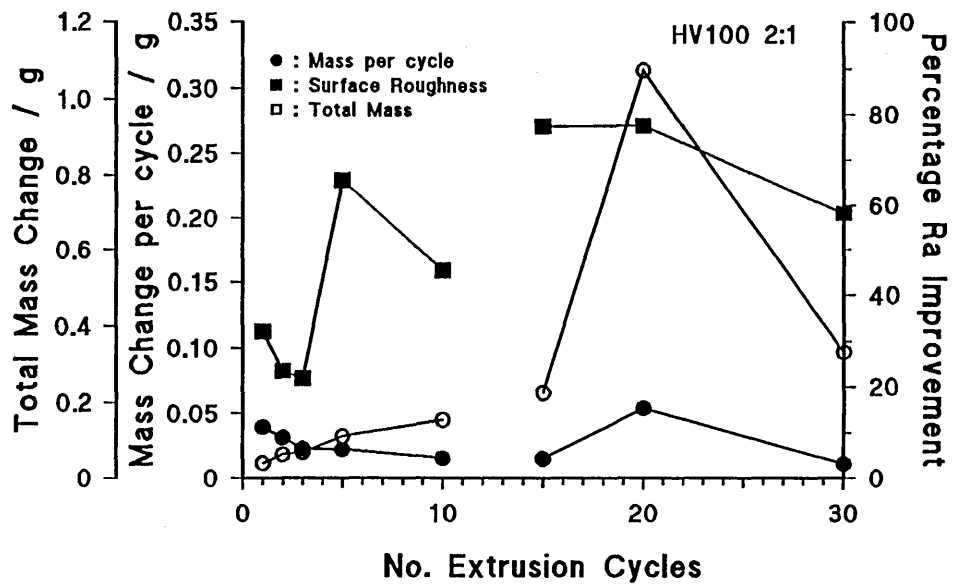
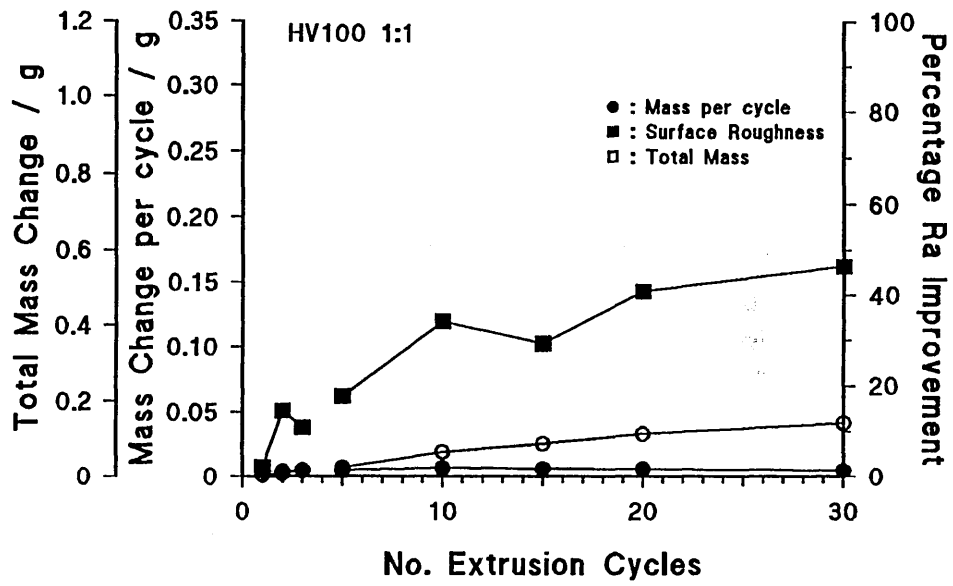
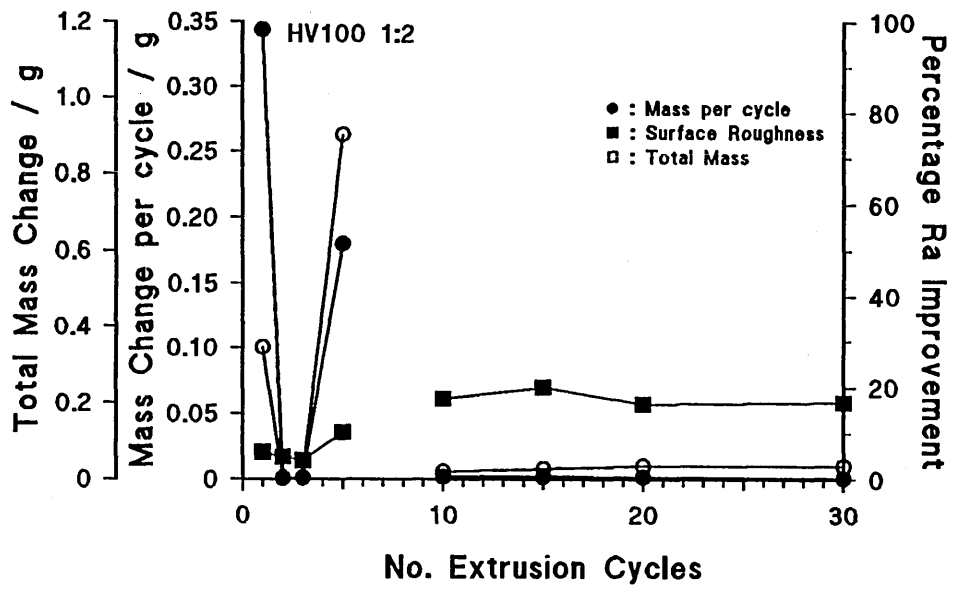


Figure 116(a) : The relationship between the change in temperature and (i) the average pressure drop, and (ii) the viscosity for the LV medium and 60 Mesh grit with a grit to polymer ratio of 0.5.

Figure 116(b) : The relationship between the change in temperature and (i) the average pressure drop, and (ii) the viscosity for the LV medium and 60 Mesh grit with a grit to polymer ratio of 1.

Figure 116(c) : The relationship between the change in temperature and (i) the average pressure drop, and (ii) the viscosity for the LV medium and 60 Mesh grit with a grit to polymer ratio of 2.

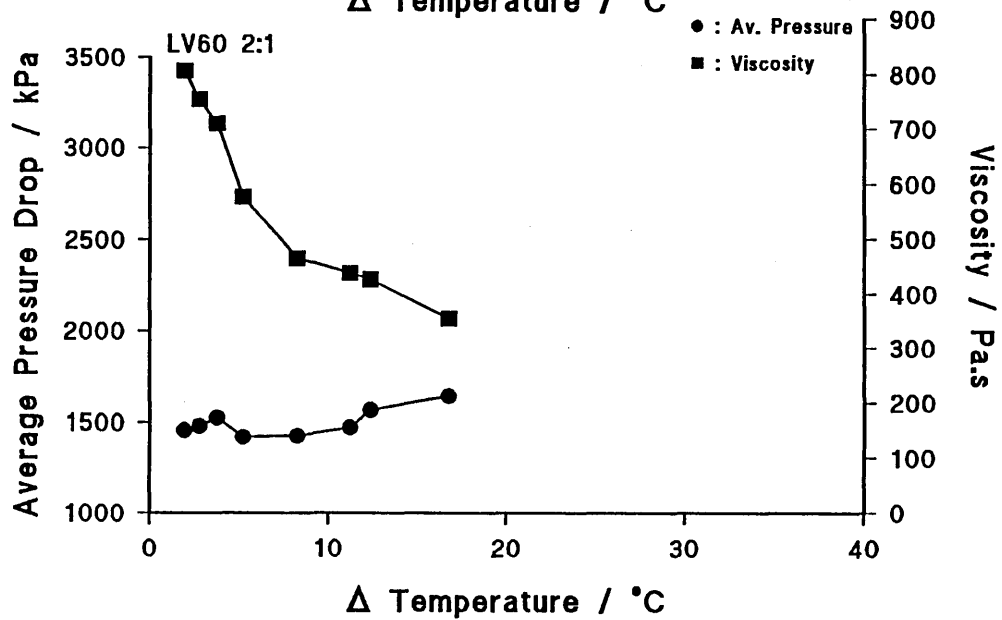
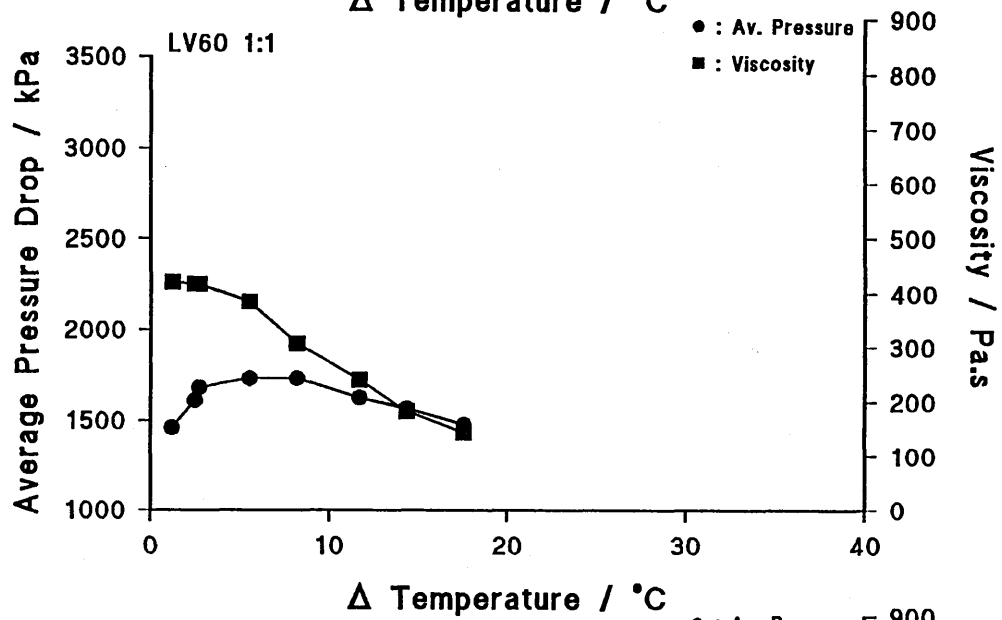
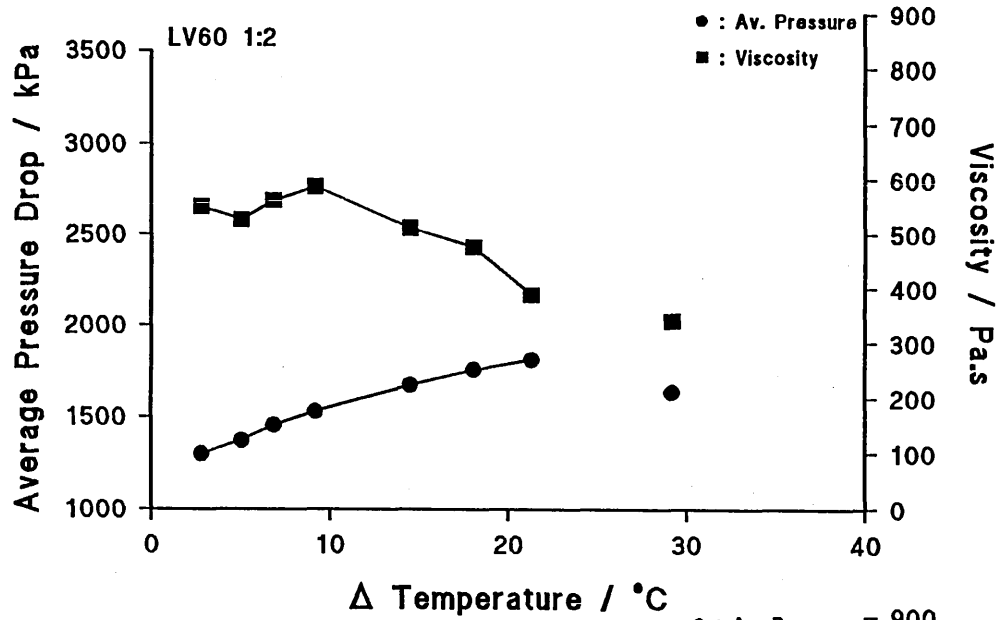


Figure 117(a) : The relationship between the change in temperature and (i) the average pressure drop, and (ii) the viscosity for the LV medium and 100 Mesh grit with a grit to polymer ratio of 0.5.

Figure 117(b) : The relationship between the change in temperature and (i) the average pressure drop, and (ii) the viscosity for the LV medium and 100 Mesh grit with a grit to polymer ratio of 1.

Figure 117(c) : The relationship between the change in temperature and (i) the average pressure drop, and (ii) the viscosity for the LV medium and 100 Mesh grit with a grit to polymer ratio of 2.

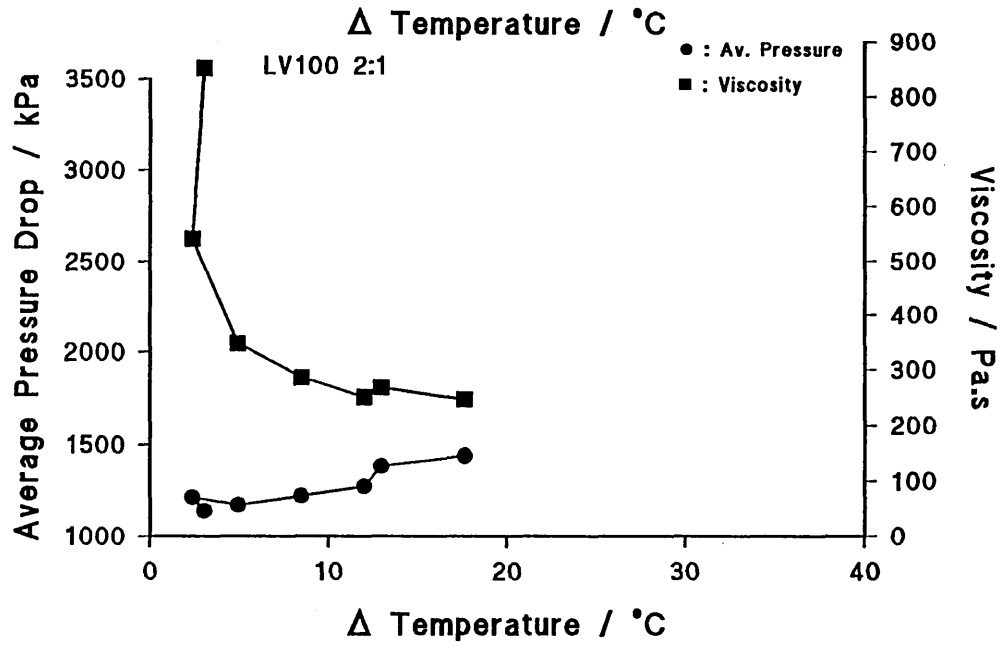
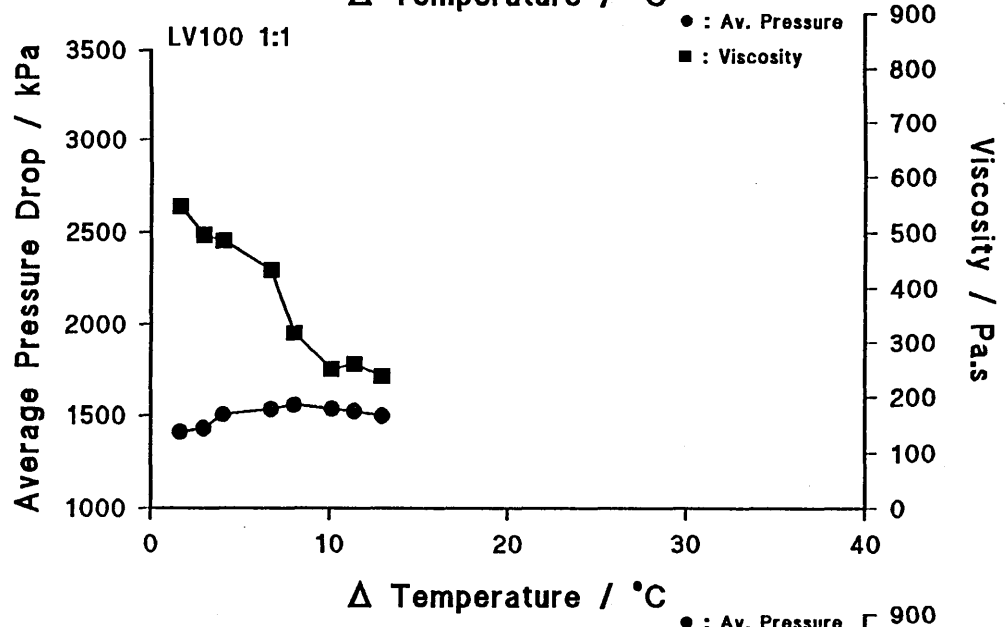
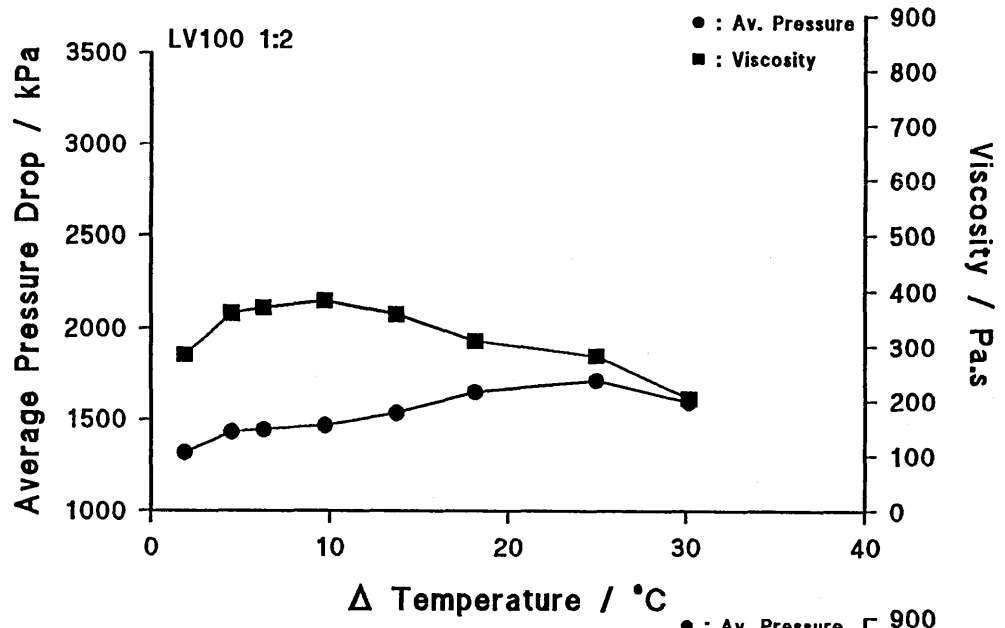


Figure 118(a) : The relationship between the change in temperature and (i) the average pressure drop, and (ii) the viscosity for the MV medium and 60 Mesh grit with a grit to polymer ratio of 0.5.

Figure 118(b) : The relationship between the change in temperature and (i) the average pressure drop, and (ii) the viscosity for the MV medium and 60 Mesh grit with a grit to polymer ratio of 1.

Figure 118(c) : The relationship between the change in temperature and (i) the average pressure drop, and (ii) the viscosity for the MV medium and 60 Mesh grit with a grit to polymer ratio of 2.

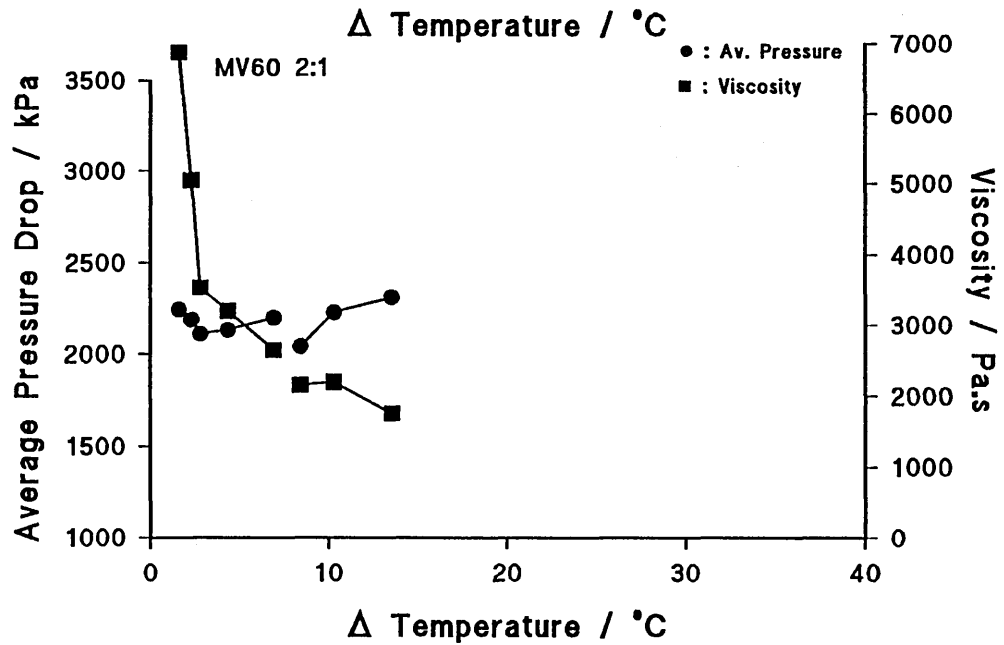
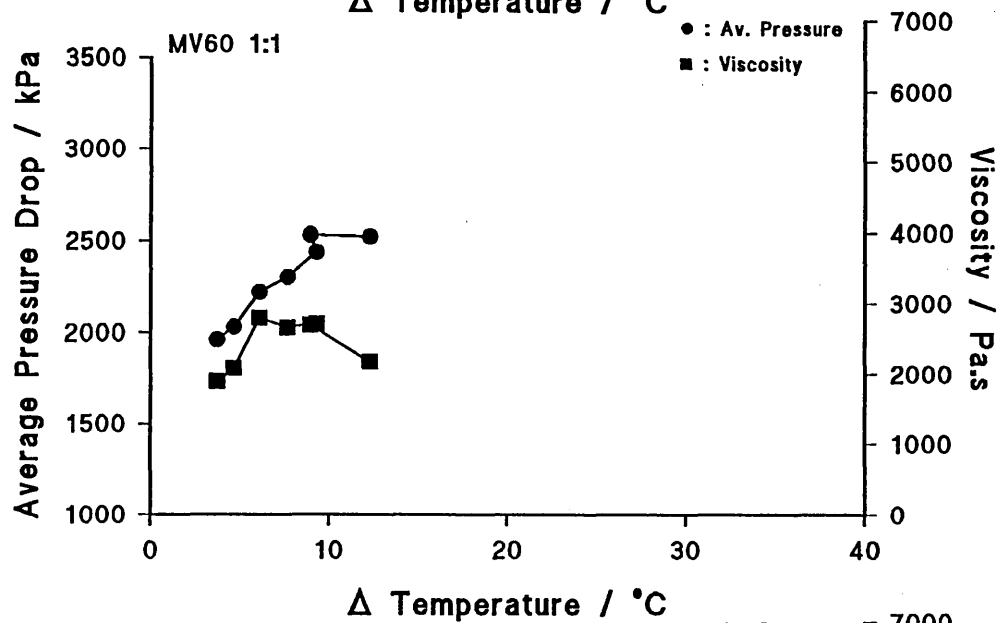
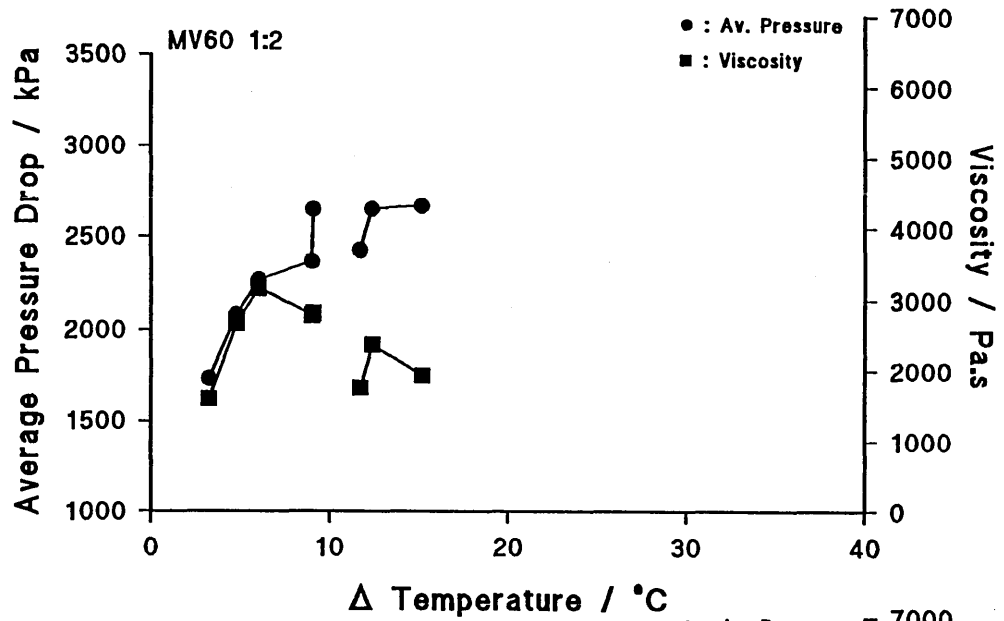


Figure 119(a) : The relationship between the change in temperature and (i) the average pressure drop, and (ii) the viscosity for the MV medium and 100 Mesh grit with a grit to polymer ratio of 0.5.

Figure 119(b) : The relationship between the change in temperature and (i) the average pressure drop, and (ii) the viscosity for the MV medium and 100 Mesh grit with a grit to polymer ratio of 1.

Figure 119(c) : The relationship between the change in temperature and (i) the average pressure drop, and (ii) the viscosity for the MV medium and 100 Mesh grit with a grit to polymer ratio of 2.

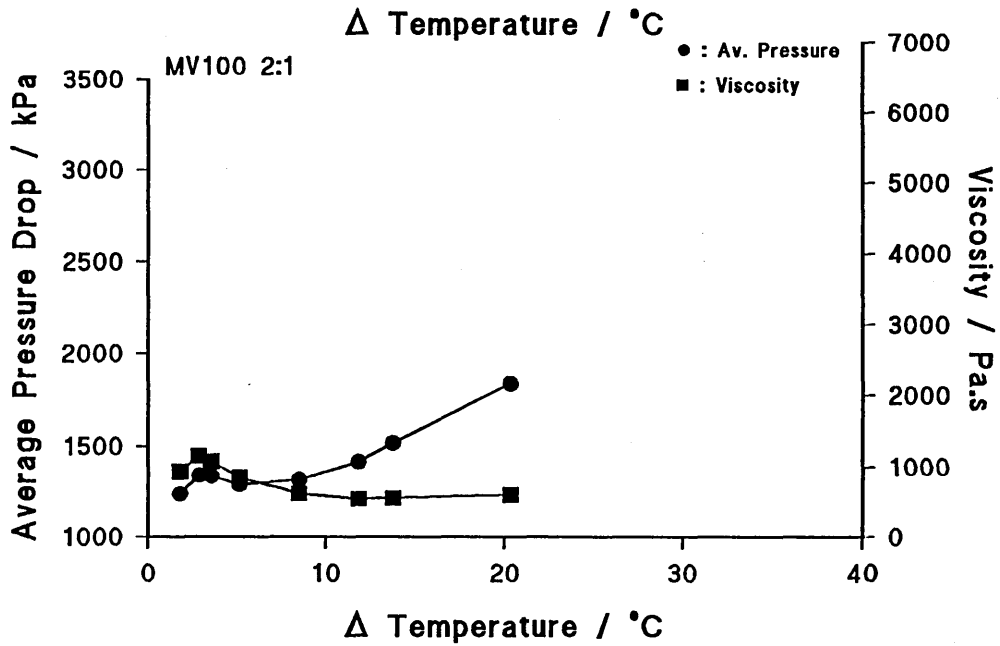
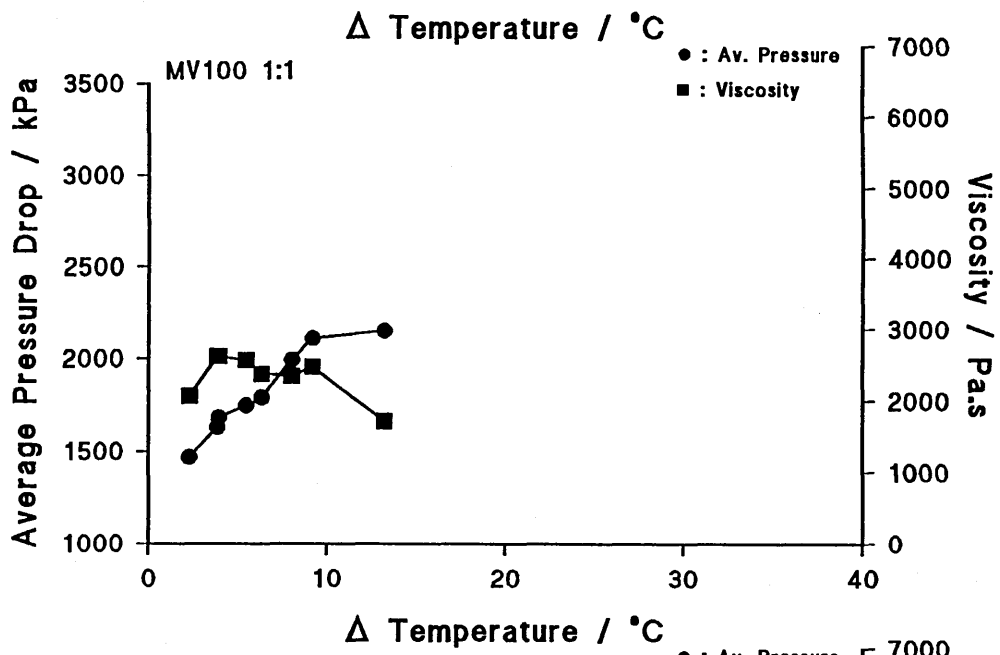
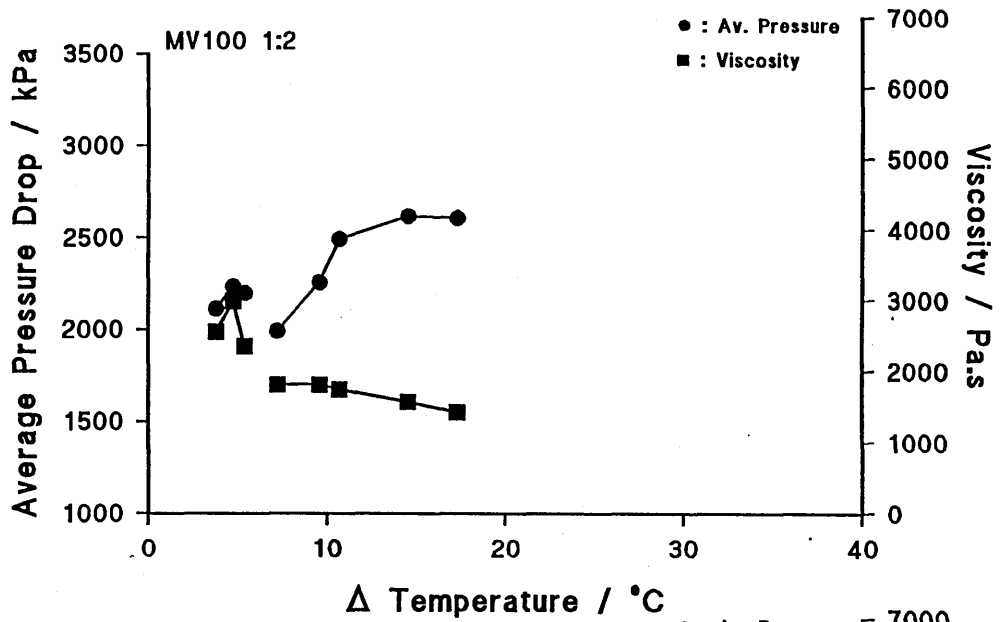


Figure 120(a) : The relationship between the change in temperature and (i) the average pressure drop, and (ii) the viscosity for the HV medium and 60 Mesh grit with a grit to polymer ratio of 0.5.

Figure 120(b) : The relationship between the change in temperature and (i) the average pressure drop, and (ii) the viscosity for the HV medium and 60 Mesh grit with a grit to polymer ratio of 1.

Figure 120(c) : The relationship between the change in temperature and (i) the average pressure drop, and (ii) the viscosity for the HV medium and 60 Mesh grit with a grit to polymer ratio of 2.

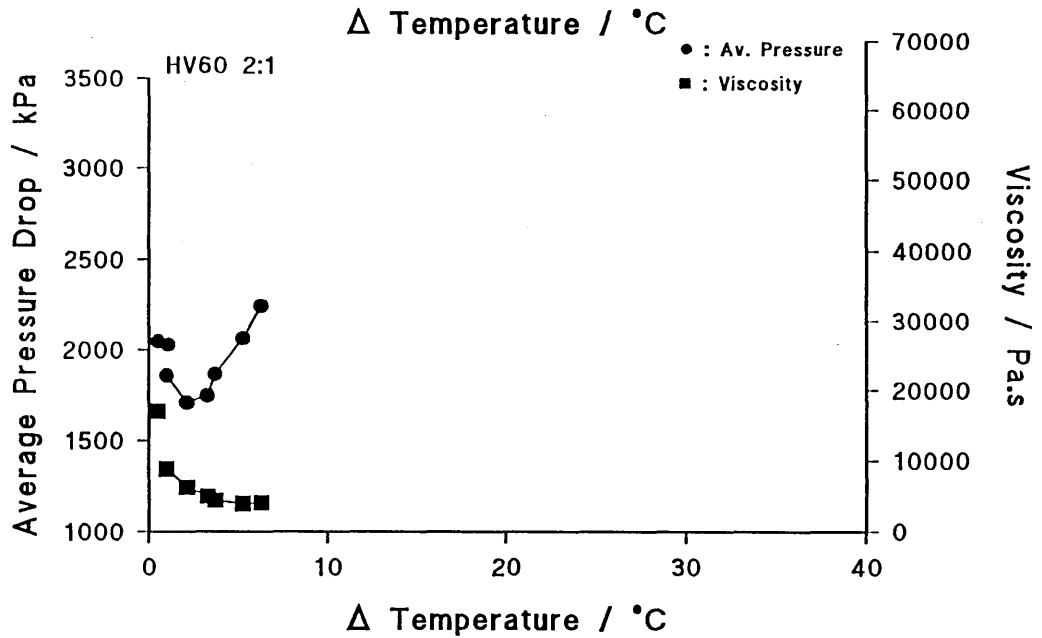
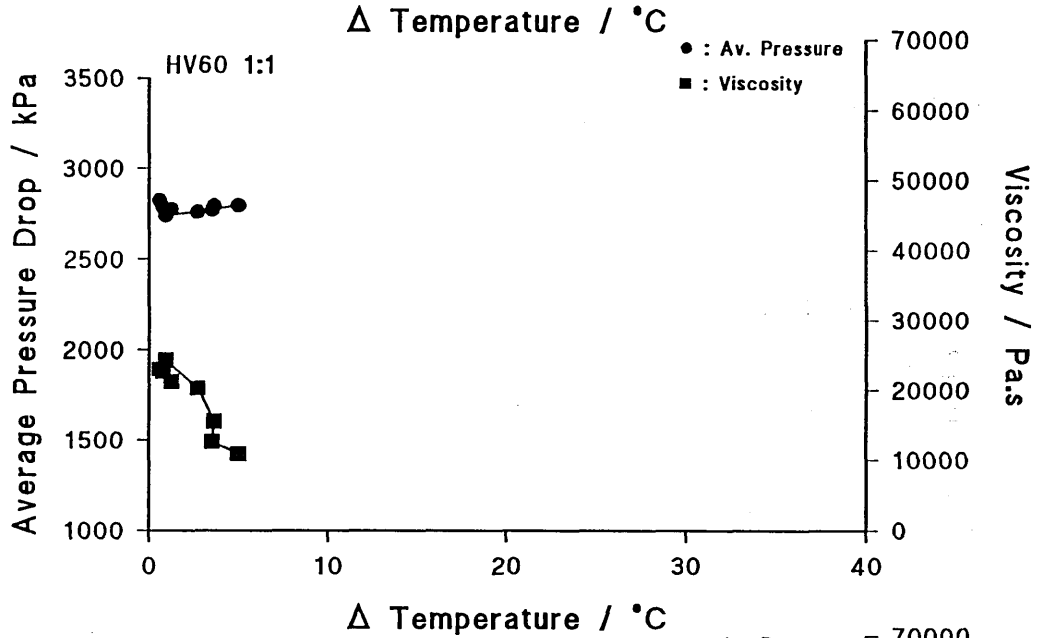
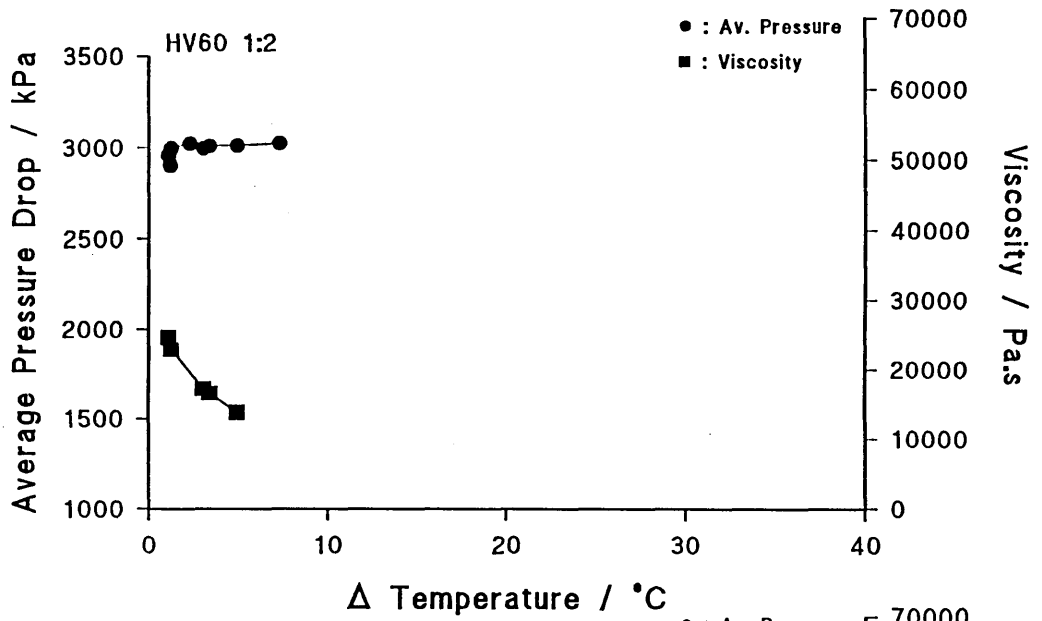


Figure 121(a) : The relationship between the change in temperature and (i) the average pressure drop, and (ii) the viscosity for the HV medium and 100 Mesh grit with a grit to polymer ratio of 0.5.

Figure 121(b) : The relationship between the change in temperature and (i) the average pressure drop, and (ii) the viscosity for the HV medium and 100 Mesh grit with a grit to polymer ratio of 2.

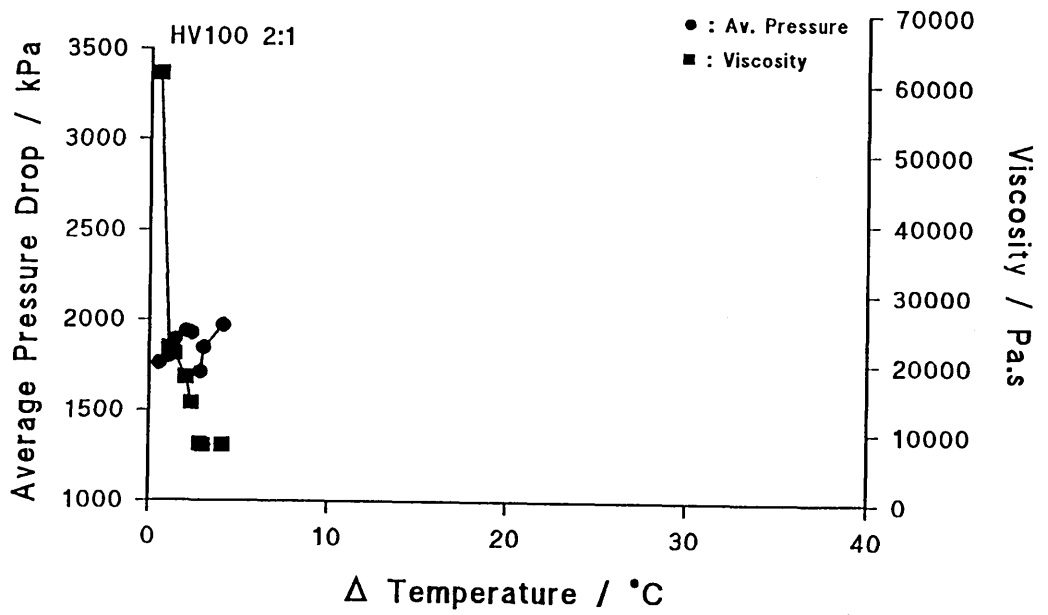
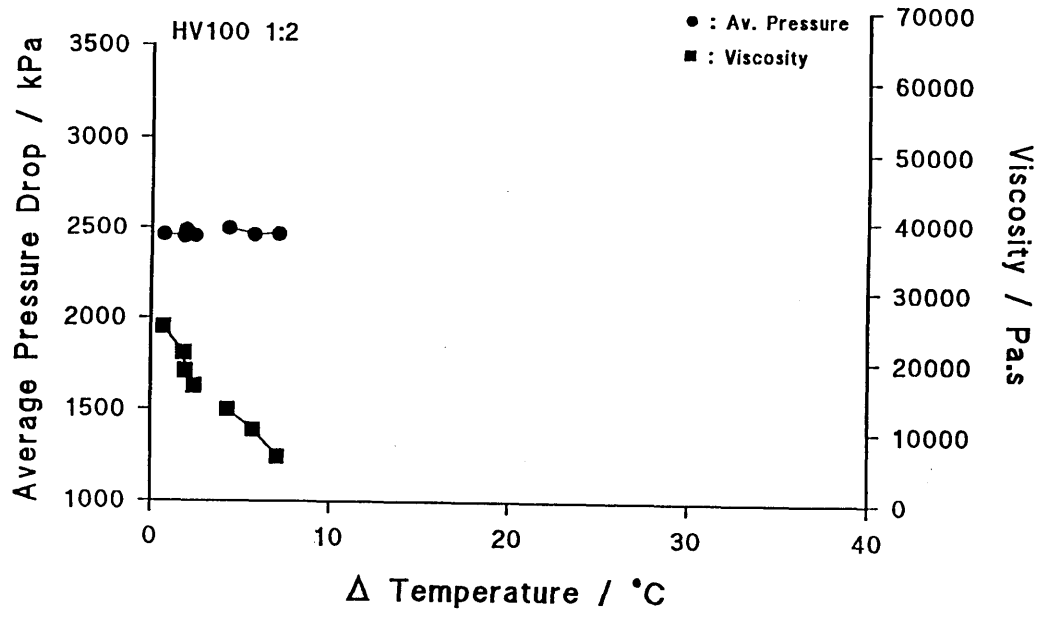


Figure 122(a) : The relationship between the temperature and pressure drop across the die for (i) the LV medium and 60 Mesh grit mixture with a grit to polymer ratio of 0.5, and (ii) the pure LV medium.

Figure 122(b) : The relationship between the temperature and pressure drop across the die for (i) the MV medium and 60 Mesh grit mixture with a grit to polymer ratio of 0.5, and (ii) the pure MV medium.

Figure 122(c) : The relationship between the temperature and pressure drop across the die for (i) the HV medium and 60 Mesh grit mixture with a grit to polymer ratio of 0.5, and (ii) the pure HV medium.

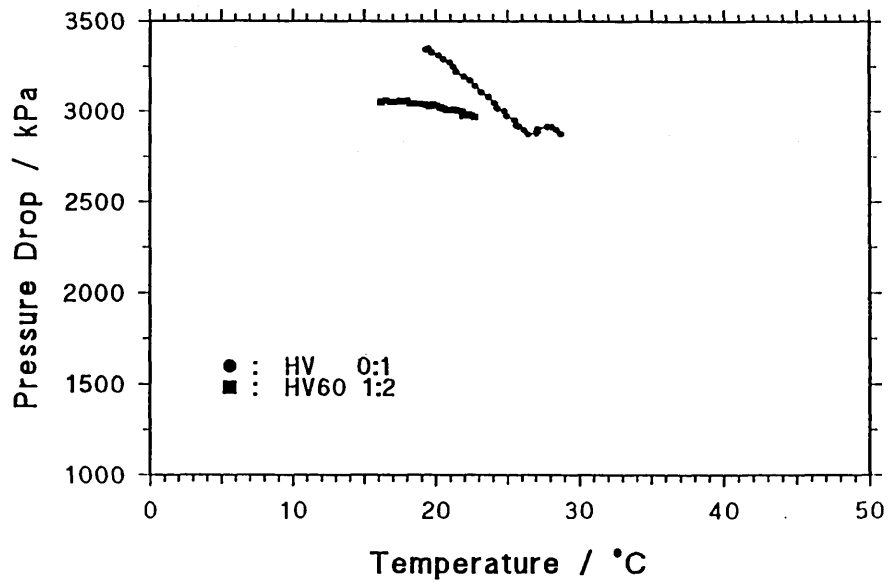
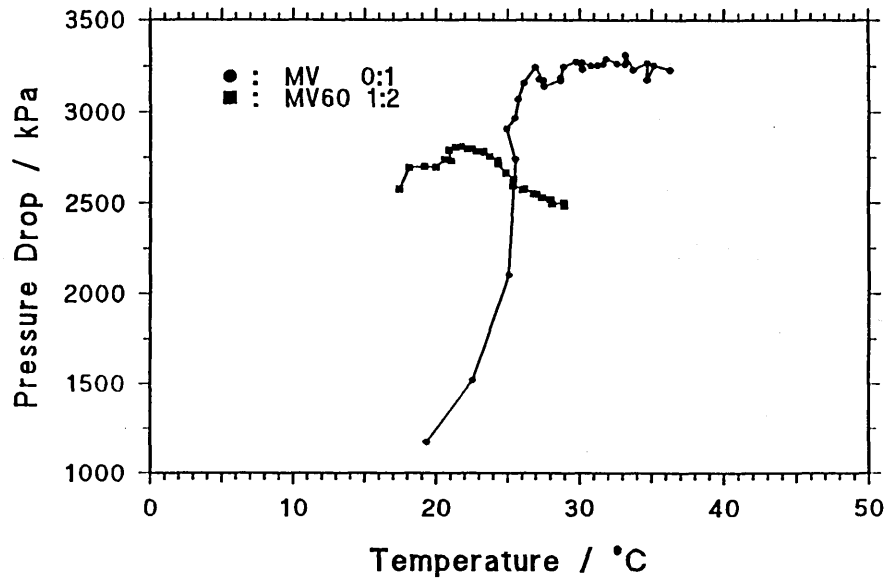
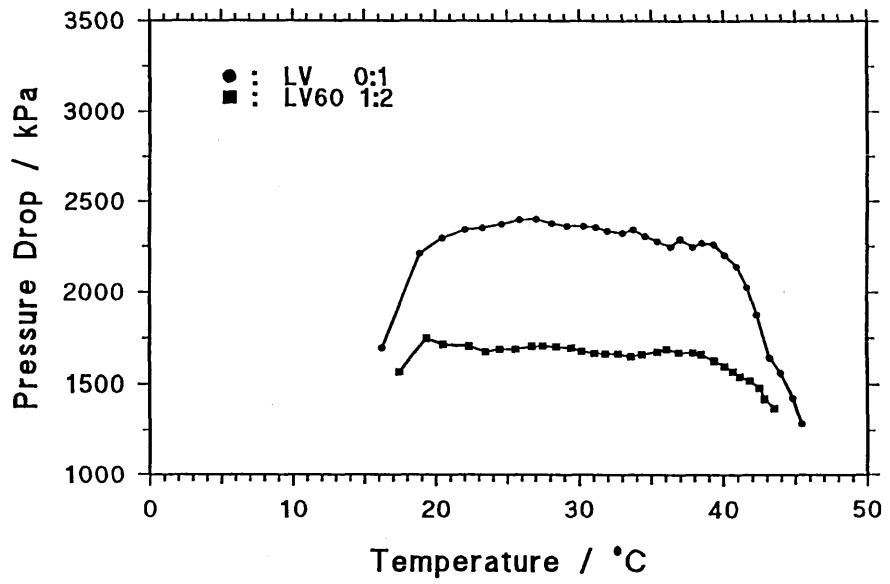


Figure 123(a) : The relationship between the temperature and (i) the viscosity, (ii) the volumetric flow rate, and (iii) the mass change per cycle for LV medium and 60 Mesh grit with a grit to polymer ratio of 0.5.

Figure 123(b) : The relationship between the temperature and (i) the viscosity, (ii) the volumetric flow rate, and (iii) the mass change per cycle for LV medium and 60 Mesh grit with a grit to polymer ratio of 1.

Figure 123(c) : The relationship between the temperature and (i) the viscosity, (ii) the volumetric flow rate, and (iii) the mass change per cycle for LV medium and 60 Mesh grit with a grit to polymer ratio of 2.

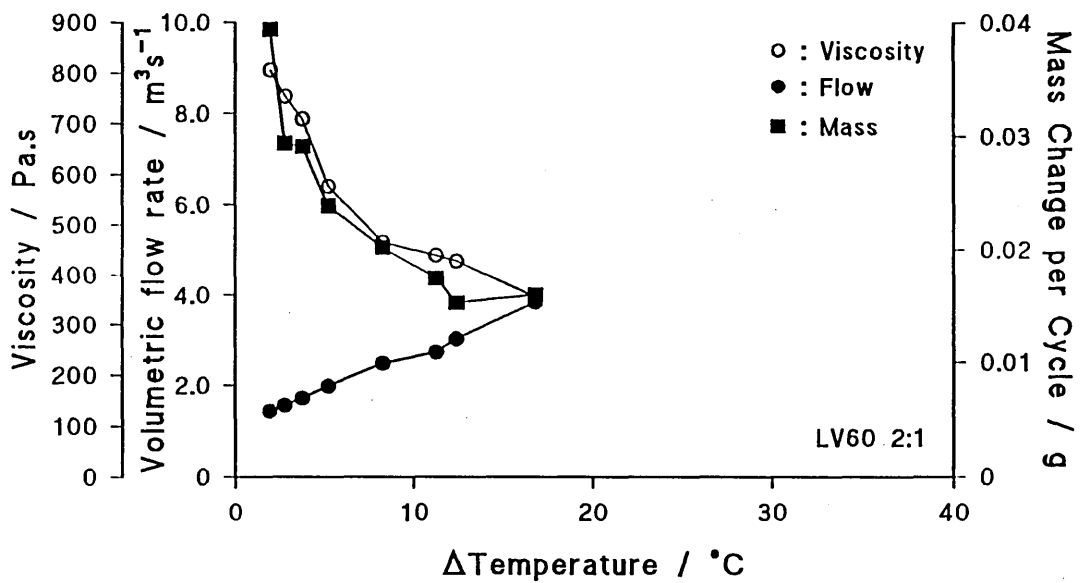
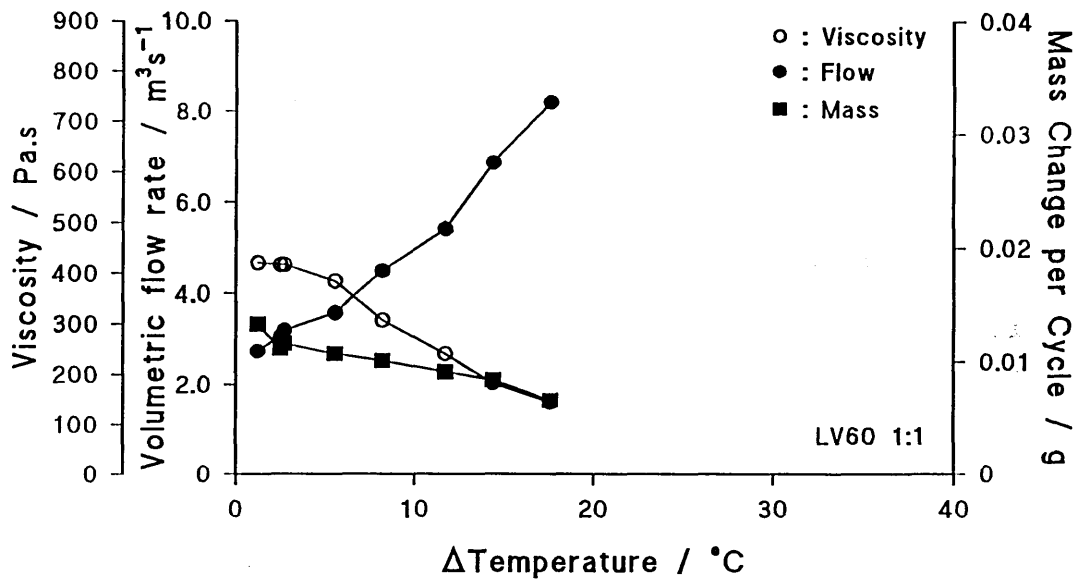
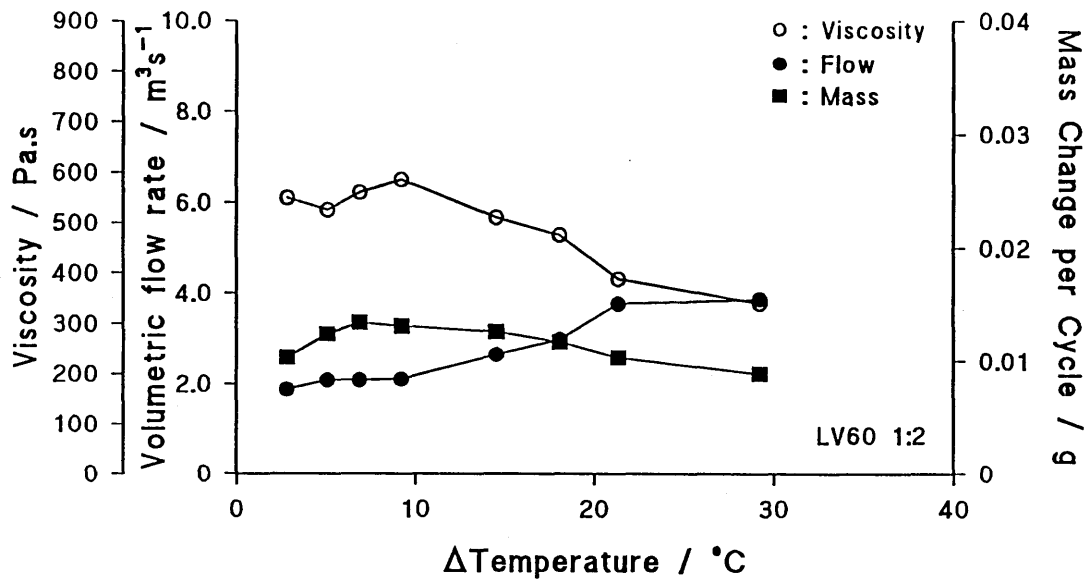


Figure 124(a) : The relationship between the temperature and (i) the viscosity, (ii) the volumetric flow rate, and (iii) the mass change per cycle for LV medium and 100 Mesh grit with a grit to polymer ratio of 0.5.

Figure 124(b) : The relationship between the temperature and (i) the viscosity, (ii) the volumetric flow rate, and (iii) the mass change per cycle for LV medium and 100 Mesh grit with a grit to polymer ratio of 1.

Figure 124(c) : The relationship between the temperature and (i) the viscosity, (ii) the volumetric flow rate, and (iii) the mass change per cycle for LV medium and 100 Mesh grit with a grit to polymer ratio of 2.

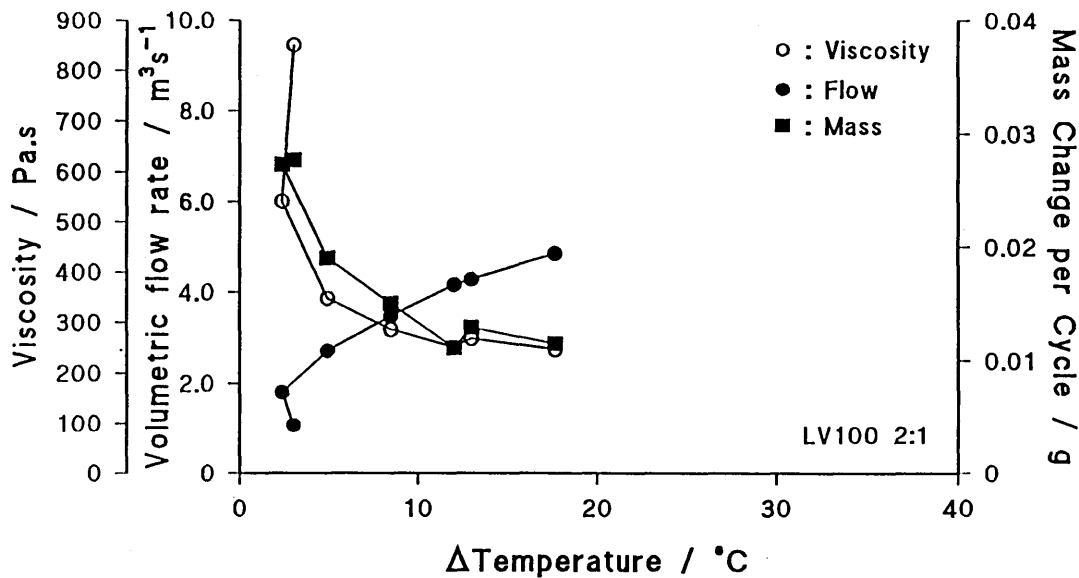
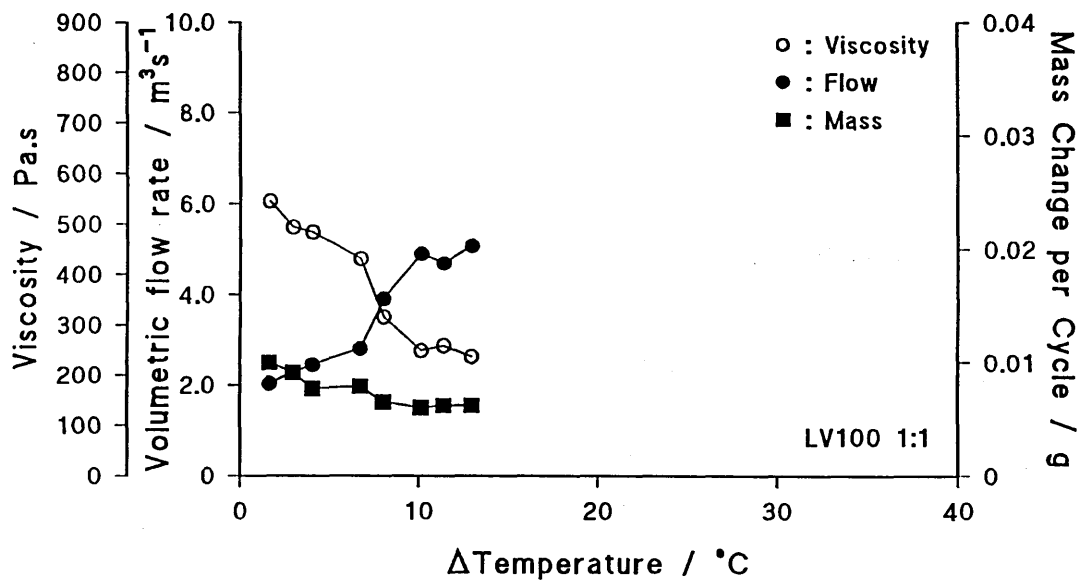
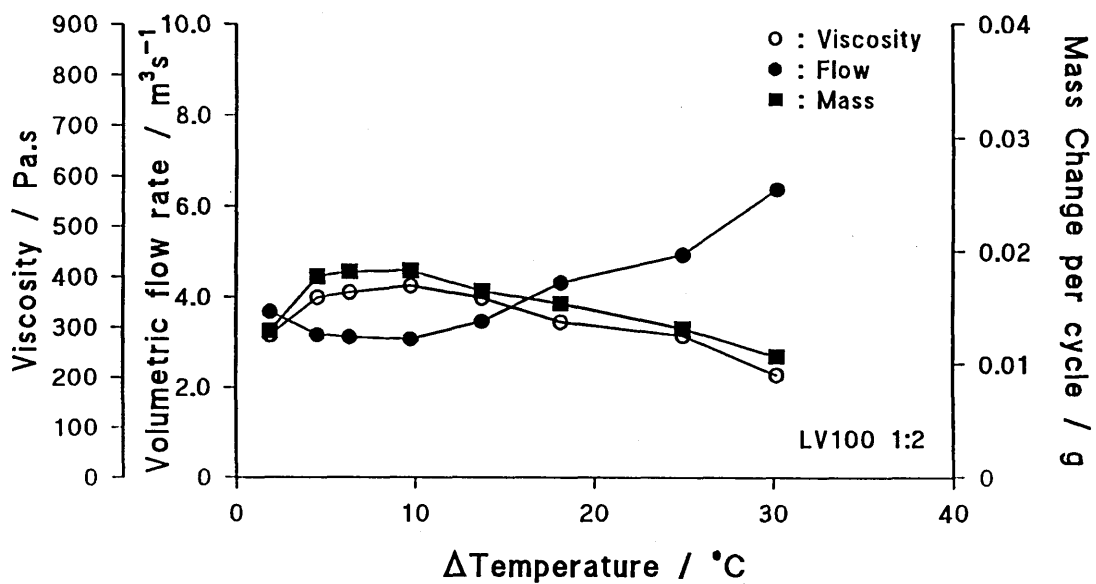


Figure 125(a) : The relationship between the temperature and (i) the viscosity, (ii) the volumetric flow rate, and (iii) the mass change per cycle for MV medium and 60 Mesh grit with a grit to polymer ratio of 0.5.

Figure 125(b) : The relationship between the temperature and (i) the viscosity, (ii) the volumetric flow rate, and (iii) the mass change per cycle for MV medium and 60 Mesh grit with a grit to polymer ratio of 1.

Figure 125(c) : The relationship between the temperature and (i) the viscosity, (ii) the volumetric flow rate, and (iii) the mass change per cycle for MV medium and 60 Mesh grit with a grit to polymer ratio of 2.

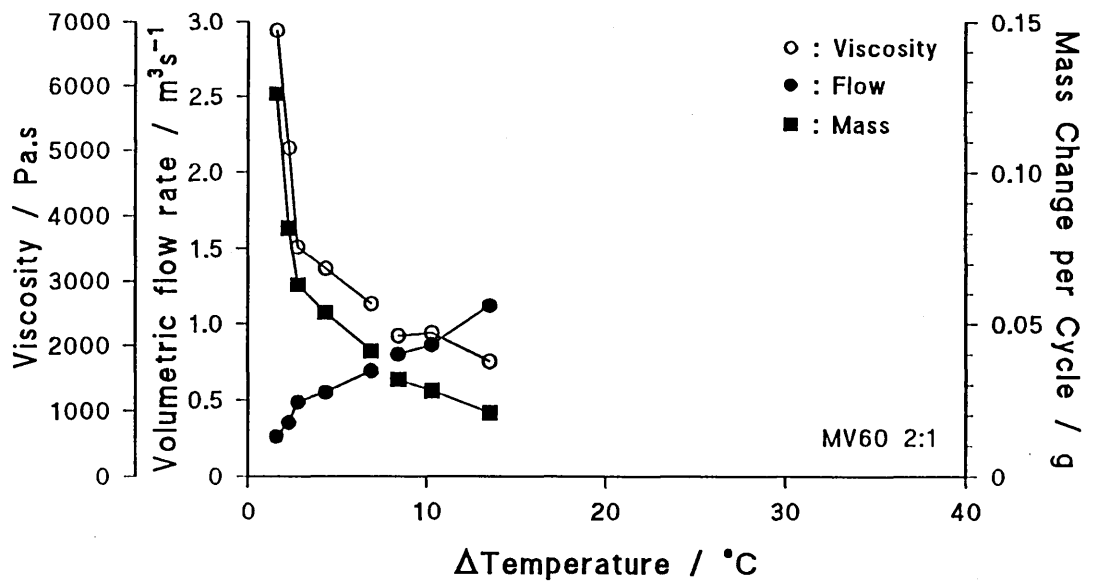
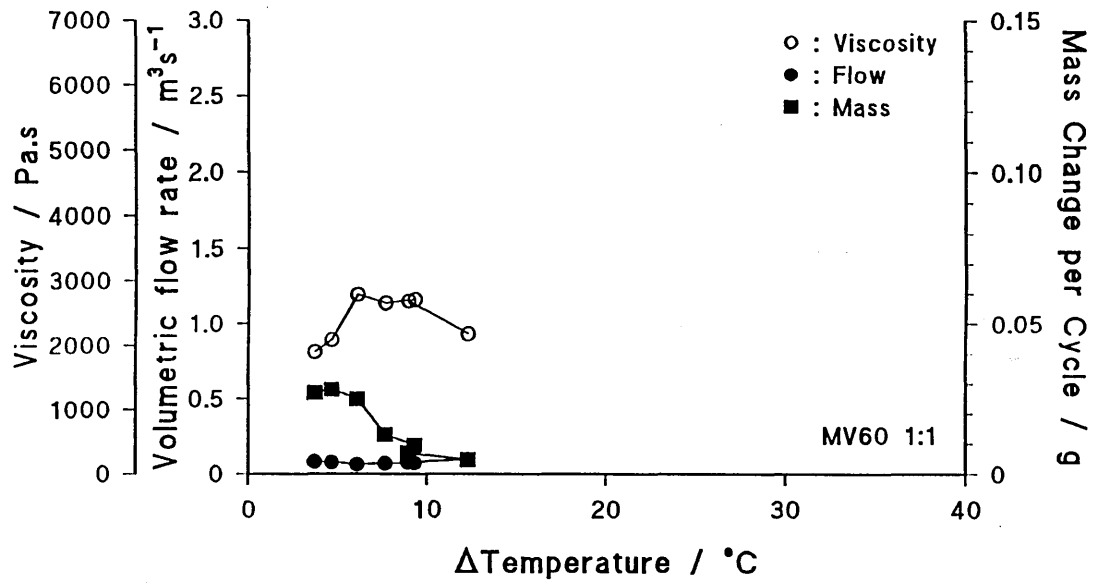
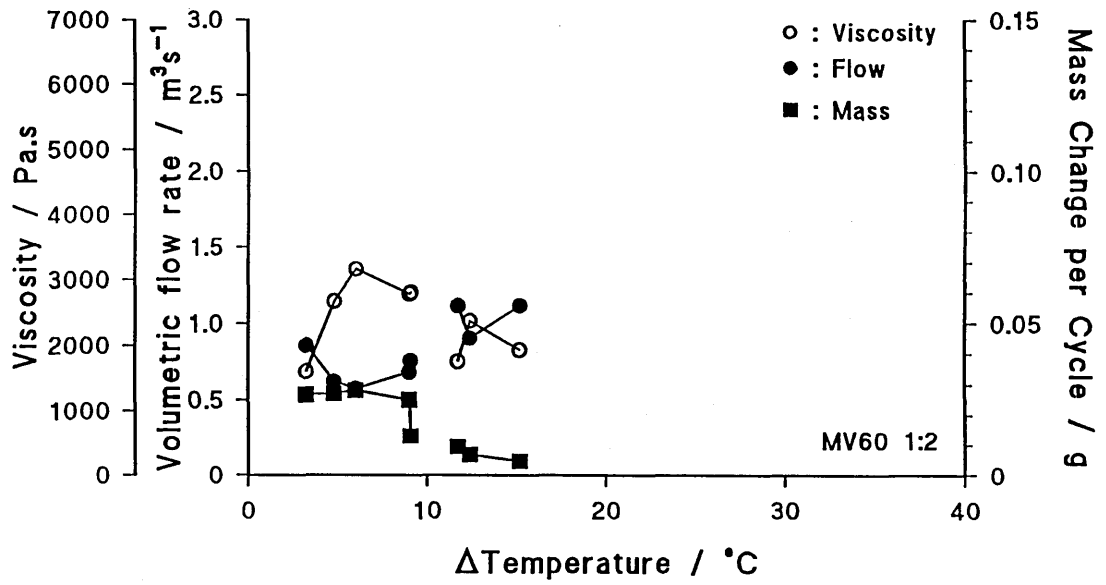


Figure 126(a) : The relationship between the temperature and (i) the viscosity, (ii) the volumetric flow rate, and (iii) the mass change per cycle for MV medium and 100 Mesh grit with a grit to polymer ratio of 0.5.

Figure 126(b) : The relationship between the temperature and (i) the viscosity, (ii) the volumetric flow rate, and (iii) the mass change per cycle for MV medium and 100 Mesh grit with a grit to polymer ratio of 1.

Figure 126(c) : The relationship between the temperature and (i) the viscosity, (ii) the volumetric flow rate, and (iii) the mass change per cycle for MV medium and 100 Mesh grit with a grit to polymer ratio of 2.

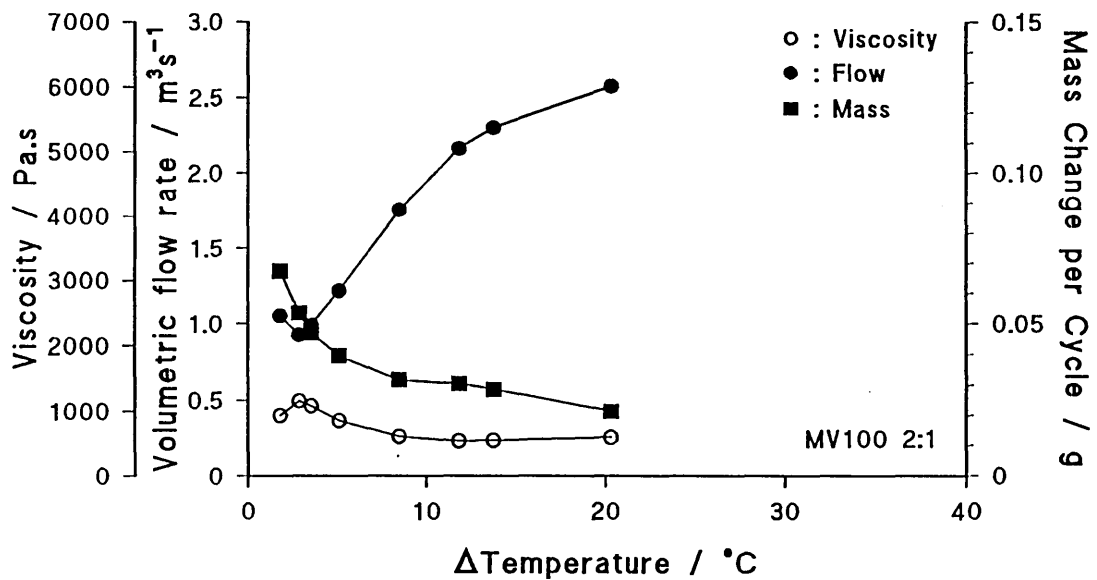
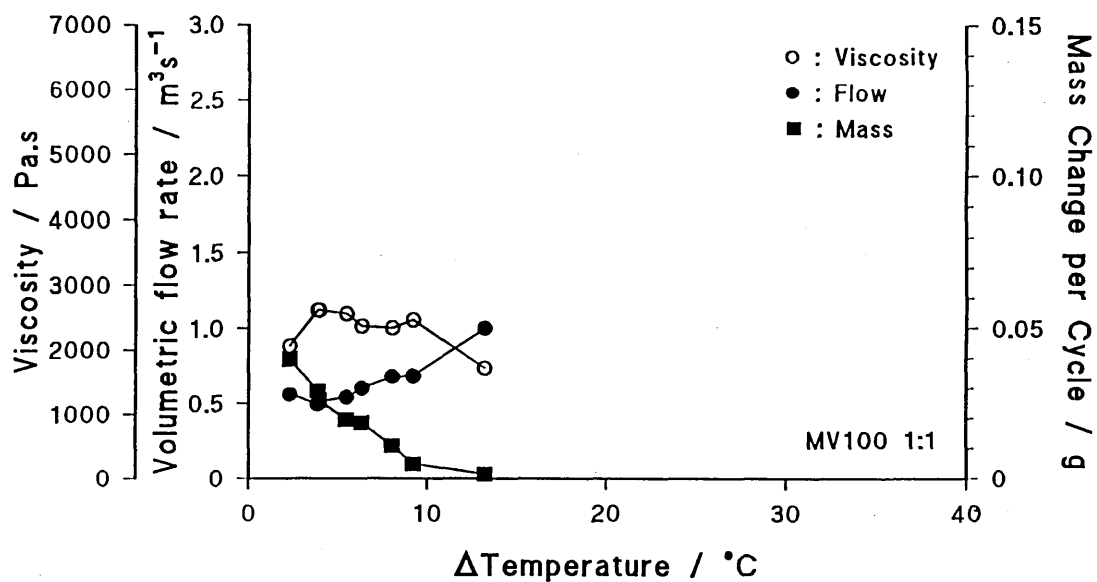
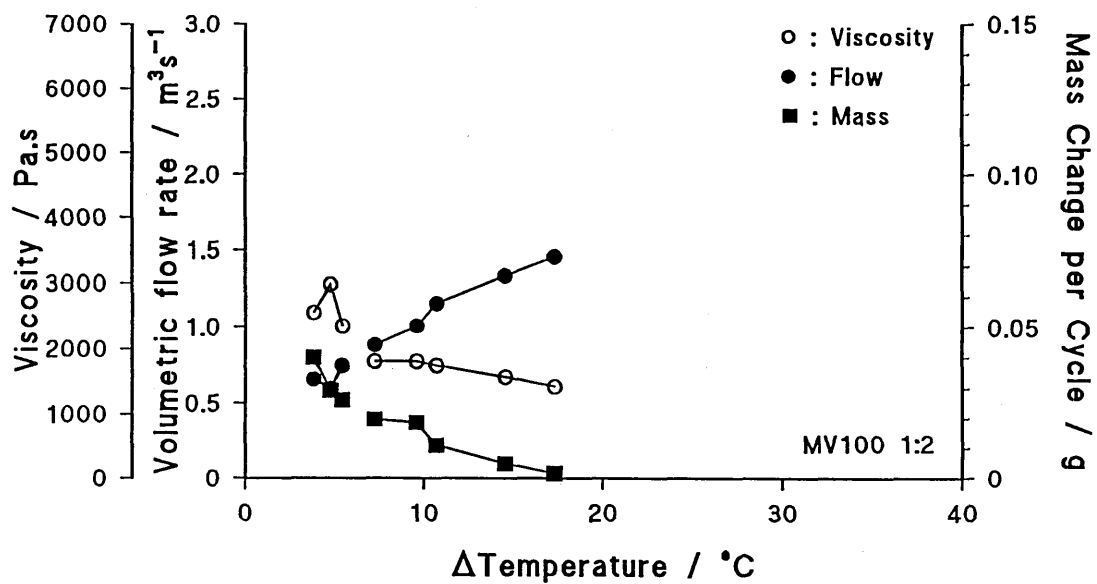


Figure 127(a) : The relationship between the temperature and (i) the viscosity, (ii) the volumetric flow rate, and (iii) the mass change per cycle for HV medium and 60 Mesh grit with a grit to polymer ratio of 0.5.

Figure 127(b) : The relationship between the temperature and (i) the viscosity, (ii) the volumetric flow rate, and (iii) the mass change per cycle for HV medium and 60 Mesh grit with a grit to polymer ratio of 1.

Figure 127(c) : The relationship between the temperature and (i) the viscosity, (ii) the volumetric flow rate, and (iii) the mass change per cycle for HV medium and 60 Mesh grit with a grit to polymer ratio of 2.

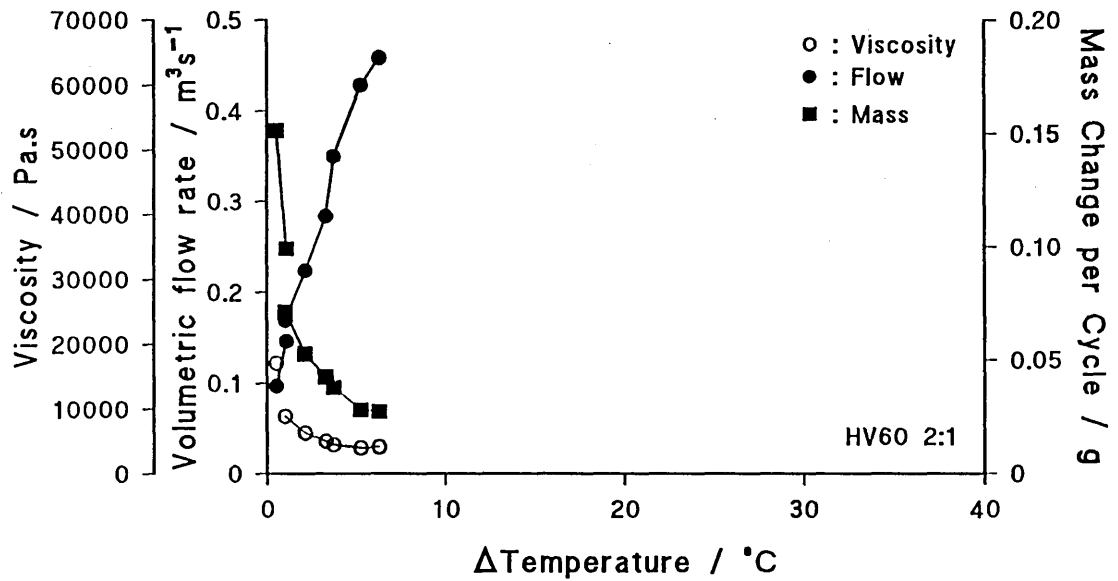
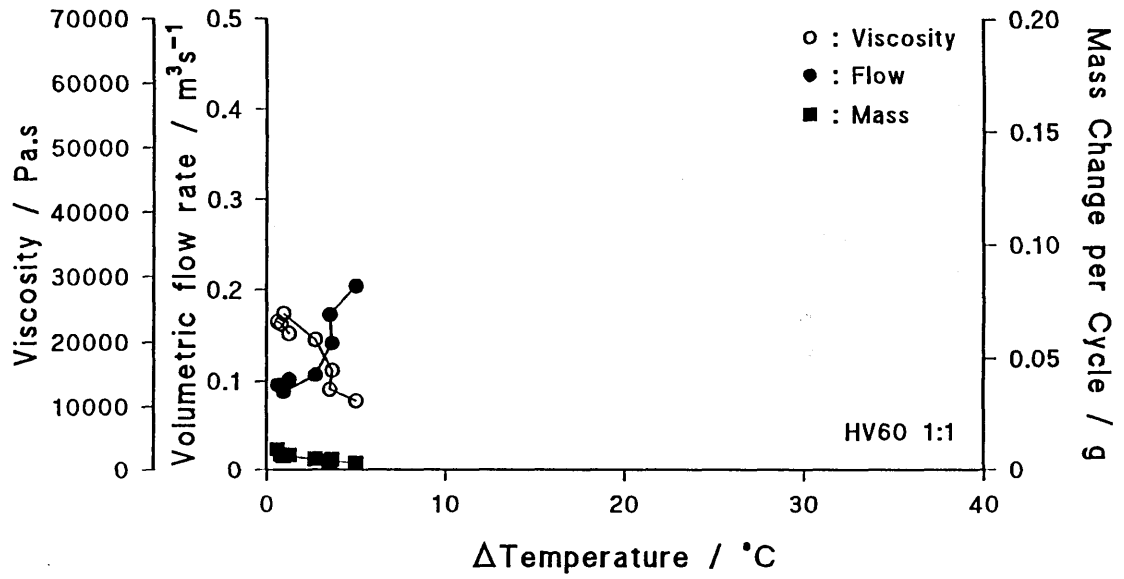
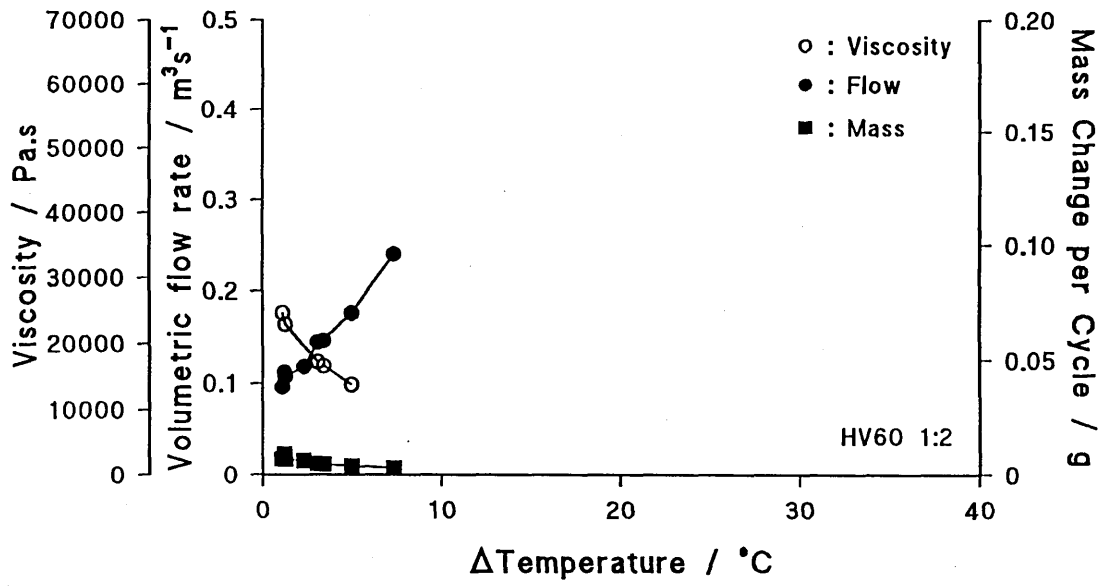


Figure 128(a) : The relationship between the temperature and (i) the viscosity, (ii) the volumetric flow rate, and (iii) the mass change per cycle for HV medium and 100 Mesh grit with a grit to polymer ratio of 0.5.

Figure 128(b) : The relationship between the temperature and (i) the viscosity, (ii) the volumetric flow rate, and (iii) the mass change per cycle for HV medium and 100 Mesh grit with a grit to polymer ratio of 2.

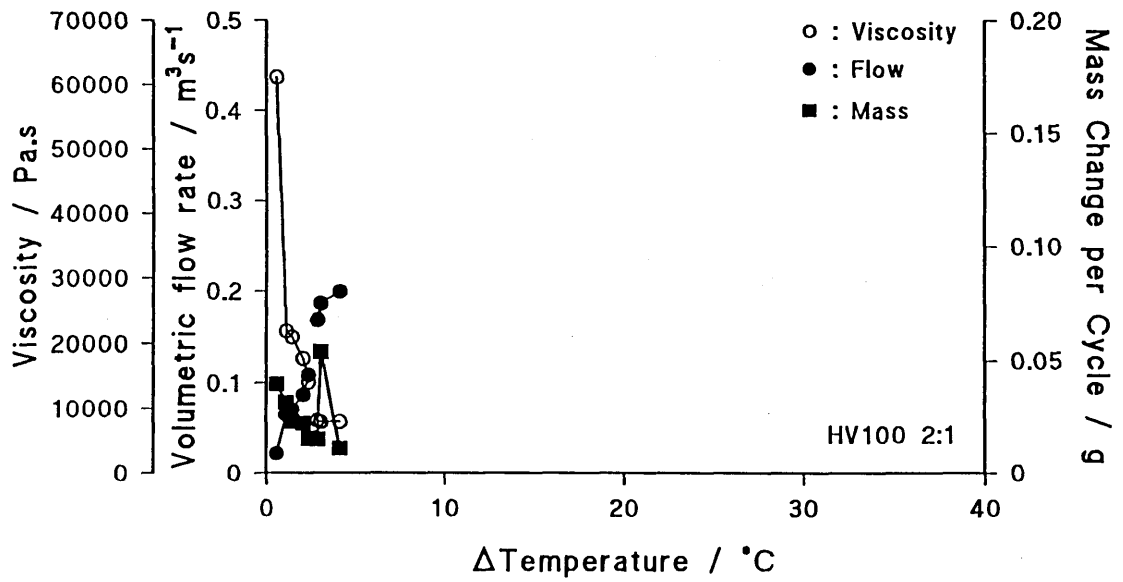
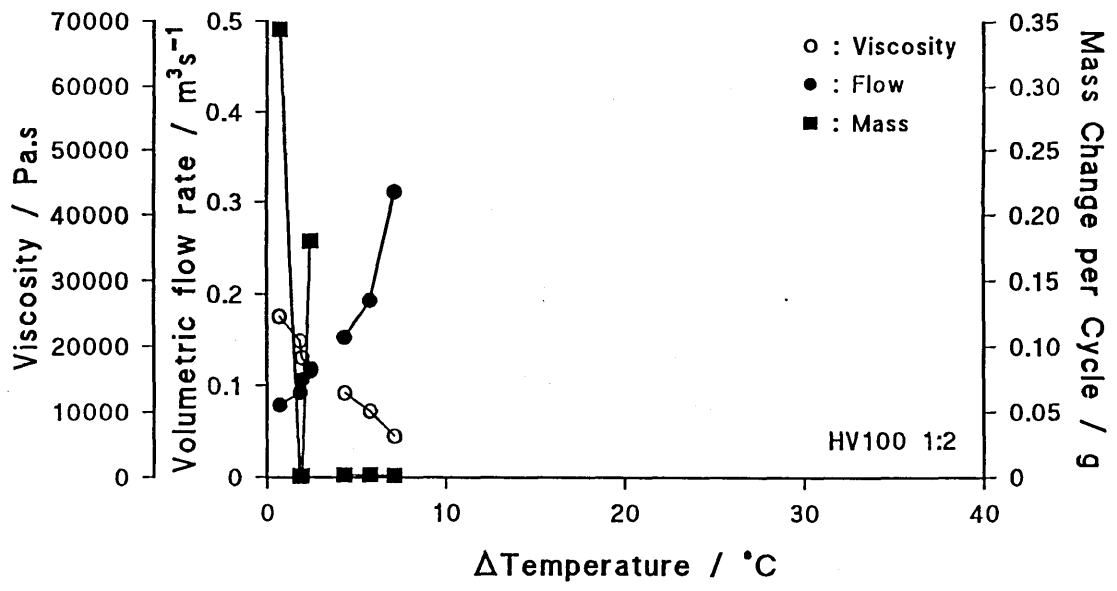


Figure 129(a) : The relationship between the number of extrusion cycles and (i) the shear stress, (ii) the viscosity, (iii) the percentage surface roughness improvement, and (iv) the total mass change for LV medium and 60 Mesh grit with a grit to polymer ratio of 0.5.

Figure 129(b) : The relationship between the number of extrusion cycles and (i) the shear stress, (ii) the viscosity, (iii) the percentage surface roughness improvement, and (iv) the total mass change for LV medium and 60 Mesh grit with a grit to polymer ratio of 1.

Figure 129(c) : The relationship between the number of extrusion cycles and (i) the shear stress, (ii) the viscosity, (iii) the percentage surface roughness improvement, and (iv) the total mass change for LV medium and 60 Mesh grit with a grit to polymer ratio of 2.

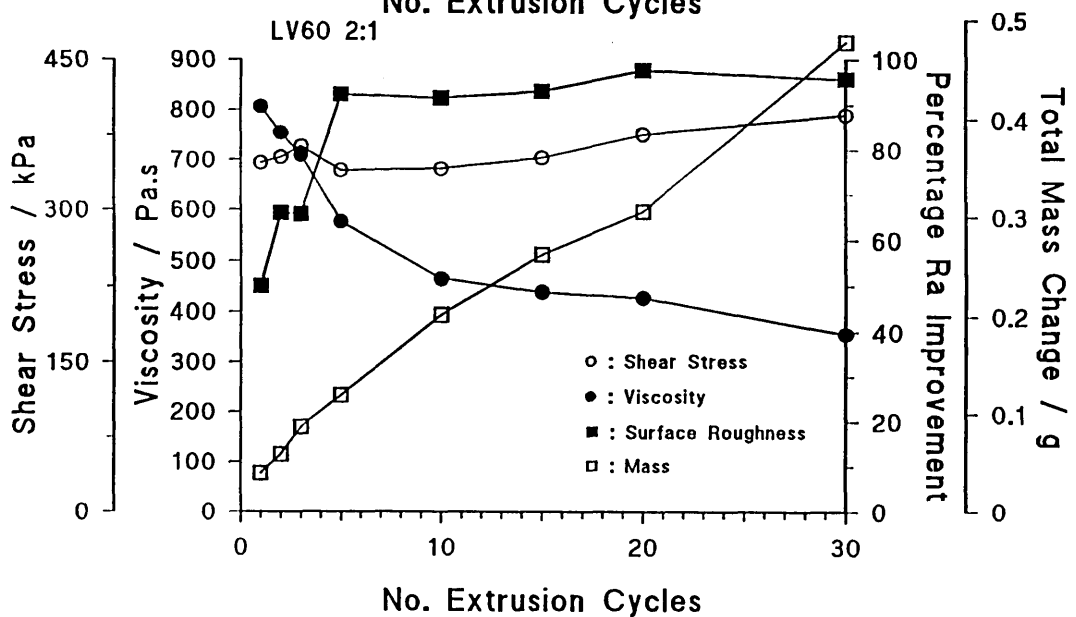
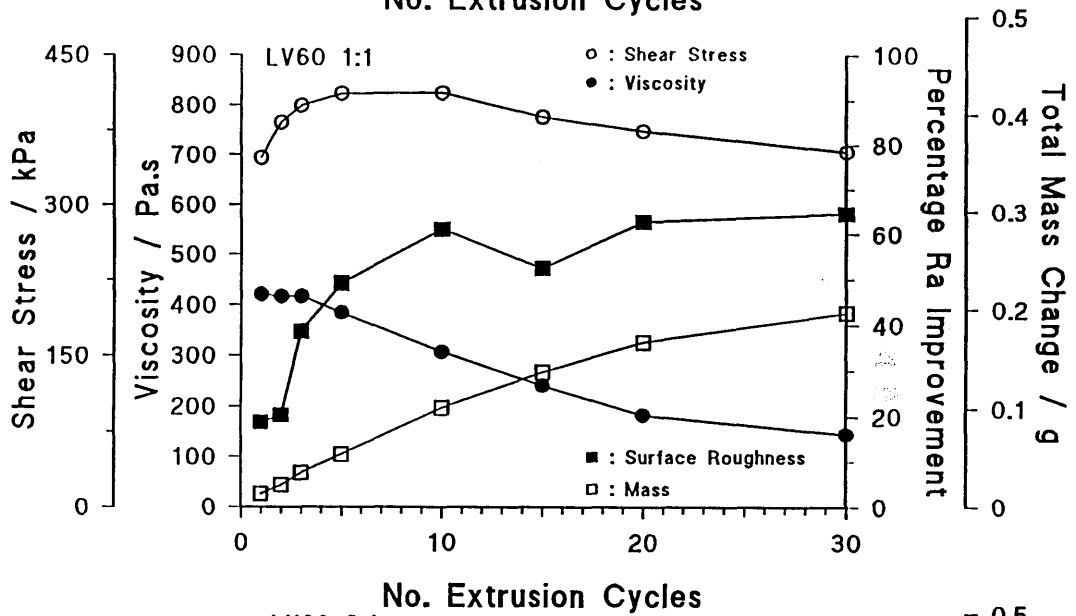
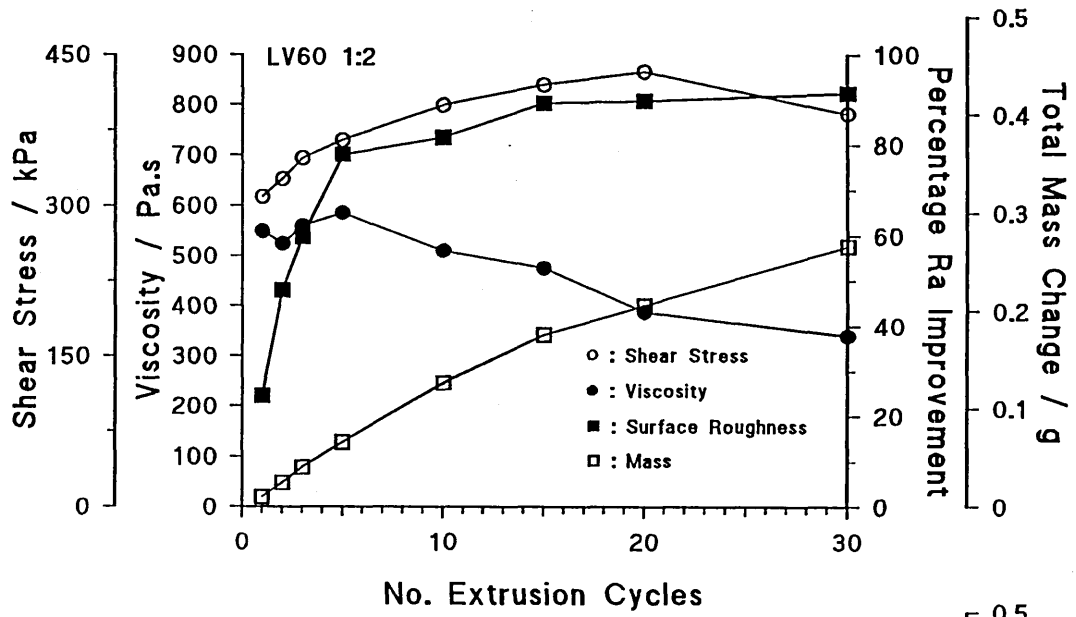


Figure 130(a) : The relationship between the number of extrusion cycles and (i) the shear stress, (ii) the viscosity, (iii) the percentage surface roughness improvement, and (iv) the total mass change for LV medium and 100 Mesh grit with a grit to polymer ratio of 0.5.

Figure 130(b) : The relationship between the number of extrusion cycles and (i) the shear stress, (ii) the viscosity, (iii) the percentage surface roughness improvement, and (iv) the total mass change for LV medium and 100 Mesh grit with a grit to polymer ratio of 1.

Figure 130(c) : The relationship between the number of extrusion cycles and (i) the shear stress, (ii) the viscosity, (iii) the percentage surface roughness improvement, and (iv) the total mass change for LV medium and 100 Mesh grit with a grit to polymer ratio of 2.

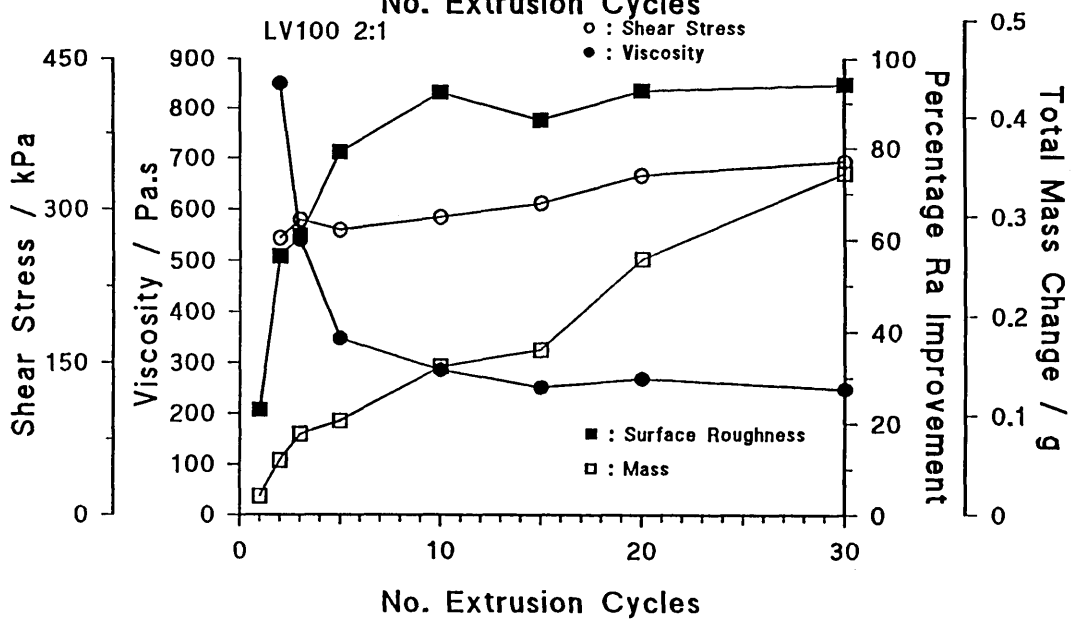
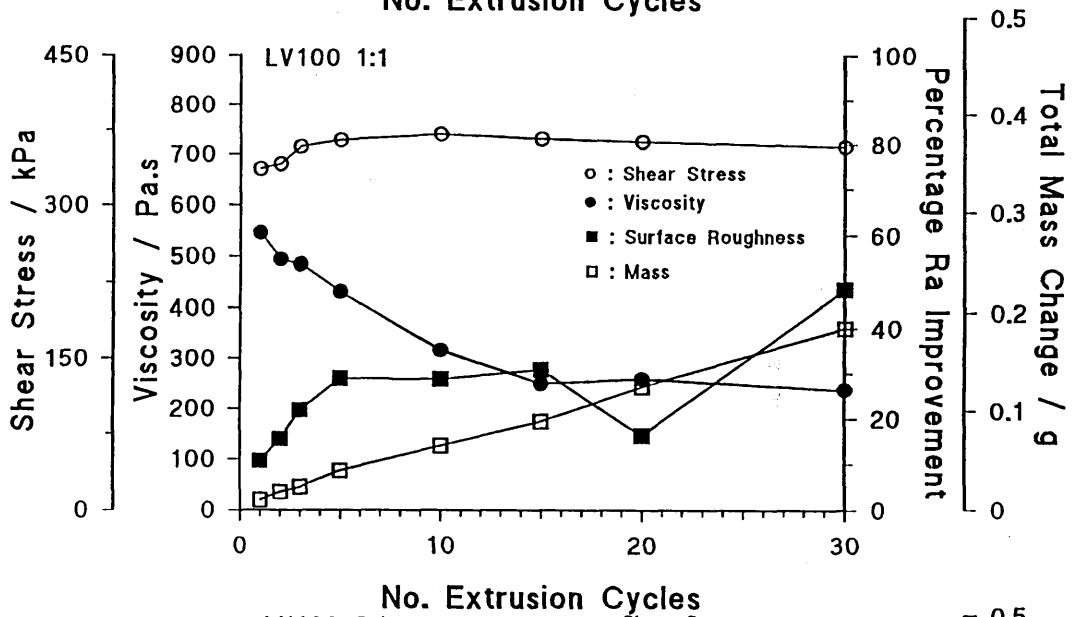
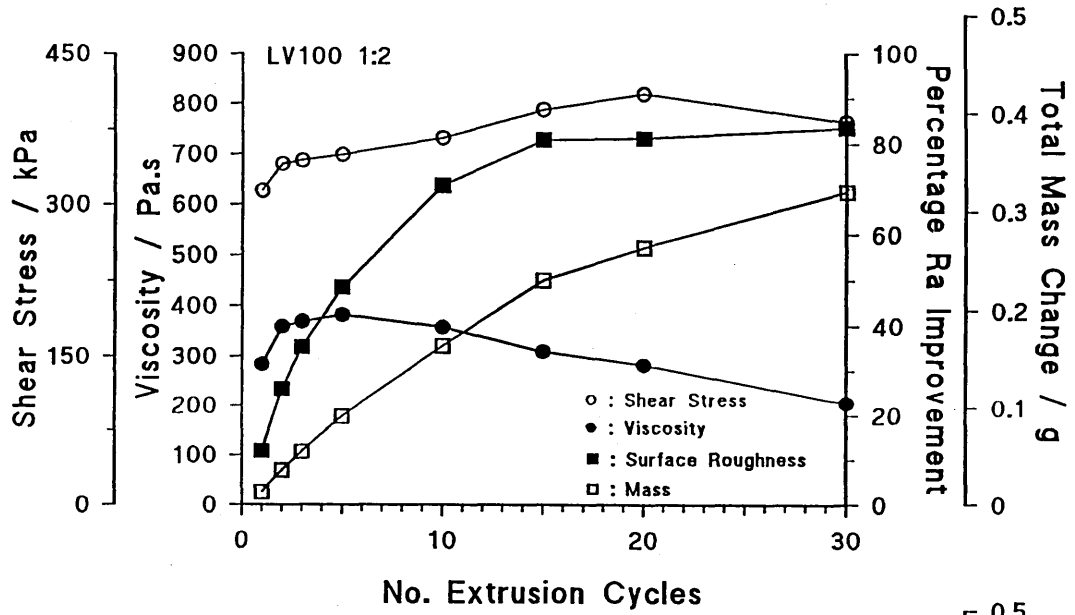


Figure 131(a) : The relationship between the number of extrusion cycles and (i) the shear stress, (ii) the viscosity, (iii) the percentage surface roughness improvement, and (iv) the total mass change for MV medium and 60 Mesh grit with a grit to polymer ratio of 0.5.

Figure 131(b) : The relationship between the number of extrusion cycles and (i) the shear stress, (ii) the viscosity, (iii) the percentage surface roughness improvement, and (iv) the total mass change for MV medium and 60 Mesh grit with a grit to polymer ratio of 1.

Figure 131(c) : The relationship between the number of extrusion cycles and (i) the shear stress, (ii) the viscosity, (iii) the percentage surface roughness improvement, and (iv) the total mass change for MV medium and 60 Mesh grit with a grit to polymer ratio of 2.

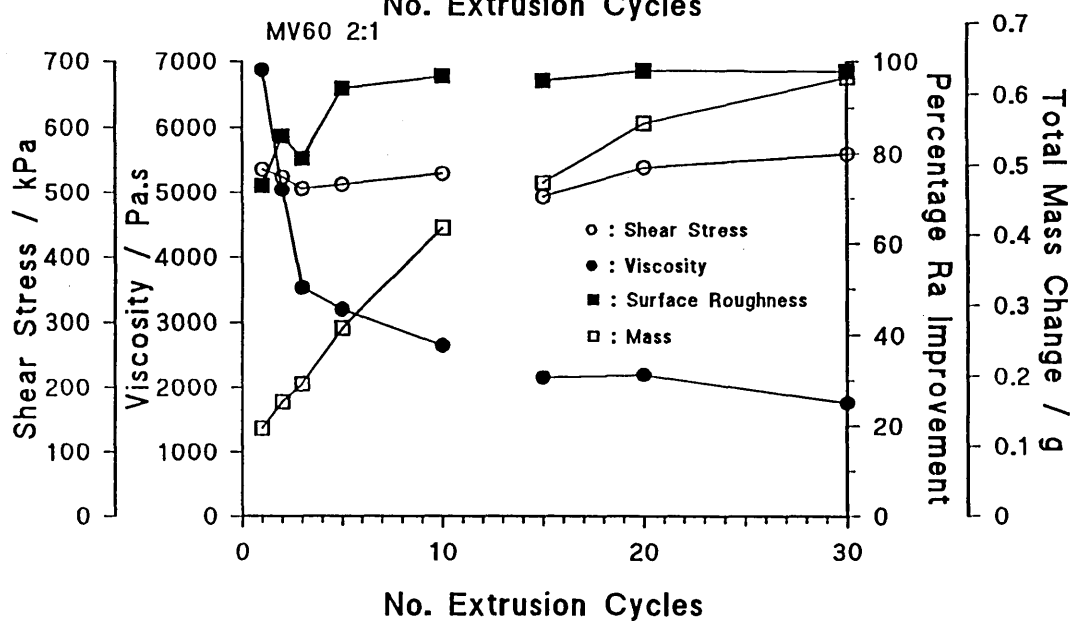
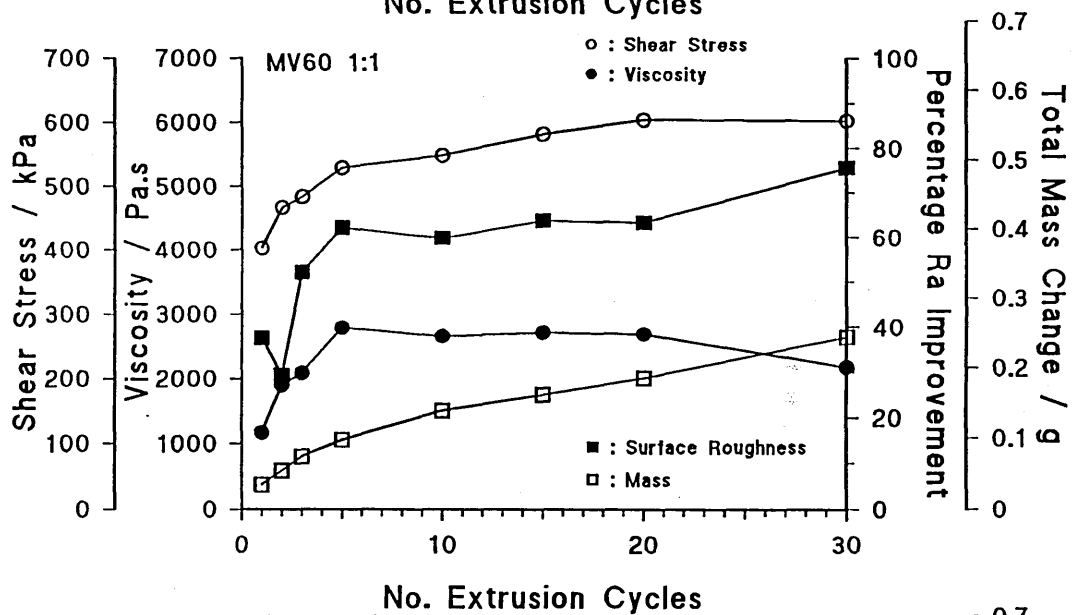
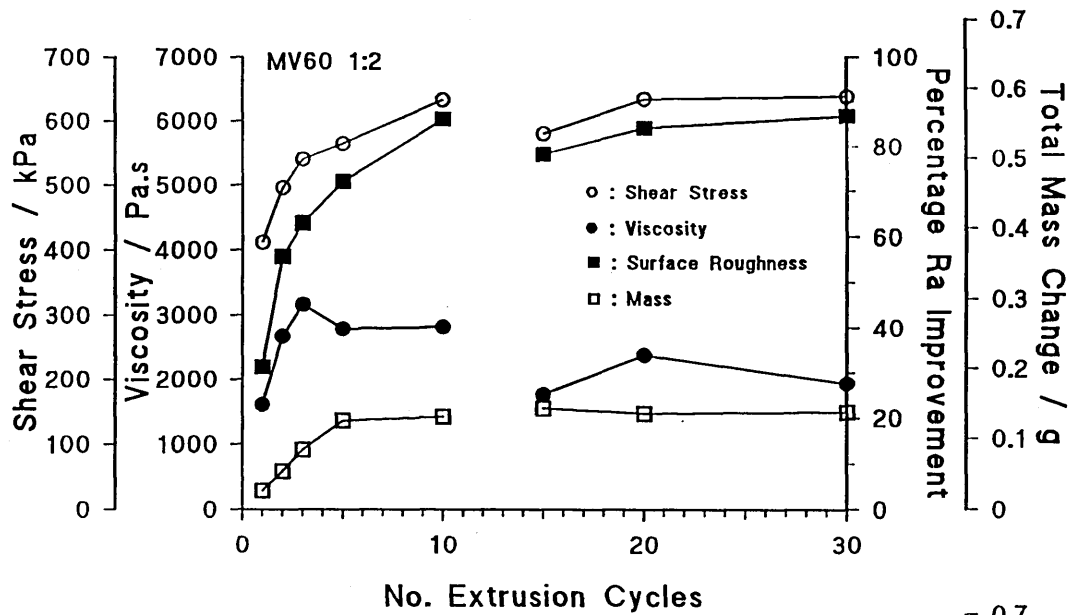


Figure 132(a) : The relationship between the number of extrusion cycles and (i) the shear stress, (ii) the viscosity, (iii) the percentage surface roughness improvement, and (iv) the total mass change for MV medium and 100 Mesh grit with a grit to polymer ratio of 0.5.

Figure 132(b) : The relationship between the number of extrusion cycles and (i) the shear stress, (ii) the viscosity, (iii) the percentage surface roughness improvement, and (iv) the total mass change for MV medium and 100 Mesh grit with a grit to polymer ratio of 1.

Figure 132(c) : The relationship between the number of extrusion cycles and (i) the shear stress, (ii) the viscosity, (iii) the percentage surface roughness improvement, and (iv) the total mass change for MV medium and 100 Mesh grit with a grit to polymer ratio of 2.

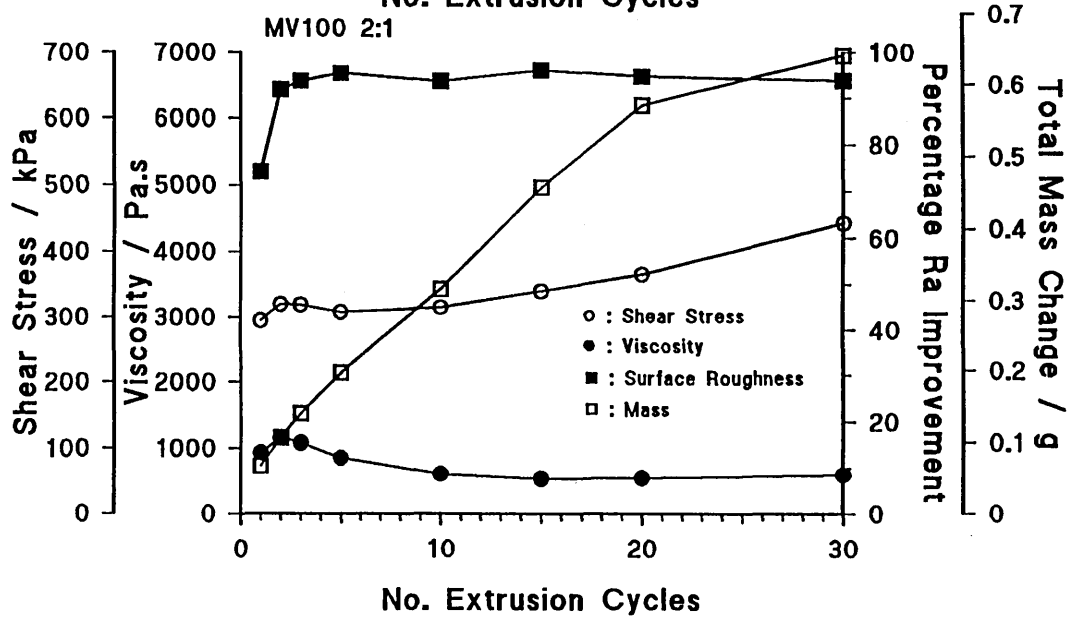
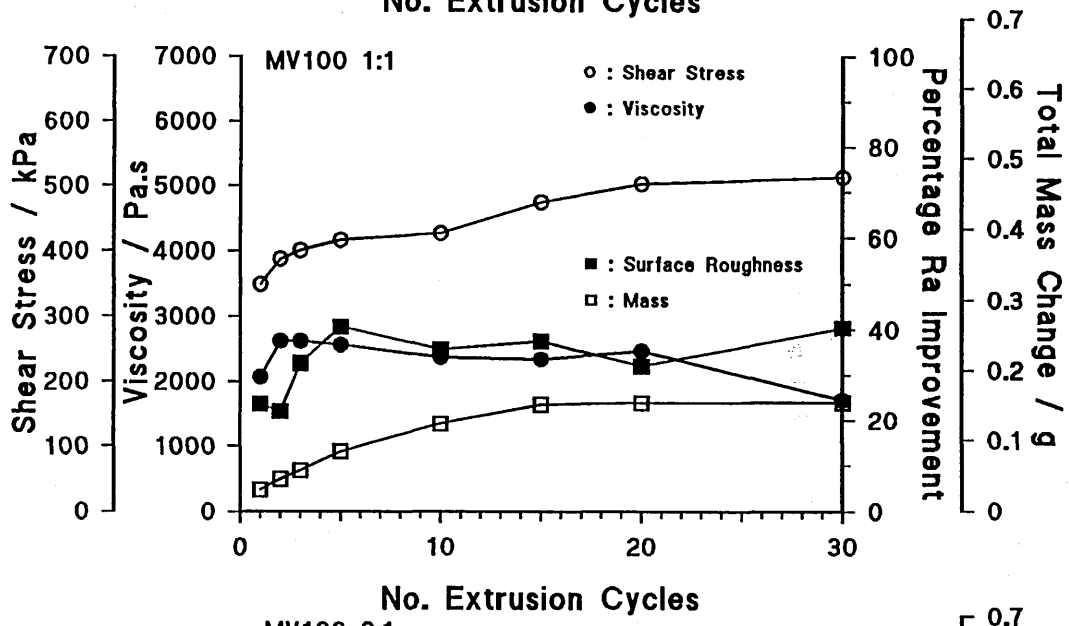
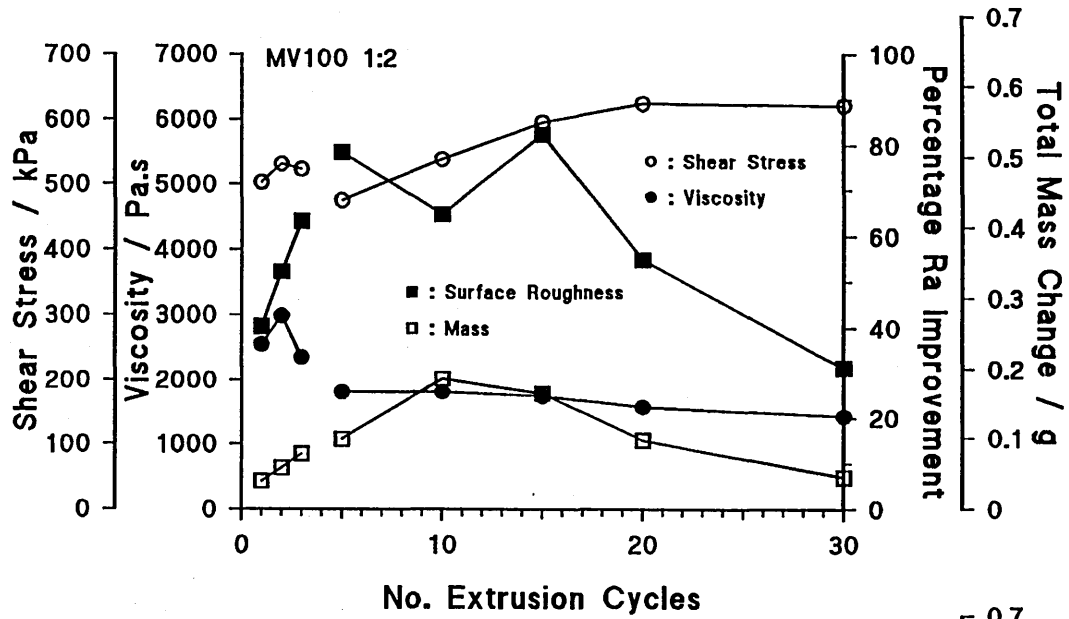


Figure 133(a) : The relationship between the number of extrusion cycles and (i) the shear stress, (ii) the viscosity, (iii) the percentage surface roughness improvement, and (iv) the total mass change for HV medium and 60 Mesh grit with a grit to polymer ratio of 0.5.

Figure 133(b) : The relationship between the number of extrusion cycles and (i) the shear stress, (ii) the viscosity, (iii) the percentage surface roughness improvement, and (iv) the total mass change for HV medium and 60 Mesh grit with a grit to polymer ratio of 1.

Figure 133(c) : The relationship between the number of extrusion cycles and (i) the shear stress, (ii) the viscosity, (iii) the percentage surface roughness improvement, and (iv) the total mass change for HV medium and 60 Mesh grit with a grit to polymer ratio of 2.

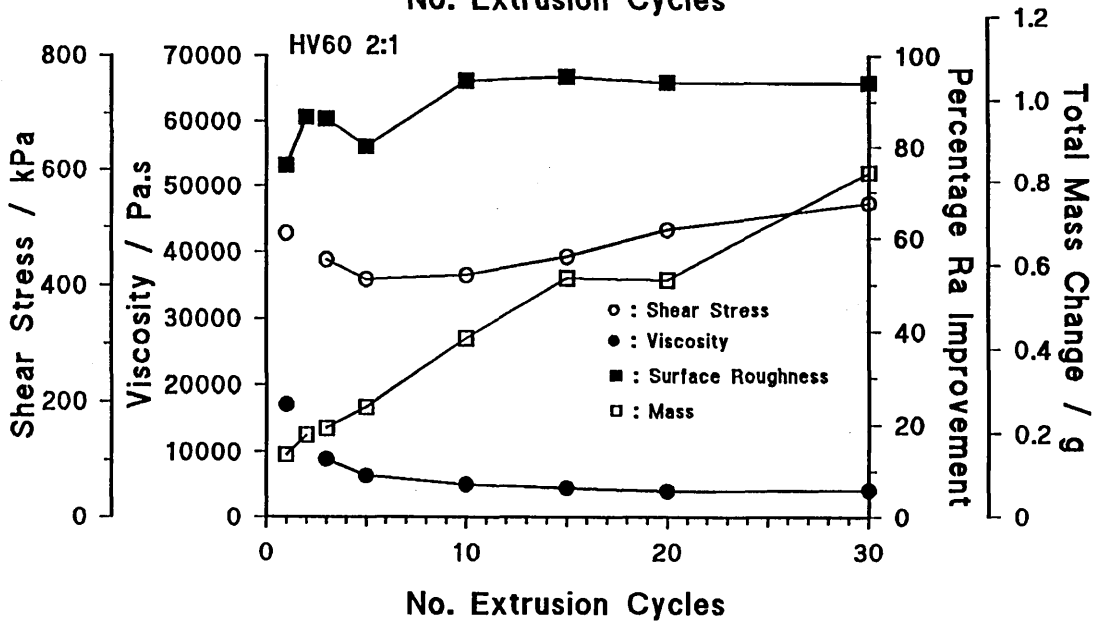
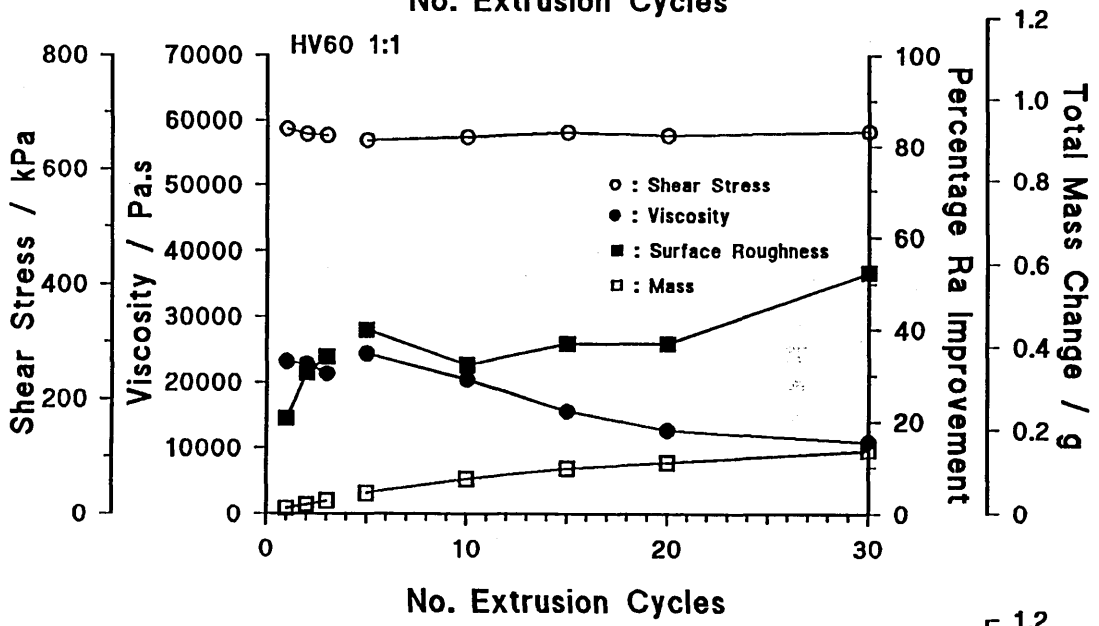
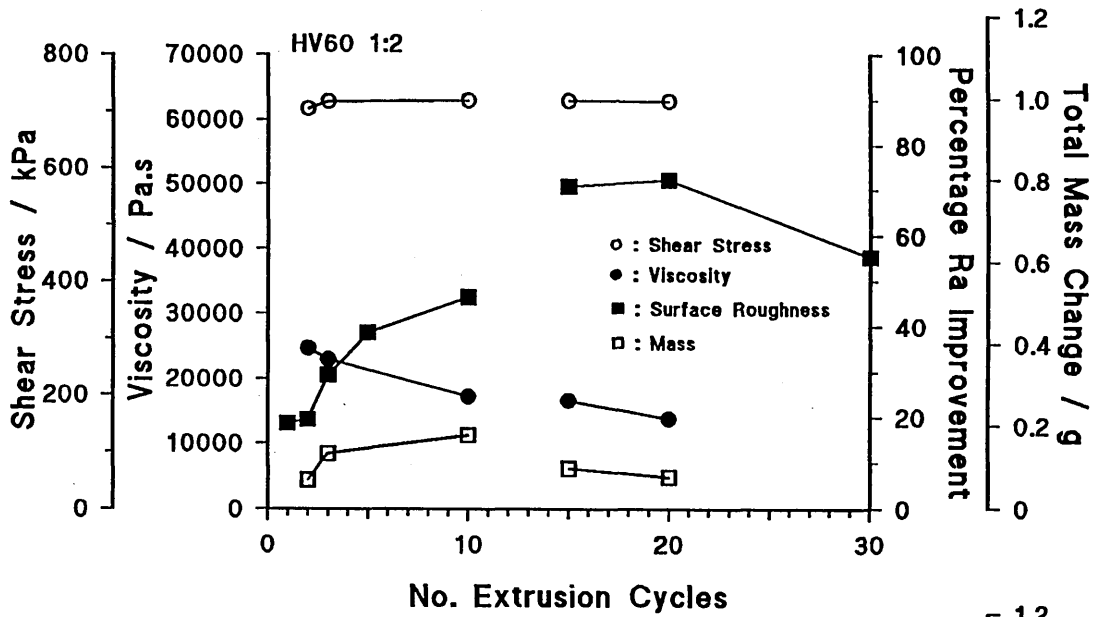


Figure 134(a) : The relationship between the number of extrusion cycles and (i) the shear stress, (ii) the viscosity, (iii) the percentage surface roughness improvement, and (iv) the total mass change for HV medium and 100 Mesh grit with a grit to polymer ratio of 0.5.

Figure 134(b) : The relationship between the number of extrusion cycles and (i) the shear stress, (ii) the viscosity, (iii) the percentage surface roughness improvement, and (iv) the total mass change for HV medium and 100 Mesh grit with a grit to polymer ratio of 1.

Figure 134(c) : The relationship between the number of extrusion cycles and (i) the shear stress, (ii) the viscosity, (iii) the percentage surface roughness improvement, and (iv) the total mass change for HV medium and 100 Mesh grit with a grit to polymer ratio of 2.

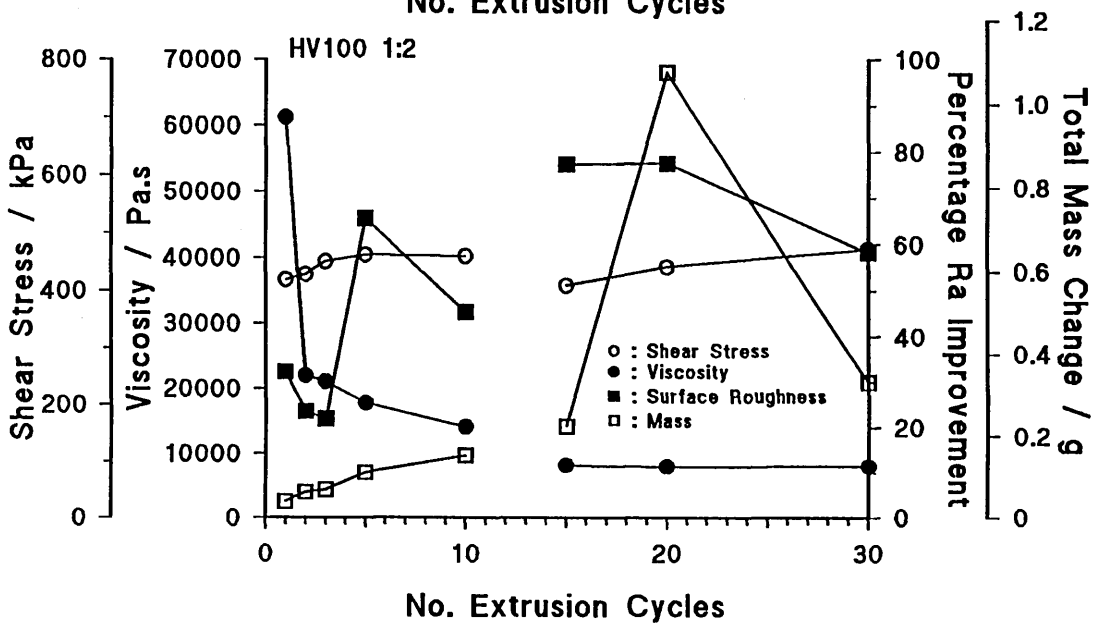
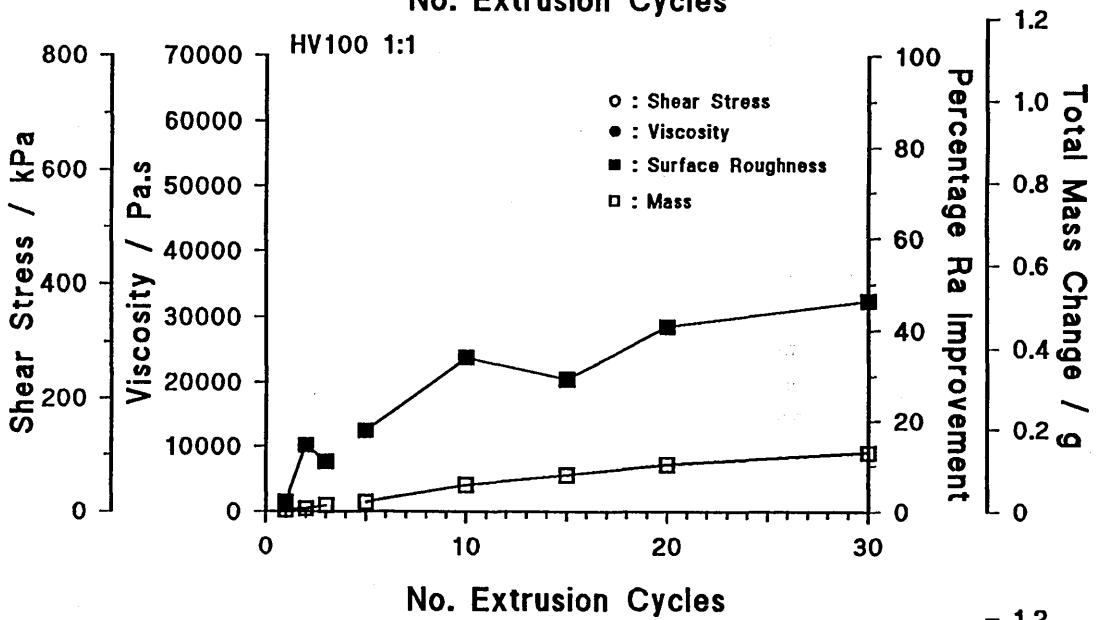
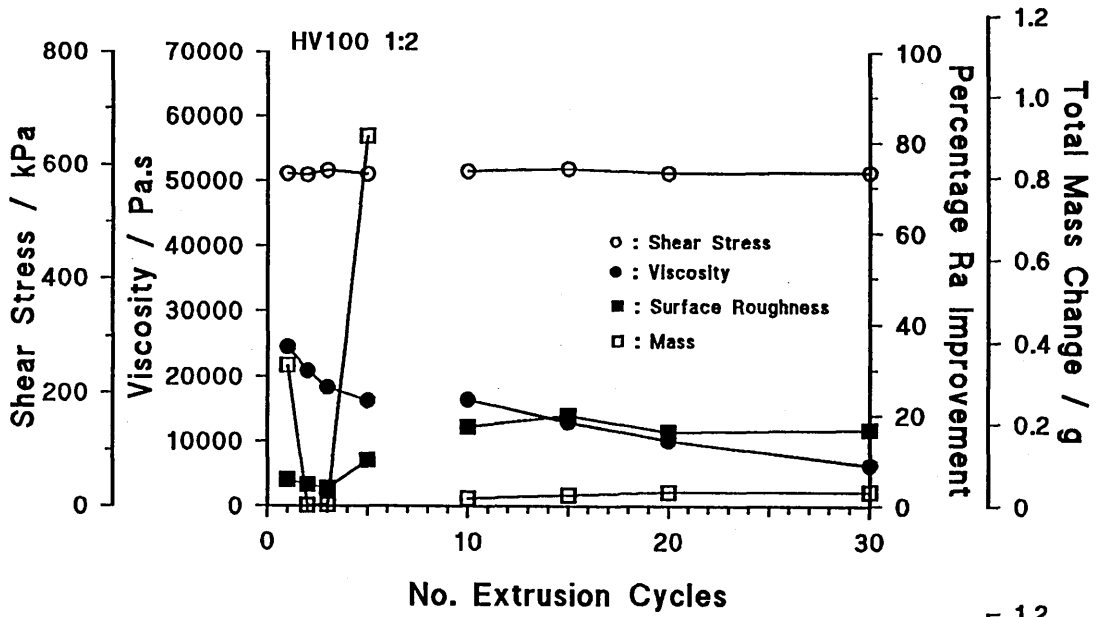
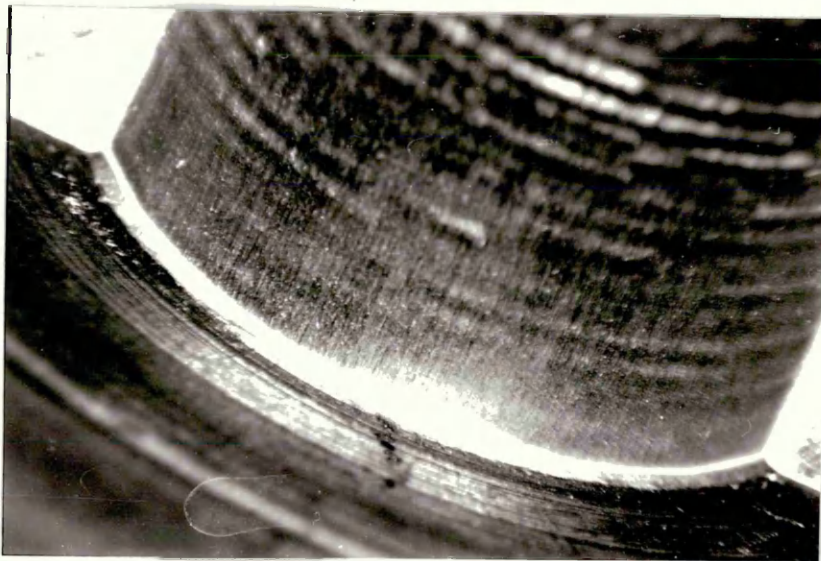
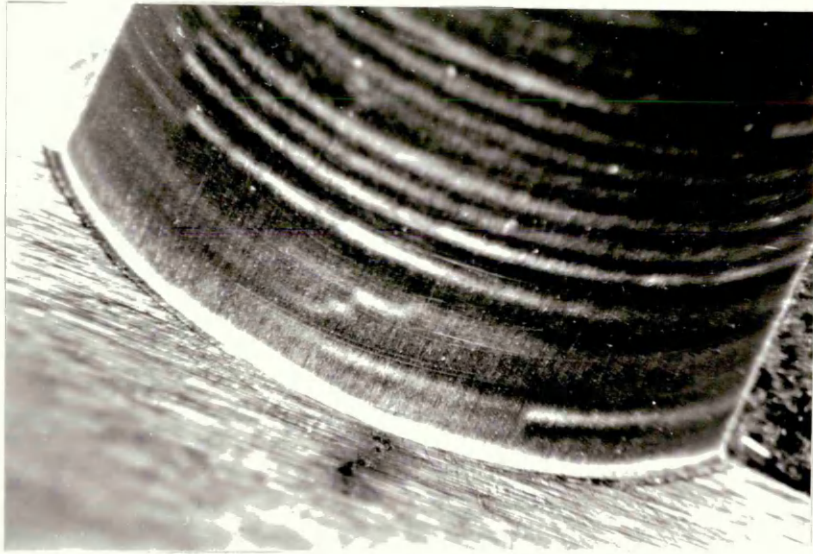


Figure 135(a) : The illustration of the surface edge condition of the die after 30 extrusion cycles using LV medium with 100 Mesh grit and a grit to polymer ratio of 1.

Figure 135(b) : The illustration of the surface edge condition of the die after 30 extrusion cycles using MV medium with 100 Mesh grit and a grit to polymer ratio of 1.

Figure 135(c) : The illustration of the surface edge condition of the die after 30 extrusion cycles using HV medium with 100 Mesh grit and a grit to polymer ratio of 1.



APPENDIX 1

A1.0 Viscosity Calculation of the LV Medium with 60 Mesh Grit and a Grit to Polymer Ratio of 0.5

A1.1 Data recorded in relation to the 30 extrusion cycle run:

Processing time:	t	= 383.4s
Average pressure drop:	P	= 1636.03kPa
Die diameter:	D	= 0.0150992m
Die length:	L	= 0.0158m
Volume of medium available:	V	= 4.462 x 10 ⁻³ m ³

A1.2 Calculation of the extruded volume from the dimensions of the medium chambers when the extremities of their forward strokes are reached:

Diameter of both medium chambers:	d	= 0.1524m
Lower medium chamber length:	L _L	= 0.038m
Upper medium chamber length:	L _U	= 0.072m

Volume of medium retained within the lower chamber:

$$\begin{aligned}V_L &= \pi (d^2/4) L_L \\ &= 0.693 \times 10^{-3} \text{m}^3\end{aligned}$$

Volume of medium retained within the upper chamber:

$$\begin{aligned}V_U &= \pi (d^2/4) L_U \\ &= 1.313 \times 10^{-3} \text{m}^3\end{aligned}$$

Volume of medium extruded on the first half cycle:

$$\begin{aligned}V_1 &= V - V_L \\ &= 3.769 \times 10^{-3} \text{m}^3\end{aligned}$$

Volume of medium extruded on the second half cycle and subsequent half cycles:

$$\begin{aligned}V_2 &= V_1 - V_U \\ &= 2.456 \times 10^{-3} \text{m}^3\end{aligned}$$

Total volume extruded during 30 extrusion cycles:

$$\begin{aligned}V_E &= (V_1 + V_2) + (V_2 \times 58) \\ &= 148.614 \times 10^{-3} \text{m}^3\end{aligned}$$

A1.3 Data calculated from the recorded data:

Flow rate: $Q = V_E / t$
 $= 0.00038762 \text{m}^3 \text{s}^{-1}$

Die radius: $r = D / 2$
 $= 0.0075496 \text{m}$

A1.4 Rheological measurements:

Shear stress: $\tau = (P r) / (2 L)$
 $= 390866.205 \text{Pa}$